OCCOQUAN RESERVOIR AND WATERSHED: A WATER QUALITY ASSESSMENT 1973–2019

Alexa María Cubas Suazo

Thesis submitted to the faculty of the Virginia Polytechnic Institute and State University in partial fulfillment of the requirements for the degree of

Master of Science

In

Civil Engineering

Adil N. Godrej, Chair

John C. Little

John T. Novak

March 31, 2021

Manassas, Virginia

Keywords: Water quality, nutrients, eutrophication, hypolimnetic oxygenation, nitrate addition, reservoir, watershed, Occoquan, trophic state

OCCOQUAN RESERVOIR AND WATERSHED: A WATER QUALITY ASSESSMENT 1973–2019

Alexa María Cubas Suazo

ABSTRACT

The Occoquan Reservoir is part of the largest indirect potable reuse systems in the United States. It in an important water supply source for the Northern Virginia area, as well as, an ecological and recreational area. Furthermore, the Occoquan Reservoir protects the water quality of the Chesapeake Bay because it acts as a trap for sediments and pollutants. Continuous water quality monitoring and evaluation is critical to preserve this important water resource. Reservoir water quality can be affected by the delivery of pollutants from point and nonpoint sources, potentially causing problems such as eutrophication, excess salinization, presence of compounds that affect human and aquatic health. Different management strategies have been implemented at the Occoquan Reservoir to nutrient loading into the reservoir and address eutrophication issues, including nitrate addition to hypolimnetic waters and installation of a hypolimnetic oxygenation system. The goal of this study is to assess how current management strategies implemented in the Occoquan Reservoir have affected the water quality from 1973 to 2019, with particular emphasis on the data since 2003. This analysis of the Occoquan Reservoir and its tributary watershed includes the evaluation of hydrometeorological data and morphometric characteristics; establishment of long-term trends for water quality constituents; and determination of the trophic state of the reservoir. Data from water samples from four different stations located at the Occoquan Reservoir and four stations located throughout the Occoquan tributary watershed were analyzed for nutrients, principal ions and metals, synthetic organic compounds (SOCs), and other water quality parameters. Long-term water quality trends were determined using Mann-Kendall test and relationship between constituents was evaluated using Principal Component Analysis (PCA). Trophic state of the reservoir was assessed using Carlson's Trophic State Index (TSI), Vollenweider Model, and Rast, Jones, and Lee's Model. Results indicate the Occoquan Reservoir is a eutrophic waterbody. However, the nitrate management strategy and the installation of the hypolimnetic system have improved reservoir water quality, reducing concentrations of nutrients and metals.

OCCOQUAN RESERVOIR AND WATERSHED: A WATER QUALITY ASSESSMENT 1973–2019

Alexa María Cubas Suazo

GENERAL AUDIENCE ABSTRACT

The Occoquan Reservoir is part of the largest indirect potable reuse systems in the United States. Indirect potable reuse refers to the planned discharge of reclaimed water into a water supply source, such as a reservoir or lake. The Occoquan Reservoir also serves as an ecological and recreational area, and serves to protects the water quality of the Chesapeake Bay because it acts as a trap for sediments and pollutants. To protect the different ecosystem services that the reservoir provides, it is critical to continuously monitoring and evaluate its water quality.

Reservoir water quality can be affected by the delivery of pollutants from industrial and municipal waste discharges (point sources), as well as, from urban and agricultural runoff (nonpoint sources). Contaminants include nutrients (such as nitrogen and phosphorus), ions, metals, and synthetic organic compounds (SOCs) that can affect human and aquatic health. Different management strategies have been implemented at the Occoquan Reservoir to reduce load of pollutants into the reservoir, particularly to reduce concentrations of nutrients, as excessive nutrients can degrade water quality. Two strategies implemented are the addition of nitrogen, in the form of nitrate, and the installation of an oxygenation system at the reservoir bottom waters. The goal of this study is to assess how current management strategies implemented in the Occoquan Reservoir have affected the water quality from 1973 to 2019, with particular emphasis on the data since 2003.

This analysis of the Occoquan Reservoir and its tributary watershed includes the evaluation of the hydrological, meteorological, and morphometric characteristics of the Occoquan Reservoir and Watershed; establishment of long-term trends for water quality constituents; and determination of the productivity (trophic state) of the reservoir. Data from water samples from four different stations located at the reservoir and four stations located throughout the watershed were analyzed for nutrients, principal ions and metals, SOCs, and other water parameters indicative of water quality. Statistical analyses were employed to determine long-term water quality trends (Mann-Kendall test) and relationship between constituents (Principal Component Analysis - PCA). The trophic state of the reservoir was assessed using three methods: Carlson's Trophic State Index (TSI), Vollenweider Model, and Rast, Jones, and Lee's Model. Results indicate the Occoquan Reservoir is eutrophic, or highly enriched with nutrients and productive. However, management strategies employed have improved the water quality and the reservoir continues to improve, though at a slow rate.

DEDICATION

This thesis is dedicated to my family,

who has loved, supported, and encouraged me all my life.

ACKNOWLEDGEMENTS

I would like to express my deepest appreciation and gratitude to my academic and thesis advisor, Dr. Adil Godrej, for providing me the opportunity to work on this research project and for his continuous support, mentorship, and scientific contributions that made possible the completion of this work. I would also like to express my deepest gratitude to my other advisory committee members, Dr. John Little and Dr. John Novak, for their valuable time, guidance, and feedback.

I would like to thank the Occoquan Program sponsors: Fairfax Water, Fairfax County, Fauquier County, Loudoun County, Prince William County, City of Manassas, and City of Manassas Park, for their financial support.

I am extremely grateful to Harry Post for his patience and collaboration throughout the data analysis process. Special thanks to Dr. Megan Rippy for her guidance on statistical methods. I would like to extend my gratitude to all the laboratory and field staff who were responsible for collecting the water quality data used in this thesis. Thank you, also, to the administrative staff who assisted me throughout the entire program.

To my Occoquan Watershed Monitoring Laboratory friends and classmates, thank for your support and friendship which made my academic experience worthwhile. Especially, I would like to thank Barbara and Robert Angelotti, Ayden Baran, Shantanu Bhide, Amelia Flanery, the Lodhi family, and Parita Shah for your friendship and advice during the completion of this project, as well as, other academic and social activities.

Finally, I would like to thank my parents, María and Jose Cubas, and my siblings, Diana and Francisco Cubas for their help, motivation, and support throughout the entire academic process. Thank you for teaching me about faith and inspiring me to pursue this degree. To all my friends who have been part of this journey for always being there, I treasure having you in my life.

TABLE OF CONTENTS

LIST OF FIGURES

LIST OF TABLES

LIST OF ABBREVIATIONS AND ACRONYMS

COD	Chemical Oxygen Demand
CSTR	Continuously-Stirred Tank Reactor
CWA	Clean Water Act
DEHP	Diethylhexyl phthalate / Bis(2-ethylhexyl) phthalate
DO	Dissolved Oxygen
DOC	Dissolved Organic Carbon
EPA	(U.S.) Environmental Protection Agency (also USEPA)
GPS	Global Positioning System
ILEC	International Lake Environment Committee
MBAS	Methylene Blue Active Substances
MCL	Maximum Contaminant Level
MCLG	Maximum Contaminant Level Goal
MHR WRF	Millard H. Robbins, Jr. Water Reclamation Facility (operated by UOSA)
N:P ratio	Nitrogen to Phosphorus ratio
NH3-N	Ammonia nitrogen
NVRC	Northern Virginia Regional Commission
OECD	Organization for Economic Cooperation and Development
OP	Orthophosphate Phosphorus
ORP	Oxidation-Reduction Potential
OWML	Occoquan Watershed Monitoring Laboratory
OWMP	Occoquan Watershed Monitoring Program
OWMS	Occoquan Watershed Monitoring Subcommittee
Ox-N	Oxidized Nitrogen
PAHs	Polycyclic Aromatic Hydrocarbons
PCA	Principal Component Analysis
PFAS	Per- and Poly- Fluorinated Alkyl Substances
PFOA	Perfluorooctanoic Acid
PFOS	Perfluorooctanesulfonate Acid
POTWs	Publicly-Owned Treatment Works
SMCL	Secondary Maximum Contaminant Level
SOCs	Synthetic Organic Compounds
TDS	Total Dissolved Solids
TKN	Total Kjeldahl Nitrogen
TN	Total Nitrogen
TOC	Total Organic Carbon
TP	Total Phosphorus
TSI	Trophic State Index
TSS	Total Suspended Solids
UNEP	United Nations Environment Programme

UOSA	Upper Occoquan Service Authority
USEPA	United States Environmental Protection Agency (also EPA)
VDEQ	Virginia Department of Environmental Quality
VPDES	Virginia Pollutant Discharge Elimination System
VSWCB	Virginia State Water Control Board (board under VDEQ)
WRF	Water Reclamation Facility

CHAPTER 1. INTRODUCTION

1.1 Overview

The Occoquan Reservoir is part of the largest indirect potable reuse systems in the United States. Indirect potable reuse refers to the planned discharge of reclaimed water into a water supply source, such as a reservoir or lake. After the reclaimed water is discharged into the receiving waterbody, water is withdrawn and treated to be used for drinking and other potable water purposes (Virginia State Water Control Board [VSWCB], 2008). In this system, highly treated water from the Millard H. Robbins, Jr. Water Reclamation Facility (MHR WRF) in Centreville, Virginia, is discharged into one of the tributaries of the Occoquan Reservoir. Water from the reservoir is withdrawn by Fairfax Water at its Griffiths Treatment Plant at Lorton, Virginia, and distributed for potable uses. In addition to being used as water supply source, the Occoquan Reservoir serves as an ecological habitat and recreational area. Furthermore, the Occoquan Reservoir is important because it protects the water quality of the Chesapeake Bay by acting as a trap for sediments and pollutants.

Due to the importance of the Occoquan Reservoir, it is key to protect and monitor its water quality. The Occoquan Watershed Monitoring Laboratory (OWML) has been in charge of collecting water quality data of the Occoquan Reservoir and Watershed. This document provides an assessment of this water quality data from 1973 to 2019. This assessment is an update to an earlier report published in 2003 (Van Den Bos, 2003), and in many cases focuses on the 2003–2019 period. It includes an analysis of the hydrometeorological and morphometric conditions of the reservoir and watershed; an analysis of long-term trends for different parameters that affect water quality including nutrients, principal ions and metals, and synthetic organic compounds; and an evaluation of the current trophic state of the reservoir.

1.2 Study Area

1.2.1 Watershed Description

The Occoquan Watershed is a 570 square mile (mi^2) basin located in Northern Virginia, United States of America. It encompasses parts of four (4) counties and the total area of two (2) cities: Fairfax County, Fauquier County, Loudoun County, Prince William County, City of Manassas, and City of Manassas Park. Figure 1-1 shows the watershed boundary and Figure 1-2 details the Occoquan Watershed land area distribution by political subdivision (Northern Virginia Regional Commission [NVRC], 2008). Located in the Occoquan Watershed are three major impoundments: Lake Jackson, Lake Manassas, and the Occoquan Reservoir. The Occoquan Reservoir, on which this assessment is focused, is one of the principal water sources for Fairfax Water, the main water purveyor for the area, supplying water to nearly two million people. The reservoir was formed with the construction of a high dam at the mouth of the Occoquan River, about eight (8) miles (Van Den Bos, 2003) before it enters the Potomac River, a tributary of the Chesapeake Bay. The Occoquan Reservoir has two (2) main tributaries: Occoquan Creek, which drains a primarily agricultural area (343 mi^2), and Bull Run, which drains an urbanizing area (185 mi^2). The remaining watershed area (42 mi^2) is drained by small tributaries of the Occoquan Reservoir located in Fairfax and Prince William Counties. The other two impoundments, Lake Manassas and

Lake Jackson, are located on the Occoquan Creek arm of the watershed. Lake Manassas serves as water supply source for the City of Manassas and Lake Jackson serves as a recreational area. These impoundments contribute to the reduction of pollutant loads coming into the Occoquan Reservoir (OWML, 1998).

Based on its geomorphological characteristics, the Occoquan Watershed mainly lies in the physiographic region of the Piedmont Province. This region is bounded by the Blue Ridge Mountains on the west side and by the Fall Line (a natural border between the Piedmont Region and Coastal Plains) on the east side. The topography of the Piedmont Province is gentle rolling with scattered peaks. It slopes gradually from approximately 200 to 300 feet above mean sea level (ft. msl) in the eastern side to approximately 800 to 900 ft. msl on the western side, becoming more rugged as it reaches the Blue Ridge mountains (NSTATE, 2016). The Piedmont Province has deeply weathered bedrock, mainly composed of crystalline igneous and metamorphic rocks, with some areas of sedimentary rocks (Triassic areas). The bedrock is generally buried under a thick blanket of saprolite (chemically weathered rocks). Parent material rocks for this region are mainly gneiss, schist, and granite. This region has thick soils, which tend to be acidic and infertile (but respond well to liming and fertilization), with sandy loam surfaces; and some subsoils are red or yellowish red because of the oxidation of iron during weathering of primary minerals (Virginia Cooperative Extension, 2000).

The Occoquan Watershed supports different land uses, as it is shown in Table 1-1. However, it can be observed that even though the watershed has become more urban throughout the years, rural uses such as agriculture (low and high tillage), pasture, and forest constituted a higher percentage (73%) of total land uses during 2010. The remaining 27% of the watershed area was distributed among urban uses that include residential, industrial, and institutional uses.

Table 1-1. Occoquan Watershed Land Use (2010) (Source: NVRC)

Land Use Category	**Watershed Area**			
	Pervious (acres)	*Impervious (acres)*	*Total Area (acres)*	*Percentage (%)*
Low Density Residential	43,314.05	4,812.67	48,126.72	13.0%
Medium Density Residential	19,781.88	4,945.47	24,727.35	6.7%
Townhouse/Garden Apt	4,953.47	2,667.25	7,620.73	2.1%
Industrial	7,185.07	7,185.07	14,370.14	3.9%
Institutional	3,421.32	1,842.25	5,263.58	1.4%
Low Tillage	22,460.45	458.38	22,918.83	6.2%
High Tillage	19,063.04	389.04	19,452.08	5.2%
Pasture	23,744.37	239.84	23,984.21	6.5%
Forested	202,208.05	2,042.51	204,250.56	55.1%
Total	**346,131.71**	**24,582.48**	**370,714.19**	**100.0%**

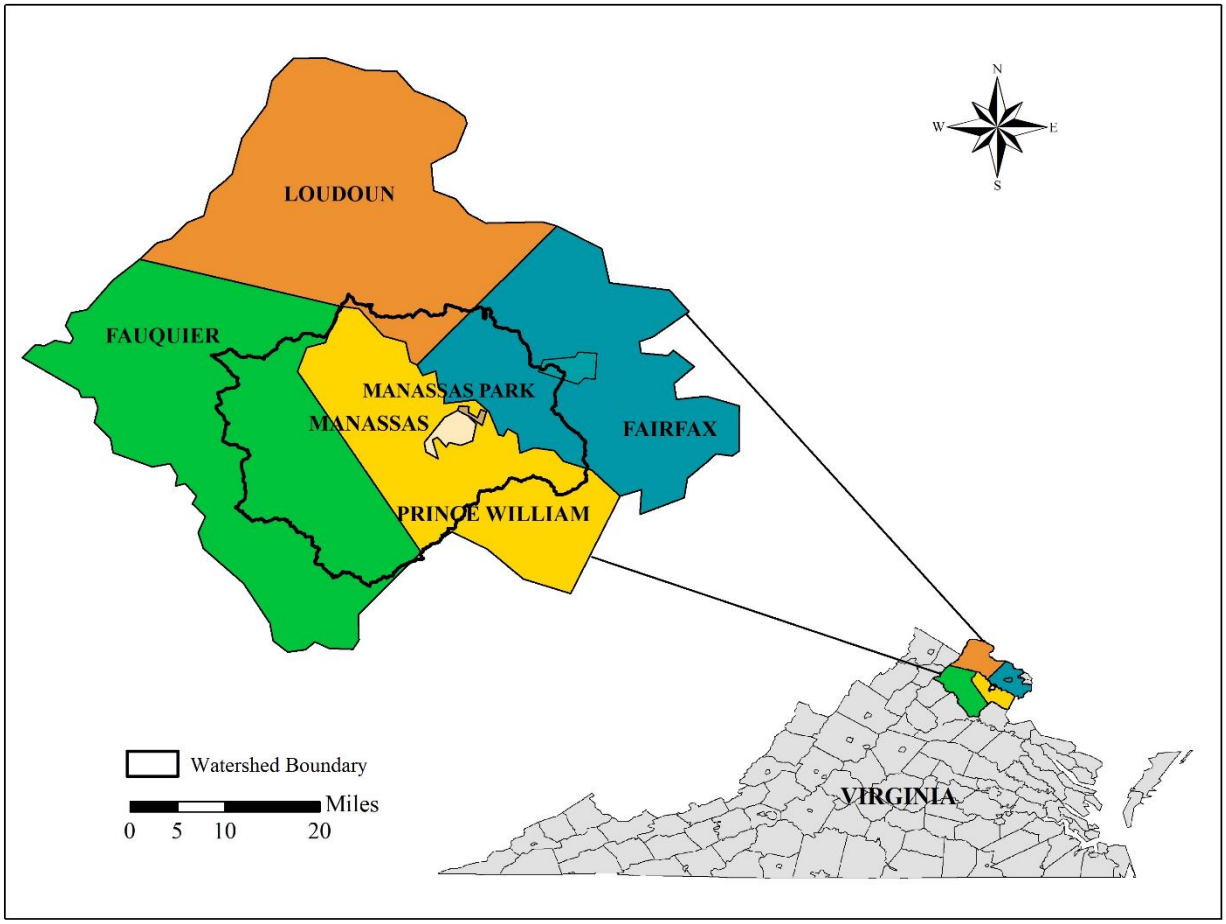

Figure 1-1. Map of the Occoquan Watershed

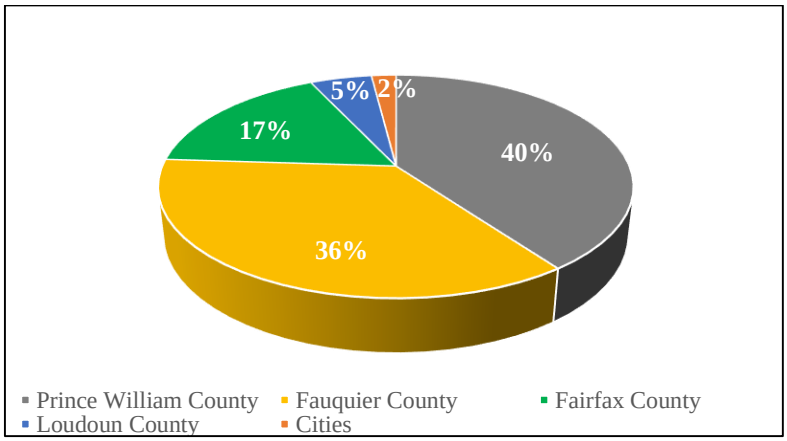

Figure 1-2. Land Area Percentage in the Occoquan Watershed by Political Subdivision (Source: NVRC)

1.2.2 History

The Occoquan Watershed was first used as a public water source for the Northern Virginia area by the Alexandria Water Company in 1950, when a low dam was built on the Occoquan River to meet the demands of the growing population. In 1957, this low head dam was replaced by the construction of a high dam which impounded the Occoquan Reservoir with an estimated storage capacity of approximately 10 billion gallons (at the time) (OWML, 1998). In 1967, Fairfax Water (formerly known as Fairfax Water County Authority) became the owner of the reservoir and the associated facilities, and currently continues to operate the system.

As a consequence of population growth, the urbanization of rural areas in the watershed, and increased agricultural activity in the western side of the basin, the Occoquan Reservoir started to present high eutrophic conditions, including massive algal blooms (mainly cyanobacteria), hypolimnetic oxygen depletion, periodic fish kills, and drinking water treatment issues, such as, taste and odor problems, and shortened filter runs. To develop a watershed management plan and help improve water quality conditions, the Virginia State Water Control Board (VSWCB) ordered an assessment of the Occoquan Reservoir and streams. This study indicated that the main cause of the eutrophication problems was the wastewater discharge from eleven publicly owned treatment works (POTWs) located in the watershed (Metcalf and Eddy, Inc., 1970). These POTWs were discharging approximately three million gallons (MGD) of secondary-treated into the reservoir, with no provisions for nutrient removal. In order to reduce the contribution of algal nutrients reaching the Occoquan Reservoir, the study recommended the implementation of one of the three (3) following alternatives:

1) Export wastewaters for treatment outside the Occoquan Watershed.
2) Provide highest treatment technically achievable; contract with local jurisdictions to purchase reclaimed water for drinking water; and limit watershed population to that which would use reclaimed water.
3) Provide highest treatment technically achievable; discharge reclaimed water to the Occoquan Watershed; and limit basin population to 100,000.

In 1971, after consideration of the options proposed in the Metcalf and Eddy study, the VSWCB adopted a modification (without the limitation on the basin population, and limiting the advanced wastewater treatment plants to no more than three, but preferably two) of the third recommendation to control point source pollution. The management plan described in “A Policy for Waste Treatment and Water Quality Management in the Occoquan Watershed” (also known as the *Occoquan Policy* §9VAC25) indicated that the Occoquan Reservoir would operate as an indirect potable water reuse system, mandated the construction of a high-performance wastewater treatment plant to replace the separate existing 11 POTWs, and required the establishment of an independent entity to continuously monitor and evaluate water quality. The Occoquan Watershed Monitoring Program (OWMP), was established by the *Policy* is executed by the OWML

1.2.3 Upper Occoquan Service Authority

In response to the mandate of the Occoquan Policy, the Upper Occoquan Sewage Authority (now called the Upper Occoquan Service Authority, or UOSA) was established to serve the four (4) jurisdictions of Fairfax County, Prince William County, City of Manassas, and City of Manassas Park. The water reclamation facility (WRF) operated by UOSA, named the Millard H. Robbins, Jr. Water Reclamation Facility (MHR WRF), was designed to have advance wastewater treatment that would provide highly reliable and efficient removal of organic matter, nutrients, potentially toxic organic compounds, and pathogens. Additionally, the plant was designed with redundancy in capacity, units, and power supplies.

Construction of MHR WRF started in 1974 and it came into operation in 1978, replacing the 11 POTWs that were providing secondary wastewater treatment at the time. MHR WRF began operations with a capacity of 10 MGD (UOSA, 2020). However, through several expansions over the years, the plant has increased its treatment capacity to 54 MGD. The treated effluent from the MHR WRF is discharged into Bull Run about 20 miles above the water supply intake at the Occoquan Reservoir (Van Den Bos, 2003). The establishment of this WRF has been crucial in the reduction of pollutant loads into the reservoir and maintaining its water quality.

The MHR WRF's treatment process includes preliminary and primary treatment of wastewater followed by an activated sludge process which operates in nitrifying mode but can accommodate for stand-by biological nitrogen removal. Afterwards, wastewater undergoes an advanced wastewater treatment process that includes lime precipitation to reduce phosphorus, recarbonation process in which pH is lowered (done in two stages and includes a settling step), multimedia filtration with granular activated carbon adsorption, post carbon filtration, and disinfection process (chlorination and dechlorination). The resulting sludge passes through sludge screens, anaerobic digesters, sludge blending, centrifuge dewatering, and drying steps so that the finished product can be used as fertilizer (UOSA, 2020).

Apart from the MHR WRF, the only other facility currently discharging in the watershed, is the Vint Hill Farms Station Wastewater Treatment Plant. Flow from this plant, however, has not exceeded 0.31 mgd (about 1% of the MHR WRF average daily flow). Another WRF that was present during the period analyzed (1973 to 2019) was the Nokesville Sewage Treatment Plant. However, the flow from this plant this plant did not exceed 0.06 mgd and it closed in July 2002.

1.2.4 Occoquan Watershed Monitoring Program

1.2.4.1 Overview

Following the Occoquan Policy mandate, the Occoquan Watershed Monitoring Subcommittee (OWMS) created the OWMP to quantify and evaluate the results of strategies implemented to protect the water quality of the reservoir and watershed. The OWMS was given the authority to create an independent facility to conduct the required monitoring program, using funds contributed by the wastewater generators and the finished water supply company (counties, cities, Fairfax Water).

This independent facility, the OWML, was established by the Department of Civil and Environmental Engineering of the Virginia Polytechnic Institute and State University in 1972. Since then, the OWML has maintained and monitored several stream and reservoir stations, as well as rain gauges located throughout the watershed (presented in Chapter 3). Water quality data obtained from these stations have been key for evaluating the suitability of indirect potable water reuse and in assisting watershed management in the decision-making process.

1.2.4.2 Stream Monitoring Stations

The OWML currently monitors eight (8) stream stations distributed throughout the Occoquan Watershed (Figure 1-3). Since the Occoquan Watershed is drained by different streams that are tributary to the Occoquan Reservoir, it is important to monitor stream water quality to be able to evaluate the effects of wastewater discharges and runoff into the reservoir. Flow and water chemistry data are maintained for each of the monitoring stations. Data collected for the stream stations are divided into either baseflow or stormflow data. During spring, summer, and fall, baseflow sampling is performed every week, while in winter it is done every two weeks. OWML field crew members take onsite measurements of stream conditions (such as temperature, pH, dissolved oxygen) and collect water grab samples which are taken to laboratory for chemical analysis. Stormflow samples are collected with automatic equipment located at stream stations (flow-weighted samples). All results are recorded in the central FoxPro database. All this information is important to determine the fluxes of nutrients and contaminants flowing into the reservoir, and the reservoir's hydrologic budget.

The criteria used to select the gauging stations and the installation process was described in a previous water quality assessment (OWML, 1993). The location of each station, distance from the dam, and drainage area are presented in Table 1-2. ST01 is located at the dam and was established to measure outflows from the Occoquan Reservoir. ST10 is used to estimate flows and loads going into the reservoir from the Occoquan Creek arm, and ST45 is used for the Bull Run tributary stream. Since some stream monitoring stations have been removed or relocated throughout the years, ST25 and ST30 have also been used to estimate values for the Occoquan Creek and ST40 has been used for Bull Run. Lastly, ST70 is used to estimate the flows and loads from Broad Run into Lake Manassas.

Table 1-3 shows the average flow (ft^3/s) for each station during the specified period of record. It should be noted that ST45 includes the flow from the MHR WRF, thus making the ST45 and ST01 areal average flow higher. All stations included in this table continuously monitor flow up to the present date.

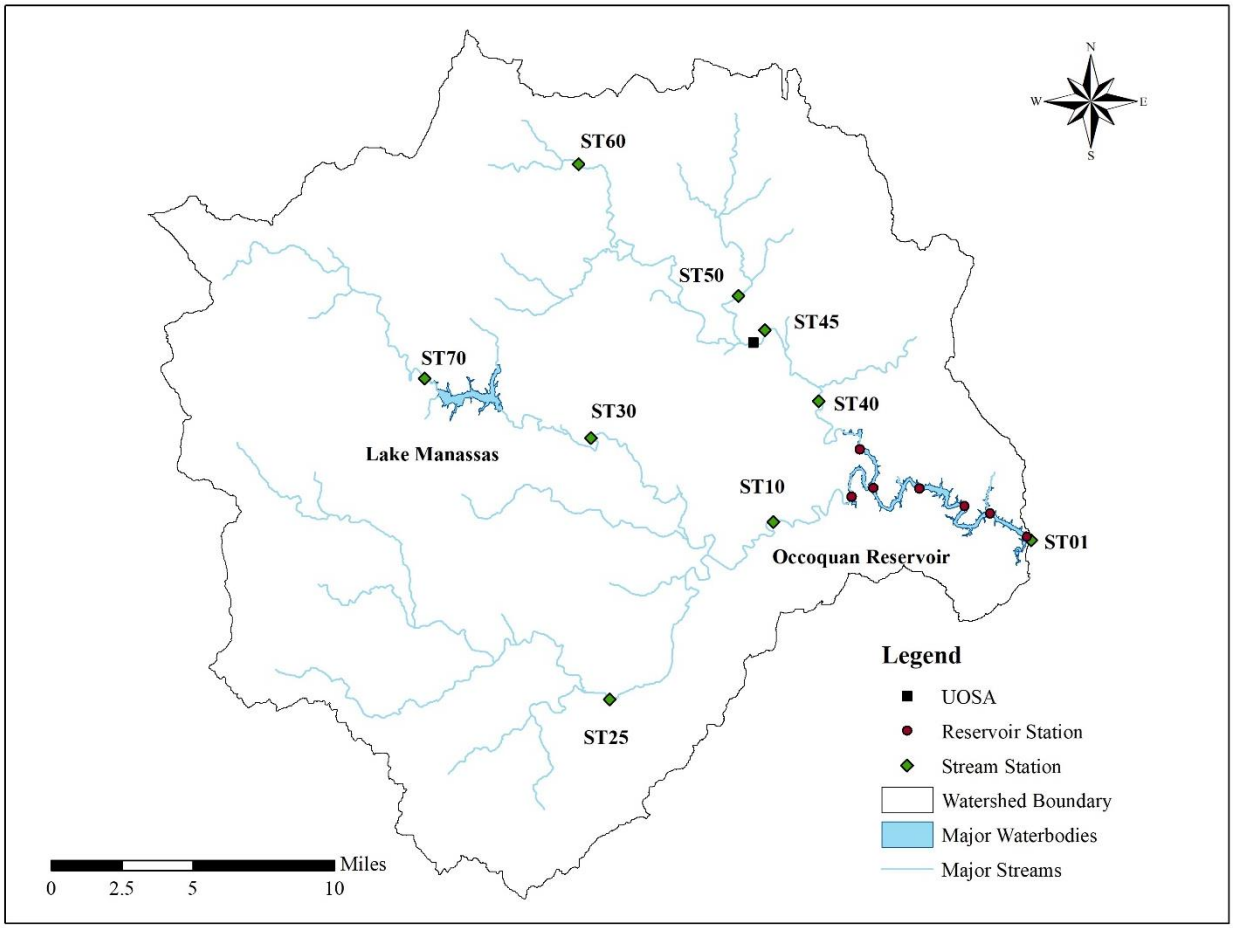

Figure 1-3. Occoquan Watershed Stream Stations

Table 1-2. Current Occoquan Watershed Stream Monitoring Stations

Station ID	Station Name	Latitude	Longitude	Distance Above Dam (mi)	Drainage Area (mi^2)
ST01	Reservoir Outlet at Occoquan Dam	38º41.636' N	77º16.637' W	0.0	570
ST10	Occoquan River near Manassas, VA	38º42.310' N	77º26.729' W	16.0	343
ST25	Cedar Run near Aden, VA	38º36.905' N	77º33.223' W	28.8	155
ST30	Broad Run near Bristow, VA	38º44.933' N	77º33.853' W	29.1	89.6
ST45	Bull Run near Manassas Park, VA	38º48.187' N	77º26.977' W	18.6	149
ST50	Cub Run near Bull Run, VA	38º49.258' N	77º27.997' W	21.8	49.9
ST60	Bull Run near Catharpin, VA	38º53.356' N	77º34.223' W	31.2	25.8
ST70	Broad Run near Buckland, VA	38º46.822' N	77º40.356' W	37.3	50.5

Table 1-3. Summary of Discharge Statistics at Occoquan Watershed Stream Monitoring Stations (includes MHR WRF discharge upstream of ST45)

Item	ST01	ST10	ST25	ST30	ST45	ST50	ST60	ST70
Start Date	1/82	12/05	10/72	10/74	11/84	10/72	5/69	10/50
End Date	11/19	11/19	11/19	11/19	11/19	11/19	11/19	11/19
Drainage Area (mi^2)	570	343	155	89.6	149	49.9	25.8	50.5
Average Flow (cfs)	712.63	376.89	163.85	83.58	224.54	60.67	26.56	54.73
Areal Average Flow (cfs/mi^2)	1.25	1.10	1.06	0.93	1.51	1.22	1.03	1.08

1.2.4.3 Reservoir Monitoring Stations

Currently, the OWML maintains seven (7) reservoir monitoring stations (Figure 1-4) and their location and distance from the dam are specified in Table 1-4. At these stations, profile measurements are taken for temperature, dissolved oxygen (DO), pH, oxidation-reduction potential (ORP), conductivity, and nitrate during site visits. Secchi depth and surface and bottom alkalinity are also measured onsite. Surface and bottom water samples are retrieved for laboratory analysis of other constituents such as nitrogen, phosphorus, organic carbon, chlorophyll-*a*, metals and synthetic organic compounds (SOCs). These samples are collected every week, except during extreme winter conditions, in which they are collected once a month or suspended, as appropriate. Metals and SOC sampling is quarterly.

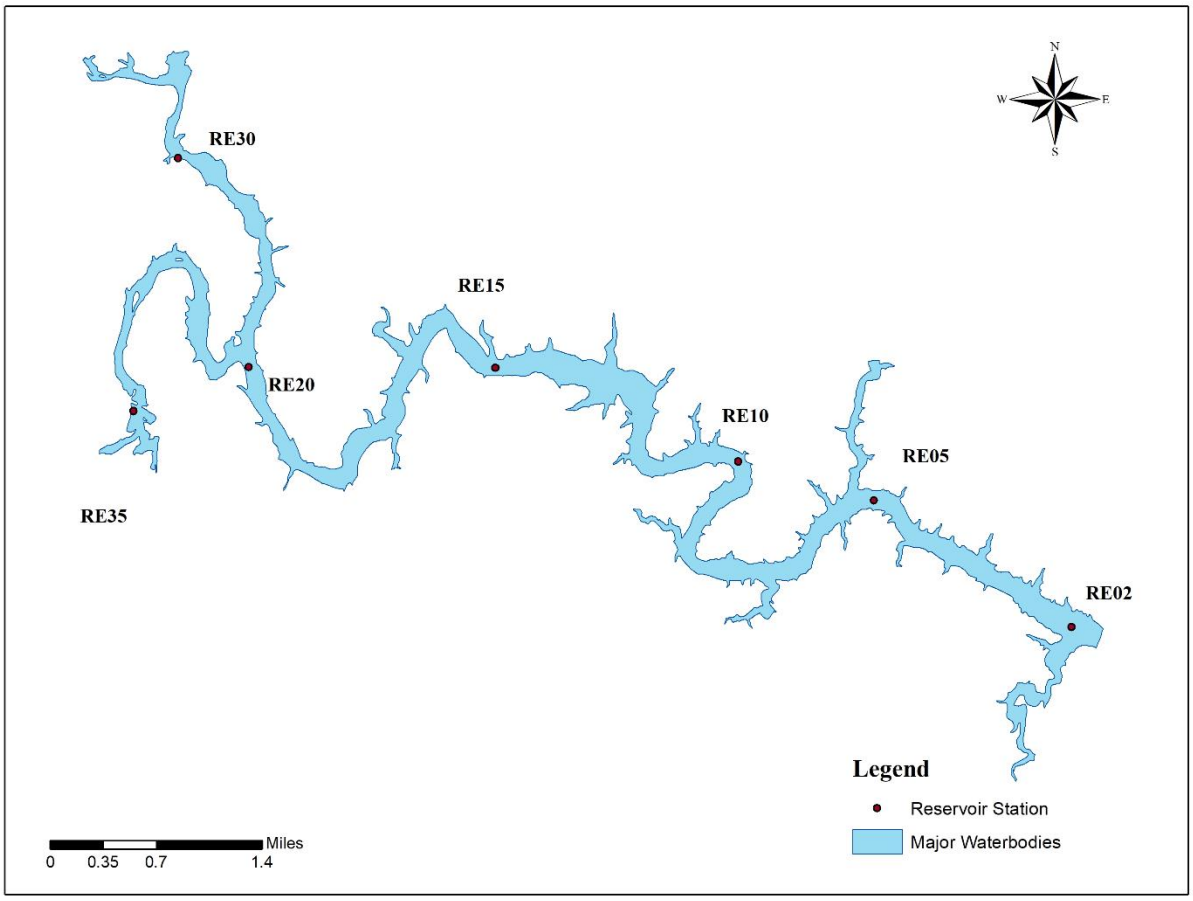

Figure 1-4. Map of the Occoquan Reservoir Monitoring Stations

Table 1-4. Current Occoquan Reservoir Monitoring Stations

Station ID	Station Name	Latitude	Longitude	Distance Above Dam (mi)
RE02	Occoquan Reservoir near Occoquan Dam	38º41.776' N	77º16.973' W	0.3
RE05	Occoquan Reservoir below Sandy Run	38º42.465' N	77º18.349' W	1.8
RE10	Occoquan Reservoir at Jacob's Rock	38º42.713' N	77º19.223' W	4.0
RE15	Occoquan Reservoir at Ryons Dam	38º43.271' N	77º21.077' W	6.1
RE20	Occoquan Reservoir below confluence	38º43.160' N	77º22.740' W	7.9
RE30	Occoquan Reservoir near Bull Run Marina	38º44.502' N	77º23.297' W	10.5
RE35	Occoquan Reservoir at Ravenwood Bridge	38º43.044' N	77º23.647' W	11.2

1.2.5 Fairfax Water

Fairfax Water (previously known as the Fairfax County Water Authority) is the main water purveyor for the Northern Virginia area and the owner of the Occoquan Reservoir. Water supplied by Fairfax Water is treated at four different locations. Two (2) of these water treatment plants are also owned and operated by Fairfax Water: James J. Corbalis Jr. treatment plant and Frederick P. Griffith Jr. treatment plant. The remaining water supplied by Fairfax Water is purchased from the McMillian and Dalecarlia plants, located in Washington DC. Fairfax Water serves nearly 2 million residents (Fairfax Water, 2020).

The James J. Corbalis Jr. Water Treatment Plant is located on the northern side of Fairfax County (near Herndon). This water treatment plant has a capacity of 225 MGD and draws water from the Potomac River. The plant opened in 1982 and was expanded and upgraded in 2008. Renovations included upgrading of the control, electrical, and ozone generation and application systems (Prince William County Service Authority [PWCSA], 2020).

The Frederick P. Griffith Jr. Water Treatment Plant is located on the southern side of Fairfax County (in Lorton). This water treatment plant draws water from the Occoquan Reservoir and can treat 120 MGD. The Griffith plant began operations in 2006, and was built to meet the Stage II Disinfection By-Product Rule implemented by the U.S. Environmental Protection Agency (USEPA), replacing three older facilities. In order to comply with this USEPA regulation, the plant incorporates ozone disinfection and granulated activated carbon filtering to remove disinfection by-product precursors, thus decreasing the possibility of formation of disinfection by-products (PWCSA, 2020).

Both the Corbalis and Griffith plants were designed so that they could be expanded if water demand increases, without interrupted service. The general water treatment process these plants follow is: coagulation and flocculation, in which chemicals are added to cause fine particles to adhere with each other and form large ‘flocs’; sedimentation, a step in which the previously formed flocs settle into the bottom of a basin and are cleared away; ozonation, where ozone is added to reduce organic material and odors; filtration, where water is passed through sand and activated carbon to remove fine particles and certain chemicals; and disinfection, a step in which chlorine is added to remove pathogens. Corrosion inhibitors are also added to prevent lead and copper from leaching into the treated water as it passes through the distribution system. Fluoride is added to the finished for teeth protection. To improve taste and odor, addition of powdered activated carbon and potassium permanganate may also be included in the treatment process (Fairfax Water, 2019).

1.2.6 Water Quality Management

Since the creation of the Occoquan Policy and establishment of the MHR WRF and the OWML, water quality conditions at the Occoquan Reservoir have improved due to regular water quality monitoring, advance wastewater treatment, and land use management. These strategies have helped reduce nutrient loads into the reservoir that caused the highly eutrophic conditions experience in the 1960s. Over the years, other management strategies have been implemented to protect the Occoquan Reservoir’s water quality and its use as a public water source, mainly by

targeting internal nutrient loading. Because the Occoquan Reservoir's productivity is mainly limited by phosphorus (Metcalf and Eddy, Inc., 1970), these strategies have focused on reducing phosphorus release from the sediments.

One of the strategies implemented at the Occoquan Reservoir is the discharge of highly nitrified effluent from the MHR WRF into the reservoir during periods of thermal stratification (summer season). When the reservoir is thermally stratified oxygen gets depleted in the hypolimnion, causing reducing conditions and phosphorus release from the sediments. The presence of nitrate in the reservoir bottom waters is useful because it keeps oxidized conditions and prevents phosphorus release. Oxidized conditions also prevent the release of other undesirable substances such as iron and ammonia. Since the MHR WRF's activated sludge basins are designed to promote complete nitrification, the effluent discharged into the reservoir serves as a source of nitrates during this period. When the nitrate-rich Bull Run inflow enters the mainstem of the Reservoir at its confluence with the Occoquan Creek arm, the waters in Bull Run are cooler (and denser) than the surface waters in the mainstem. Therefore, much of the Bull Run flow 'dives' into the hypolimnion (cooler bottom waters during summertime), where the oxidized nitrogen is needed during summer after deoxygenation. A much smaller fraction of the Bull Run flow enters the epilimnion (water top layer waters) and is diluted by other flow, hence keeping the nitrate concentration low.

The other strategy implemented to keep oxidized conditions in the reservoir was the installation of a hypolimnetic oxygenation system in 2012 by Fairfax Water. This system replaced a previously existing destratification aeration system. The goal of the new system is to keep the bottom waters aerated rather than to break stratification as the previous system did. Fairfax Water also applied copper sulfate to the reservoir (up until 2011) to control algae (caused by excessive nutrients) which may be toxic and may be problematic to the water treatment process.

1.3 Objectives

The goal of this study is to assess how current water quality management strategies implemented in the reservoir have affected the water quality in the Reservoir from 1973 to 2019, focused on the years (2003–2019) since the previous water quality assessment of 2003.

The objectives of this assessment are to:

1) Evaluate the current water quality of the reservoir by determining long-term trends of important water quality parameters.
2) Assess how the nitrate management strategy and the installation of the hypolimnetic oxygenation system in the reservoir has further improved reservoir water quality.
3) Determine the trophic state of the Occoquan Reservoir.
4) Determine any areas of emerging concern.

CHAPTER 2. LITERATURE REVIEW

Freshwater bodies such as lakes and reservoirs are important ecosystems that enhance the quality of life of people by supplying drinking water, food, fiber, medicine, and energy (USEPA, 2009a). Lakes/reservoirs also provide water for agriculture and industrial activities, serve as recreational areas, and constitute an important habitat for wildlife. In addition, lakes and reservoirs can act as important sinks for pollutants, reducing transport of contaminants to downstream coastal marine environments. For instance, Harrison et al. (2009) showed that lentic systems are important sinks for nitrogen because it can get buried in sediments or may be denitrified. In their study, they estimated lentic waters removed approximately one third of the nitrogen estimated to enter surface freshwaters. Reservoirs, in particular, accounted for 33% of the nitrogen removed. Maavara et al. (2015) studied phosphorus retention in reservoirs and estimated a retention of 12% of the global river phosphorus load in 2000 and predicted a 17% retention by 2030. Reservoirs have been also shown to be possible sinks for organic carbon that is transported from rivers to oceans (Mulholland and Elwood, 1982; Phyoe and Wang, 2019).

The ecosystem services lake and reservoirs are able to provide can vary depending on many factors such as meteorological conditions, morphometry, geography/geomorphology, and watershed characteristics. These factors influence the hydrologic and chemical characteristics of the waterbody, which consequently affect the composition of biological communities and water quality.

2.1 Meteorology, Morphometry, Geography

Meteorological conditions, including precipitation, temperature, wind, solar radiation, humidity, and snowmelt, affect water levels and internal chemical and biological processes occurring in lakes/reservoirs. Climate variables, particularly precipitation and temperature, are important because they determine timing and magnitude of runoff. Nutrient runoff, warmer temperatures, and intense storm events have been observed to exacerbate algal growth (Salas and Subburayalu, 2019). Temperature and morphometric characteristics also influence the distribution of algal blooms. For example, nuisance algae (cyanobacteria) favor temperatures greater than 15°C (Paerl et al., 2001). In addition, water temperature affects other water quality parameters such as pH, oxygen demand and solubility, and concentrations of nitrogen, phosphorus, chlorophyll-*a*, and metals (Yang et al., 2017).

One important phenomenon that affects water chemistry and is influenced by climatic and morphometric variables is thermal stratification. Thermal stratification occurs in lakes/reservoirs of moderate or high depths (usually greater than 6 meters). Temperature at the surface becomes warmer than temperature at the bottom due to solar radiation and insufficient wind force (Wetzel, 2001). Because water density depends on temperature (decreases with increasing temperature after reaching its maximum value at 4ºC), a density gradient forms, diving the water column into three distinct layers or zones. The upper zone, called the epilimnion, is warmer, less dense, usually more turbulent, and has abundant oxygen because it is in contact with the atmosphere. The middle layer, called the metalimnion, is the transition zone between the surface and bottom waters where temperature change is most rapid as a function of depth. And the deepest layer is the hypolimnion,

which has no contact with the atmosphere. Due to the lack of contact with the atmosphere and lack of oxygen circulation from the epilimnion (because of the density gradient), oxygen at the hypolimnion can get depleted. Oxygen depletion can affect water chemistry because it causes reducing conditions, which promote the release of constituents including phosphorus, ammonia, iron, and manganese from sediments, thus degrading water quality. Noor Halini et al. (2011) study of the effects of thermal stratification on a reservoir, for example, found that DO decreased significantly with depth, and iron and manganese concentrations were highest during the strongest period of stratification. As the weather changes from warmer to cooler months, the surface water begins to cool and density differences in the water column reduce, making it easier for currents caused by wind or storm events to mix the entire water column (called the overturn).

Morphometric characteristics (e.g., size, shape, depth) of a lake/reservoir provide information regarding storage capacity, stratification and mixing patterns, and sedimentation and flushing rates. The mean depth of a lake is related to how productive that lake is (Vollenweider, 1975). Additionally, the depth of a lake and its water temperature determine hypolimnion thickness during thermal stratification. Hypolimnetic thickness influences oxygen consumption rates in bottom waters during stratification (Charlton, 1980). The morphometric characteristics of a lake and watershed, as well as the geographical and meteorological (particularly precipitation) conditions, influence residence times. The residence time of a lake/reservoir controls the concentrations and accumulative capacity of contaminants entering the waterbody (Ambrosetti et al., 2003).

Morphometry, namely mean depth, and temperature have been observed to affect eutrophication (excess nutrients) and lake restoration efficiency. Genkai-Kato and Carpenter (2005) studied lake susceptibility to regime shifts (i.e., clear water state to high turbidity changes). They concluded that eutrophication tends to occur more in warmer temperatures and that efforts to restore a waterbody were less likely to be successful because of higher internal phosphorus loading from sediments. Additionally, they observed that lakes with intermediate mean depths (approximately 10 meters) were most susceptible to changes and least restorable.

Geographic characteristics, such as topography and soil type, influence the form, toxicity, and mobility of pollutants (i.e., if contaminants are dissolved, adsorbed, or precipitated) (Durães et al., 2018). Characteristics such as soil permeability, temperature, moisture, and land slopes, may increase or decrease contaminant transport rates. Areas with highly permeable soils may absorb contaminants readily and divert them to the subsurface. In the case of nitrogen transport, studies have shown that nitrate is less likely to leach from soils with high clay content. On the contrary, soils with high sand content tend to present more nitrate leaching (Donner et al., 2004). Soil temperature and moisture have direct effects on nitrogen mineralization, nitrification, and denitrification (Lupon et al., 2015; Seitzinger, 1988). A study on the delivery of nutrients to streams indicated temperature, soil permeability, and stream density (ratio of stream length to drainage area) as variables with significant influence on land-water delivery of nitrogen to streams (Smith et al., 1997). Phosphorus delivery to streams was significantly influenced only by soil permeability and stream density.

Lastly, watershed characteristics, such as land use, also determine the quantity of runoff flowing into the waterbody, as well as the constituents being transported (U.S. Geological Survey [USGS],

2021). Land use changes, such as changes in crop cover and fertilizer application, have been demonstrated to influence nutrient cycling (Donner et al., 2004). Urbanization has increased contaminant transport to aquatic systems due to larger volumes of wastewater discharges and increased impervious areas. Impervious surface areas result in higher contaminant transport because they increase runoff rates and reduce infiltration capacity (Salas and Subburayalu, 2019).

2.2 Eutrophication and Nutrient Sources

One of the water quality problems that rivers, lakes and reservoirs, estuaries, and coastal oceans face is eutrophication. Eutrophication is the overenrichment of a waterbody with nutrients, organic matter, and sediments, thus increasing primary productivity (Lewtas et al., 2015). Eutrophication is characterized by the proliferation of algal blooms, which leads to water quality and ecosystem degradation including effects such as high turbidity, unpleasant tastes and odors, oxygen depletion in bottom waters, fish kills, food web alterations, and biodiversity loss (Paerl et al., 2001). Additionally, some algae, such as certain species of blue-green algae or cyanobacteria, are toxic and pose a health hazard. Cyanobacteria blooms have been linked to animal (Carmichael, 1994), and human poisoning (Hawkins et al., 1985; Yuan et al., 2006).

Eutrophication has affected many waterbodies worldwide. A survey of the state of lakes and reservoirs around the world (1988–1993) prepared by the International Lake Environment Committee (ILEC) in collaboration with the United Nations Environment Programme (UNEP) estimated that 48% of 61 lakes studied in North America were eutrophic (Matsui et al., 1995). Additionally, the USEPA 2012 survey of lakes in the United States indicated 40% of lakes studied had excessive phosphorus levels and 35% had excessive levels of nitrogen (USEPA, 2016a). Estuaries that have been affected by nutrient enrichment, seasonal algal blooms, and low DO concentrations include the Chesapeake Bay, Long Island Sound, and other smaller estuaries (Trench et al., 2012).

Eutrophication can be classified as natural or cultural. Natural eutrophication is the slow, aging process that lakes/reservoirs undergo which constitutes an increase in nutrients and sediments. Natural eutrophication can also occur when the waterbody is located in an area with naturally nutrient rich soils (Lewtas et al., 2015). However, this natural process may be accelerated by anthropogenic activities, a phenomenon known as cultural eutrophication. Cultural eutrophication is the primary type of eutrophication currently affecting waterbodies (Smith and Schindler, 2009). Anthropogenic activities such as changes in catchment (e.g., land use changes, clearing of forests, urbanization) result in increased point source (industrial and municipal waste discharge) and nonpoint source pollution (agricultural and urban runoff) in aquatic systems which lead to eutrophication problems (Salas and Subburayalu, 2019).

The primary nutrients influencing eutrophication are nitrogen and phosphorus (Vollenweider, 1968). Nitrogen and phosphorus are essential nutrients that can be found in aquatic systems, as they are important for plant and animal growth and survival. Nutrients can be released into the environment from natural processes such as the decomposition of plant and animal material. They can also be transported into waterbodies from several watershed sources such as agricultural runoff (e.g., fertilizer application), urban runoff, wastewater discharges (point source), and atmospheric

deposition (industrial, automotive, biogenic emissions). USEPA (2016b) mentioned agricultural runoff as the leading source affecting river and lake water quality. However, urbanization has also contributed to increasing concentrations of nitrogen and phosphorus runoff (Hobbie et al., 2017). Boyer et al. (2002), on the other hand, analyzed the contribution of atmospheric deposition, fertilizer use, food and feed, fixation in agricultural lands, and fixation in forests as nitrogen sources for 16 catchments, and mentioned atmospheric deposition as the largest source, overall. However, the relative importance of each source varied by catchment and depended strongly on land use. In addition to the previously mentioned watershed sources, internal loading of nutrients from sediments constitute an important source (Beutel, 2016; Wu et al., 2017). Lastly, for nitrogen, some autotrophic and heterotrophic bacteria are able to fix nitrogen from the atmosphere. Cyanobacteria are mostly responsible for planktonic fixation in freshwater. However, rates are only high when they represent a large portion of the total biomass (Howarth et al., 1988).

Phosphorus is considered the nutrient that limits growth in most freshwater because it is found in lower concentrations compared to other essential nutrients. Phosphorus lacks an atmospheric source that other nutrients such as nitrogen have, and can get sedimented (Grundy, 1971). In waterbodies, it can be present as organic (associated with a carbon-based molecule) or inorganic phosphorus (form that can be assimilated by plants, i.e., orthophosphate), and it can be dissolved or particulate (Wang and Wang, 2009). Specific inputs of phosphorus include erosion from rocks and minerals, runoff, point sources and recycling from sediment (Genkai-Kato and Carpenter, 2005).

2.3 Trophic State Indices and Models

Lakes/reservoirs can be assessed and classified depending on their trophic state (from the Greek word *trophe* meaning "nourishment") (Yang et al., 2008). In general terms, the trophic state concept is related to two main aspects: the nutrient input or in-lake concentrations and the productivity or biological structure of a lake (USEPA, 1979).

There are different trophic state indices (TSI) and models that have been developed to assess the productivity of a waterbody. Indices and models are useful because they provide a way to qualitatively and quantitatively describe the current and possible future conditions of waterbody to aid in management decision-making processes (USEPA, 2000b). Terms generally used to describe trophic states are oligotrophic, mesotrophic, eutrophic, and hypereutrophic. Oligotrophic refers to waterbodies that are nutrient-poor, have low primary production, low biomass, high biological diversity, and DO is present in the hypolimnion throughout stratification. Eutrophic waterbodies, on the contrary, are nutrient-rich, have high primary production and net biomass, low biological diversity, and DO tends to get depleted during stratification. Mesotrophic refers to an intermediate state between the oligotrophic and eutrophic states, and is used to describe fairly productive waterbodies. Hypereutrophic refers to an extreme eutrophic condition, with high concentrations of nutrient (usually caused by anthropogenic factors) (Bhagowati and Ahamad, 2019).

TSIs have been either based on a typological concept, where a lake can be classified into a specific group (i.e., oligotrophic, eutrophic), or a continuum concept, where the trophic state of a lake is a

gradual increase from a range of possibilities (i.e., not a distinct type but ranging from presenting general characteristics of oligotrophy to general characteristics of eutrophy) (USEPA, 1979). In addition, TSIs can be based on a single variable or multiple variables. Variables that have been used to assess trophic states include nutrients (nitrogen and phosphorus), algal chlorophyll, Secchi depth (water clarity), and DO concentration (Bhagowati and Ahamad, 2019). Examples of multivariate index are the Shannon-Brezonik TSI, which is based on seven variables, and the USEPA 1974 Index, which used a percentile-based system to rank lakes based on six variables (Brezonik, 1984). One of the arguments against single variable indices is that no single indicator can adequately describe a trophic status. On the other hand, disadvantages of multivariate indices are that it requires measurements of several variables which can be costly and time consuming, changes in a variable may be overlooked, one change may trigger changes in other variables, and it does not give information on which variable has changed (USEPA, 2000b).

Among the most used indices is one developed by Robert Carlson, which classifies the trophic state of a waterbody according to algal biomass (Carlson, 1977). Carlson used the continuum concept and a numerical scale to assess the trophic state. He related algal biomass to Secchi depth since it is affected by algal density, and then related Secchi depth to algal chlorophyll and total phosphorus through regression models. The resulting index outputs a number between 0 and 100.

Models used to determine lake productivity can generally be classified as static models or dynamic models (Bryhn and Håkanson, 2007). Static models quantify cause (i.e., nutrient input) and effect (i.e., productivity) relationships based on a steady-state assumption (constant nutrient input for a long time). Static models apply statistical approaches (usually regression) to data from lakes, without providing detailed descriptions of all the interactions within a lake. Dynamic models, on the other hand, approximate the biological, chemical, and physical processes that influence aquatic plant growth within a waterbody, including parameters such as light, temperature, nutrient loading, among others, and simulate changes over time (Bryhn and Håkanson, 2007; Rast et al., 1983; Tapp, 1978).

Among the most influential of these static models has been the Vollenweider Input-Output Model (Cheng et al., 2010). As part of a study conducted by the Organization for Economic Cooperation and Development (OECD) on eutrophication in approximately 200 waterbodies in North America, Western Europe, Australia, and Japan, Vollenweider quantified the relationship between nutrient input and lake productivity — primarily based on data from European lakes (Jones and Lee, 1982; Jones and Lee, 1986). Vollenweider's initial relationship between nutrient concentrations, nutrient loadings, and trophic states took into consideration the effects of mean depth (i.e., the greater the mean depth of the lake, the more phosphorus loading it could receive before it became eutrophic) (Jones and Lee, 1986; Vollenweider, 1968). This relationship was subsequently modified to include the effect of flushing rates and surface area of the lake receiving light (Vollenweider, 1975). In 1976, Vollenweider then developed a relationship between annual phosphorus loading (taking into account mean depth and residence time) and algal chlorophyll concentrations (Vollenweider, 1976).

Rast and Lee (1978) then developed these relationships for the U.S. waterbodies (38 waterbodies) included in the OECD study, following Vollenweider's approach. Rast and Lee also developed

two additional relationships, one between the normalized phosphorus loading and Secchi depth, and another between normalized phosphorus load and hypolimnetic oxygen depletion rate. These relationships were updated in 1982 by including an additional 40 waterbodies (Jones and Lee, 1982).

Throughout the years, several other static (e.g., Larsen and Mercier, 1976; Nürnberg, 1984) , as well as dynamic models (e.g., Malmaeus and Håkanson, 2003; Thomann et al., 1976) have been developed to assess and forecast water quality conditions in lakes and reservoirs. Each method of assessing trophic state has its advantages and disadvantages. Static models provide a means for a faster estimation of nutrient concentrations and effects on lake productivity. The OECD models, in particular, have the advantage of being applicable to a wide range of lakes and reservoirs. Dynamic models present a more accurate representation of the processes occurring in a lake or reservoir. However, the ability to model these interactions may be limited due to the extensive data collection that may be required and the uncertainty of driving variables (Rast et al., 1983; Tapp, 1978). When deciding which model to use, it is thus important to understand its limitations and take time and cost requirements into consideration.

2.4 Water Quality Criteria

During the mid-twentieth century, the Unites States experienced environmental degradation due to modernization and economic growth and a lack of adequate environmental protections (Stets et al., 2015). To help improve water quality, the U.S. Congress established the Federal Water Pollution Control Act of 1948. The act was extensively revised and amended in 1972, and became known as the Clean Water Act (CWA). Additional amendments were done in 1977, 1981, 1987, and 2014. Currently, the CWA is the main law governing surface water pollution. Under the CWA, the USEPA and state have established technology-based effluent limitations and water quality standards to protect water quality (Congressional Research Service, 2016). These water quality standards, along with recommended criteria, provide a benchmark for water quality assessment. This section will discuss criteria and recommended values that serve as reference for the trophic conditions of a lake. Other relevant criteria, such as for SOCs, will be presented in the Results and Discussion chapter.

To address the eutrophication problem, USEPA (2000a) developed recommended criteria for four (4) variables: total nitrogen, total phosphorus, chlorophyll-*a*, and Secchi depth. These variables were chosen because they are representative of the causes and effects of eutrophication. Rather than developing values that applied to all the waterbodies, recommended criteria were determined using an ecoregion approach. Areas with relatively similar geographic and ecological characteristics (soil, land cover, climate, etc.) were assigned a recommended value for these variables. Values were obtained empirically and are representative of surface waters that have been least impacted by anthropogenic activities and that protect aquatic life and recreational uses. Recommended aggregate reference values for Ecoregion IX Southeastern Temperate Forested Plains and Hills, in which Northern Virginia is located, were 20 µg/l for total phosphorus, 0.36 mg/l for total nitrogen, 4.93 µg/l for chlorophyll-*a* (fluorometric), and 1.53 m for Secchi depth.

Ecoregions were further divided into sub-ecoregions and additional reference values were provided. These recommended values may serve as reference to assess water quality conditions.

The VSWCB, now the Virginia Department of Environmental Quality, or VDEQ, established criteria chlorophyll-*a* and total phosphorus criteria for 121 man-made lakes and reservoirs, including the Occoquan Reservoir, with the purpose of protecting aquatic life and recreational uses from the effects of nutrient enrichment. These criteria state that the 90th percentile of the chlorophyll-*a* data should not exceed 35 µg/l in each of the two most recent monitoring years. The criteria also indicate that if algaecide treatment was applied, the median of the total phosphorus data collected during this time should not exceed 40 µg/l. Data should correspond to samples collect at one meter or less from the surface, within the lacustrine zone of the reservoir, and during the period from April 1 to October 31(VSWCB, 2017b).

In addition, because nitrogen can be found in many forms (organic and inorganic) and states (oxidized and reduced), and some of them can cause adverse effects, certain standards have been established. Nitrogen in the form of ammonia can stimulate phytoplankton growth, and when it is present in the unionized form it is toxic to aquatic organisms, especially at higher pH and temperature. Furthermore, since it can be converted to nitrate, which is an aerobic process, it can induce oxygen demand. The VDEQ criteria for total ammonia nitrogen was established depending on pH and temperature to protect aquatic life. For instance, the chronic criteria for total ammonia nitrogen where freshwater mussels and early life stages of fish are present at pH 7 and 20°C is 1.9 mg/l (VSWCB, 2020). Another form of nitrogen that can affect water quality is nitrate because at high concentrations it can be harmful to infants, causing a condition named methemoglobinemia (in which infants do not get enough oxygen), also known as blue baby syndrome (Beutel, 2016). The USEPA National Drinking Water Standard (USEPA, 2009b) and the VDEQ criterion (VSWCB, 2019) for waters used as a public water supply for nitrate is 10 mg/l (measured as nitrogen) to prevent adverse effects to human health.

Other related water quality variables include DO, water temperature, and pH. These variables provide information of the mixing status, DO concentrations and depletion rates, solubility of chemical species, and indicate if conditions are suitable for sensitive fish species (USEPA, 2000b). The VDEQ criteria for Class III nontidal waters (Coastal and Piedmont Zones) indicate a daily water maximum temperature criteria of 32°C, minimum DO value of 4.0 mg/L, DO daily average of 5.0 mg/L, and pH values from 6 to 9. It should be noted that for the Occoquan Reservoir, the DO and pH criteria only apply to the epilimnion when thermally stratified. When no thermal stratification is present the DO and pH criteria applies throughout the water column (VSWCB, 2017a).

2.5 Lake Management

Lake/reservoir management refers to the different strategies employed to maintain or improve the water quality of a lake, to enhance its designated uses, as well as to prevent anticipated issues (Cooke et al., 2005). Restoration, on the other hand, refers to the use of ecologically sound principles to return a lake or reservoir to a close approximation of its original condition.

Strategies that have been employed to reduce eutrophication of waterbodies have targeted nitrogen, carbon, and phosphorus (Grundy, 1971). Studies have indicated that eutrophication can be controlled if the amount of limiting nutrient input into the lake/reservoir is decreased (Schindler, 2006). Therefore, throughout the years, eutrophication has generally been diminished by improving wastewater treatment, which reduces external sources of nutrient loading into lakes/reservoirs. However, nonpoint sources and internal nutrient loading from sediments can delay the lake recovery process. To address this, other strategies such as implementing best management practices and runoff control measures have also been applied to better control nonpoint sources. Internal loading has been addressed through methods such as hypolimnetic aeration and oxygenation (Beutel and Horne, 1999), hypolimnetic withdrawal (Dunalska et al., 2007; Nürnberg, 2020), phosphorus inactivation (Augustyniak et al., 2019), sediment oxidation — which includes nitrate addition (Ripl, 1976), and dredging (Björk, 1988; Van der Does et al., 1992). Additional in-lake restoration techniques have also been used to directly target primary production reduction. Examples include algaecide application, biomanipulation, and water level drawdown.

To effectively assess the feasibility of lake management strategies, it is important to determine the designated water use and evaluate the overall physical, chemical, and biological processes that occur in aquatic systems (Lewtas et al., 2015). This includes analysis of the morphometric characteristics of the lake and the characteristics of the tributary watershed which can provide information on sources, distribution transport, and fate of nutrient and contaminants to establish control programs (Trench et al., 2012). Additionally, evaluation of chemical and biological parameters such as temperature, DO, pH, alkalinity, nitrogen, phosphorus, electrical conductivity, water column transparency, algal chlorophyll, can provide a diagnostic of current water conditions to determine restoration techniques.

As population continues to grow and water demand increases, continued protection and monitoring of water resources will be required. The Nygrén et al. (2017) study of eutrophic lake management in the future mentions climate change, increasing agriculture, lack of funding, increased water demand usage due to population growth, and chemical contaminants in waterbodies as areas of future concern for managers. Additionally, recent research has shown the presence of several emerging organic contaminants in surface waters, providing a new area for concern. Emerging organic contaminants include pharmaceuticals, hormones, surfactants, pesticides, personal care products, disinfection by-products, algal toxins, taste-and-odor compounds, among others (Pal et al., 2014).

CHAPTER 3. METHODOLOGY

3.1 General Process

This thesis contains a historical hydrobiochemical assessment of the Occoquan Watershed and Reservoir, and consists of four (4) main parts:

- Hydrometeorological assessment, which includes analysis of precipitation data and morphometric conditions of the Occoquan Reservoir that affect water quality.
- Water quality analysis for the watershed and reservoir, which includes the calculation of the hydrologic balance and loads into the reservoir, establishment of long-term trends, and determination of relationships between constituents.
- Trophic state assessment of the Occoquan Reservoir.
- Analysis of SOCs.

In order to perform this assessment, long-term water quality data from four (4) principal stream monitoring stations and four (4) principal reservoir stations were analyzed. The selected stream monitoring stations represent the main inflows and outflows of the reservoir: ST01—which is located at the Occoquan Reservoir high dam at the reservoir outlet station; ST10—which represents the inflow coming from the Occoquan Creek arm; and ST40 and ST45 which correspond to the Bull Run arm inflow. Two stations were included to represent Bull Run's inflow to present a complete timeline since ST40 went out of service in 2012, and ST45 information dates back only to 1986.

The four (4) reservoir monitoring stations that were selected out of the total seven (7) stations likewise represent key points of the reservoir: RE02 located near the Occoquan Dam which is the outlet point of the reservoir; RE15 representing water quality data at a mid-section of the reservoir, approximately six (6) miles from the dam and downstream of the confluence of the two main tributaries and above Ryons Dam[1]; RE30 located approximately 1.5 miles above the confluence and used to represent the reservoir water quality in the Bull Run arm; and, RE35 located approximately two (2) miles from the confluence and used to represent water quality in the Occoquan Creek arm.

It should be noted that since 1973, sampling stations have been removed or relocated. For this reason, data from ST20 and ST25, RE01 and RE02, and RE25 and RE35 were combined to present the water quality for the complete period of record. Due to the close proximity of these stations to one another, results should not be significantly affected.

Water quality constituents for the stream and reservoir stations can be categorized in the following ways: water quality parameters, nutrients, organic carbon, principal metals, major ions, and SOCs. Water quality parameters include temperature, DO, pH, alkalinity, conductivity, total suspended solids (TSS) and turbidity. Reservoir station analysis includes ORP, hardness, Secchi depth, and

[1] Also often called Ryans Dam. "The dam was built by Fred B. Ryons, a Colonel in WW I and a military engineer with an interest in hydroelectric energy." https://www.midcopw.net/mid-county-history.html, visited 06 January 2021.

chlorophyll-*a*, in addition to the previously mentioned parameters. Nutrients studied include nitrogen and phosphorus in the following forms: ammonia nitrogen (NH3-N), total Kjeldahl nitrogen (TKN), oxidized nitrogen (Ox-N) which corresponds to nitrite and nitrate forms, total nitrogen (TN), orthophosphate phosphorus (OP), and total phosphorus (TP). Organic carbon for the reservoir was analyzed as dissolved organic carbon (DOC) and total organic carbon (TOC). Chemical oxygen demand (COD) was used to characterize organic matter content in the stream stations. An analysis of sodium and chloride (ions) is included for reservoir stations, as well as iron and manganese (metals). Lastly, SOC information for both stream and reservoir stations is presented.

Data in this assessment are generally presented as time series and/or seasonal averages. Seasonal analyses are important since many variables exhibit seasonality as a result of temperature, precipitation and flow. The seasons in this assessment are considered as detailed below:

- Winter → December (of the previous year), January, February
- Spring→ March, April, May
- Summer→ June, July, August
- Fall→ September, October, November

Annual data are also presented from December of the previous year through November for consistency among seasons. Concentration values that were below detection limits, or censored data, were set as half the detection limit for this analysis.

Statistical analyses in this thesis include the Mann-Kendall test, to determine trends for constituents, and Principal Component Analysis (PCA), to determine relationships between parameters. A trophic state assessment was also performed for the Occoquan Reservoir using Carlson's TSI, the Vollenweider Model, and the Rast, Lee, Jones Model.

The majority of the calculations for this study were completed in Microsoft Excel. Temperature and DO isopleths, as well as PCA were performed using Matlab, and Trend analysis was performed in the R programming language.

3.2 Thiessen Rain

The OWML manages a database with precipitation records that date back to 1951. This database has been updated throughout the years as new rain stations have been established and other stations are no longer used. Currently, rainfall data are obtained from fifteen (15) stations distributed across the Occoquan Watershed (Figure 3-1). The OWML manages the operation of thirteen (13) rain gauges (Table 3-1), which work under the tipping-bucket principle. In this type of gauge, rain water flows from a funnel into a two-bucket receptacle located on a pivot. When one of the buckets is filled to 0.01 inches, the bucket tilts, releasing the collected water and bringing the other bucket under the funnel to be filled. When the bucket tips, it sends an electric signal to record the measurement. The data are stored in a computer file every 10 minutes. One of the two remaining gauges is operated by the National Weather Service (DULL) and the other is operated by Fairfax

Water (LRTN). The information from these two gauges is provided to OWML as daily records. The UOSA gauge is actually a full weather station operated by OWML, and provides rainfall, relative humidity, air temperature, solar insolation, wind speed and direction, and reflected radiation (from the earth to the sky) data.

Using the rainfall measurements obtained from each gauge, the daily average precipitation for the Occoquan Watershed was estimated by applying the Thiessen Polygon method. This method assigns an area of influence for each gauge based on the assumption that the data recorded at any station can be applied halfway to the next station in any direction. The areas of influence are constructed by plotting the rain gauge network, connecting the adjacent stations with a line, and then bisecting these lines perpendicularly to form different polygons. Rainfall measurements obtained from each gauge are then multiplied by its respective area of influence. This value is then divided by the watershed area to obtain a weighted average of rainfall for the basin. The Thiessen polygons for the Occoquan Watershed are also shown in Figure 3-1.

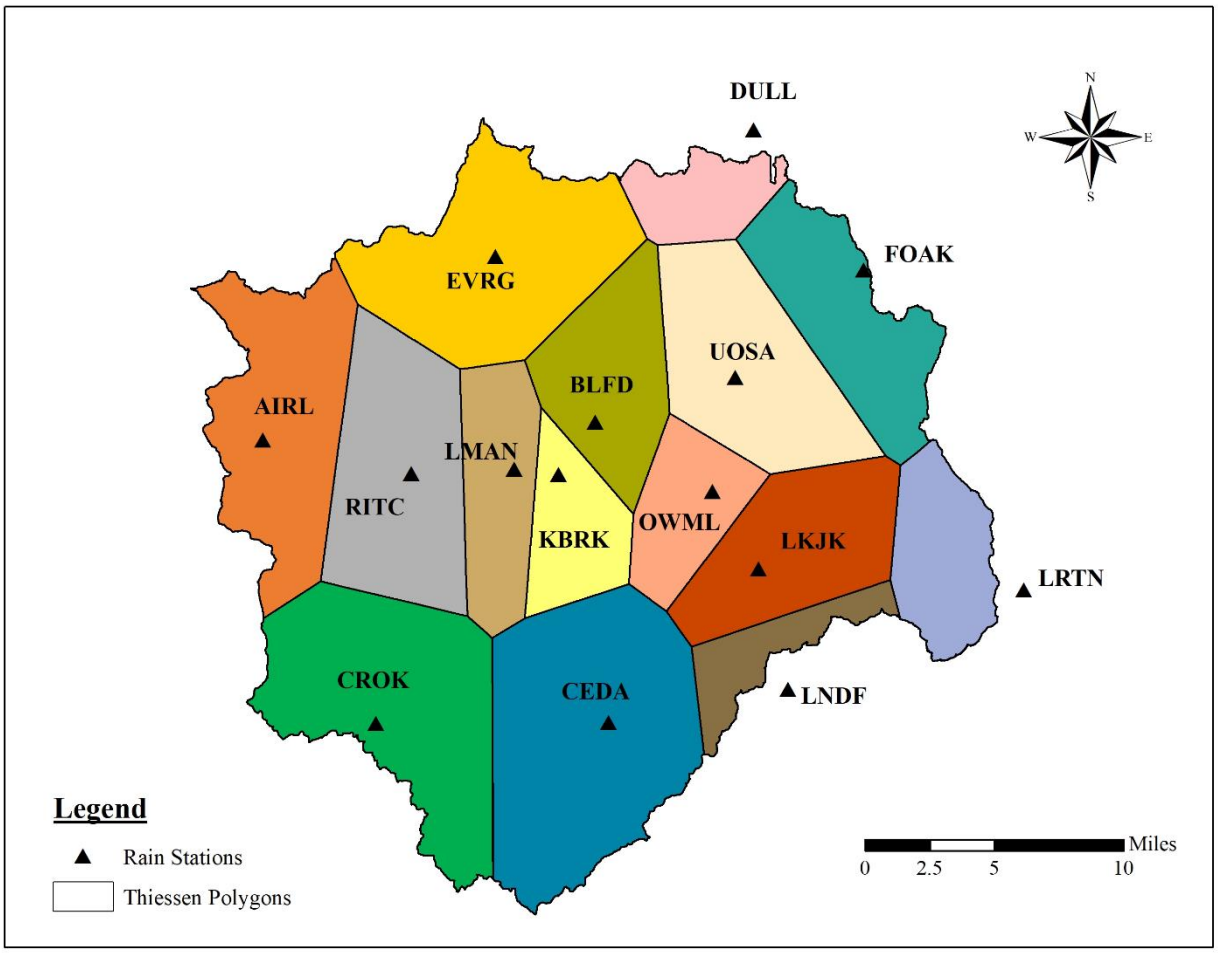

Figure 3-1. Rain Gauge Network and Thiessen Polygons for the Occoquan Watershed

Table 3-1. OWML Rain Gauge Network

#	Station ID	Rain Gage Name	Area (Acres)	Latitude	Longitud	Operator	Period of Record
1	OWML	Occoquan Watershed Monitoring Laboratory	14,208	38°44.920' N	77°28.834' W	OWML	1978-Present
2	DULL	Dulles International Airport	10,432	38°57.071' N	77°26.891' W	National Weather Service	1963-Present
3	LRTN	Lorton Water Treatment Plant	16,064	38°41.486' N	77°15.523' W	Fairfax Water	1977-Present
4	LMAN	Lake Manassas Water Treatment Plant	17,408	38°45.748' N	77°37.337' W	OWML	1984-Present
5	LNDF	Prince William County Regional Landfill	9,536	38°38.241' N	77°25.687' W	OWML	1995-Present
6	BLFD	Balls Ford Road Yardwaste Facility	21,504	38°47.300' N	77°33.829' W	OWML	1995-Present
7	LKJK	Lake Jackson Dam	25,024	38°42.299' N	77°26.889' W	OWML	1997-Present
8	AIRL	Airlie	33,088	38°46.793' N	77°48.131' W	OWML	2001-Present
9	CEDA	Cedar Run Wetlands	48,704	38°37.198' N	77°33.387' W	OWML	2001-Present
10	FOAK	Fair Oaks Police Department	24,000	38°52.309' N	77°22.227' W	OWML	2001-Present
11	RITC	C. Hunter Ritchie Elementary School	31,872	38°45.629' N	77°41.754' W	OWML	2001-Present
12	CROK	Crockett Park	40,960	38°37.247' N	77°43.366' W	OWML	2001-Present
13	EVRG	Evergreen Fire Department	38,912	38°52.902' N	77°38.066' W	OWML	2001-Present
14	KBRK	Kingsbrook	13,504	38°45.556' N	77°35.434' W	OWML	2004-Present
15	UOSA	Upper Occoquan Service Authority	29,888	38°48.748' N	77°27.803' W	OWML	2006-Present

3.3 Stream Flow Data

As mentioned in Chapter 1, there are currently eight (8) stream monitoring stations. Stream gauges continuously measure the river stage, which refers to the height of the water surface at a given location. In order to determine volumetric flow rates, stage-discharge relation curves (i.e., rating curves) were developed and programmed into the data logger at each station. On-site discharge measurements are performed periodically to detect changes in the rating relationship. The only station for which direct flow rating is not performed is ST01 (outflow station); instead, the flow rating curve is determined by applying the broad-crested weir equation to the crest of the Occoquan Dam and adding discharges to the water treatment plant. Stream base flows are recorded hourly and storm base flows are recorded every 15 minutes. All recordings are stored in the OWML Microsoft FoxPro Database.

Three significant issues with the gauging stations were explained in a previous report (OWML, 1998). The first two issues were backwater problems in ST10 and ST70 due to the increase in elevation in the Occoquan Dam (2-ft increase) and raising of the pool elevation of Lake Manassas (5-ft), respectively. These issues were addressed by installing ultrasonic meters that measure changes in frequency to determine water velocity (Doppler shift) and use acoustics to determine water depth. The third issue was related to the accuracy of outflow measurements obtained at ST01. At this station, the equation used to calculate flows does not include the deformation of the concrete surface. Additionally, since the outflow for this station did not include the discharges into the water treatment plant, they had to be added manually as stated previously. The third issue still remains as the methods and location for estimating the reservoir outflow cannot be updated.

Stream flow measurements from ST10, ST25, ST30, ST40 and ST45 were used to determine reservoir inflow and outflow values. Flows at ST10 were used to calculate the inflow corresponding to Occoquan Creek and ST45 to calculate the inflow from Bull Run. Since measurements from each station are associated with a specific drainage area (Table 1.2), these flows were scaled up to estimate the flow of ungauged areas upstream of the Occoquan Dam. The inflow of ST10 was scaled to match an area of 369 mi^2, corresponding to the total drainage area of the Occoquan Creek arm. The flow from ST45 was scaled to match a drainage area of 201 mi^2,

corresponding to Bull Run's total drainage area. It should be noted that flow from the MHR WRF was subtracted before scaling up the flow. When there were no data for ST10, due to backwater problems, the flow from ST20/25 was scaled up, and ST30 flow was added to the result to determine the total inflow from Occoquan Creek as described by Van Den Bos (2003). For Bull Run, flows from ST40 were used before ST45 came into operation.

3.4 Hydrologic Balance

The hydrologic balance for the Occoquan Reservoir was estimated using the precipitation data calculated with the Thiessen Polygon method, area-capacity data obtained from hydrographic surveys, pool elevation data and stream flow data measured by the laboratory. The inputs for the reservoir include direct inflow from its two tributary streams, Occoquan Creek and Bull Run, effluent from POTWs, and precipitation. Outflows from the reservoir include flow over the dam, water withdrawn for treatment and distribution (Fairfax Water's Lorton treatment works, originally the Occoquan plant and now the new Griffith plant), water released through blow-off valves, and/or evaporation. In earlier years, there was some periodic generation of power at the Occoquan dam, and those flows have also been accounted for in those years.

Direct annual rainfall into the reservoir was determined by multiplying the precipitation values obtained from the rain gauges and the application of the Thiessen polygon method by the yearly average surface area of the reservoir. Surface area values were calculated using the measured daily pool elevations and the area-capacity data. Total reservoir inflow was the sum of the inflow from Occoquan Creek (ST10 scaled flow), Bull Run (ST45 scaled flow), the flows from the POTWs (MHR WRF, Vint Hill Farms Station Wastewater Treatment, Nokesville Sewage Treatment Plant) that were in operation during the period of record and the precipitation values.

Total reservoir outflow was calculated as the sum of the discharges at the Occoquan Dam and the water withdrawn by the water treatment plant (ST01 flow values) plus evaporation losses. Evaporation losses from 1983 to 2008 were estimated as explained in Van Den Bos (2003) using data from evaporation maps published by the U.S. Department of Commerce Weather Bureau (Kohler et al., 1959), which indicate an annual average evaporation of 35.8 inches. This value was converted to the appropriate units and multiplied by the median reservoir surface area. Evaporation rates were estimated in two groups: one value for the period of May–October (70% of the annual average) and one value for the period of November–April (30% of the annual average). The two evaporation rates obtained were summed to get a total annual evaporation flow. The evaporation values from 2009 to 2019 were estimated using the wind speed, air temperature, relative humidity and radiation data measured and recorded since 2008 at the UOSA station. With this data, and the calculated daily surface areas, the evaporation water flow was calculated using the Penman equation modified by Shuttleworth (Shuttleworth, 2007):

$$E_{mass} = \frac{mR_n + \gamma * 6.43(1 + 0.536 * U_2)\delta_e}{\lambda_v(m + \gamma)}$$

where:

$E_{mass} = evaporation\ rate\ (mm/day)$

$m = slope\ of\ the\ saturation\ vapor\ pressure\ curve$ (k$P_a/°C$)

$R_n = net\ irradiance\ (MJ/m^2\ d)$

$\gamma = psychrometric\ constant = 0.0016286 * P/\gamma$ (k$P_a/°C$)

$U_2 = windspeed\ (m/s)$

$\delta_e = vapor\ pressure\ deficit$ (kP_a)

$\lambda_v = latent\ heat\ of\ vaporation = 2.45\ MJ/kg$

The resultant evaporation value was converted to the appropriate units (ft/day) and then multiplied times the reservoir surface area to obtain the value in ft^3/year, which was used in the hydrologic balance data.

3.5 Load Balance

A load balance for TN, TP, TSS, and sodium was calculated for the Occoquan Reservoir. The process followed was similar to the one performed for the hydrologic balance, where loads calculated for ST10 were scaled up to obtained an estimate of the loads coming from the 369 mi^2 corresponding to the Occoquan Creek arm of the watershed, and loads calculated for ST45 were scaled up to estimate incoming loads from the 201 mi^2 corresponding to the Bull Run side of the watershed. Where data were not available for ST10, values from ST20/25 were scaled up (to match an area corresponding to the Occoquan Creek arm minus ST30 drainage area) and then added to ST30 to obtain a total value for the Occoquan Creek branch. ST40 was used for Bull Run when data from ST45 were not available. Loads from the MHR WRF were subtracted before scaling up.

Constituent loads for each station were determined following the Daily Flow Data Integration Model described by Johnston (1999). In this model, loads for baseflow conditions are calculated by multiplying constituent concentrations obtained through laboratory analysis of the baseflow samples collected by the associated flow rate for that particular date. Concentrations for days where there were no samples were estimated by interpolating between consecutive baseflow sampling events to obtain load values for the entire period. Loads related to storm events were calculated by multiplying the average constituent concentration from the flow-weighted composite sample or Event Mean Concentration in (mg/l), the event mean flow rate (ft^3/s), the duration time of the storm (days), and the corresponding conversion factor to obtain the final result in pounds (lbs). This model uses the simple substitution method (half the detection limit) to infill missing non-detect values. Loads from 1983 to 2015, were calculated with this method using the Microsoft Excel spreadsheets developed by Johnston (1999) and daily average flows for baseflow calculations. From 2016 to 2019, loads where calculated using the URUNME software developed by Lodhi et al. (2020) using the continuous stream flow data collected. The only station which is still currently calculated with daily average values is ST01.

In addition to the non-point source loading, which refers to the previously mentioned Occoquan Creek and Bull Run loads, inputs to the reservoir include loadings from POTWs and atmospheric deposition. Loads from POTWs were calculated using data provided by UOSA and Vint Hill

Farms Station Wastewater Treatment. Nokesville data were also included for the period where it was in operation. It should be noted that only the MHR WRF was included as POTWs for sodium calculation, since it was the only one for which sodium data are available. The concentration used was the median value (66.6 mg/l) of sodium measurement taken in the plant. Atmospheric deposition data were only available for nitrogen and phosphorus and were obtained from a study of the performance of a constructed wetland in Manassas, Virginia (Carleton et al., 2000). Estimated median annual atmospheric deposition rate (wetfall plus dryfall) for nitrogen was 11.74 lb/acre/yr and 0.34 lb/acre/yr for phosphorus. To obtain total atmospheric loading, these values were multiplied by the average annual reservoir surface area values previously calculated. Output loads correspond to the loads calculated with data from ST01.

3.6 Trend Analysis

A trend analysis was performed for water quality variables of the Occoquan Watershed and Reservoir stations to determine if values are increasing, decreasing or staying stable over time. Trend analyses are apt when evaluating gradual changes (monotonic trends) in water quality such as those due to urbanization or implementation of best management practices. For example, the Chesapeake Bay Program has performed trend analyses since the 1990s to detect water quality responses to nutrient reduction actions and to measure progress toward Bay restoration goals (Chesapeake Bay Program, 2008).

Trend analysis is a statistical procedure in which a null hypothesis is evaluated. H_o indicates no trend is present. If the test shows that the significance level is at or below an established significance level (*p*-value), the null hypothesis is rejected and the alternative hypothesis (increasing or decreasing trend) is accepted. Failure to reject H_o does not mean no trend is present, rather it is an indication that there is not enough evidence to conclude a trend exists at a certain confidence interval. Different statistical methods can be used to identify trends and estimate rates of change; these methods can be parametric, nonparametric, or mixed type. For this assessment, the method used was the Mann-Kendall nonparametric test. Nonparametric tests are more robust for non-normal distributions and against outliers and large data gaps (Meals et al., 2011).

The Mann-Kendall test is a nonparametric form of regression analysis used to determine monotonic trends. The test assumes that the data are independent and that the distribution remains constant over time (Helsel and Hirsch, 2002). The Mann-Kendall test determines a trend by evaluating the sign difference between latter measurements (y_j) and earlier measurements (y_i) throughout the length of the dataset *n*, using the following formula:

$$S = \sum_{i=1}^{n-1} \sum_{j=i+1}^{n} sign(y_j - y_i)$$

If the difference between the latter and earlier data is positive ($y_j > y_i$), a value of 1 is assigned. On the contrary, if the difference is negative, a value of –1 is given. 0 is assigned when there is no difference. These assigned integers are then summed to find *S*. A trend is upward or increasing when *S* is a large positive value, downward or decreasing when *S* is a large negative value, and no trend when *S* is a small value. A test statistic τ (Kendall tau) is also calculated using *S* to provide

a measure of the strength of the monotonic relation between x and y and ranges from –1 to +1. Positive τ values indicate an upward trend (concentrations increase with time) and negative τ values indicate a downward trend (concentrations decrease with time). The formula to determine τ is the following:

$$\tau = \frac{S}{n(n-1)/2}$$

Additionally, the statistical significance is checked using Z scores, which are calculated with the formula shown below, where S is the previously calculated test statistic and σ_s is the standard deviation. If the value of $Z > Z_{\alpha/2}$, the null hypothesis is rejected at a specified level of significance in a two-sided test. p-values are presented in this study to indicate the significance of τ for each parameter analyzed. Trends in this study were considered significant when $p \leq 0.1$.

$$Z_s = \begin{cases} \frac{S-1}{\sigma_s} & if\ S > 0 \\ 0 & if\ S = 0 \\ \frac{S+1}{\sigma_s} & if\ S < 0 \end{cases}$$

Lastly, the rate of change for a trend can be calculated as the median of the slope of all the individual pairs of data, also called the Sen slope estimator formula (Meals et al., 2011; Sen, 1968):

$$\beta_1 = median(\frac{y_j - y_i}{x_j - x_i})$$

3.7 Principal Component Analysis

PCA was used to identify dominant patterns in nutrient data (nitrogen and phosphorus) and principal ions (sodium and chloride) at the Occoquan Reservoir in time (season) and space (stations). Forms analyzed for nitrogen were NH3-N, TKN, Ox-N, and TN. Phosphorus was analyzed as OP and TP. In addition, PCA was used to identify possible drivers of the observed patterns. Parameters included as possible drivers of the nutrient and principal ion patterns were temperature, pH, DO, alkalinity, TSS, ORP, DOC, TOC, and rainfall.

PCA is an ordination method that helps summarize and visualize the relationships contained in multivariate data by reducing data dimensionality (i.e., replacing the original variables with linear combinations of these variables). Each new variable, or component, is orthogonal to all other components. The patterns which emerge following the analysis are called PC modes. PC1 is the first principal direction along which the samples show the largest variation (best fit line). PC2 is the second most important direction along which the samples vary (i.e., the next best fit line perpendicular to PC1), and so on. Linear algebra methods are used to determine the PC modes (eigenvectors and new coordinate axes), latent scores which represent the fraction of variance explained by each PC mode (eigenvalues), and PC scores which refer to each of the observations from the original data transformed into PC space. PCA assumes normally distributed residuals, is sensitive to outliers, and does not reflect any nonlinear relationships between variables.

To identify possible variables that can be driving patterns, Vector Projection (also called Environmental Factor Projection) or through Constrained PCA can be performed. In order to use these methods, variables have to be previously evaluated and classified as dependent (the variables for which we want to see the patterns and whose value depends on other variables) or independent (variables that have an effect on the dependent variables). In Vector Projection, PCA is only performed on the dependent variables. Data corresponding to the independent variables is then projected or regressed into PC space to evaluate their association with the dominant patterns. Constrained PCA only shows the patterns that can be explained by the previously defined independent variables. It is done by performing multiple linear regression on the original data followed by PCA on the regressed data. For the present water quality assessment, the Vector Projection method was chosen in order to identify all patterns occurring in the reservoir and then evaluate the relationship of these patterns with other parameters. Confidence intervals for the independent variables were calculated to determine if the variables regressed are significant predictors of the dependent variables.

Before performing PCA, stopping rules must be applied in order to determine how many PC modes are actually meaningful and warrant further evaluation. For this assessment, a resampling-based approach that keeps PC modes that are significantly greater than random at $p<0.05$ (one-sided test, refers to upper bound only) was employed. In this method (Peres-Neto et al., 2003), PCA is performed on the original data where PC modes, latent scores, and PC scores are calculated. Then, the data within each variable is randomized (resampled without replacement) and PCA is performed on the new randomized data. Latent scores are saved and the process is repeated for N iterations (generally N = 10,000 as done in Rippy et al. (2017)), each time saving all the latent scores from the different randomized matrices. The 50^{th}, 90^{th}, and 95^{th} percentiles for the eigenvalues at each mode are estimated. PC modes where the latent scores (eigenvalues) of the original data exceeded the 95^{th} percentile threshold calculated were interpreted as dominant patterns. PC modes below the 50^{th} percentile threshold were considered random patterns and not evaluated further.

Once the stopping rule and PCA were performed, a non-parametric bootstrapping method was employed to calculate confidence bounds and determine which variables contributed significantly to the patterns represented by each PC mode. For this assessment, 95% and 90% confidence bounds about the PC modes and scores were calculated following the process and code specified by Babamoradi et al. (2013). In summary, the original data were resampled with replacement and PCA was performed on the new data. This process is repeated (N = 10,000) and each of the bootstrapped PC modes and latent scores were corrected for both inversion (i.e., being out of order relative to the empirical data) and reflection (i.e., being ordered correctly but multiplied by −1). Confidence bounds were then estimated from this data.

PCA was performed independently for surface and bottom data and graphs were presented by station as well as by seasons. Significant PC modes were illustrated using biplots, where the x-axis is PC1 and y-axis is PC2. The magnitude and direction of each plotted vector indicates the contribution of that variable to the PC mode. Vectors leaning along the x-axis mainly contribute to PC1, while vectors leaning along the y-axis mainly contribute to PC2. Variables with longer

vectors contribute more to the PC mode than shorter vectors. All PCA calculations were performed in Matlab programming language developed by Mathworks.

3.8 Trophic State Assessment

The trophic state of an aquatic system indicates its level of productivity. Based on the trophic state, a waterbody can be classified as oligotrophic, mesotrophic, eutrophic, or hypereutrophic. As explained in section 2.3, oligotrophic waterbodies are nutrient poor and have low productivity, while eutrophic waterbodies are nutrient rich and have high primary production. Mesotrophic indicates an intermediate state between oligotrophic and eutrophic, and hypereutrophic refers to highly enriched waterbodies. There are different models and classification systems (e.g., TSI) designed to rate the biological productivity of a waterbody. For this assessment, the trophic state of the Occoquan Reservoir was analyzed using three (3) different methods: Carlson's TSI; the Vollenweider Model; and the Rast, Lee, Jones Model.

Carlson's TSI is an empirically derived multi-parameter index that evaluates the trophic state of a lake/reservoir based on algal biomass. The index is calculated using three different variables: Secchi depth, chlorophyll-*a*, and TP concentrations. The formulas used to calculate this index, given by Carlson (1977), include the following:

$$TSI\ (SD) = 60 - 14.41 \ln(SD)$$

$$TSI\ (CHL) = 9.81 \ln(CHL) + 30.6$$

$$TSI\ (TP) = 14.42 \ln(TP) + 4.15$$

where SD refers to Secchi depth in meters, CHL equals chlorophyll-*a* concentration in µg/l, and TP refers to total phosphorus also in µg/l. The resulting TSI is a dimensionless number between 0 and 100. TSI values less than 30 are common in oligotrophic lakes and reservoirs. Values from 50 to 70 correspond to eutrophic lakes/reservoirs, and values higher than 70 are classified as hypereutrophic (Wetzel, 2001) The three parameters when transformed to indices should give the same value. However, caution should be used when using Secchi depth as an indicator in highly colored lakes or lakes containing high non-algal particulate matter. TP may not be the appropriate indicator in lakes where phosphorus is not the limiting nutrient or in lakes with high orthophosphate concentrations. The best number may be the one derived from the chlorophyll-*a* formula (Carlson, 1977). When values calculated with different variables do not provide the same TSI value, it is recommended to use chlorophyll-*a* and Secchi depth during summer, and TP during the other seasons. The Carlson TSI for the Occoquan Reservoir was calculated using surface water data of these three variables from 1973 to 2019.

The trophic state of the Occoquan Reservoir was also assessed using the input-output model developed by Richard A. Vollenweider (Vollenweider, 1968, 1975). This empirical model is used to predict lake eutrophication based on nutrient loading. The nutrient loading concept indicates

that there is relation between the amount of a nutrient flowing into a waterbody and its response to that nutrient input (Wetzel, 2001). Vollenweider quantitatively defined the relationship between nutrient loading and planktonic algal trophic response. Through a mass balance approach, Vollenweider related nutrient loadings to lake morphometry (mean depth) and hydrology (i.e., retention time, hydraulic loading) to predict total lake nutrient concentration. The model follows these assumptions: nutrient load is instantaneously and completely mixed (continuously-stirred tank reactor - CSTR); the waterbody is at steady-state, so that concentrations in the lake are equal to the outflow; inflow and outflow rates are equivalent; phosphorus is the main nutrient limiting algal growth; nutrient (i.e., TP) can be lost via advection (i.e., through outlet station) or by transport into sediment (loss rate is first-order reaction); there is no phosphorus internal loading to the water column from sediments. The Vollenweider Model can be expressed as:

$$P_L = \frac{L_P}{q_s + v_s}$$

where

$P_{Lake} = total\ concentration\ of\ phosphorus\ in\ lake\ (\frac{g}{m^3})$

$L_p = annual\ TP\ loading\ per\ unit\ of\ lake\ surface\ area\ (\frac{g}{m^2 yr})$

$q_s = areal\ hydraulic\ loading = \frac{mean\ depth\ of\ lake}{hydraulic\ retention\ time}\ (\frac{m}{yr})$

$v_s = apparent\ settling\ velocity\ (\frac{m}{yr})$

As part of his model, Vollenweider plotted (log-log plot) L_p against q_s, and defined TP loading values for the trophic boundaries. Following the Vollenweider Model, L_p for the Occoquan Reservoir was calculated and plotted against q_s from 1974 to 2019. These values were then compared against trophic boundaries to illustrate the trophic state of the reservoir for each year of the record period. Lp was calculated by dividing the previously calculated loads by the average surface area. Mean depth of the reservoir was calculated as the average volume divided by the average surface area, and the hydraulic retention time was determined by dividing the reservoir volume by the total outflow obtained from the hydrologic balance. The phosphorus concentrations used to determine the phosphorus loading trophic boundaries for this assessment were 10 µg/l for mesotrophic, 25 µg/l for eutrophic, and 60 µg/l for hypereutrophic (Olem and Flock, 1990). Phosphorus loading boundaries were calculated by using these values in the Vollenweider formula with an apparent settling velocity of 10 m/yr (as defined by Vollenweider).

Lastly, the effect of nutrient loading on the Occoquan Reservoir was evaluated by predicting chlorophyll-*a* concentrations using Rast, Jones, and Lee's model (Rast et al., 1983). This empirical model was developed following Vollenweider's approach on data from several U.S. lakes and reservoirs to derive a regression that relates phosphorus loads to their chlorophyll-*a* concentration. In order to use the Rast, Jones, Lee model, the assumptions previously mentioned for predicting phosphorus lake concentration must be met. Additionally, productivity must be mainly planktonic

algae (rather than attached or aquatic macrophytes), the lake must present only moderate amounts of turbidity or color from other sources rather than algae, and the hydraulic residence time for the growing season should be a minimum of two weeks. The results of this model were presented on a graph of chlorophyll-*a* as a function of normalized phosphorus loads, with the best fit line of the graph representing the relation between the two variables.

As indicated in the previous assessment (Van Den Bos, 2003), the resulting relation derived by Rast et al., (1983) was used to predict summer chlorophyll-*a* concentrations (µg/l) at the Occoquan Reservoir using the following expression:

$$chla = 0.394 P_{Lake}^{\ 0.8319}$$

where P_{Lake} is the same as the predicted in-lake steady state mean TP concentration described in Vollenweider's model (in mg/m^3). Predicted values for the reservoir were graphed and compared to observed chlorophyll-*a* concentration from 1974 to 2019. The observed values were calculated as an area-weighted average from concentrations measured at RE02, RE15, RE30, and RE35 during summer.

CHAPTER 4. RESULTS AND DISCUSSION

4.1 Hydrometeorological Conditions

4.1.1 Introduction

Hydrometeorology is the science that utilizes meteorological data to help develop solutions to hydrologic problems (Bruce and Clark, 1966). It studies the circulation of water between the ocean, land surfaces and the atmosphere, and deals with parameters such as rainfall, evaporation, streamflow, and runoff. These parameters are important to engineers for calculating safe water yields, determining required storage capacity of dams, designing spillways, and estimating water losses, among other uses. These sections present rainfall calculations for the Occoquan Watershed, reservoir pool elevation data, morphometric information that influence the internal processes of the reservoir, and the hydrologic budget.

4.1.2 Precipitation and Pool Elevation

Figure 4-1 shows the daily Thiessen-weighted average rainfall from 1951 to 2019. It can be observed there have been three (3) rain events that have exceeded 5 inches of rain for this period. The highest occurred in June 1972 due to Hurricane Agnes, which caused a peak rainfall value of over 7 inches. The next two high rain events occurred in July 1956, with 6.19 inches of rain and August 1955, with 5.40 inches. More recently, smaller peaks have occurred in 2008, 2010 and 2018, which all had one day with total rainfalls of 4 inches

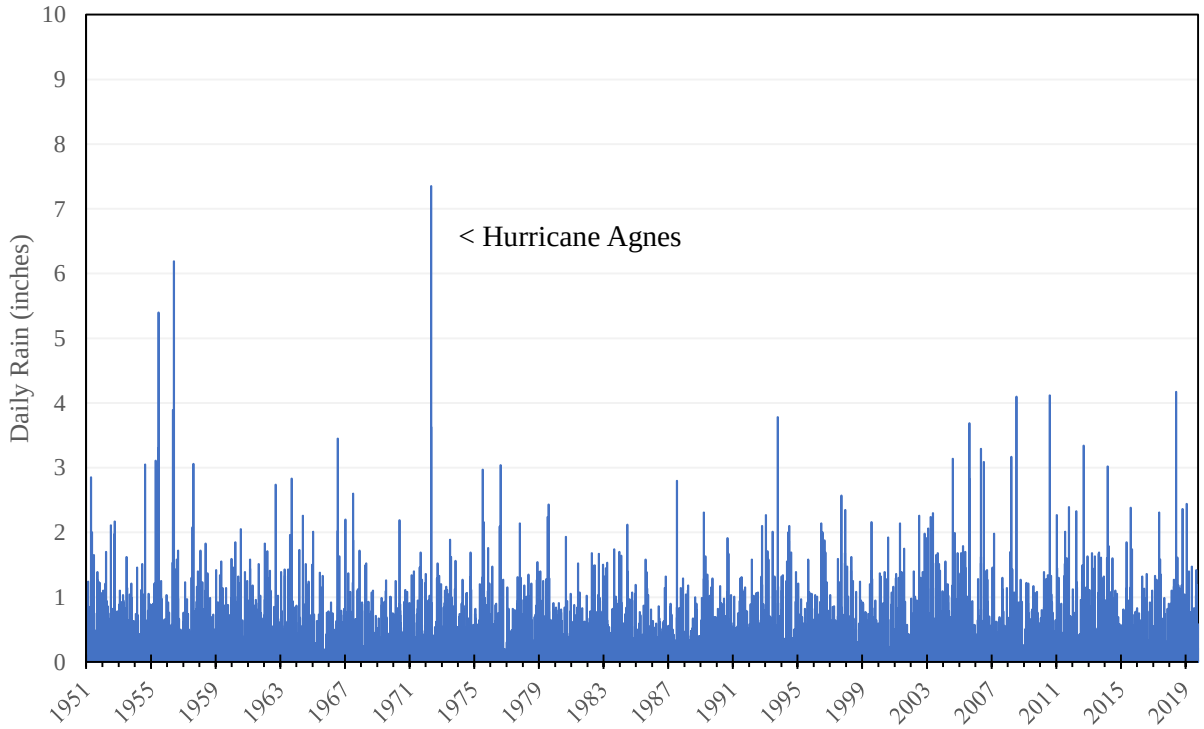

Figure 4-1. Daily Thiessen Average Rain in the Occoquan Watershed, 1951–2019

Of the total number of days in the 69-year period of record, 42% were days with rain (Figure 4-2). The season that had more rain days was summer; however, rain events were distributed almost evenly throughout the seasons. The seasonal distribution of rainfall is further detailed in Figure 4-3. In this graph, the x-axis indicates the quantity of rainfall on a particular day, in inches, and the y-axis represents the percentage of occurrences of rain events that were less than that particular value of rainfall. For example, in fall, 93% of all events had less than 1 inch of rain and all days (100%) had less than 4.1 inches of rain. Seasonal median values are 0.10 inches for winter, and 0.13 inches for the rest of the seasons (for those days that had rain).

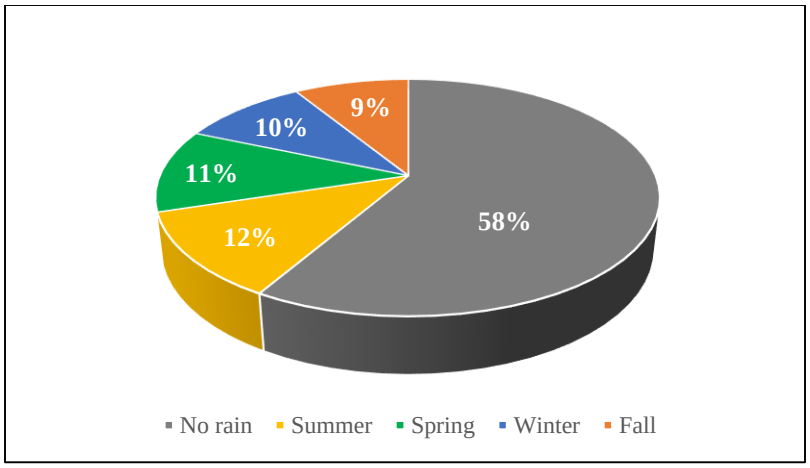

Figure 4-2. Overall Daily Rainfall Distribution for the Occoquan Watershed, 1951–2019

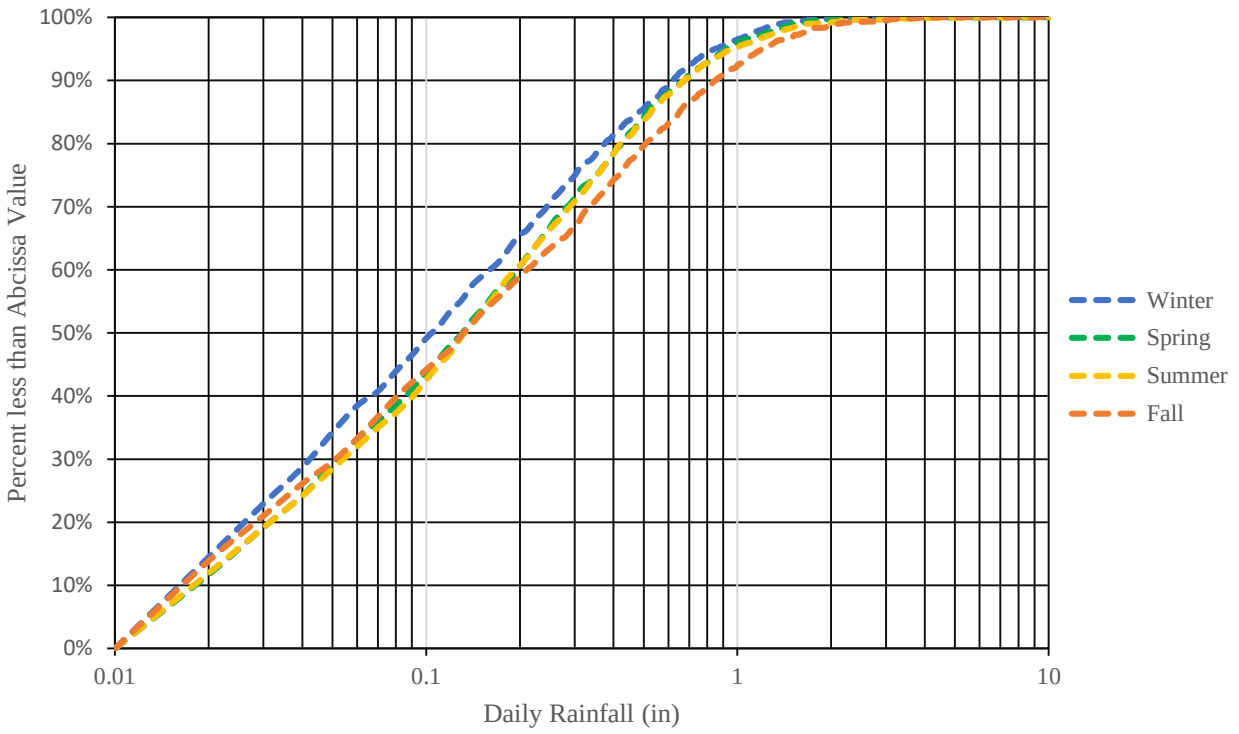

Figure 4-3. Seasonal Distribution of Daily Rainfall in the Occoquan Watershed, 1951–2019 (days with rain only)

Finally, total yearly values from 1951 to 2019 are shown in Figure 4-4. It can be observed that the year with most rainfall was 1979, with a total of 62.43 inches of rain, followed by 2003 with 58.50 inches, and 2018 with 54.34 inches of rainfall. Since 1951, there have been nine dry years (1957, 1959, 1969, 1986, 1988, 1997, 2002, 2007, 2016) and nine wet years (1952, 1955, 1956, 1972, 1975, 1979, 1984, 2003, 2018). This means that for dry years, total rainfall was less than the 69-year average by more than one standard deviation, and for wet years it was more than one standard deviation above it.

The average rainfall for the period under analysis was approximately 40 inches, with summer having the highest average rain, 11.54 inches, and winter having the lowest value, 7.96 inches. Rainfall statistics are summarized for each season in Table 4-1. It can be observed that during the period of record, summer was the season with most days with rain, as well as higher average and median rainfall values, followed by spring. For winter, however, even though it had more days with rain than fall, there seem to be more rainfall during fall, as the averages and median values are higher.

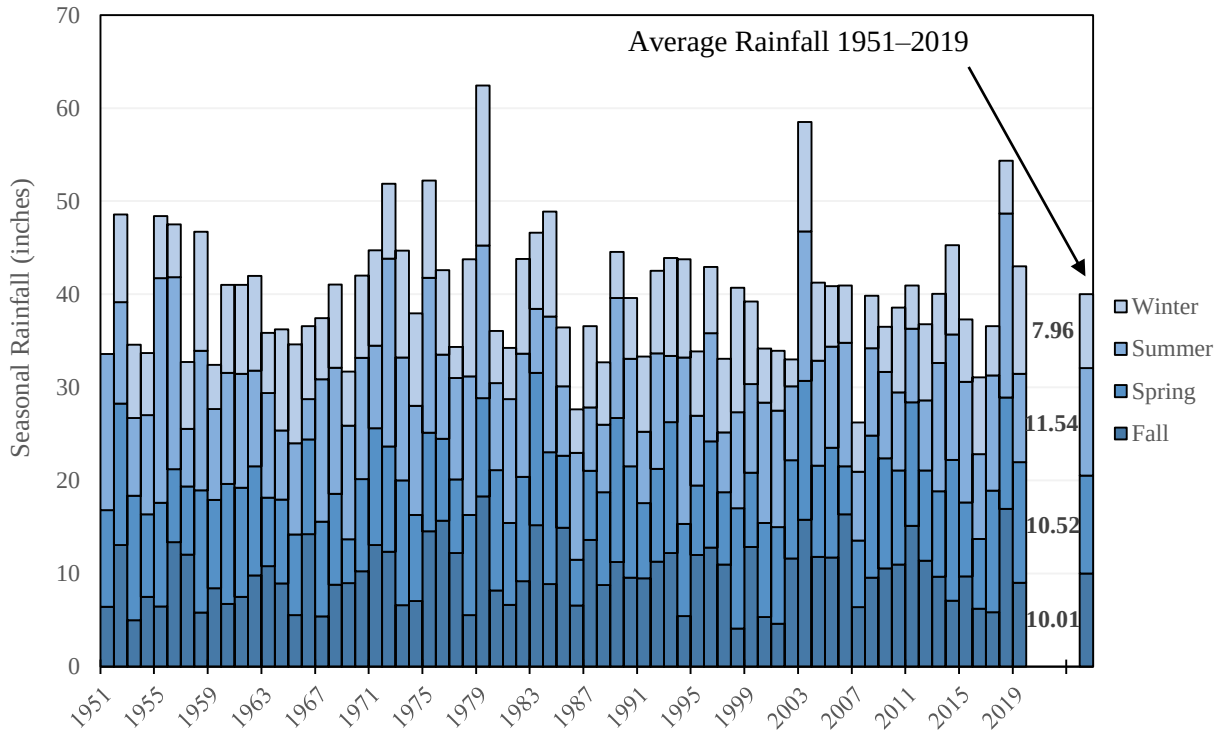

Figure 4-4. Seasonal Thiessen Average Rainfall in Occoquan Watershed, 1951–2019

Table 4-1. Seasonal Rainfall Statistics 1951–2019

Season	Mean (inches)	Median (inches)	Standard Deviation (inches)
Winter	7.96	7.92	2.76
Spring	10.52	10.16	2.63
Summer	11.54	11.28	3.81
Fall	10.01	9.68	3.45
Total	**40.03**	**39.84**	**6.81**

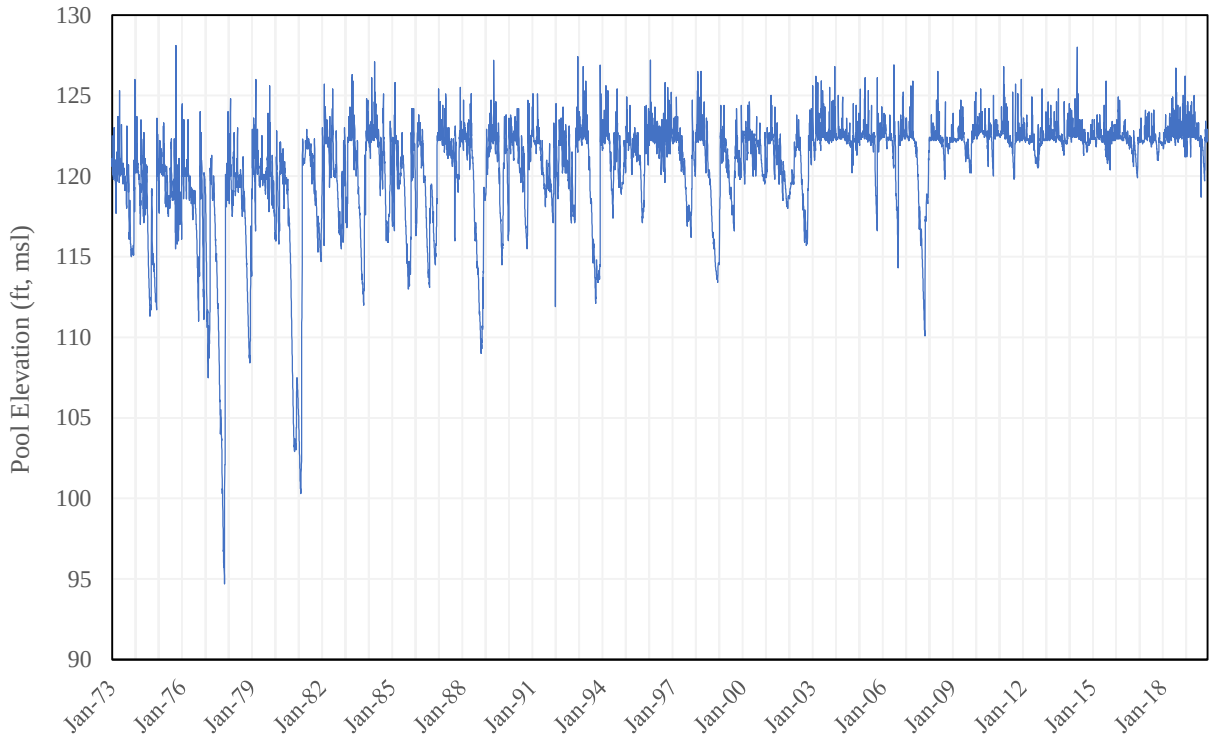

Figure 4-5. Time Series of Daily Pool Elevation of the Occoquan Reservoir, 1973–2019

Figure 4-5 shows how the daily pool elevations have varied from 1973 to 2019. Pool elevation records started in January 1973 and are measured at ST01. The lowest pool elevation for the 47-year period occurred in October 1977, in which the water elevation fell to 94.7 ft. msl. These low values were seen throughout the entire month, averaging approximately 97 ft. msl. Another period with low pool elevations occurred from September 1980 to January 1981, for which the lowest elevation was approximately 100 ft. msl. Note that the dam elevation was raised from 120 ft. msl to 122 ft. msl in 1982, and the drawdown in the previous year was likely due to the construction activity related to the weir crest elevation. Since the year 2000, the period with lowest observed pool elevations was in October 2007, with an average 111.9 ft. msl for the month, and a low point of 110 ft. msl. Interestingly, the only year that had low pool elevations that was classified as a dry year was 2007.

4.1.3 Morphometry

Morphometry is the measurement of the physical features of a reservoir and its tributary watershed. It is important to evaluate the size and shape of a reservoir because it affects nearly all chemical and biological parameters (Wetzel, 2001). The morphometry of a reservoir can help us understand internal processes such as turbulence, sedimentation and resuspension, lake stratification, and nutrient availability. Knowing how these processes work in the Occoquan Reservoir can help predict changes in the system and mitigate any undesirable impact on the aquatic life. Additionally, it can help reservoir managers be prepared for any changes in storage capacity and water quality that might affect its function as a water supply source.

Table 4-2 presents a summary of important morphometric parameters of the reservoir. It has an elongated and narrow shape (900 ft. maximum width) and is relatively shallow with a mean depth of 16.7 ft. The deepest part of the reservoir, known as the lacustrine (lake-like) zone, is the area located near the dam and has a maximum depth of approximately 65 ft. The riverine shape of the reservoir makes it function like a plug flow system, which means there is limited mixing in the direction of the flow (OWML, 1998). The volume of the reservoir is 8.33 billion gallons, which is important because it influences the dilution capacity and is used to calculate flushing rates. The average hydraulic residence time for the Occoquan Reservoir is approximately 19.6 days.

Table 4-2. Occoquan Reservoir Morphometric Parameters

Parameter	Value	Source
Watershed Drainage Area	570 mi^2 (1,480 km^2)	OWML, 1998
Pool Area	1539 acres (6.23 km^2)	2010 Hydrographic Survey
Volume	8.33 billion gallons (31.4 $\times 10^6 m^3$)	2010 Hydrographic Survey
Watershed Area: Pool Area	238:1	Calculated
Length	14 mi (22.5 km)	Van Den Bos, 2003
Mean Depth	16.7 ft. (5.1 m)	Calculated
Maximum Depth	65 ft. (20m)	Grizzard, 2001
Maximum Width	900 ft. (275 m)	Van Den Bos, 2003
Dam Height	122 ft. (37.2 m) msl	OWML, 1998
Average Hydraulic Residence Time	19.6 days	Van Den Bos, 2003
Shoreline Development Index	10.9	OWML, 1998
Natural Safe Yield	65 mgd (250,000 m^3/d)	Van Den Bos, 2003
Reclaimed Water Addition	34 mgd (130,000 m^3/d)	UOSA, 2019

The pool surface area and storage capacity of the reservoir stated in Table 4-2 were obtained from the most recent hydrographic survey completed in 2010. This survey was by done by the OWML staff as explained in (OWML, 2011) using Global Positioning System (GPS) satellites to locate determined points along the reservoir, and an ultrasonic sounder which measured depth at each location. With the coordinates of the points and the corresponding values of depths referenced to the mean sea level, a topographic map was created and the area/volume were calculated using the Surfer for Windows software. The surface area and volume presented in the table refer to the values obtained at full pool elevation (122 ft. msl – height of the dam).

The Shoreline Development Index, D_L, is the ratio of a lake's shoreline length to the shoreline length of a perfectly circular lake that has the same area, and provides a measure of how far the lake is from the ideal circular lake. A perfectly circular lake would have a shoreline development index of 1. The Occoquan Reservoir's shoreline development index of 10.9 indicates a long shoreline, with lots of indentations (coves and inlets). The length is obvious from a quick look at a map of the Reservoir, but the indentations are not. The formula for the Shoreline Development Index is as follows:

$$D_L = \frac{L}{2\sqrt{\pi A}}$$

where *L*=shoreline length, and *A*=surface area, both in compatible units (such as ft. and ft^2).

Figure 4-6 and Figure 4-7 were graphed using the data from the topographic survey to show how volume and surface area change with respect to depth. Values in Figure 4-6 are expressed in absolute terms and are graphed with respect to mean sea level. On the other hand, values for Figure 4-7 are expressed as percentage with respect to the depth of the reservoir (the difference between the full pool elevation and each elevation above the mean sea level at which information was provided). For example, the reservoir is at 50% of its volume at approximately a 10 ft. depth.

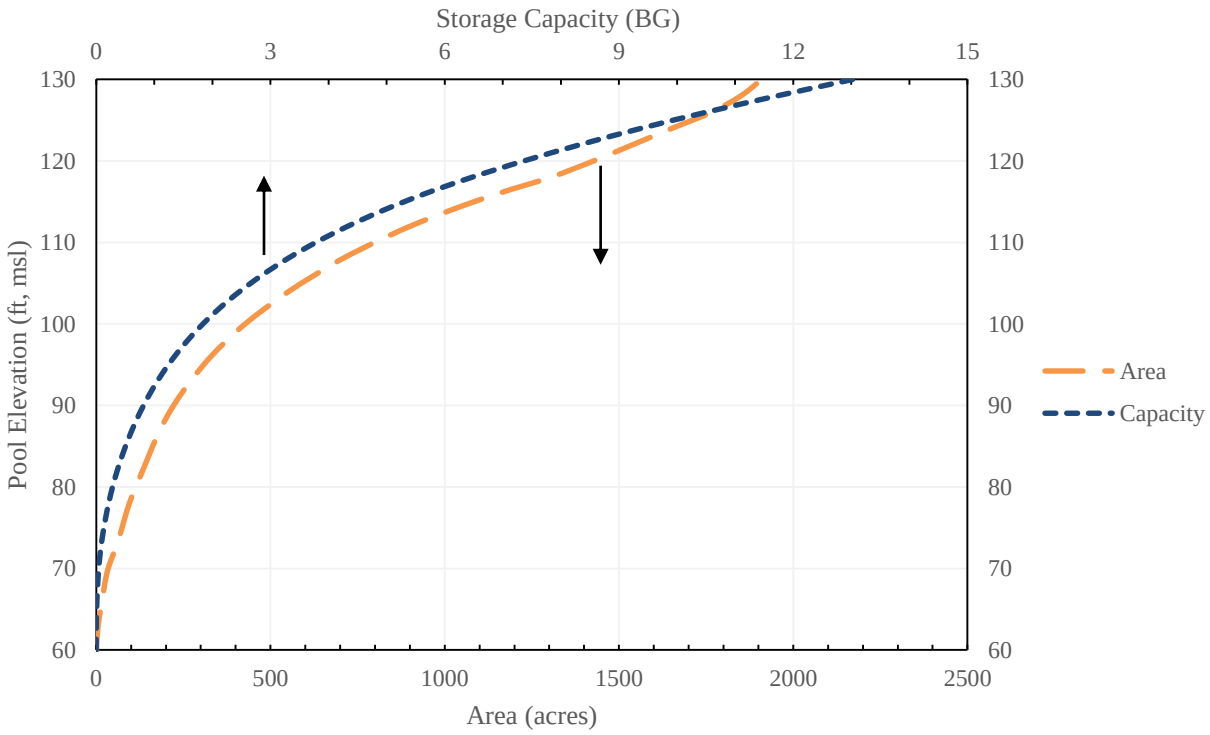

Figure 4-6. Area-Capacity Curve for the Occoquan Reservoir Expressed as a Value (2010 Hydrographic Survey)

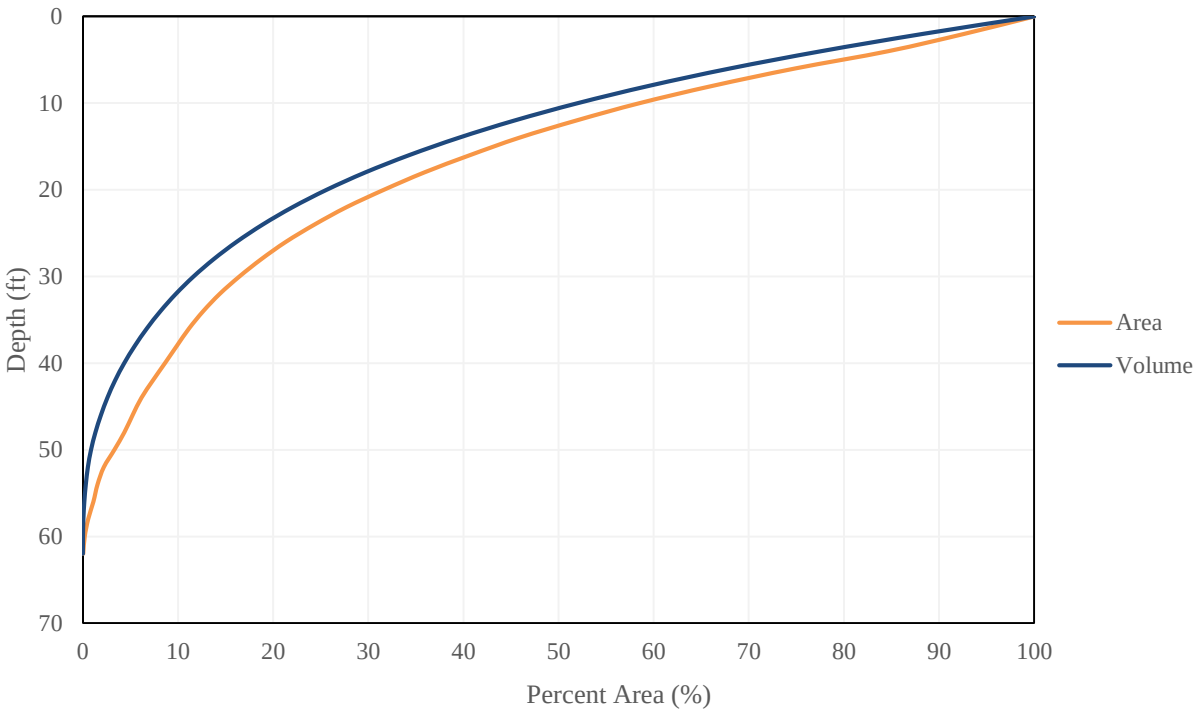

Figure 4-7. Area-Capacity Curve for the Occoquan Reservoir Expressed as a Percentage (2010 Hydrographic Survey)

Using the area values obtained from the hydrographic survey, along with daily pool elevations values shown in Figure 4-5, daily surface area was estimated for the Occoquan Reservoir from 1995 to 2019 and is shown in Figure 4-8. It can be observed that pool area is maintained mainly between 1200 and 1800 acres. Values that have gone below this range have occurred during 1998, 2002, 2006, and 2007. The dips in 2002 and 2007 may be likely due to low rainfall, since these were dry years according to the classification in the precipitation section. Surface area estimates were useful for the subsequent calculation of precipitation and evaporation volumes for the hydrologic balance that will be shown in the next section.

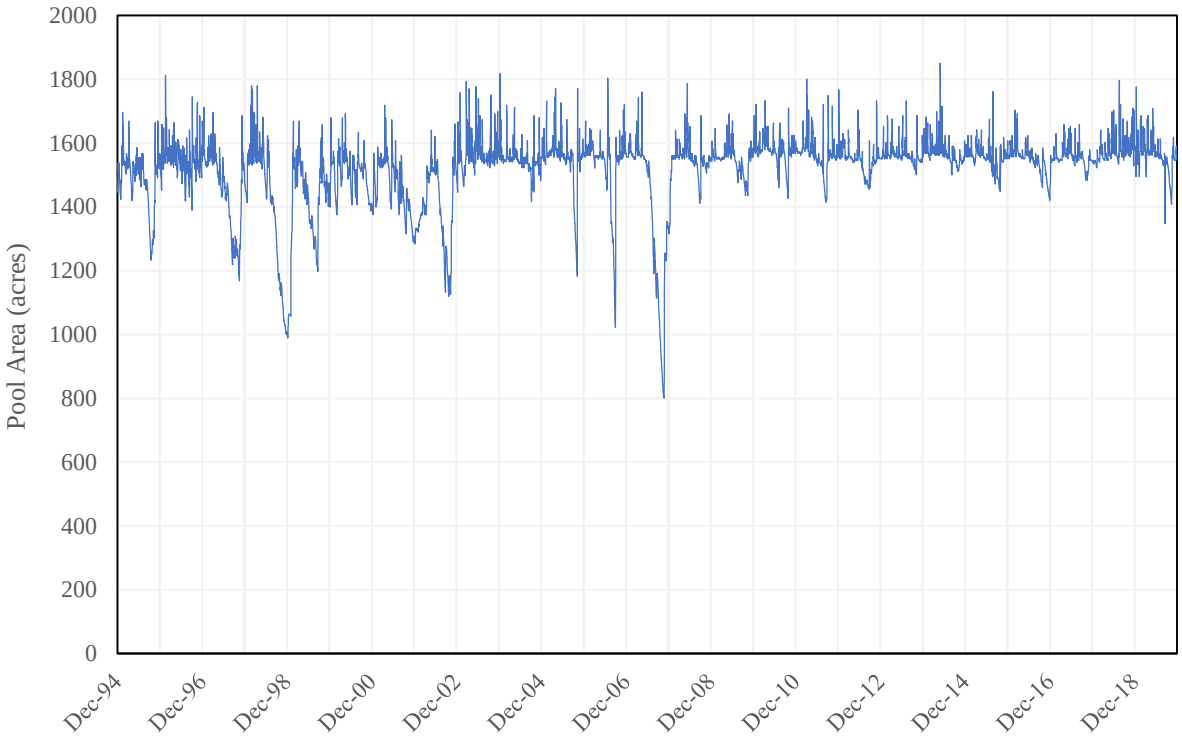

Figure 4-8. Time Series of Daily Surface Area of the Occoquan Reservoir, 1995–2019

There are records of storage capacity for 1957, 1995, 2000, 2005 and 2010 (Table 4-3). As it was explained in a previous assessment (OWML, 1998), there are differences between the original information from 1957 (11.25 BG) and the hydrographic survey performed in 1995 (8.52 BG), likely due to following reasons: (1) normal reservoir storage loss due to deposition and internal generation of sediment from settling organic matter which can be up to 2% annually, (2) difference in methods employed to determine contour lines to calculate values, (3) resuspension of sediments due to high internal water velocities during large runoff events. Since the 1995 survey, however, storage capacity values in the subsequent surveys have not experienced a significant change (Figure 4-9). From 1995 to 2010, the storage capacity of the reservoir decreased approximately 2.2%. Assuming that the original 11.25 BG estimate from fairly low-resolution survey maps was in error, the low rate of storage loss since 1995 is likely due to periodic flushing of sediments during high flow events.

Table 4-3 Summary of Storage Capacity Values for Different Surveys

Year	Storage Capacity (BG)	Method
1957	11.25	Original estimate from topographic maps
1995	8.52	Hydrographic Survey using GPS/Acoustic Sounding System
2000	8.31	Hydrographic Survey using GPS/Acoustic Sounding System
2005	8.27	Hydrographic Survey using GPS/Acoustic Sounding System
2010	8.33	Hydrographic Survey using GPS/Acoustic Sounding System

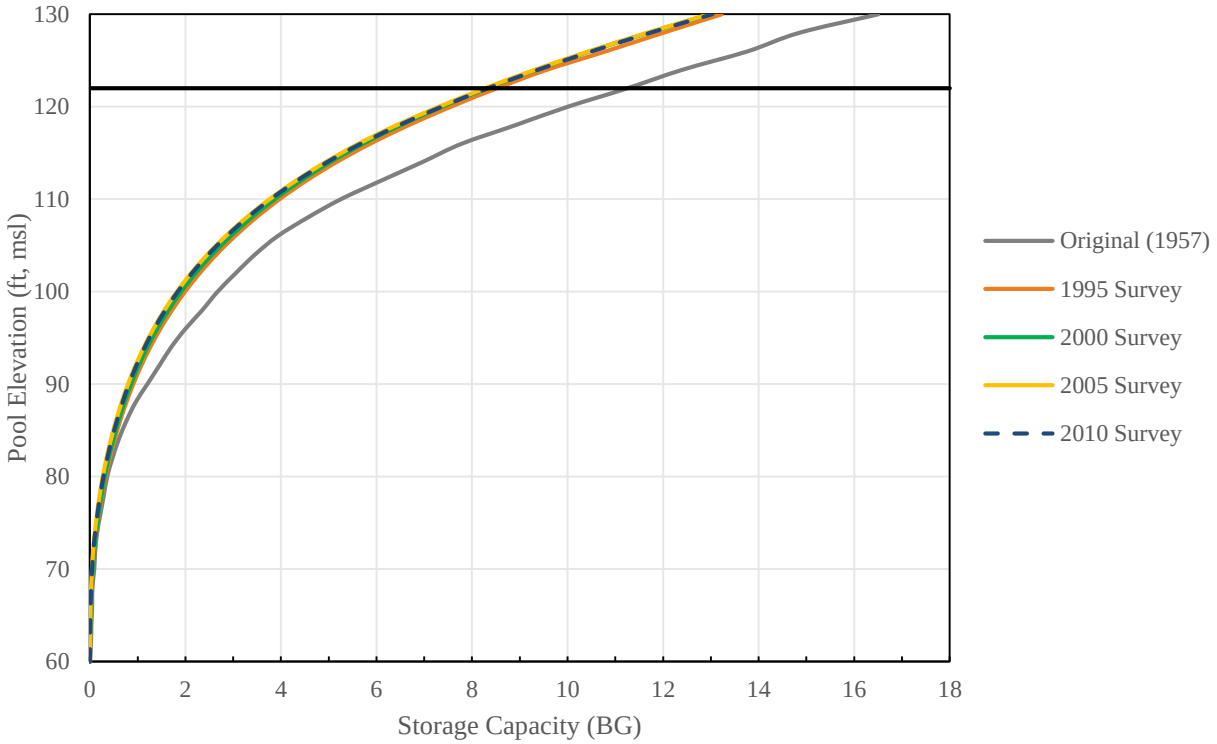

Figure 4-9. Occoquan Reservoir Storage Change 1957–2019

4.1.4 Hydrologic Budget for the Occoquan Reservoir

The hydrologic balance estimated for the Occoquan Reservoir for 1983 to 2019 is shown in Table 4-4. It can be observed that the majority of the inflow corresponds to the Occoquan Creek flow. On average, from 1983 to 2019, 56% of the inflow comes from the Occoquan Creek, while 37% corresponds to Bull Run (Figure 4-10). This is likely because the Occoquan Creek has a larger drainage area (369 mi^2) than Bull Run (201 mi^2). During the period of record, there were three POTWs that contributed to the stream flow: Nokesville, Vint Hill, and the MHR WRF. However, as it can be observed in Table 4-4 and Figure 4-11, the highest contribution comes from the MHR WRF, averaging a daily discharge of 34 million gallons in 2019. Nokesville has not been in operation since 2002. Precipitation inputs correspond to roughly only 1% of total inflow.

As shown in Table 4-4, the majority of the flow that is lost from the Occoquan Reservoir occurs via overflow at the spillway and for water abstracted for treatment. Evaporation only accounts for an average of 1% of the water loss of the reservoir.

Table 4-4. Hydrologic Data for the Occoquan Reservoir, 1983–2019

Year	Inflows						Outflows			Difference	
	Occoquan Creek	*Bull Run*	*MHR WRF*	*Other POTWs*	*Direct Rain*	***Total Inflow***	*Occoquan Dam*	*Reservoir Evaporation*	***Total Outflow***	*Inflow - Outflow*	
	(Annual flow in cubic feet x 10^10)										*(%)*
1983	1.633	0.799	0.045	0.001	0.029	2.508	2.479	0.022	2.502	0.006	0.25
1984	2.148	1.194	0.051	0.001	0.032	3.427	3.429	0.024	3.453	-0.026	-0.75
1985	0.764	0.547	0.045	0.001	0.022	1.380	1.192	0.022	1.213	0.167	12.11
1986	0.500	0.352	0.049	0.001	0.017	0.919	1.010	0.022	1.031	-0.112	-12.21
1987	0.973	0.666	0.062	0.001	0.025	1.728	1.982	0.024	2.006	-0.278	-16.08
1988	0.825	0.648	0.065	0.001	0.019	1.560	1.606	0.021	1.627	-0.067	-4.31
1989	1.445	0.701	0.082	0.001	0.029	2.257	2.280	0.024	2.304	-0.047	-2.06
1990	0.947	0.601	0.081	0.001	0.026	1.656	1.884	0.023	1.908	-0.252	-15.22
1991	0.804	0.509	0.081	0.001	0.022	1.416	1.477	0.023	1.500	-0.084	-5.95
1992	1.096	0.589	0.091	0.001	0.027	1.806	1.696	0.023	1.720	0.086	4.76
1993	1.801	0.987	0.095	0.001	0.027	2.910	3.354	0.021	3.375	-0.465	-15.98
1994	1.648	1.019	0.107	0.001	0.029	2.805	3.077	0.024	3.100	-0.296	-10.54
1995	0.718	0.558	0.095	0.001	0.018	1.389	1.549	0.019	1.568	-0.179	-12.91
1996	2.505	1.221	0.110	0.001	0.024	3.861	3.556	0.020	3.576	0.285	7.39
1997	1.136	0.727	0.107	0.001	0.017	1.987	2.079	0.018	2.097	-0.110	-5.55
1998	1.803	1.031	0.118	0.001	0.021	2.973	3.126	0.019	3.145	-0.171	-5.76
1999	0.439	0.589	0.114	0.001	0.020	1.162	1.153	0.019	1.172	-0.010	-0.84
2000	0.574	0.562	0.119	0.001	0.019	1.274	1.510	0.020	1.530	-0.256	-20.11
2001	0.556	0.519	0.123	0.000	0.018	1.217	1.288	0.019	1.307	-0.091	-7.46
2002	0.259	0.405	0.117	0.000	0.017	0.797	0.770	0.018	0.788	0.009	1.09
2003	2.472	1.711	0.150	0.000	0.033	4.367	4.846	0.020	4.866	-0.499	-11.42
2004	1.267	0.812	0.136	0.000	0.023	2.238	2.453	0.020	2.473	-0.235	-10.50
2005	1.158	0.954	0.141	0.000	0.023	2.276	2.395	0.020	2.415	-0.139	-6.11
2006	1.297	0.945	0.145	0.001	0.023	2.411	2.483	0.020	2.503	-0.092	-3.82
2007	0.735	0.470	0.139	0.000	0.013	1.358	1.473	0.018	1.490	-0.133	-9.77
2008	0.858	0.885	0.146	0.001	0.022	1.913	2.053	0.020	2.074	-0.161	-8.40
2009	0.927	0.785	0.147	0.001	0.020	1.880	1.841	0.018	1.859	0.021	1.13
2010	1.428	0.852	0.157	0.001	0.022	2.459	2.650	0.022	2.672	-0.212	-8.63
2011	1.242	0.834	0.155	0.001	0.023	2.255	2.282	0.020	2.302	-0.048	-2.11
2012	1.081	0.657	0.149	0.001	0.021	1.909	1.920	0.022	1.941	-0.032	-1.69
2013	1.199	0.802	0.155	0.001	0.023	2.179	2.272	0.022	2.294	-0.114	-5.25
2014	2.013	1.222	0.167	0.001	0.026	3.429	3.203	0.022	3.225	0.204	5.95
2015	1.103	0.939	0.160	0.001	0.021	2.225	2.109	0.022	2.132	0.093	4.19
2016	0.993	0.778	0.158	0.001	0.017	1.948	2.019	0.024	2.043	-0.095	-4.89
2017	0.664	0.630	0.154	0.001	0.021	1.470	1.553	0.024	1.577	-0.107	-7.25
2018	2.163	1.389	0.175	0.002	0.031	3.760	4.108	0.024	4.132	-0.373	-9.91
2019	1.564	1.051	0.168	0.002	0.024	2.809	3.311	0.025	3.336	-0.527	-18.78

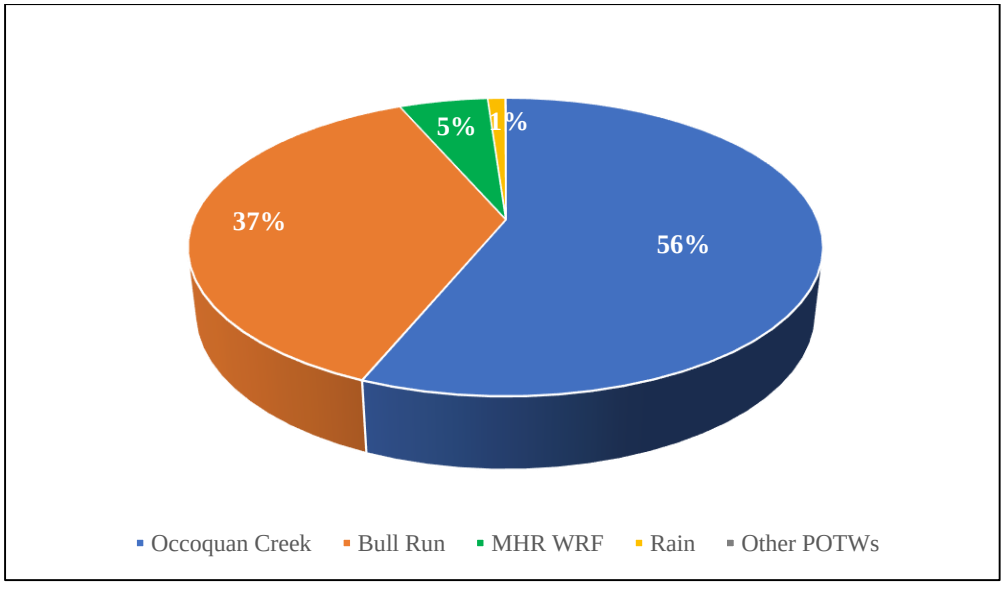

Figure 4-10. Distribution of Inflow to the Occoquan Reservoir, 1983–2019

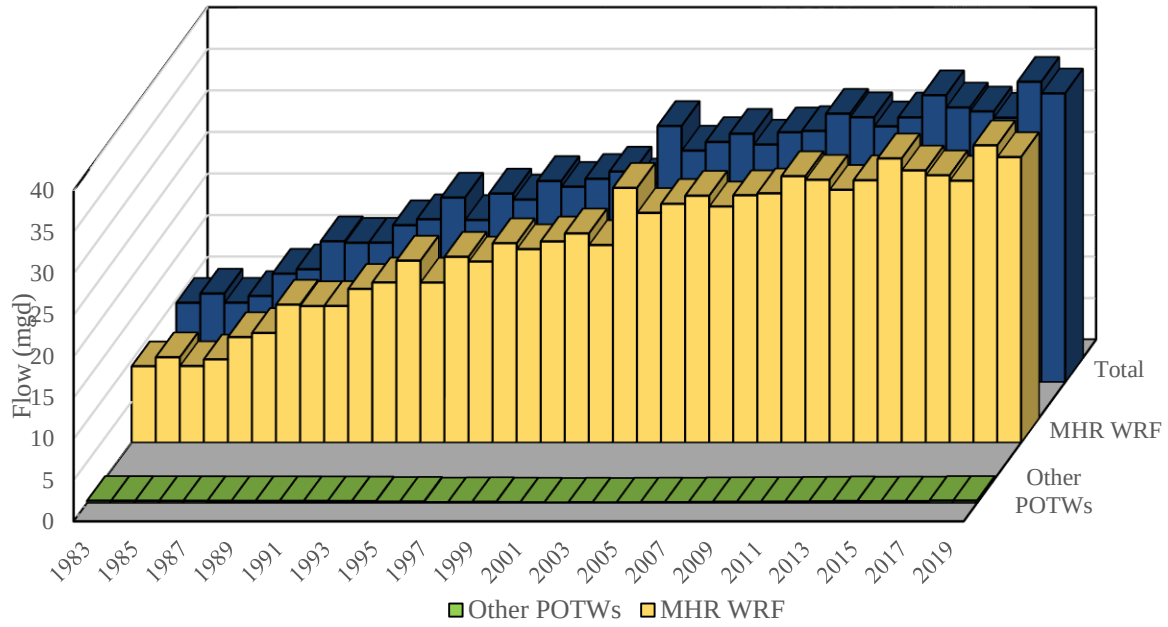

Figure 4-11. Occoquan Watershed POTWs Annual Flow, 1983–2019

Figure 4-12 shows that the relationship between rainfall and runoff for the Occoquan Watershed is best expressed as linear. The calculated average runoff for the period of record is 15.25 inches. This value can also be predicted from the graph reading the value for the y-axis corresponding to the 40.03 inches of average rainfall calculated for the period of record.

On average, the difference between total inflow and total outflow for the period of record is approximately 5%. However, as Table 4-4 and Figure 4-13 show, when analyzing each individual year there are differences of up to -20%. Figure 4-13, demonstrates that for the majority of the years, the outflow is greater than the inflow. This may be an indication that either the outflow values are overestimated or inflow values may be underestimated. Annual inflow vs annual outflow values were graphed to further illustrate the relationship between inputs and outputs for the reservoir, and compared to the 1:1 relationship it would follow if inflow would equal total outflow (Figure 4-14).

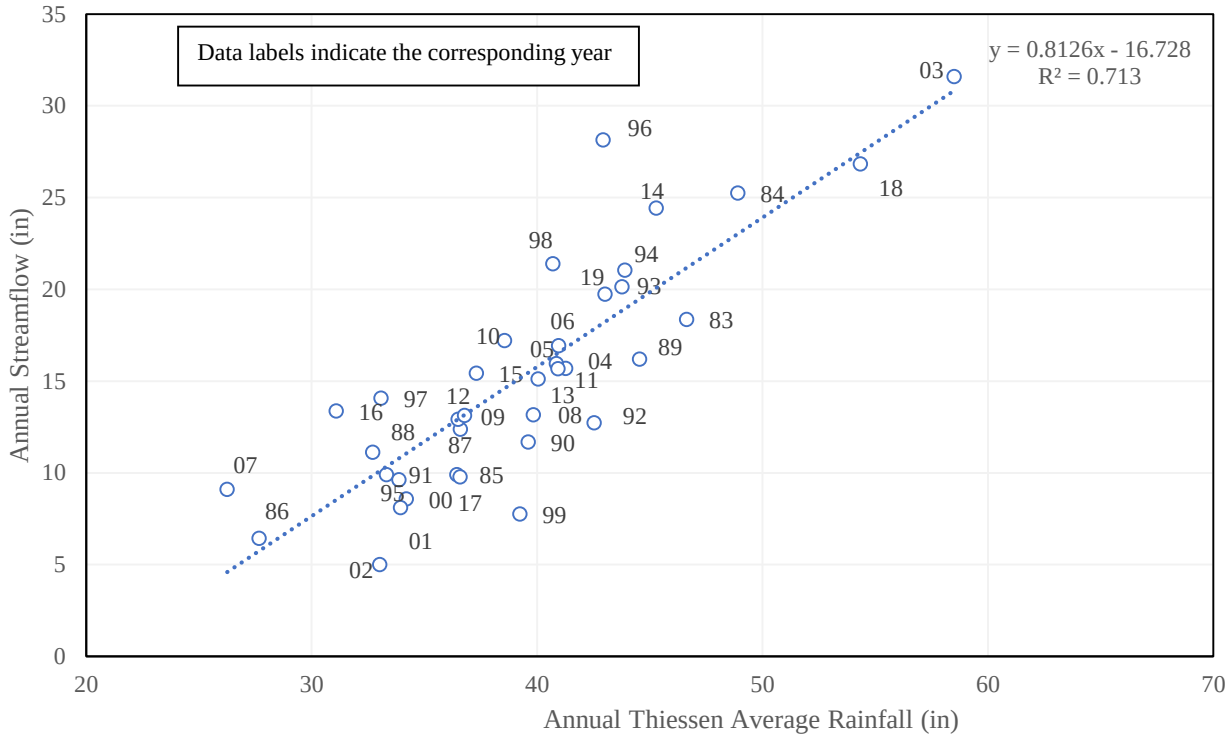

Figure 4-12. Streamflow and Rainfall Relation at the Occoquan Watershed

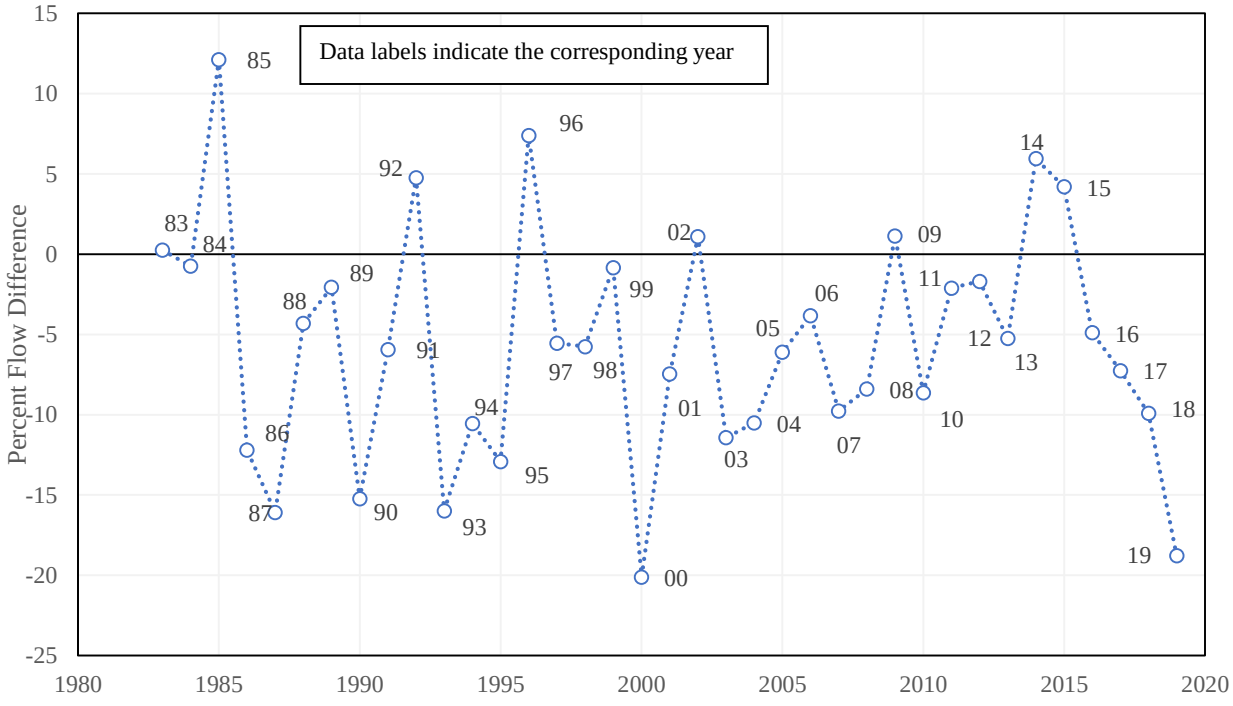

Figure 4-13. Occoquan Watershed Inflow and Outflow Difference

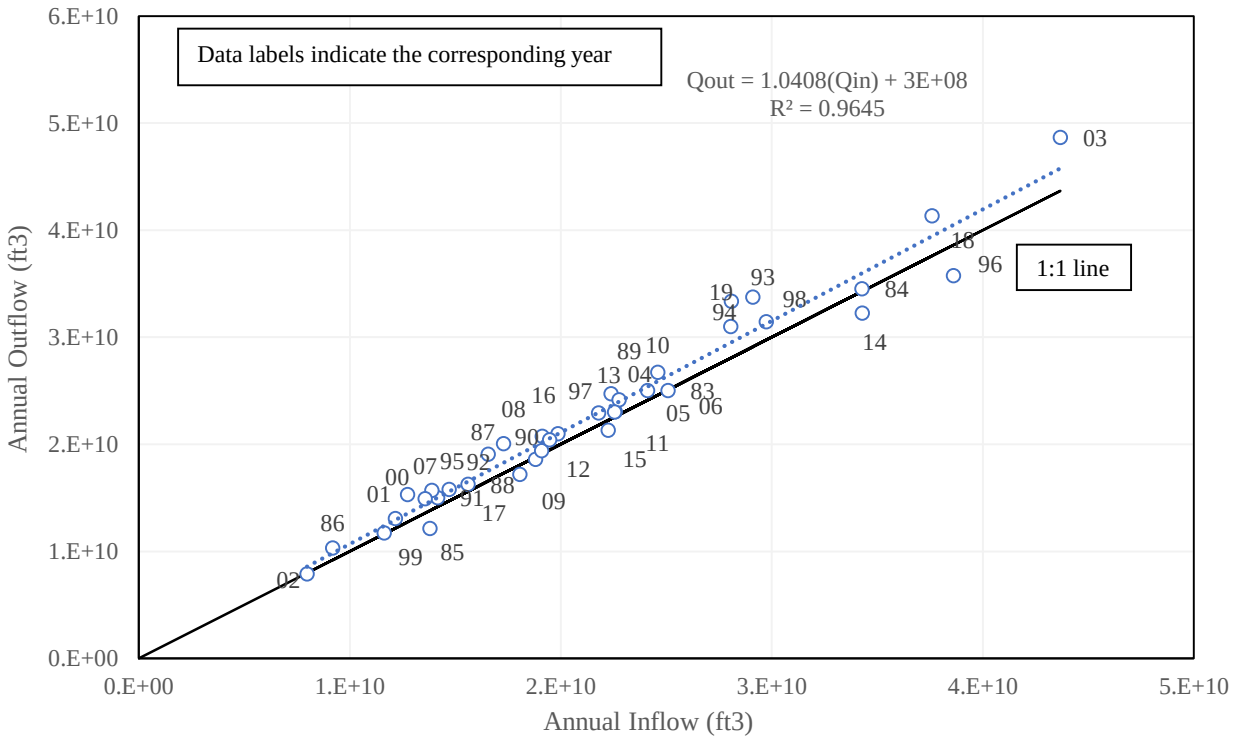

Figure 4-14. Comparison of Annual Inflows and Outflows at the Occoquan Watershed, 1983–2019

4.2 Watershed Water Quality

4.2.1 Introduction

Studying stream water quality helps identify pollutants coming from the watershed and determine effects on biodiversity and water withdrawn for usage. In order to perform an analysis on the Occoquan Watershed, flow information and water chemistry data obtained from the stream monitoring stations were used to (1) monitor variations in the concentrations of constituents through time and location, and (2) determine the loads of pollutants flowing into the Occoquan Reservoir. This section presents an analysis of important water chemistry parameters from four (4) main stream stations: ST01, which corresponds to the outflow point of the reservoir, ST10 which represents the inflow from one of the two main tributaries (Occoquan Creek arm), and ST40/45 which characterize the inflow from Bull Run, the other main tributary. Load calculations were performed using data from ST01, ST25, ST30, ST40, and ST45. Data are mainly presented as seasonal average concentrations. Tables from the Mann-Kendall analysis are provided to indicate increasing or decreasing trends and statistical significance.

4.2.2 Millard H. Robbins, Jr. Water Reclamation Facility Water Quality

Due to the water quality degradation that the Occoquan Reservoir experienced in the 1960s, UOSA was established as mandated by the Occoquan Policy and the WRF managed by UOSA came into

operation in 1978. This WRF was designed to have advanced wastewater treatment to be able to comply with the stringent permit limitations set by the VSWCB (now the Virginia Department of Environmental Quality, or VDEQ) and the USEPA for indirect discharges to a public water supply. Initially, the plant started with a capacity of 10 mgd; however, it is now able to treat 54 mgd. This WRF is not only able to work under nitrification mode, but can also accommodate for stand-by biological nitrogen removal.

Table 4-5 shows the current effluent limits set for the MHR WRF in the Virginia Pollutant Discharge Elimination System (VPDES) and Virginia State Water Control Law permit. During summer, when thermal stratification is present, the plant is allowed to discharge oxidized nitrogen, instead of removing it completely, to improve the water quality of the reservoir. Highly nitrified effluent is discharged to prevent the release of phosphorus that could increase the growth of undesired algal species in the reservoir (more about this later in the lake analysis section). However, because the drinking water limit of nitrate is 10 mg/l, the MHR WRF is required by the Occoquan Policy to completely remove nitrogen when reservoir nitrate concentrations (as N) at the Fairfax Water Griffith plant intake reach 5 mg/l or higher values.

The MHR WRF has been in operation for approximately 40 years and has constituted 5–10% of the annual inflow to the reservoir in the last 15 years (Figure 4-15). For this reason, MHR WRF effluent discharges are constantly monitored to ensure compliance. Figure 4-16 shows monthly average concentrations for COD, TP, TSS, MBAS, TKN, and turbidity from 2005 to 2019. It can be observed that average monthly concentrations of these parameters have been maintained at concentrations within their respective limits. A summary of the MHR WRF's effluent water characteristics for the entire period of record is also shown (Figure 4-17). The concentrations graphed correspond to median values from 1982 to 2019 and compare to the permit limits, where appropriate. Median values are all under the limits established in the *Occoquan Policy*.

Table 4-5. Permit Limits for the MHR WRF Effluent, VDEQ 2018

Water Quality Parameter	Monthly Average	Unit
Chemical Oxygen Demand (COD)	10.0	mg/l
Total Phosphorus (TP)	0.1	mg/l
Total Suspended Solids (TSS)	1.0	mg/l
Methylene Blue Active Substances (MBAS)	0.1	mg/l
Unoxidized nitrogen (TKN)	1.0	mg/l
Turbidity	0.5	NTU

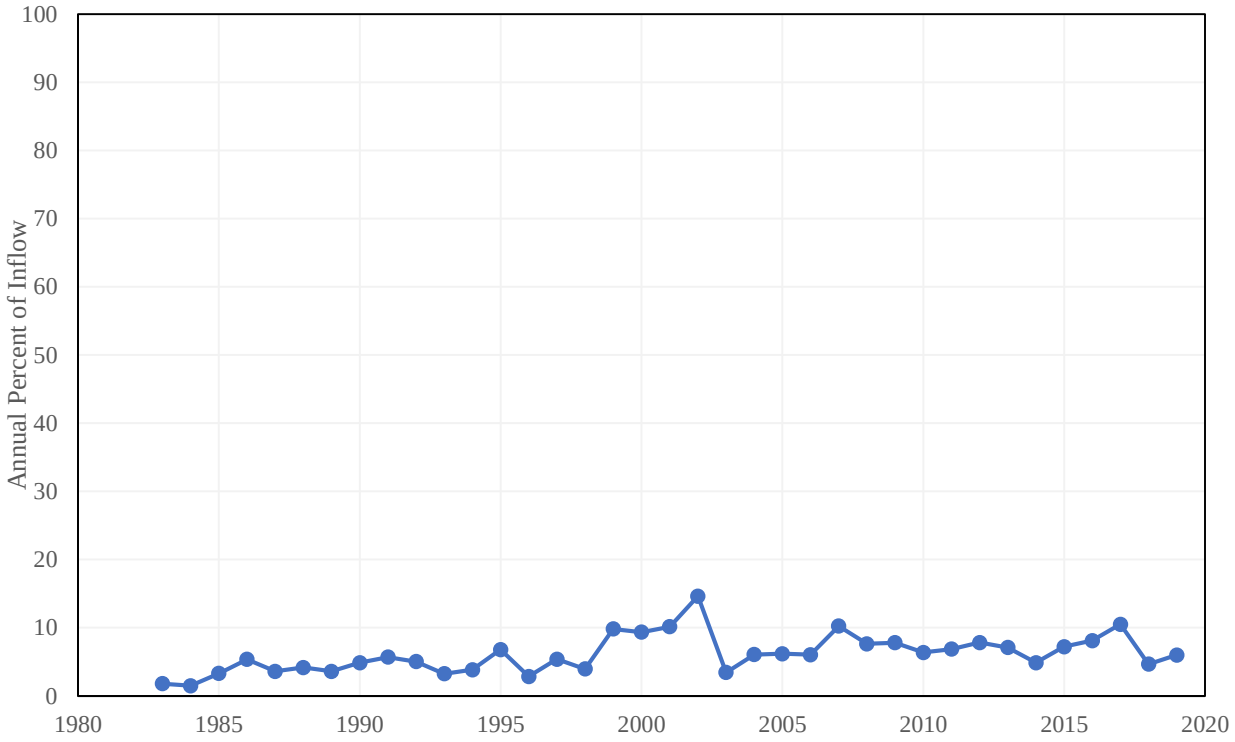

Figure 4-15. Annual Percentage of the MHR WRF Contribution to Reservoir Inflow, 1983–2019

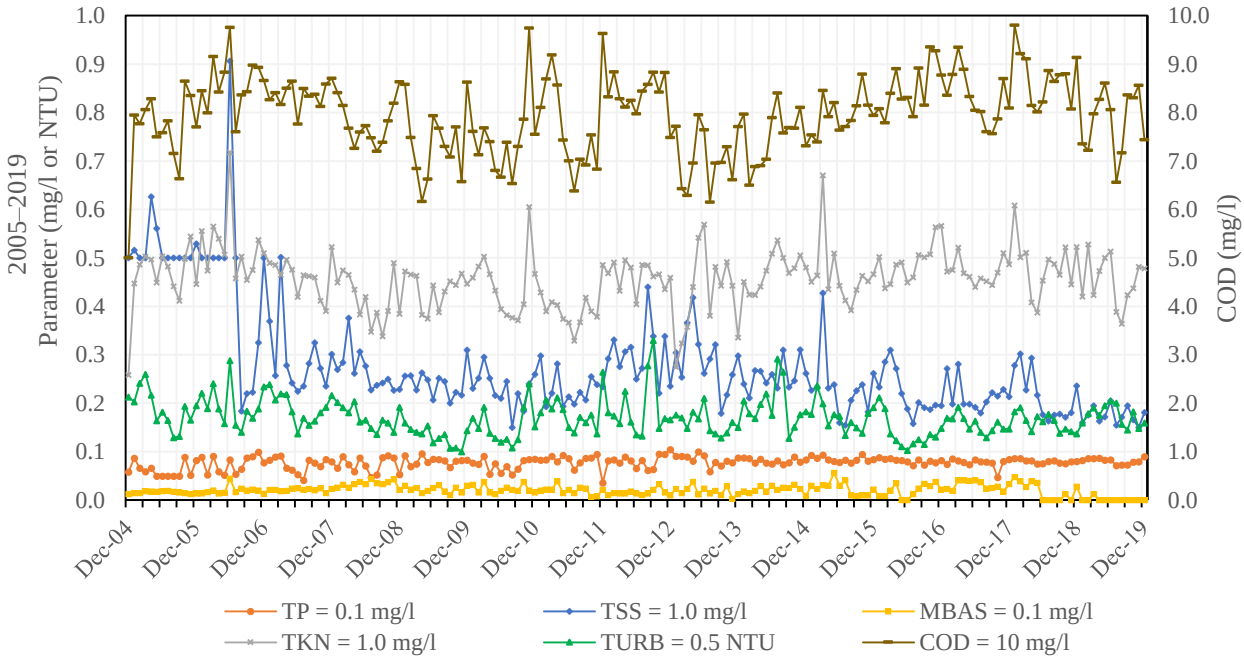

* TP = total phosphorus; MBAS = methylene blue active substances; TURB = Turbidity; TSS = total suspended solids; TKN = total Kjeldahl nitrogen; COD = chemical oxygen demand.

Figure 4-16. Monthly Average Concentrations of the MHR WRF Final Effluent Water Quality Parameters, 2005–2019

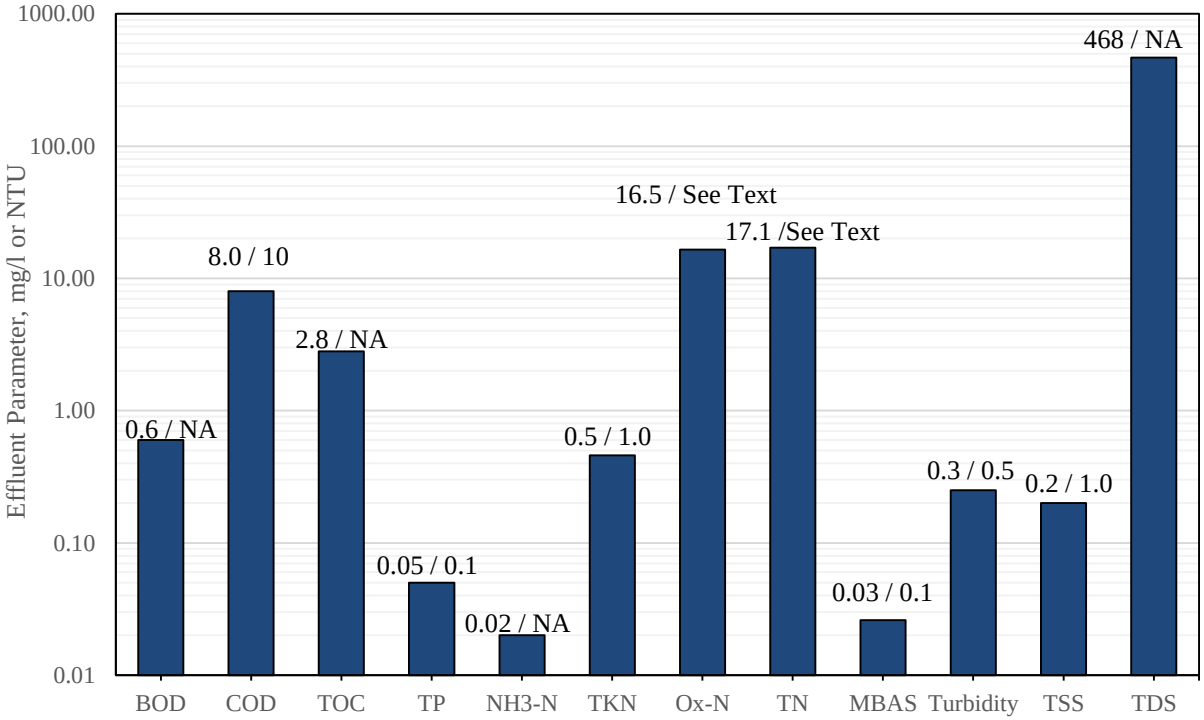

* BOD = biochemical oxygen demand; COD = chemical oxygen demand; TOC = total organic carbon; TP = total phosphorus; NH3-N = ammonia nitrogen; TKN = total Kjeldahl nitrogen; Ox-N = oxidized nitrogen; TN= total nitrogen; MBAS = methylene blue active substances; TURB = Turbidity; TSS = total suspended solids; TDS = total dissolved solids.

Figure 4-17. Median Values of MHR WRF Effluent Water Quality Parameters, 1982–2019

4.2.3 Water Quality in Tributary Streams

4.2.3.1 Temperature

Water temperature is important because it effects the chemical and biological processes of a stream or reservoir. It defines the type of organisms that live in the waterbody, since different organisms survive at different temperatures. Temperature also drives chemical reactions occurring in streams, therefore, having an effect on other parameters such as pH, and the concentrations of dissolved constituents found in the water. Additionally, water temperature of the streams has an effect on the circulation pattern of the Occoquan Reservoir.

Table 4-6 presents the seasonal average temperature, median and standard deviation for the entire period of record of the stations that characterize the reservoir inflow: ST10, ST40 and ST45. Table 4-7 shows the values for ST01, representing outflow average temperature. Additionally, Figure 4-18 presents seasonal average temperature by year from 1973 to 2019 with its respective standard deviation (gray bars). As anticipated, the highest average temperatures can be observed in summer, reaching up to 30°C, followed by fall with temperatures ranging from 13°C to 22°C, then spring

with values between 12°C and 20°C, and finally winter, the coolest season with average temperatures falling to 1°C. Temperatures at the inflow points tend to be lower than the outflow, particularly during summer and fall, which may be caused by the effects of solar radiation on the higher surface area and lower horizontal velocities of the Occoquan Reservoir. Comparing average temperatures between the stations corresponding to Bull Run, it can be observed that ST45, which is farther from the reservoir, has higher temperatures in all seasons than ST40. In winter and spring, ST45 average and median temperatures for the entire period of record are higher than ST01. Daily water temperatures have not exceeded the VDEQ maximum temperature criteria of 32°C for Class III nontidal waters, on stations on the inflow stations (ST10,40,45). ST01 has only had four days in which the temperature was slightly higher than (less than 34°C) this maximum during the entire period of record.

It can also be observed in Figure 4-18 that there is an upward trend for temperature at the four (4) stations and seasons. This trend was then confirmed by the Mann-Kendall test results (Table 4-8). Kendall tau and Sen Slope values included on the table are all positive, indicating an upward trend for temperature. The Sen Slope is a value that represents the magnitude of the trend. Bold values in the table correspond to those trends that are significant at a 90% confidence interval or greater ($p \leq 0.1$). It can be observed that temperature trends for ST10, ST40, and ST45 are significant for all seasons, with the exception of the summer trend for ST45. On the other hand, the only significant trend for ST01 occurs during winter. DO and alkalinity trends that are displayed on this table will be discussed in subsequent sections.

Table 4-6. Seasonal Average Temperature (°C) at Inflow Stream Stations, 1973–2019

Season	ST10			ST40			ST45		
	Mean	*Median*	*Standard Deviation*	*Mean*	*Median*	*Standard Deviation*	*Mean*	*Median*	*Standard Deviation*
Winter	4.22	4.00	2.43	4.31	4.00	3.00	6.04	6.00	2.82
Spring	15.02	15.30	5.22	14.64	15.00	5.00	16.18	16.30	4.85
Summer	25.56	26.00	2.55	23.99	24.00	2.50	25.44	25.80	2.20
Fall	16.26	16.00	5.63	15.62	15.50	5.24	17.43	17.40	5.24

Table 4-7. Seasonal Average Temperature (°C) at Outflow Stream Station, 1979–2019

Season	ST01		
	Mean	*Median*	*Standard Deviation*
Winter	5.14	5.00	2.56
Spring	15.52	16.00	5.80
Summer	27.21	27.50	2.40
Fall	18.84	19.00	5.40

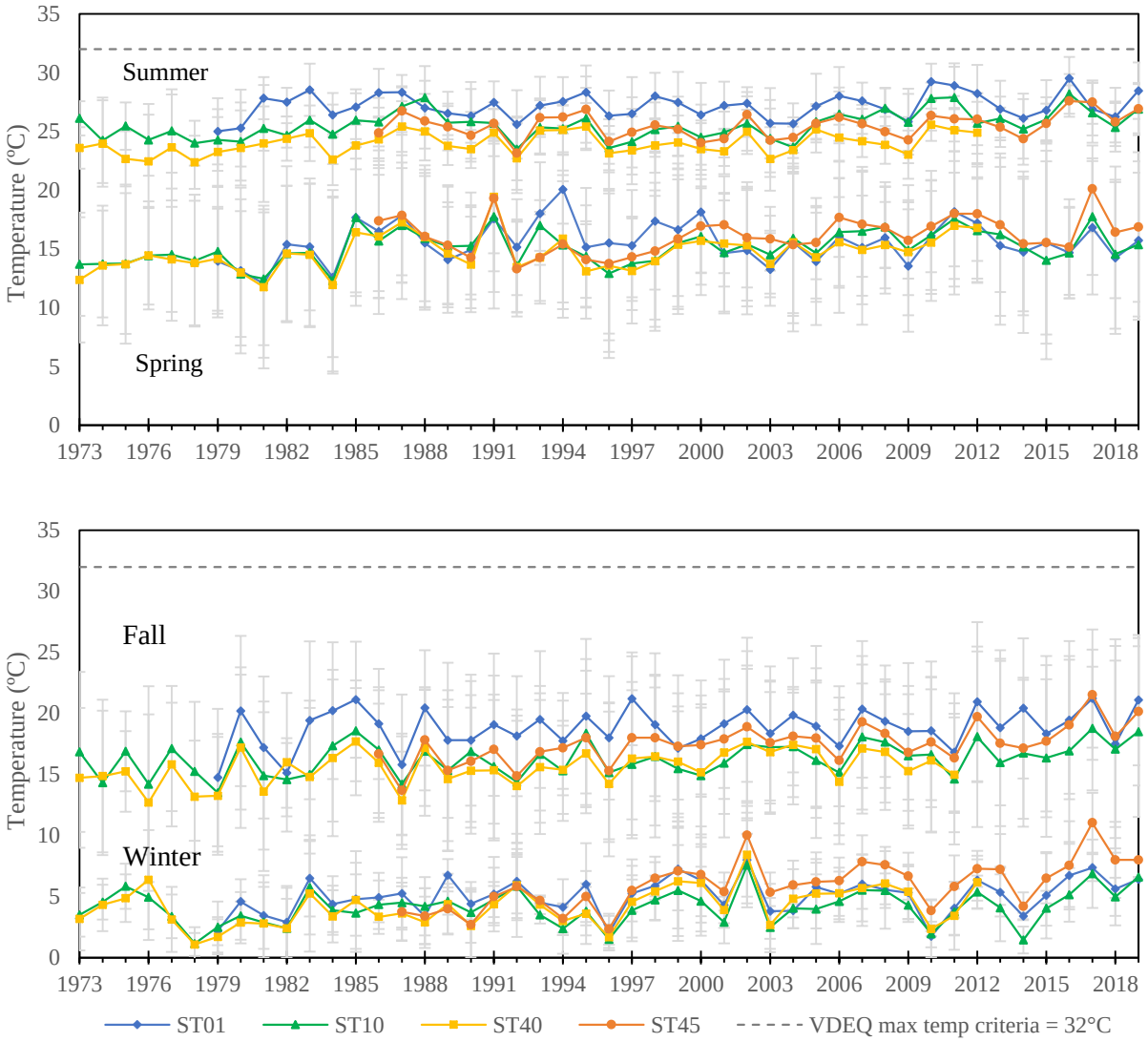

Figure 4-18. Seasonal Average Temperature at Stream Stations, 1973–2019

Table 4-8. Mann-Kendall Trends for Stream Temperature, Dissolved Oxygen, and Alkalinity, 1973–2019

Station	Season	Temperature				Dissolved Oxygen				Alkalinity			
		Sen Slope	*Kendall Tau*	*p-value*	*Trend*	*Sen Slope*	*Kendall Tau*	*p-value*	*Trend*	*Sen Slope*	*Kendall Tau*	*p-value*	*Trend*
ST01	Winter	0.042	0.222	**0.042**	↗	-0.021	-0.190	**0.082**	↘	0.394	0.295	**0.007**	↗
	Spring	0.013	0.073	0.507	↗	-0.010	-0.105	0.340	↘	0.490	0.556	**3.6E-07**	↗
	Summer	0.007	0.039	0.728	↗	0.003	0.026	0.822	↗	0.464	0.461	**2.3E-05**	↗
	Fall	0.032	0.157	0.151	↗	-0.022	-0.257	**0.018**	↘	0.465	0.371	**0.001**	↗
ST10	Winter	0.024	0.179	**0.078**	↗	0.012	0.209	**0.039**	↗	0.450	0.475	**2.6E-06**	↗
	Spring	0.046	0.302	**0.003**	↗	-0.010	-0.230	**0.023**	↘	0.384	0.537	**1.2E-07**	↗
	Summer	0.036	0.276	**0.006**	↗	-0.029	-0.465	**4.2E-06**	↘	0.455	0.502	**7.2E-07**	↗
	Fall	0.043	0.254	**0.012**	↗	-0.019	-0.243	**0.016**	↘	0.527	0.412	**4.7E-05**	↗
ST40	Winter	0.059	0.272	**0.014**	↗	0.014	0.209	**0.059**	↗	1.206	0.662	**2.0E-09**	↗
	Spring	0.053	0.299	**0.007**	↗	-0.032	-0.323	**0.003**	↘	1.140	0.754	**8.0E-12**	↗
	Summer	0.027	0.226	**0.041**	↗	-0.065	-0.461	**3.0E-05**	↘	0.847	0.710	**1.2E-10**	↗
	Fall	0.054	0.290	**0.010**	↗	-0.012	-0.132	0.241	↘	0.913	0.525	**2.7E-06**	↗
ST45	Winter	0.131	0.519	**2.5E-05**	↗	0.022	0.224	**0.070**	↗	0.602	0.280	**0.023**	↗
	Spring	0.056	0.207	**0.088**	↗	-0.007	-0.041	0.744	↘	0.709	0.540	**7.6E-06**	↗
	Summer	0.028	0.166	0.173	↗	-0.034	-0.326	**0.007**	↘	0.551	0.561	**3.2E-06**	↗
	Fall	0.086	0.433	**3.5E-04**	↗	-0.033	-0.330	**0.006**	↘	0.180	0.194	0.109	↗

4.2.3.2 Dissolved Oxygen

DO is an indicator of the biochemical processes occurring in a waterbody. The amount of DO available has an effect on the survival of aquatic organisms, as well as the solubility of inorganic nutrients and trace metals. For instance, low DO levels can cause fish kills, the release of sediment phosphorus, iron, manganese, and ammonia. Oxygen is added to the waterbody from the atmosphere or through photosynthesis from aquatic plants, and its solubility is dependent mainly on water temperature. Warmer waters hold less DO than cooler waters. Other factors that influence DO levels are barometric pressure (low pressure, low oxygen solubility) and salinity (high salinity, low oxygen holding capacity). Oxygen sinks are due to metabolic respiration of aquatic plants, animals and bacteria.

Tables 4-9 and 4-10 summarize DO levels from 1973 to 2019 for each station. The overall average DO for the outflow lies between 6–11 mg/l and 7–13 mg/l for the inflow stations. The lowest DO values during winter and fall are observed at ST01, while the lowest spring and summer values are observed at ST40 and ST45, respectively. Figure 4-19 presents the seasonal average values for each year by station and its standard deviation. In general terms, higher DO levels are seen in winter, followed by spring, then fall, and finally summer, following the expected opposite pattern as temperature. The only exception is ST01, which shows lower DO values in fall rather than summer. The lowest DO average value (4 mg/l) for the period of record occurred during the fall of 2009 at ST01 and the highest (14 mg/l) occurred in winter 2014 at station ST45.

In general terms, significant results from the Mann-Kendall statistical test for DO show a slightly negative trend for all seasons except winter (Table 4-8). During winter, there is a slightly upward trend at ST10, ST40, and ST45, while ST01 shows a downward trend, all at a significant level (p<0.1). In spring, there is a negative trend at all stations, although the only significant trends occur at ST10 and ST40. Summer trends at ST10, ST40, and ST45 are all negative with a high confidence

interval, while ST01 is positive but not statistically significant. During fall, significant negative trends can be observed at ST01, ST10, and ST45.

In the previous water quality assessment (Van Den Bos, 2003), it was shown that from 1973 to 2002 there were 20 days in which ST01 presented DO levels that were less than the 4 mg/l minimum daily value specified in the VDEQ water quality criteria, four (4) days from ST10 and three (3) days for ST40. Table 4-11 presents the dates for which this has occurred in ST01 since then (2003–2019). In the last 17 years, there have been 38 days were records of the daily DO concentration being less than 4 mg/l, most of which occurred during fall (35 records for fall). ST10 and ST40 records show no values less than 4 mg/l since 2002, and ST45 show no minimum DO level violations for the entire period of record (1986–2019).

Table 4-9. Seasonal Average Dissolved Oxygen (mg/l) at Inflow Stream Stations, 1973–2019

Season	ST10			ST40			ST45		
	Mean	*Median*	*Standard Deviation*	*Mean*	*Median*	*Standard Deviation*	*Mean*	*Median*	*Standard Deviation*
Winter	12.64	12.80	1.08	12.71	12.80	1.18	13.15	13.00	1.31
Spring	10.17	10.00	1.45	9.99	9.95	1.60	10.39	10.20	1.84
Summer	7.54	7.61	1.18	7.82	7.72	1.48	7.41	7.40	1.08
Fall	9.17	9.20	1.84	9.47	9.40	1.78	9.22	9.00	1.85

Table 4-10. Seasonal Average Dissolved Oxygen (mg/l) at Outflow Stream Station, 1979–2019

Season	ST01		
	Mean	*Median*	*Standard Deviation*
Winter	10.64	10.80	1.56
Spring	10.24	10.30	1.72
Summer	7.87	8.07	1.64
Fall	6.00	6.00	1.83

Table 4-11. Dissolved Oxygen Concentrations under 4mg/l at Stream Outflow Station (ST01), 2003–2019

Date	*DO (mg/l)*	*Date*	*DO (mg/l)*	*Date*	*DO (mg/l)*
07/26/2004	3.83	11/05/2007	3.81	11/08/2010	3.52
09/07/2004	2.59	11/13/2007	3.65	09/19/2011	3.67
09/13/2004	2.47	08/18/2008	3.76	09/26/2011	2.8
09/20/2004	2.95	10/14/2008	2.88	10/03/2011	3.24
10/18/2004	3.36	10/20/2008	2.2	09/24/2012	3.41
08/29/2005	1.96	10/27/2008	3.43	10/12/2012	2.71
09/06/2005	2.65	09/08/2009	0.86	10/22/2012	3.98
09/12/2005	3.22	09/14/2009	1.36	09/23/2013	2.47
09/26/2005	2.21	09/21/2009	1.53	10/14/2016	3.03
10/03/2005	3.19	09/29/2009	1.88	09/30/2019	3.28
10/17/2005	3.89	10/05/2009	2.62	10/07/2019	2.31
10/24/2005	3.1	10/25/2010	2.76	10/15/2019	2.72
09/11/2006	1.6	11/01/2010	3.23		

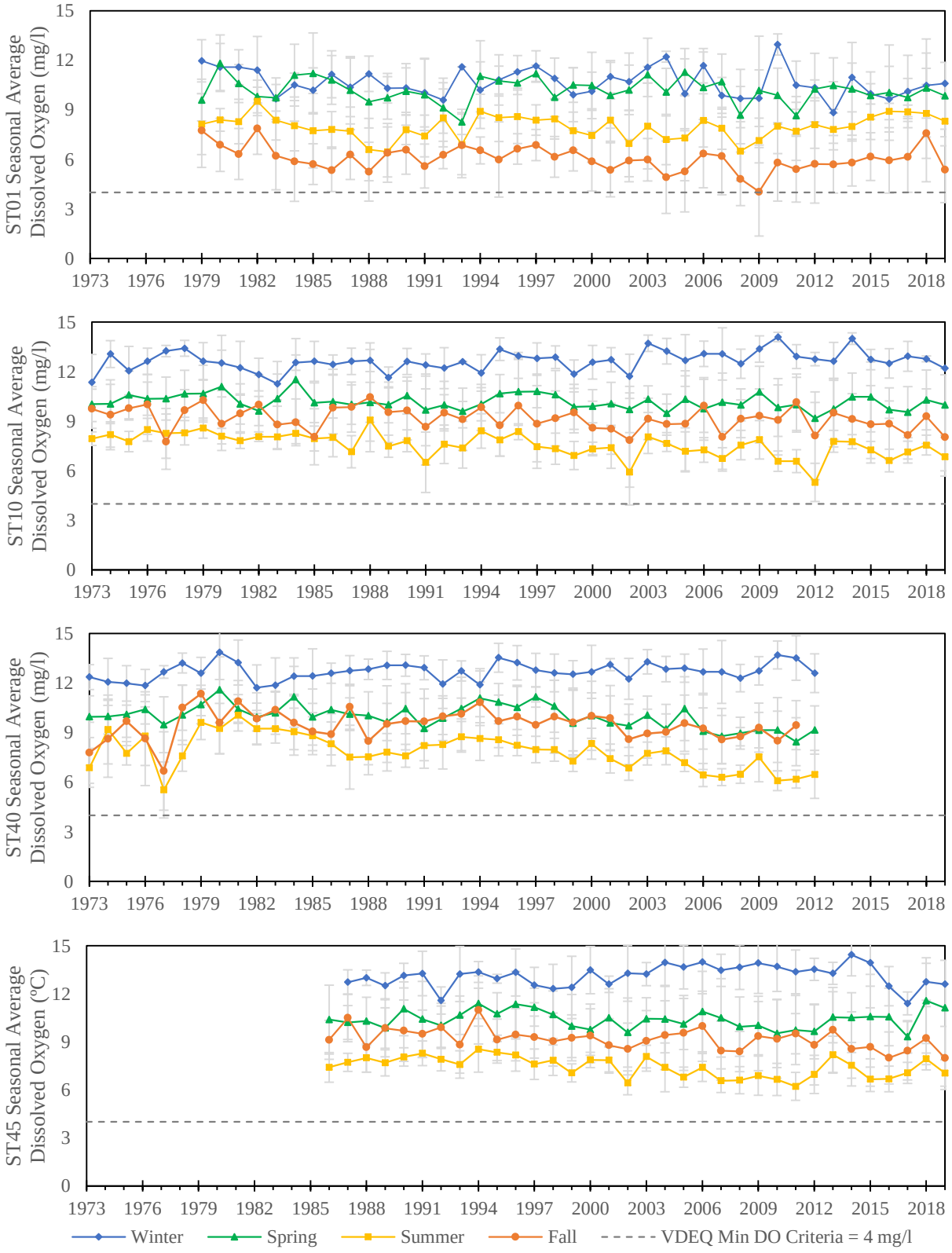

Figure 4-19. Seasonal Average Dissolved Oxygen by Station, 1973–2019

4.2.3.3 pH and Alkalinity

One of the master variables that controls the chemistry of an aquatic system is pH, which is the measure of hydrogen ion (H^+) activity. The pH value of a waterbody is obtained by taking the negative log of the hydrogen ion concentration. It indicates whether the water is acidic (high H^+ activity – low pH) or basic (low H^+ activity – high pH), and its importance lies in the fact that it determines the solubility and biological availability of other chemical species. The VDEQ water quality criteria states Class III nontidal waters should have pH values between 6 and 9. Linked to pH, alkalinity is the capacity of water to neutralize a strong acid, and indicates a waterbody's ability to resist changes in pH. High alkalinity in natural waters is due to the presence of carbonates and bicarbonates, which are mainly derived from the watershed (surrounding soils, rocks, atmosphere). Other factors that can influence alkalinity, and therefore pH, are rain, snowmelt, anthropogenic factors such as urbanization and mining operations, and biologic processes occurring in the waterbody, such as photosynthesis and denitrification. USEPA recommends a minimum alkalinity of 20 mg/l expressed as $CaCO_3$ to protect freshwater productivity (USEPA, 1986).

Table 4-12 presents the average and median pH from 1973 to 2019 by season. Average values were calculated by converting the measured pH to H+ concentrations, averaging the concentrations and then converting back to pH scale. It can be observed that mean values range from 6.5 to 7.4 pH units. Comparing all stations, the reservoir outflow (ST01) shows lower average pH in all seasons, except for summer, and the Bull Run inflows show higher pH (both ST40/45). Figure 4-20 shows pH time series for the entire period by season. It can be observed from the graph that during the earlier years there were a few values below the VDEQ minimum of pH 6, especially during winter. However, since the 1990s, there have been no measured pH daily values less than 6 in the reservoir outflow and inflow stations. During the entire period, there have been only three occurrences with pH values slightly higher than 9, two (pH values of 9.1 and 9.3) observed in summer 2010 at ST01, and one (pH 9.4) observed in fall 1988 at ST10.

Table 4-12. Seasonal Average and Median pH at Stream Stations, 1973–2019*

Season	ST01		ST10		ST40		ST45	
	Mean	*Median*	*Mean*	*Median*	*Mean*	*Median*	*Mean*	*Median*
Winter	6.5	7.0	6.6	7.1	6.7	7.3	7.4	7.5
Spring	6.9	7.3	7.0	7.2	7.1	7.4	7.4	7.5
Summer	7.2	7.6	7.1	7.3	7.3	7.4	7.3	7.4
Fall	6.9	7.0	7.1	7.2	7.3	7.5	7.4	7.5

*Seasonal Average of H+ concentration; median value of measured pH.

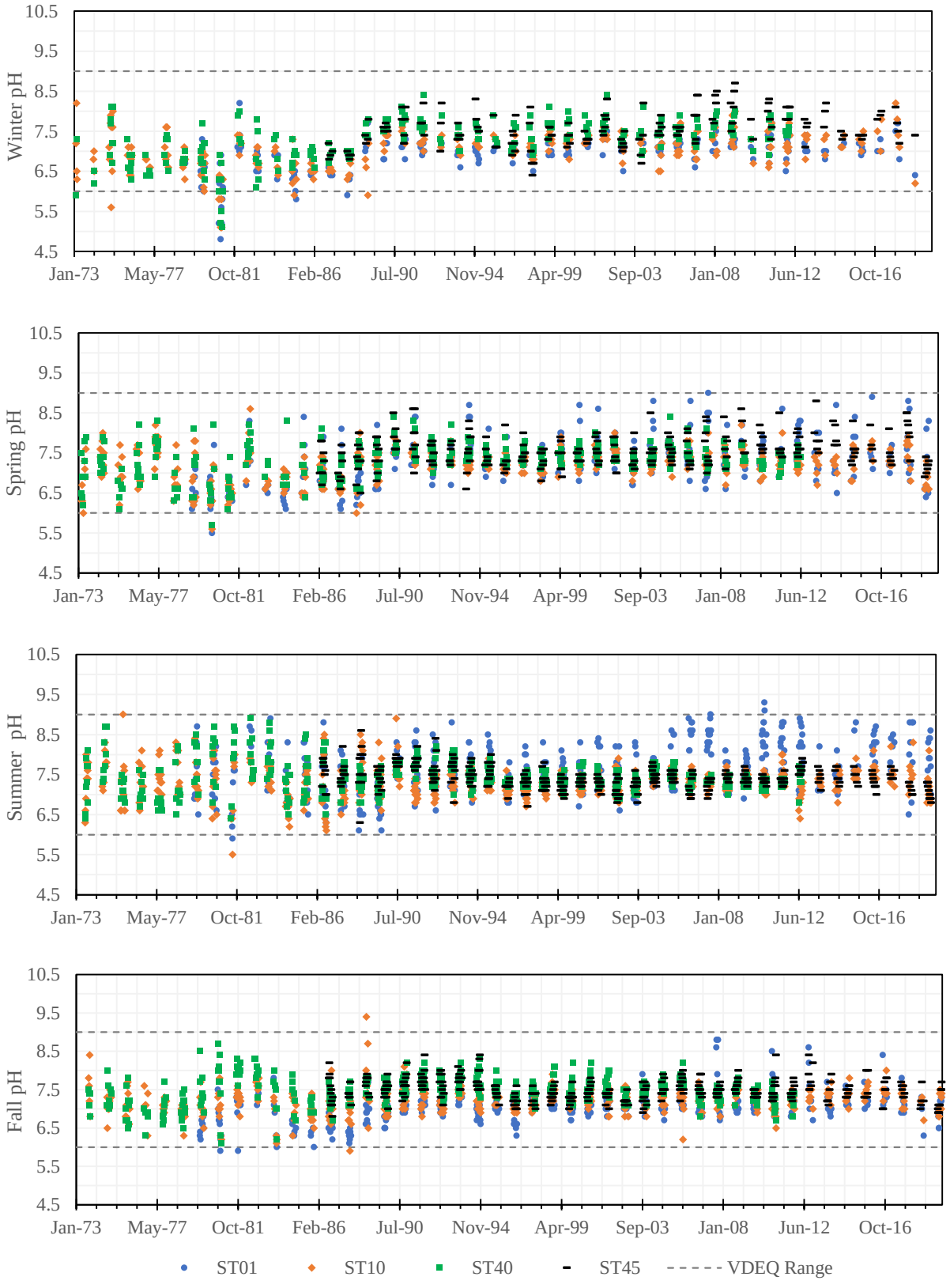

Figure 4-20. pH Values of Stream Stations by Season, 1973–2019

Similar trends are observed for alkalinity in Figure 4-21. Bull Run total alkalinity seasonal averages are higher than in the rest of the stations, and Occoquan Creek averages tend to be higher than the reservoir outflow. Average total alkalinity for the entire period of record ranges from 37 to 52 mg/l as $CaCO_3$ for the reservoir outflow, 37 to 55 mg/l as $CaCO_3$ for the Occoquan Creek, and from 55 to 82 mg/l as $CaCO_3$ for the Bull Run stations. Higher average values are observed during the fall and lower in spring at all stations. Since 2004, there have been no daily values less than the recommended 20 mg/l. The higher Bull Run values may be due to the effect of total alkalinity values of the MHR WRF effluent, which are much higher than that of the natural waters. The MHR WRF's average total alkalinity for the entire period of record (1982–2019) ranges between 70 to 94 mg/l as $CaCO_3$, the lowest average corresponding to the summer average and the highest occurring in winter. Average values for ST45, which is closer to the MHR WRF, are higher than ST40 values. A comparison between seasonal averages of the MHR WRF effluent total alkalinity and the alkalinity after the effluent has been mixed with the natural waters (Bull Run-ST40/45) is shown in Figure 4-22.

Mann-Kendall test results show an increasing trend for alkalinity for the four stations analyzed and during all seasons at a significant level (ST45 fall value is the only one for which the confidence interval is slightly less than 90% confidence), Table 4-8. It can be observed that the slope for the trends at ST40 and ST45 is higher than that of the other stations. As mentioned before, this may be due to the influence of the MHR WRF discharge. Another factor that may contribute to higher alkalinity values is the process of biological denitrification. This increase in alkalinity can be considered positive because it can help buffer pH changes from acid rain and atmospheric deposition.

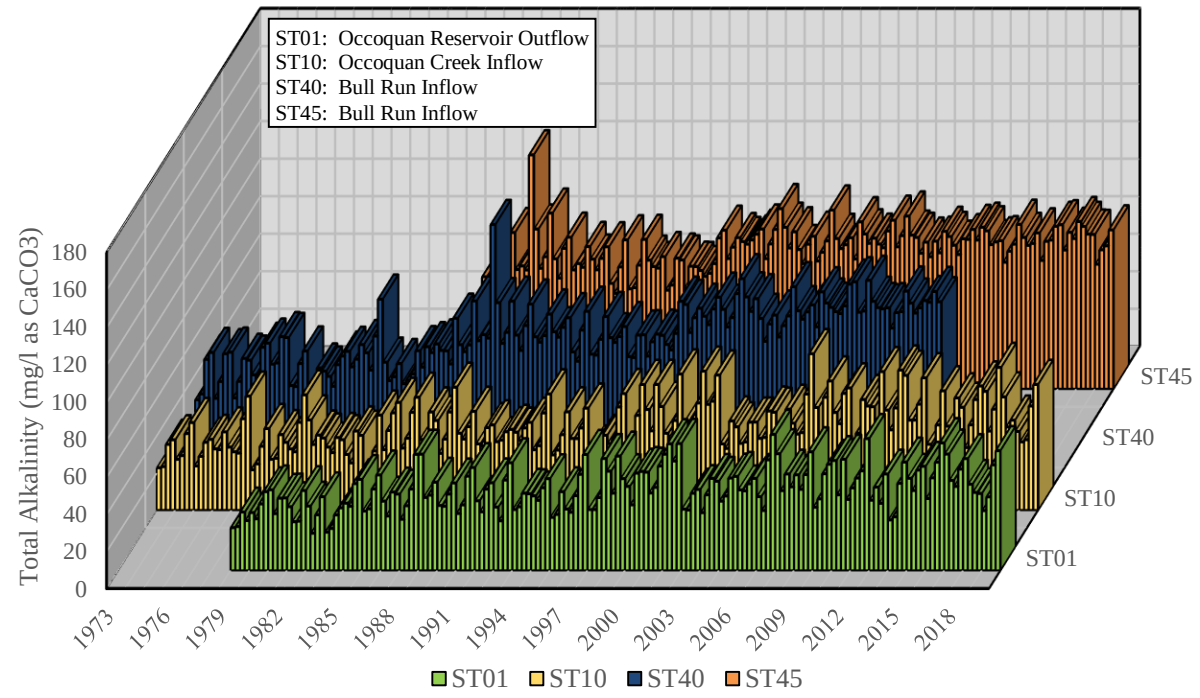

Figure 4-21. Seasonal Average Total Alkalinity at Stream Stations, 1973–2019

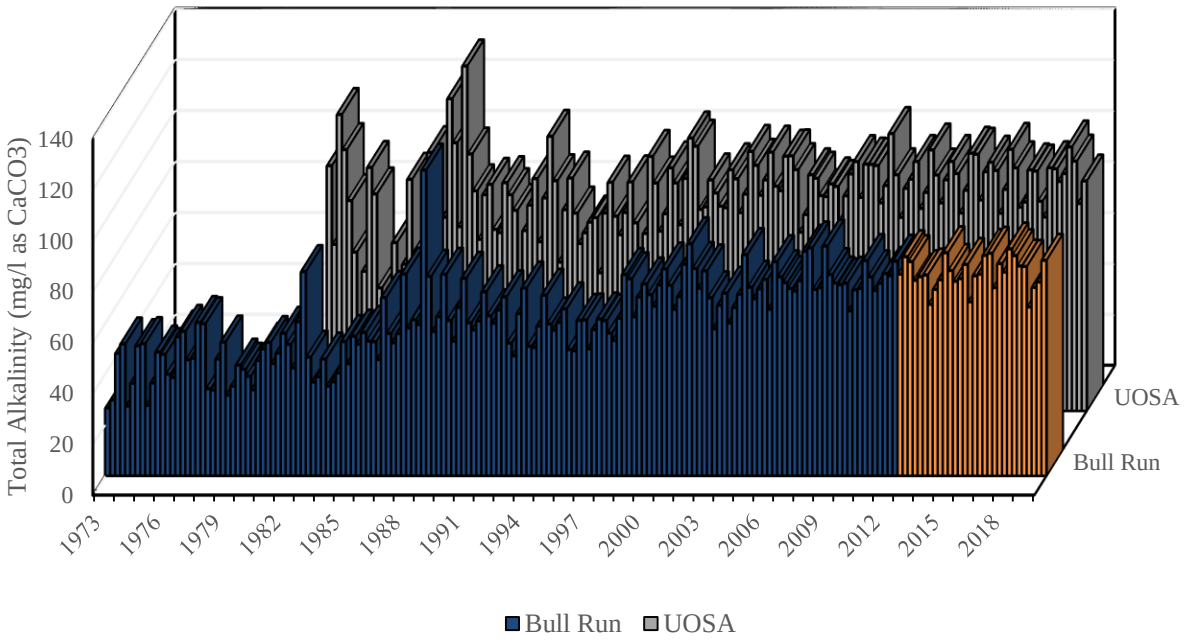

Figure 4-22. Bull Run and MHR WRF Seasonal Average Total Alkalinity Comparison, 1973–2019

4.2.3.4 Total Dissolved Solids and Conductivity

Total dissolved solids (TDS) is a parameter that indicates the amount of mass of minerals, salts, metals anions, cations, and small quantities of organic matter dissolved in water. It usually includes calcium, magnesium, potassium, sodium, bicarbonates, chlorides, and sulfates. The National Secondary Drinking Water Standards recommends a limit of 500 mg/l for TDS, because high levels may cause aesthetic problems in water, such as bitter/salty taste and discoloration, corrosion of fixtures, and reduced efficiency of water filter and equipment. Since TDS is not easily measured and data were not readily available for all stations, conductivity measurements were used as a surrogate for TDS to assess the effects of TDS in the reservoir. Conductivity is a measure of the degree in which a solution is able carry an electric current and corresponds to the sum of the contribution of all ions present (Thomas, 1986). TDS and conductivity measurements taken at ST45 have made it possible to determine a TDS to conductivity ratio of 0.6:1 for the Occoquan Watershed, as shown in Figure 4-23. Conductivity seasonal averages from 1973 to 2019 are presented in Figure 4-24. Higher conductivity is observed at Bull Run compared to the other stations, averaging 473 µS/cm at ST40 and 561 µS/cm at ST45 for the entire period of record. The Occoquan Creek and the reservoir outflow, on the other hand, average 194 µS/cm and 232 µS/cm, respectively. Values for all seasons seem to be increasing in the recent years at all stations. Mann-Kendall test results for conductivity presented in Table 4-13 confirm this upward trend for all seasons and all stations at a 95% or higher confidence interval. These upward trends may be the result of urban runoff. Additionally, the higher values observed at ST40 and ST45 may be the influence of the MHR WRF discharge. Figure 4-25 compares seasonal average TDS for the MHR WRF from 1993 to 2019, which tends to be higher, to seasonal averages at ST45 for the period of record (1989–2019). Average TDS for the MHR WRF for the entire period of record is 466 mg/l, while the average TDS at ST45 is 350 mg/l. In spite of this increase, TDS estimated values based on the previously mentioned ratio of 0.6:1 for ST01, which is the outlet station, have not exceed the recommended limit of 500 mg/l. The combination of this higher conductivity water from Bull Run with the Occoquan Creek water, which shows lower average conductivity, may be the reason why ST01 conductivity values are not as high.

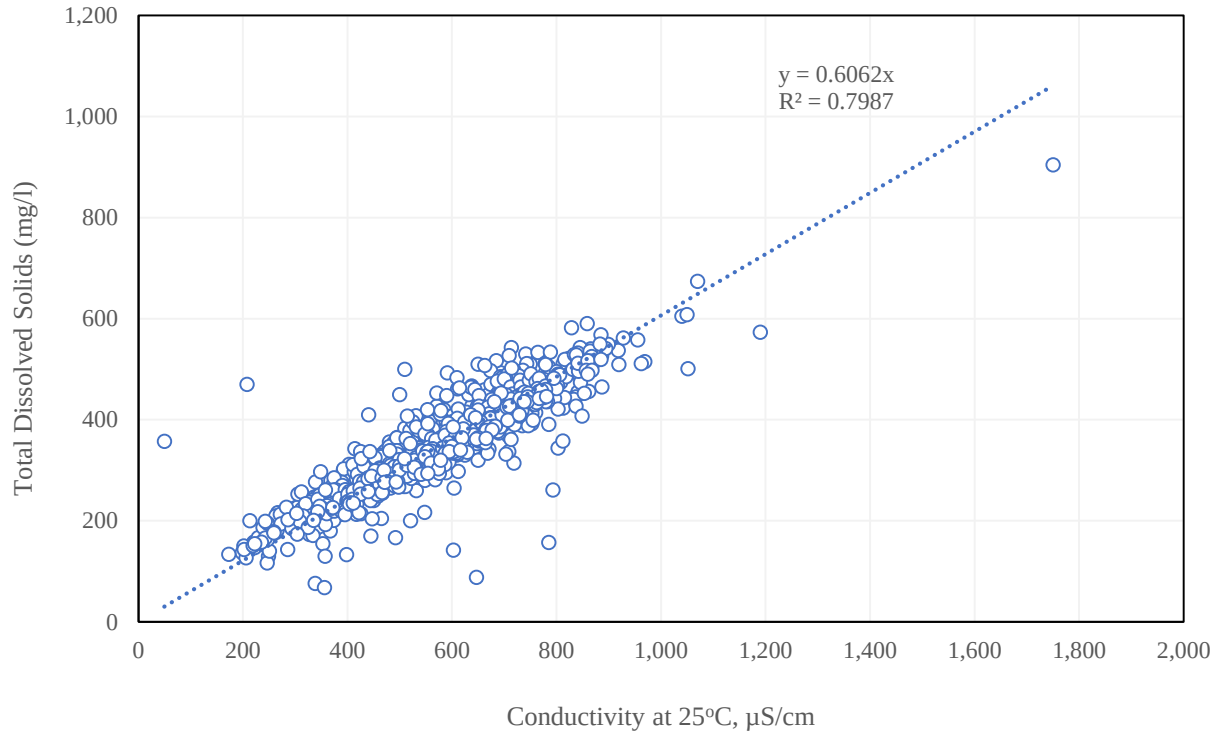

Figure 4-23. Specific Conductance and Total Dissolved Solids Correlation for ST45, 1989–2019

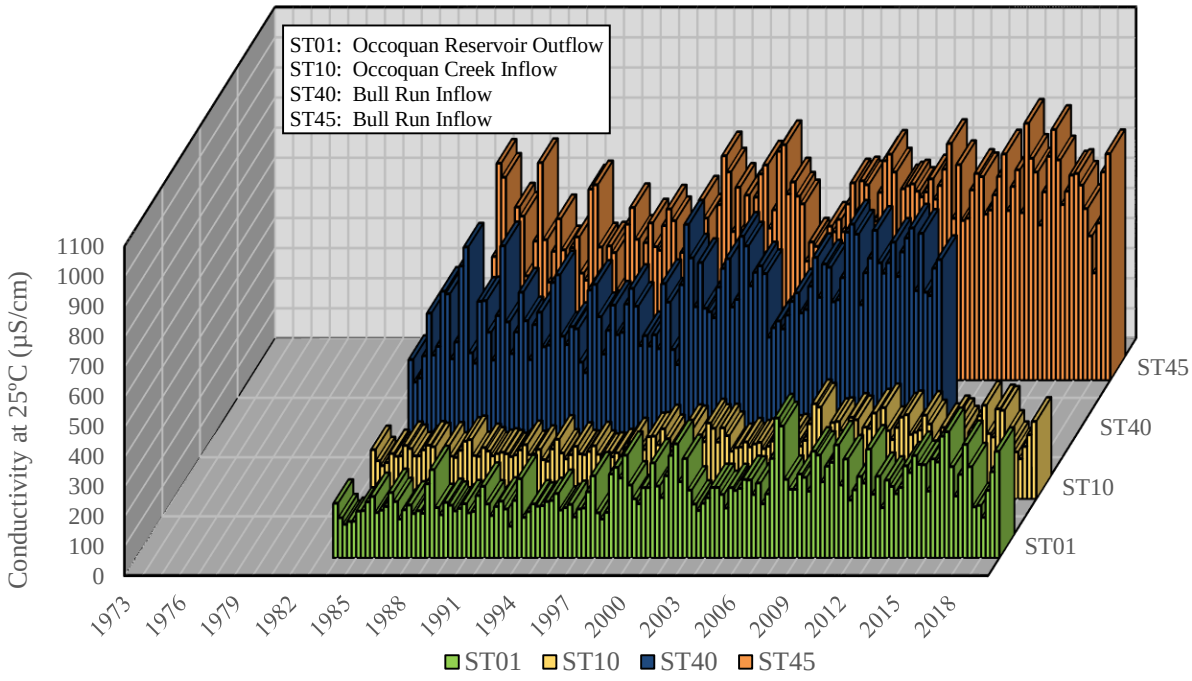

Figure 4-24. Seasonal Average of Specific Conductance at Stream Stations, 1983–2019

Table 4-13. Mann-Kendall Trends for Stream Conductivity, Total Suspended Solids, and Turbidity, 1973–2019

Station	Season	Conductivity				Total Suspended Solids				Turbidity			
		Sen Slope	*Kendall Tau*	*p-value*	*Trend*	*Sen Slope*	*Kendall Tau*	*p-value*	*Trend*	*Sen Slope*	*Kendall Tau*	*p-value*	*Trend*
ST01	Winter	3.773	0.432	**2.2E-04**	↗	-0.032	-0.123	0.261	↘	-0.105	-0.120	0.363	↘
	Spring	5.036	0.594	**3.6E-07**	↗	-0.066	-0.225	**0.040**	↘	-0.095	-0.108	0.412	↘
	Summer	3.544	0.448	**1.3E-04**	↗	-0.011	-0.068	0.537	↘	0.016	0.124	0.344	↗
	Fall	4.115	0.414	**3.2E-04**	↗	-0.041	-0.281	**0.010**	↘	-0.048	-0.153	0.234	↘
ST10	Winter	2.971	0.463	**7.4E-05**	↗	-0.072	-0.189	**0.063**	↘	-0.102	-0.157	0.232	↘
	Spring	3.086	0.610	**2.4E-07**	↗	-0.035	-0.132	0.193	↘	0.086	0.131	0.318	↗
	Summer	2.966	0.568	**1.2E-06**	↗	-0.021	-0.073	0.474	↘	-0.022	-0.053	0.695	↘
	Fall	3.137	0.532	**3.9E-06**	↗	0.002	0.006	0.963	↗	0.013	0.006	0.973	↗
ST40	Winter	13.146	0.635	**1.4E-06**	↗	-0.099	-0.399	**3.0E-04**	↘	-0.180	-0.360	**0.017**	↘
	Spring	11.903	0.645	**9.5E-07**	↗	-0.141	-0.472	**1.9E-05**	↘	-0.200	-0.383	**0.011**	↘
	Summer	7.796	0.429	**0.001**	↗	-0.136	-0.256	**0.020**	↘	-0.098	-0.249	0.102	↘
	Fall	5.332	0.271	**0.041**	↗	-0.131	-0.463	**3.5E-05**	↘	-0.088	-0.178	0.245	↘
ST45	Winter	9.184	0.394	**0.001**	↗	-0.020	-0.118	0.344	↘	-0.122	-0.295	**0.023**	↘
	Spring	11.060	0.615	**3.6E-07**	↗	0.029	0.095	0.441	↗	-0.097	-0.193	0.139	↘
	Summer	6.004	0.426	**4.2E-04**	↗	-0.007	-0.016	0.906	↘	-0.057	-0.113	0.392	↘
	Fall	4.931	0.244	**0.044**	↗	-0.022	-0.125	0.306	↘	-0.057	-0.209	0.103	↘

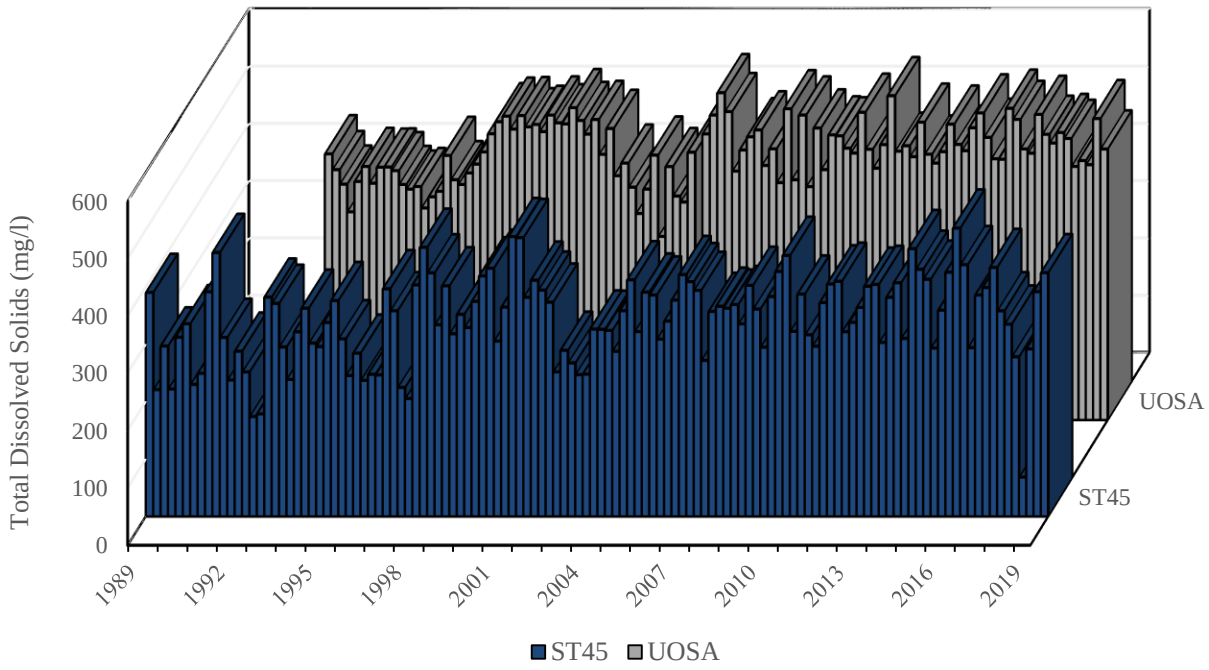

Figure 4-25. ST45 and MHR WRF Seasonal Average Total Dissolved Solids Comparison, 1989–2019

4.2.3.5 Total Suspended Solids and Turbidity

TSS is a parameter used to describe organic and inorganic particulate matter that are suspended in a waterbody (USEPA, 1986). It is an important water quality metric because suspended matter provides areas for bacterial growth and can interfere with the water disinfection process. Turbidity is a related parameter, and it refers to the reduction of water clarity due to the presence of suspended particles (e.g., clay, silt, organic matter) (American Public Health Association, 1999). These parameters themselves do not pose a major health threat. However, they are both measured because they are indicators of the presence of organic matter, disease-causing microorganisms, nutrients, or other compounds that can affect water quality.

Figures 4-26 shows seasonal average concentrations for TSS for the Occoquan Reservoir inflows and outflows by year. It can be observed that after its peak in the 1970s, average TSS concentrations have been maintained below 30 mg/l at all stations. Since the year 2003, the highest TSS seasonal average concentrations observed at each station were 26 mg/l at Bull Run (ST45) during summer 2019, 25 mg/l at ST01 during winter 2016, and 20 mg/l at the Occoquan Creek during summer 2013. TSS seasonal averages are highest at the Occoquan Creek, but are lower when they reach the outlet station. Lower averages observed at ST01 may be due to the effect of the reservoir sediment trap efficiency that will be further discussed in the load section.

Figure 4-27 shows average seasonal turbidity for the period of record. Values range from 2 to 43 NTU at ST01, 4 to 25 NTU at ST10, and 2 to 16 NTU at Bull Run stations. Turbidity average values at the Occoquan Creek were higher than at Bull Run stations. It can be observed that like TSS, there are peaks for turbidity at ST01 during winter 2016, ST10 during summer 2013, and at ST45 during summer 2019. Turbidity peaks are typically due to runoff events caused by erosion from overland and stream flow.

Mann-Kendall test results for TSS and turbidity are shown in Table 4-13. In general terms, trends for both parameters seem to be going downward with time, with a few exceptions showing an upward trend. Significant trends, however, are all downward, for TSS at ST01 (during spring and fall, at ST10 during winter, and at ST40 during all seasons) and, for turbidity (at ST40 during spring and winter, and at ST45 during winter).

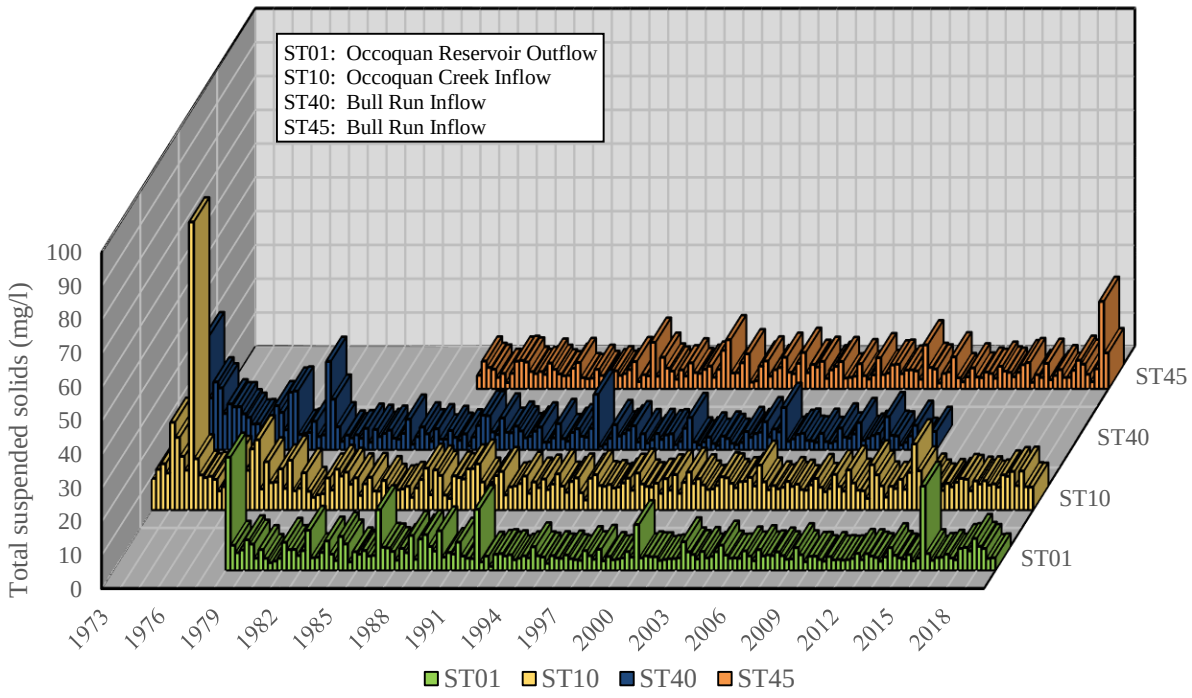

Figure 4-26. Seasonal Average of Total Suspended Solids at Stream Stations, 1973–2019

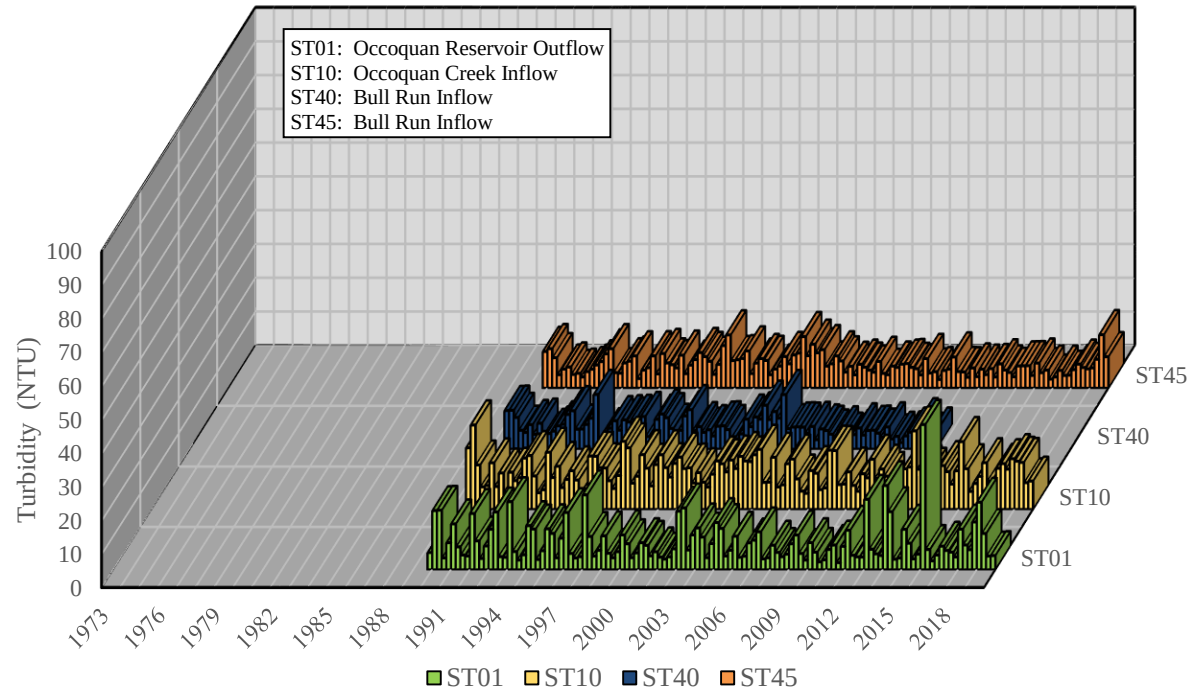

Figure 4-27. Seasonal Average Turbidity at Stream Stations, 1973–2019

4.2.3.6 Nitrogen

As mentioned in the Literature Review section, nitrogen is an essential element and nutrient that is found in the environment in organic and inorganic forms, and exists in different oxidized and reduced states. Figures 4-28 to 4-31 show seasonal average concentrations for NH3-N, TKN, Ox-N, and TN for the reservoir inflow and outflow stations, from 1973 to 2019. TKN refers to the total concentration of organic and ammonia nitrogen, and oxidized nitrogen is the sum of NO_2^- and NO_3^-. From the beginning of the period of record until Fall 2004, measurements for NH3-N, TKN, Ox-N, were taken for each station, and TN concentrations were calculated by summing TKN and Ox-N values. However, since 2004, the inverse operation has been performed, as the OWML started measuring TN concentrations instead of TKN. TKN is now calculated as the difference between TN and Ox-N.

It may be observed in Figure 4-28, that NH3-N seasonal averages from 1973 to 2019 range between 0.02 and 0.22 mg/l at ST01, 0.01 and 0.25 mg/l at ST10, 0.01 and 2.57 mg/l at ST40, and 0.01 and 0.74 mg/l at ST45. The highest average values for NH3-N can be seen at Bull Run from 1976 to 1978. However, since the MHR WRF came into operation in 1978, NH3-N concentrations have been greatly reduced. Other peaks observed in Bull Run occurred during winter 1988 which had average concentrations of 0.74 mg/l at ST45 and 0.5 mg/l at ST40. Since 2003, seasonal average NH3-N concentrations have been $\leq$0.14 mg/l for all stations. For this period, higher NH3-N averages were observed at ST01 during winter than the rest of the stations. During fall, higher values were generally observed at the Occoquan Creek. There was little difference between stations during spring and summer. Higher total seasonal averages from 2003 to 2019 at the reservoir and the Occoquan Creek were observed during fall, as also at Bull Run during winter. It is important that ammonia nitrogen levels remain low because high values can be harmful to aquatic life, particularly to fish. The VDEQ has established criteria for ammonia nitrogen depending on pH and temperature (VSWCB, 2020). For example, the criteria for total ammonia nitrogen for pH 7 and a temperature of 20°C is 1.9 mg/l. Total NH3-N average for the entire period was record was 0.07 mg/l at ST01, 0.08 mg/l at ST10, 0.11 mg/l at ST40, 0.06 mg/l at ST45.

Table 4-14 shows Mann-Kendall test results for the nitrogen forms discussed in this document. NH3-N values at ST01 present a decreasing trend for all seasons. However, the only significant trend occurs during winter. Significant trends for ST10 and ST40 also present decreasing values during winter and fall for the former station, and during winter for the latter. Meanwhile at ST45, values for spring, summer, and fall present an upward trend at *p*-values greater than 0.05. The double-headed horizontal arrow observed at ST45 during winter indicates the trend is neither increasing or decreasing (Sen Slope is also zero).

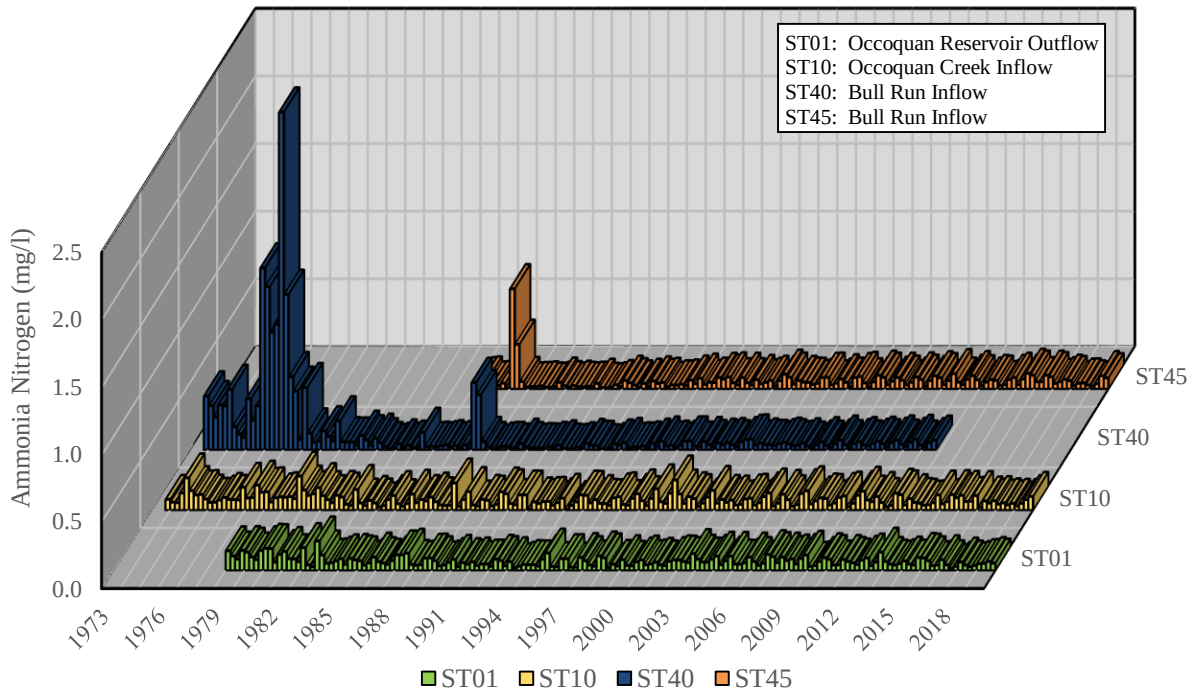

Figure 4-28. Seasonal Average Ammonia Nitrogen at Stream Stations, 1973–2019

Table 4-14. Mann-Kendall Trends for Stream Nitrogen Species, 1973–2019

Station	Season	Ammonia Nitrogen				Total Kjeldahl Nitrogen				Oxidized Nitrogen				Total Nitrogen			
		Sen Slope	*Kendall Tau*	*p-value*	*Trend*	*Sen Slope*	*Kendall Tau*	*p-value*	*Trend*	*Sen Slope*	*Kendall Tau*	*p-value*	*Trend*	*Sen Slope*	*Kendall Tau*	*p-value*	*Trend*
ST01	Winter	-0.001	-0.257	**0.019**	↘	-0.004	-0.236	**0.031**	↘	-8.8E-06	-0.001	1.000	↘	-0.006	-0.088	0.425	↘
	Spring	-1.9E-04	-0.087	0.431	↘	-0.002	-0.140	0.200	↘	0.002	0.072	0.515	↗	-3.8E-04	-0.012	0.919	↘
	Summer	-0.001	-0.174	0.113	↘	0.003	0.225	**0.040**	↗	0.003	0.076	0.493	↗	0.005	0.098	0.375	↗
	Fall	-0.001	-0.139	0.204	↘	0.001	0.113	0.301	↗	0.015	0.244	**0.025**	↗	0.013	0.251	**0.021**	↗
ST10	Winter	-0.001	-0.346	**0.001**	↘	-0.008	-0.329	**0.001**	↘	-0.008	-0.271	**0.009**	↘	-0.015	-0.388	**1.8E-04**	↘
	Spring	-7.3E-19	-0.003	0.985	↘	-0.004	-0.263	**0.010**	↘	-0.002	-0.141	0.174	↘	-0.009	-0.310	**0.003**	↘
	Summer	2.4E-05	0.007	0.955	↗	-0.003	-0.185	**0.068**	↘	-0.004	-0.187	**0.072**	↘	-0.007	-0.269	**0.010**	↘
	Fall	-0.001	-0.168	**0.099**	↘	-0.004	-0.227	**0.025**	↘	-0.002	-0.085	0.417	↘	-0.006	-0.194	**0.062**	↘
ST40	Winter	-0.003	-0.413	**2.3E-04**	↘	-0.007	-0.250	**0.026**	↘	0.092	0.340	**0.003**	↗	0.064	0.309	**0.007**	↗
	Spring	-0.001	-0.166	0.140	↘	-0.004	-0.134	0.236	↘	0.092	0.442	**9.7E-05**	↗	0.076	0.414	**2.7E-04**	↗
	Summer	3.4E-04	0.078	0.490	↗	-3.5E-04	-0.008	0.954	↘	0.115	0.249	**0.029**	↗	0.115	0.275	**0.016**	↗
	Fall	-0.001	-0.111	0.327	↘	-0.002	-0.063	0.578	↘	0.094	0.135	0.244	↗	0.091	0.144	0.214	↗
ST45	Winter	0.000	-0.010	0.951	↔	0.005	0.194	0.118	↗	-0.071	-0.254	**0.039**	↘	-0.065	-0.223	**0.070**	↘
	Spring	0.001	0.254	**0.037**	↗	0.008	0.276	**0.022**	↗	-0.059	-0.251	**0.038**	↘	-0.045	-0.226	**0.062**	↘
	Summer	0.002	0.475	**8.5E-05**	↗	0.016	0.629	**2.4E-07**	↗	-0.120	-0.394	**0.001**	↘	-0.089	-0.226	**0.062**	↘
	Fall	0.002	0.589	**1.1E-06**	↗	0.012	0.447	**2.1E-04**	↗	-0.197	-0.390	**0.001**	↘	-0.169	-0.330	**0.006**	↘

TKN seasonal average concentrations for ST01 were less than 1.0 mg/l for all years except 1982, in which an average concentration of 1.05 mg/l was observed during the summer and winter (Figure 4-29). At ST10, peak concentrations occurred from 1974 to 1979, reaching a maximum of 2.28 mg/l. Since 1980, the highest concentration observed was 0.98 mg/l during summer 2001. At the Bull Run stations, high average TKN concentrations can be observed before 1979, however, the highest average concentration occurred in summer 2017, where values rose up to 4.26 mg/l.

Other peak average concentrations observed were 2.98 mg/l in summer 2016, 2.47 mg/l in fall 2009, and 2.12 mg/l in summer 2009. Since 2003, in general terms, TKN average concentrations at Bull Run were higher than at the Occoquan Creek and the outflow station (Figure 4-29). Keeping TKN levels low helps prevent oxygen depletion caused by nitrifying bacteria, as well as further eutrophication, since nitrogen is a nutrient that can promote algal blooms.

TKN values at ST10 indicate a downward significant trend (Table 4-14). Values for ST40 also show a downward trend, but the only significant value occurs during winter. Trends at ST45, on the other hand, are positive and significant for spring, summer, and fall. ST01 shows a statistically significant downward trend during winter and an upward trend for summer. Values for spring and fall at ST01 are not significant.

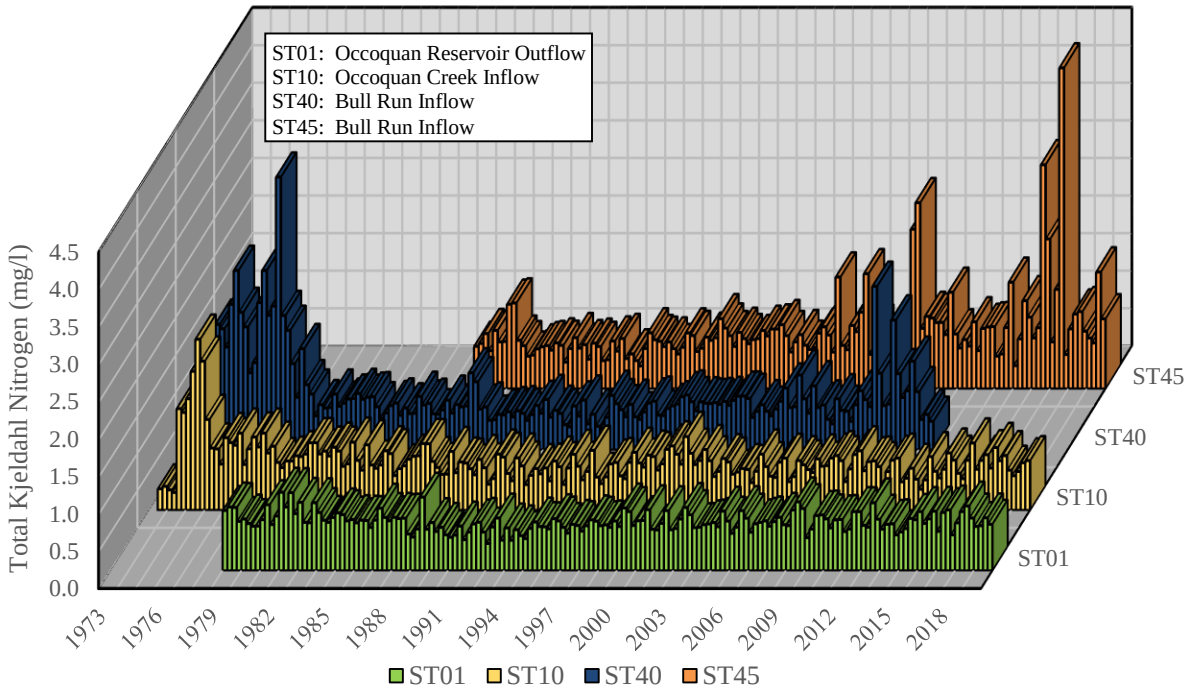

Figure 4-29. Seasonal Average Total Kjeldahl at Stream Stations, 1973–2019

Ox-N seasonal averages concentrations at Bull Run station are significantly higher than at the Occoquan Creek and the outflow station, as can be noted from Figure 4-30. These values range between 0.60 and 16 mg/l, and are high due to the MHR WRF discharges when operating in nitrification mode. Despite this, it can be observed that average values at the reservoir outflow station have been maintained low, less than 3.5 mg/l, due to dilution with resident waters and denitrification processes. Since the 1990s, all values at ST01 have been less than the 10 mg/l (measured as nitrogen) National Drinking Water Standard indicated for nitrate by the USEPA, as well as the VDEQ criteria, to prevent adverse effects to human health. Indeed, Ox-N concentrations at ST01 since the 1990s have not exceeded 4.82 mg/l. Average concentrations at ST10 were less than 1.95 mg/l during the entire period of record.

Due to the nitrate addition process, TN values follow a similar pattern as Ox-N, with higher values observed at Bull Run compared to Occoquan Creek and reservoir outflow (Figure 4-31). Occoquan Creek average values are lower than ST01 values during all seasons. Values for the Occoquan Creek and ST01 have been maintained less than 3 mg/l during all seasons. Bull Run values range between 2 to 15 mg/l and are higher during summer and fall. Mann-Kendall test results for Ox-N and TN also follow similar trends (Table 4-14). At ST01, significant *p*-values show an increasing trend during fall for both parameters. ST10 values indicate a decreasing trend for all seasons, and are significant during winter and summer for Ox-N and during all seasons for TN. Significant results for the Bull Run stations show an upward trend at ST40 and declining trend at ST45.

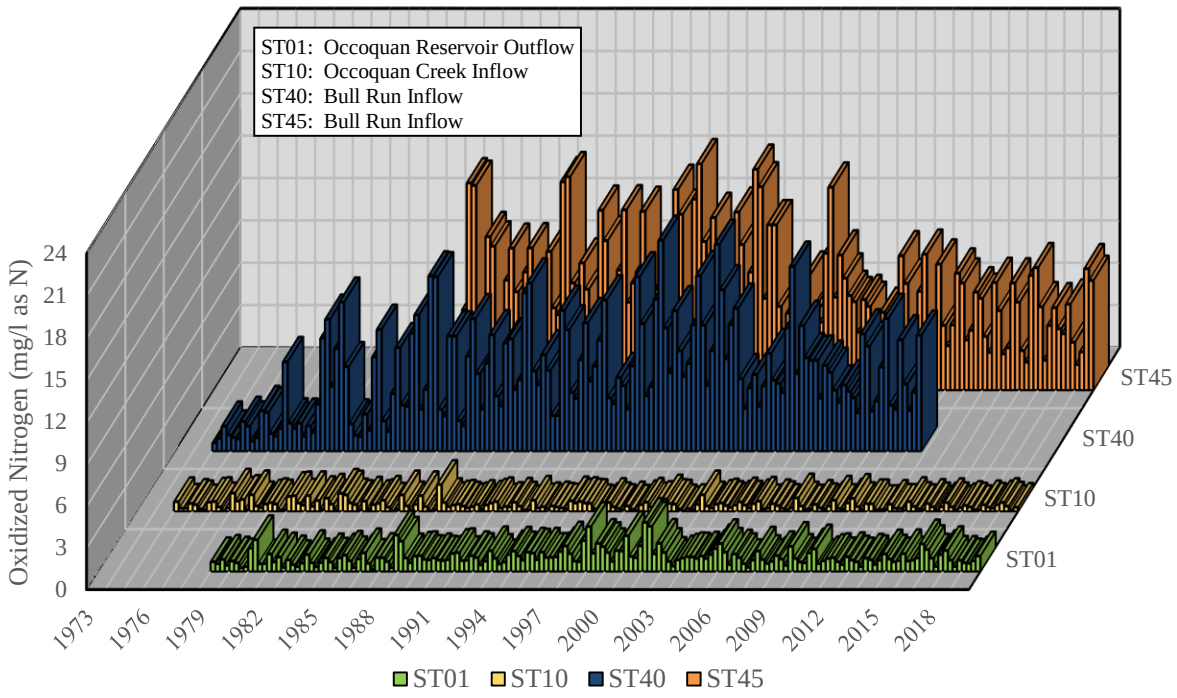

Figure 4-30. Seasonal Average Oxidized Nitrogen at Stream Stations, 1973–2019

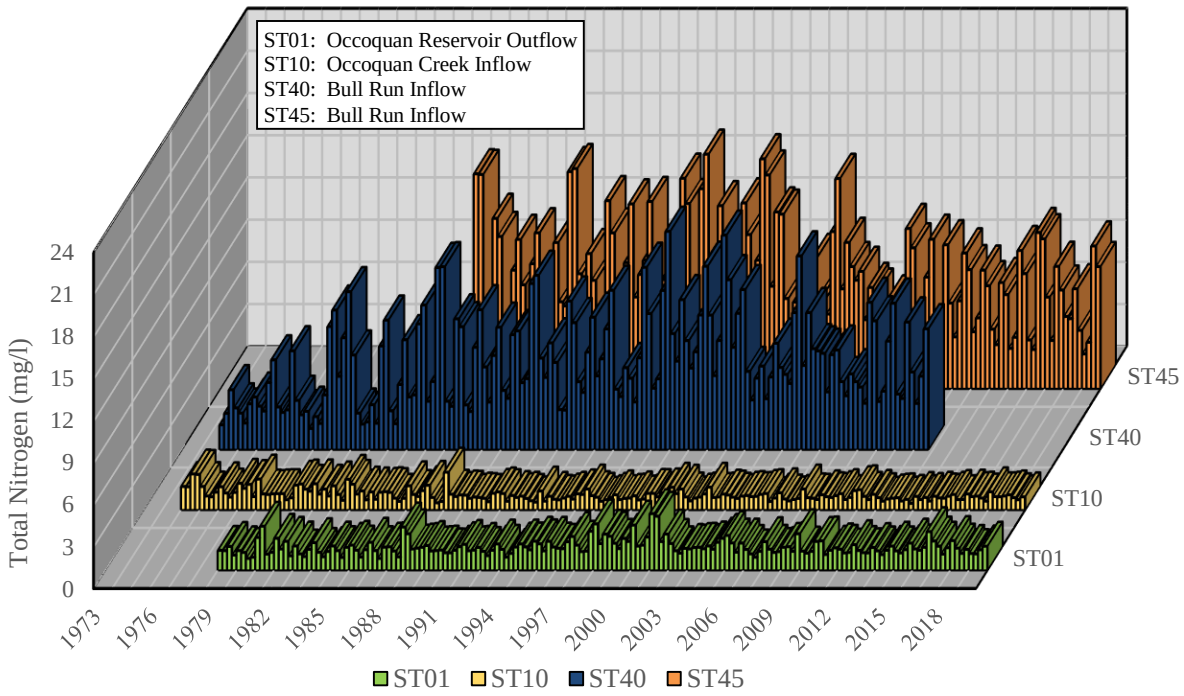

Figure 4-31. Seasonal Average Total Nitrogen at Stream Stations, 1973–2019

4.2.3.7 Phosphorus

Phosphorus is a chemical element that plays an essential role in the metabolism of plants, animals and humans. However, because it is not found in high concentrations in the environment when compared to other essential elements, it is considered a limiting nutrient. In spite of this, when there is excess phosphorus in a waterbody it can also cause eutrophication. For this reason, it is important to monitor its concentration. Some sources of phosphorus are fertilizers, manure, organic wastes and industrial effluents.

Figures 4-32 and 4-33, show seasonal average concentrations for OP (or soluble reactive phosphorus) and TP for the Occoquan Reservoir Inflow and Outflows. OP concentrations average 0.01 mg/l as P for ST01, 0.02 mg/l as P for ST10 and ST45, and 0.05 mg/l as P for ST40, for the entire period of record. The higher average values at ST40 are due to high concentrations observed before the MHR WRF came into operation, with values reaching a maximum average concentration for 0.93 mg/l as P during fall 1973. Since the year 2003, all seasonal average values at both Bull Run and Occoquan Creek have been ≤0.05 mg/l as P. Average values at the outflow station, ST01, range between 0.01 to 0.04 mg/l. During spring, summer, and fall the lowest values are observed at ST01 and the highest at ST45.

Average TP values for the entire period of record are 0.04 mg/l for ST01, 0.06 mg/l for ST10, 0.08 mg/l for ST40, and 0.04 mg/l at ST45. Like OP, TP values for Bull Run have decreased since the MHR WRF's startup. Seasonal TP concentrations since 2003 range from 0.02 to 0.14 mg/l at the

reservoir outlet, 0.03 to 0.12 mg/l at Occoquan Creek, and 0.03 to 0.09 mg/l at Bull Run stations. With the exception of these two maximum values, one during winter 2016 at ST01 (0.14 mg/l), and one during fall 2006 at ST10 (0.12 mg/l), average concentrations were all below 0.1 mg/l. It should be noted that the ST01 peak value coincides with peak values observed for TSS. Higher average concentration observed during winter 2016 was due to two rainfall events that occurred during the February. OP and TP significant trends at ST01, ST10 and ST40 show a decreasing tendency (Table 4-15). ST45 values, on the hand, present an upward trend for all seasons.

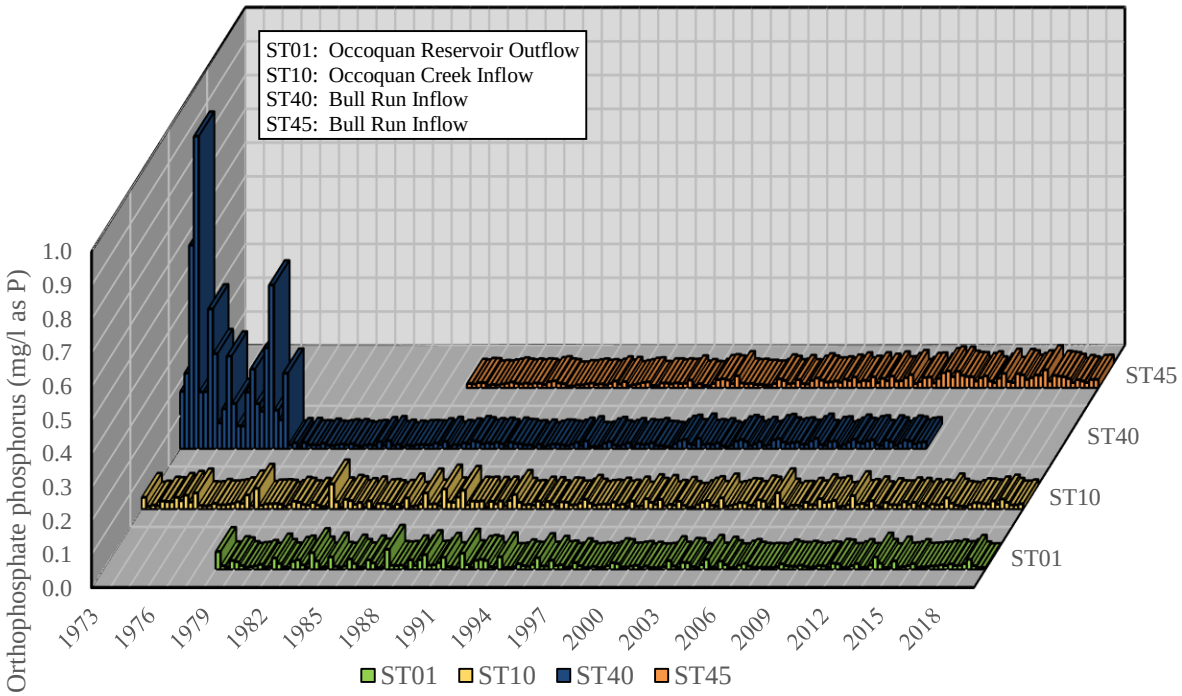

Figure 4-32. Seasonal Average Orthophosphate Phosphorus at Stream Stations, 1973–2019

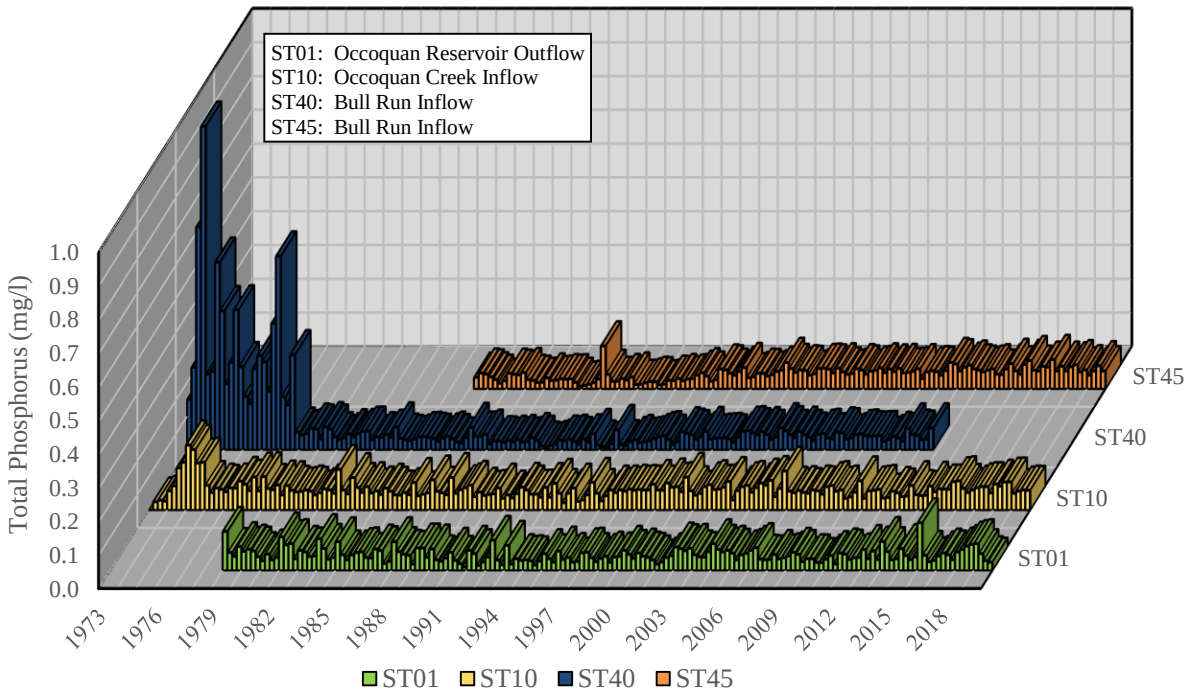

Figure 4-33. Seasonal Average Total Phosphorus at Stream Stations, 1973–2019

Table 4-15. Mann-Kendall Trends for Stream Phosphorus, 1973–2019

Station	Season	Orthophosphate Phosphorus				Total Phosphorus			
		Sen Slope	*Kendall Tau*	*p-value*	*Trend*	*Sen Slope*	*Kendall Tau*	*p-value*	*Trend*
ST01	Winter	-4.9E-04	-0.292	**0.008**	↘	-2.7E-04	-0.077	0.486	↘
	Spring	-2.0E-04	-0.328	**0.003**	↘	-2.2E-04	-0.110	0.317	↘
	Summer	-3.5E-05	-0.189	**0.089**	↘	-2.2E-05	-0.015	0.902	↘
	Fall	3.4E-05	0.061	0.582	↗	-9.1E-05	-0.069	0.537	↘
ST10	Winter	-2.7E-04	-0.290	**0.005**	↘	-4.5E-04	-0.170	**0.099**	↘
	Spring	-5.2E-05	-0.091	0.373	↘	-2.4E-05	-0.021	0.847	↘
	Summer	-2.5E-05	-0.041	0.693	↘	2.1E-05	0.023	0.826	↗
	Fall	6.6E-05	0.073	0.474	↗	9.0E-05	0.065	0.527	↗
ST40	Winter	-3.9E-04	-0.342	**0.002**	↘	-0.001	-0.324	**0.003**	↘
	Spring	-3.1E-05	-0.043	0.709	↘	-0.001	-0.299	**0.007**	↘
	Summer	-8.8E-05	-0.037	0.744	↘	-0.001	-0.197	**0.077**	↘
	Fall	1.8E-04	0.114	0.315	↗	-0.001	-0.154	0.172	↘
ST45	Winter	4.7E-04	0.424	**0.001**	↗	0.001	0.448	**3.1E-04**	↗
	Spring	4.4E-04	0.475	**9.0E-05**	↗	0.001	0.479	**7.5E-05**	↗
	Summer	0.001	0.542	**7.0E-06**	↗	0.002	0.580	**1.5E-06**	↗
	Fall	0.001	0.564	**3.0E-06**	↗	0.002	0.537	**8.7E-06**	↗

4.2.3.8 Chemical Oxygen Demand

COD is a parameter that indirectly quantifies the organic content present in an aquatic system. It measures of the amount of oxygen that is consumed during the oxidation of organic matter. High COD levels indicates high organic matter content that can be oxidized, which can lead to oxygen depletion.

Figure 4-34 shows COD seasonal averages from 1982 to 2019. Values range between 9 to 30 mg/l at ST01, 10 to 26 mg/l at ST10, 6 to 40 mg/l at ST40, and 3 to 30 mg/l at ST45. After its peak in 1988 and 1989, COD values at the Bull Run stations have been less than 15 mg/l. Values at Bull Run tend to be lower than at the Occoquan Creek station and ST01 during all seasons. In the last 15 years, the MHR WRF has not exceeded the permitted COD limit of 10 mg/l, as can also be seen for the 2005–2019 period in Figure 4-16. Seasonal averages for the entire period of record are higher during summer, averaging 17.62 mg/l at ST01, 16.92 mg/l at ST10, 11.23 mg/l at ST40, and 11.49 mg/l at ST45.

Mann-Kendall test results for chemical oxygen demand show a downward trend at ST10, ST40, ST45. However, significant trends occur only during spring at ST40, and during spring, summer and fall at ST45 (Table 4-16). Values for ST01 are not statistically significant.

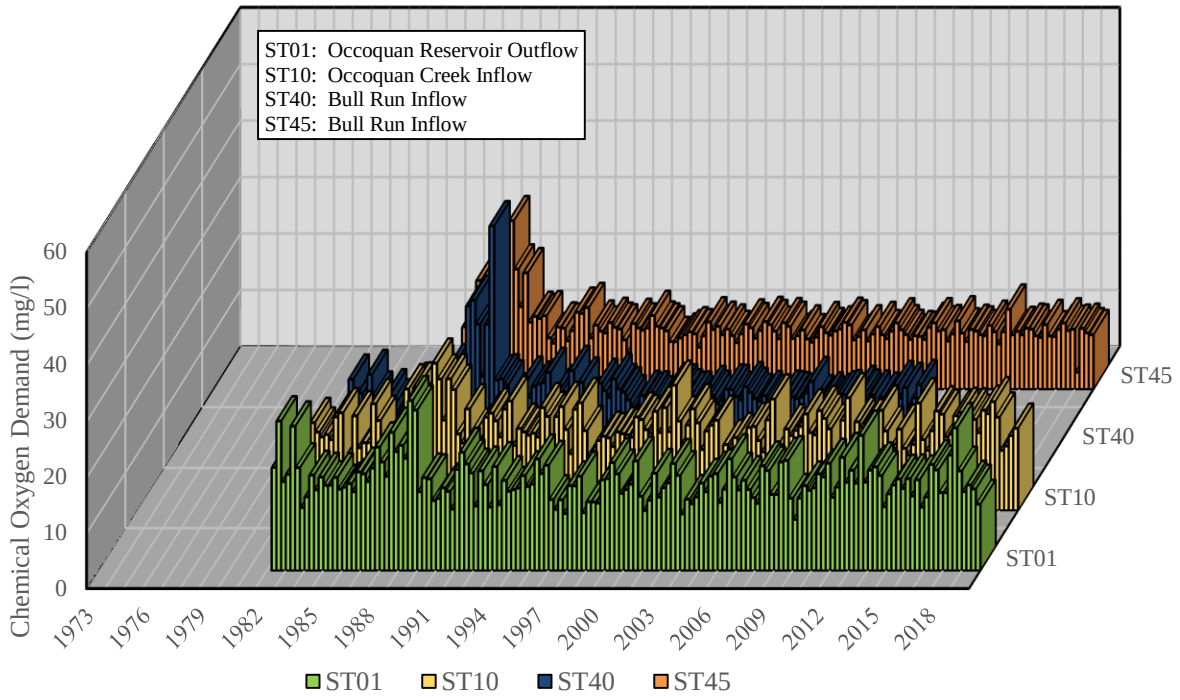

Figure 4-34. Seasonal Average Chemical Oxygen Demand at Stream Stations, 1973–2019

Table 4-16. Mann-Kendall Trends for Stream Chemical Oxygen Demand, 1973–2019

Station	Season	Chemical Oxygen Demand			
		Sen Slope	*Kendall Tau*	*p-value*	*Trend*
ST01	Winter	-0.059	-0.180	0.120	↘
	Spring	-0.028	-0.063	0.589	↘
	Summer	0.012	0.038	0.744	↗
	Fall	-0.048	-0.107	0.352	↘
ST10	Winter	-0.046	-0.134	0.250	↘
	Spring	-0.003	-0.007	0.960	↘
	Summer	-0.034	-0.104	0.365	↘
	Fall	-0.036	-0.093	0.421	↘
ST40	Winter	-0.008	-0.060	0.656	↘
	Spring	-0.088	-0.375	**0.003**	↘
	Summer	-0.047	-0.170	0.185	↘
	Fall	-0.057	-0.177	0.175	↘
ST45	Winter	-0.064	-0.279	**0.024**	↘
	Spring	-0.035	-0.205	**0.091**	↘
	Summer	-0.054	-0.319	**0.008**	↘
	Fall	-0.045	-0.191	0.116	↘

4.2.3.9 Loads

As mentioned in the Methodology chapter, the load balance for TN, TP, TSS, and sodium was estimated. A sodium load balance was included in this assessment due to recent concerns with salinity levels in the Occoquan Reservoir. Load balance tables include inputs from watershed nonpoint sources, POTWs and atmospheric deposition. Nonpoint sources were calculated using the flow values from the hydrologic balance (section 4.1.4) and baseflow/storm concentrations from ST10 (ST25 and ST30 where no data was available for ST10) and ST40/45 recorded in the Occoquan Laboratory database. Input from POTWs was estimated using water quality data provided by the plants (MHR WRF, Vint Hill, and Nokesville - for the period when it was in use). POTWs load for sodium only includes load coming from the MHR WRF, and was obtained by multiplying the median value of 66.6 mg/l by the corresponding flow. Atmospheric deposition was estimated for nitrogen and phosphorus using values obtained from a study of the performance of a constructed wetland in Manassas, Virginia (Carleton et al., 2000). Percent removal was calculated as the difference between all the inputs (nonpoint, POTWs, and atmospheric deposition) and the outputs (loads from ST01).

Tables 4-17 to 4-20, present the load balance from 1983 to 2019 for the four constituents previously mentioned. It can be observed that nitrogen loads flowing into the reservoir range from 1.5 to 6.3 million pounds, phosphorus input ranges from 77,000 to 549,000 lbs, sediment input values vary from 48 to 357 million pounds, and sodium input values go from 10 to 43 million pounds. The highest input value for all constituents occurred during 2003 and are associated with a peak inflow during this year.

Median values for load input during the period of record were 3.1 million pounds for nitrogen, 201,000 lbs, 111 million pounds for sediments, and 23 million pounds for sodium. The majority load input to the reservoir, as it is indicated in each of the tables, correspond to nonpoint sources, contributing to 65% of the incoming nitrogen, 97% of incoming phosphorus, 74% for sodium, and almost all sediment input. POTWs load accounts for 34% of the total input for nitrogen, 3% for phosphorus, close to zero percent for sediments, and 26% for sodium. The higher nitrogen percentage is due to the high nitrate effluent discharge to the reservoir as a water quality strategy. Atmospheric deposition accounts for less than 1% of the input. Mann-Kendall statistical tests were performed on nonpoint sources and loads from POTWs since they account for most of the input. It can be observed in Table 4-21 that nonpoint sources did not showed any statistically significant trends. On the other hand, loads from POTWs show an increasing trend for nitrogen, phosphorus, and sodium, which is the result of the increasing flow from the MHR WRF. Sediment POTWs load is not significant.

Figure 4-35 is a comparison of the natural flow and load in Occoquan Creek and Bull Run. Flows and loads do not take into account the POTWs contribution and were calculated by divided by their respective drainage area to provide the result on a unit area basis. It can be noticed that the majority of flow and loads from Bull Run are higher than values for the Occoquan Creek. This may be because the Bull Run side of the watershed is more urbanized than the Occoquan Creek side, therefore is more influenced by runoff events. Since runoff is a function of rainfall, and they both contribution to pollutant loading, their relationship is presented in Figure 4-36. This figure shows that nitrogen, phosphorus, and sediment loads tend to increase with increasing rainfall. This linear relationship is less apparent for sodium.

Finally, Figure 4-37 is a graphic representation of the 'Percent Removal' column from Tables 4-17 to 4-20, and shows the ability of the reservoir for pollutant retention. Phosphorus and sediments are more readily retained than nitrogen. Overall, the difference between load input and output for nitrogen is 28%, 55% for phosphorus, and 83% sediments. Sodium, on the other hand, presents a negative percent removal, indicating higher sodium loads at the outlet station. Currently, there is no explanation for this phenomenon.

Table 4-17. Occoquan Reservoir Total Nitrogen Load Balance, 1983–2019

Total Nitrogen (lb/yr)						
Year	*Nonpoint Sources*	*POTWs*	*Atmospheric Sources*	*Total Input*	*Total Outflow*	*Percent Removal*
1983	2.60E+06	5.27E+05	2.01E+04	3.14E+06	2.53E+06	19.5%
1984	3.99E+06	5.40E+05	2.13E+04	4.55E+06	3.52E+06	22.6%
1985	1.70E+06	5.86E+05	1.98E+04	2.30E+06	1.27E+06	44.7%
1986	8.60E+05	6.65E+05	1.93E+04	1.54E+06	1.05E+06	31.9%
1987	2.96E+06	6.73E+05	2.18E+04	3.65E+06	2.21E+06	39.5%
1988	1.85E+06	7.06E+05	1.91E+04	2.58E+06	1.56E+06	39.3%
1989	2.66E+06	1.01E+06	2.10E+04	3.69E+06	2.36E+06	36.1%
1990	1.18E+06	1.10E+06	2.09E+04	2.30E+06	1.90E+06	17.3%
1991	1.08E+06	1.12E+06	2.10E+04	2.22E+06	1.45E+06	34.7%
1992	1.68E+06	1.16E+06	2.09E+04	2.86E+06	2.04E+06	28.8%
1993	2.89E+06	1.07E+06	1.97E+04	3.98E+06	3.16E+06	20.5%
1994	2.82E+06	1.24E+06	2.15E+04	4.09E+06	2.88E+06	29.5%
1995	1.56E+06	1.01E+06	1.74E+04	2.59E+06	1.94E+06	25.2%
1996	3.93E+06	1.26E+06	1.81E+04	5.20E+06	4.15E+06	20.3%
1997	1.85E+06	1.24E+06	1.71E+04	3.11E+06	2.63E+06	15.3%
1998	2.79E+06	1.31E+06	1.67E+04	4.11E+06	3.28E+06	20.3%
1999	1.44E+06	1.35E+06	1.66E+04	2.80E+06	1.76E+06	37.2%
2000	1.34E+06	1.40E+06	1.76E+04	2.76E+06	1.82E+06	34.0%
2001	1.52E+06	1.51E+06	1.72E+04	3.04E+06	1.92E+06	36.9%
2002	1.26E+06	1.41E+06	1.64E+04	2.68E+06	1.66E+06	38.2%
2003	4.79E+06	1.44E+06	1.83E+04	6.25E+06	5.52E+06	11.7%
2004	2.20E+06	1.25E+06	1.82E+04	3.47E+06	2.60E+06	24.9%
2005	2.82E+06	1.61E+06	1.81E+04	4.45E+06	3.00E+06	32.5%
2006	2.34E+06	1.69E+06	1.80E+04	4.05E+06	3.13E+06	22.7%
2007	1.13E+06	1.03E+06	1.65E+04	2.18E+06	1.46E+06	33.0%
2008	1.95E+06	9.11E+05	1.81E+04	2.88E+06	1.39E+06	51.7%
2009	1.68E+06	1.14E+06	1.81E+04	2.83E+06	2.00E+06	29.6%
2010	2.28E+06	1.22E+06	1.85E+04	3.52E+06	2.59E+06	26.4%
2011	1.94E+06	1.18E+06	1.83E+04	3.15E+06	2.49E+06	21.0%
2012	1.44E+06	1.21E+06	1.81E+04	2.67E+06	1.94E+06	27.3%
2013	1.82E+06	1.19E+06	1.83E+04	3.03E+06	2.18E+06	27.9%
2014	2.92E+06	1.24E+06	1.84E+04	4.17E+06	2.91E+06	30.3%
2015	2.18E+06	1.10E+06	1.82E+04	3.30E+06	1.93E+06	41.4%
2016	1.84E+06	1.17E+06	1.82E+04	3.03E+06	1.83E+06	39.6%
2017	1.21E+06	1.17E+06	1.82E+04	2.40E+06	1.67E+06	30.4%
2018	3.15E+06	1.22E+06	1.85E+04	4.38E+06	3.97E+06	9.3%
2019	2.38E+06	1.15E+06	1.83E+04	3.55E+06	2.89E+06	18.6%
Total	**65.3%**	**34.1%**	**0.6%**	**1.22E+08**	**8.86E+07**	**27.7%**

Table 4-18. Occoquan Reservoir Total Phosphorus Load Balance, 1983–2019

	Total Phosphorus (lb/yr)					
Year	*Nonpoint Sources*	*POTWs*	*Atmospheric Sources*	*Total Input*	*Total Outflow*	*Percent Removal*
1983	2.51E+05	4.14E+03	5.82E+02	2.56E+05	1.34E+05	47.7%
1984	4.02E+05	4.39E+03	6.16E+02	4.07E+05	2.24E+05	45.0%
1985	1.22E+05	3.12E+03	5.73E+02	1.26E+05	6.29E+04	50.1%
1986	7.29E+04	3.23E+03	5.59E+02	7.66E+04	3.38E+04	55.9%
1987	2.48E+05	3.43E+03	6.31E+02	2.52E+05	9.77E+04	61.2%
1988	1.34E+05	4.92E+03	5.52E+02	1.39E+05	7.03E+04	49.5%
1989	3.66E+05	3.99E+03	6.09E+02	3.71E+05	1.17E+05	68.3%
1990	1.84E+05	3.84E+03	6.06E+02	1.88E+05	5.69E+04	69.8%
1991	1.37E+05	3.03E+03	6.09E+02	1.41E+05	5.62E+04	60.1%
1992	1.73E+05	3.92E+03	6.04E+02	1.77E+05	5.57E+04	68.6%
1993	3.53E+05	4.92E+03	5.71E+02	3.58E+05	2.07E+05	42.2%
1994	2.94E+05	5.41E+03	6.22E+02	3.00E+05	1.52E+05	49.3%
1995	1.16E+05	2.79E+03	5.04E+02	1.20E+05	5.46E+04	54.4%
1996	3.55E+05	3.42E+03	5.24E+02	3.59E+05	1.42E+05	60.5%
1997	1.73E+05	3.41E+03	4.95E+02	1.77E+05	8.28E+04	53.2%
1998	3.39E+05	4.77E+03	4.85E+02	3.44E+05	1.75E+05	49.3%
1999	1.27E+05	3.75E+03	4.79E+02	1.31E+05	3.58E+04	72.7%
2000	1.22E+05	3.90E+03	5.11E+02	1.26E+05	4.81E+04	61.8%
2001	1.38E+05	5.51E+03	4.98E+02	1.44E+05	4.00E+04	72.3%
2002	8.26E+04	5.83E+03	4.74E+02	8.89E+04	2.58E+04	71.0%
2003	5.39E+05	9.54E+03	5.31E+02	5.49E+05	2.77E+05	49.5%
2004	2.42E+05	5.87E+03	5.26E+02	2.48E+05	1.02E+05	59.0%
2005	3.38E+05	6.34E+03	5.25E+02	3.45E+05	1.42E+05	59.0%
2006	3.52E+05	7.62E+03	5.21E+02	3.60E+05	1.32E+05	63.3%
2007	9.04E+04	7.03E+03	4.78E+02	9.79E+04	5.47E+04	44.1%
2008	2.00E+05	7.08E+03	5.23E+02	2.08E+05	6.23E+04	70.0%
2009	1.36E+05	7.57E+03	5.25E+02	1.44E+05	5.31E+04	63.2%
2010	1.50E+05	7.26E+03	5.34E+02	1.58E+05	6.36E+04	59.7%
2011	1.83E+05	7.84E+03	5.31E+02	1.91E+05	9.05E+04	52.7%
2012	1.26E+05	7.81E+03	5.26E+02	1.35E+05	7.23E+04	46.3%
2013	2.17E+05	8.24E+03	5.31E+02	2.26E+05	8.44E+04	62.6%
2014	2.51E+05	8.61E+03	5.33E+02	2.60E+05	1.54E+05	40.9%
2015	1.92E+05	8.61E+03	5.28E+02	2.01E+05	6.25E+04	68.9%
2016	2.68E+05	8.06E+03	5.26E+02	2.77E+05	8.61E+04	68.9%
2017	1.25E+05	7.48E+03	5.28E+02	1.33E+05	4.62E+04	65.2%
2018	3.72E+05	8.84E+03	5.35E+02	3.81E+05	2.05E+05	46.2%
2019	2.45E+05	8.64E+03	5.29E+02	2.54E+05	2.20E+05	13.5%
Total	**97.2%**	**2.5%**	**0.2%**	**8.45E+06**	**3.78E+06**	**55.3%**

Table 4-19. Occoquan Reservoir Total Suspended Solids Load Balance, 1983–2019

Total Sediment (lb/yr)						
Year	*Nonpoint Sources*	*POTWs*	*Atmospheric Sources*	*Total Input*	*Total Outflow*	*Percent Removal*
1983	1.16E+08	2.21E+04		1.16E+08	4.23E+07	63.5%
1984	2.28E+08	2.11E+04		2.28E+08	6.28E+07	72.5%
1985	9.29E+07	1.86E+04		9.29E+07	1.31E+07	85.9%
1986	5.52E+07	2.31E+04		5.53E+07	3.96E+06	92.8%
1987	1.44E+08	3.00E+04		1.44E+08	2.55E+07	82.3%
1988	9.43E+07	3.37E+04		9.43E+07	5.41E+06	94.3%
1989	2.61E+08	4.08E+04		2.61E+08	5.22E+07	80.0%
1990	1.14E+08	2.64E+04		1.14E+08	1.01E+07	91.1%
1991	6.66E+07	2.19E+04		6.67E+07	1.33E+07	80.0%
1992	8.94E+07	2.32E+04		8.94E+07	9.43E+06	89.5%
1993	1.78E+08	3.08E+04		1.78E+08	5.40E+07	69.7%
1994	1.74E+08	4.55E+04		1.74E+08	3.40E+07	80.4%
1995	6.29E+07	2.58E+04		6.29E+07	8.65E+06	86.3%
1996	1.91E+08	2.84E+04		1.91E+08	3.10E+07	83.8%
1997	9.96E+07	3.14E+04		9.96E+07	1.53E+07	84.7%
1998	1.81E+08	4.77E+04		1.81E+08	4.22E+07	76.7%
1999	7.34E+07	4.51E+04		7.34E+07	4.16E+06	94.3%
2000	6.34E+07	3.47E+04		6.34E+07	7.08E+06	88.8%
2001	8.74E+07	2.73E+04		8.74E+07	5.25E+06	94.0%
2002	4.84E+07	1.79E+04		4.84E+07	2.21E+06	95.4%
2003	3.57E+08	1.20E+05		3.57E+08	5.03E+07	85.9%
2004	1.53E+08	4.50E+04		1.53E+08	2.25E+07	85.4%
2005	1.94E+08	4.71E+04		1.94E+08	2.45E+07	87.4%
2006	1.74E+08	4.49E+04		1.74E+08	1.80E+07	89.7%
2007	5.39E+07	2.75E+04		5.39E+07	7.16E+06	86.7%
2008	1.11E+08	2.54E+04		1.11E+08	8.62E+06	92.2%
2009	7.95E+07	2.30E+04		7.95E+07	7.08E+06	91.1%
2010	1.15E+08	2.39E+04		1.15E+08	1.19E+07	89.6%
2011	1.10E+08	2.35E+04		1.11E+08	2.14E+07	80.6%
2012	6.32E+07	2.94E+04		6.33E+07	1.22E+07	80.8%
2013	1.29E+08	3.00E+04		1.29E+08	1.65E+07	87.3%
2014	1.63E+08	2.85E+04		1.63E+08	4.34E+07	73.4%
2015	6.97E+07	2.40E+04		6.97E+07	5.66E+06	91.9%
2016	6.69E+07	2.26E+04		6.69E+07	1.35E+07	79.9%
2017	5.87E+07	2.09E+04		5.87E+07	5.18E+06	91.2%
2018	1.97E+08	2.37E+04		1.97E+08	3.20E+07	83.7%
2019	1.29E+08	1.84E+04		1.29E+08	2.99E+07	76.8%
Total	**100.0%**	**0.0%**	**0.0%**	**4.64E+09**	**7.72E+08**	**83.4%**

Table 4-20. Occoquan Reservoir Total Sodium Load Balance, 2002–2019

Total Soluble Sodium (lb/yr)						
Year	*Nonpoint Sources*	*POTWs*	*Atmospheric Sources*	*Total Input*	*Total Outflow*	*Percent Removal*
2002	5.40E+06	4.85E+06		1.02E+07	1.38E+07	-34.8%
2003	3.64E+07	6.24E+06		4.26E+07	5.04E+07	-18.4%
2004	1.73E+07	5.65E+06		2.30E+07	2.76E+07	-20.0%
2005	1.81E+07	5.85E+06		2.39E+07	2.58E+07	-7.9%
2006	1.17E+07	6.05E+06		1.77E+07	2.35E+07	-32.4%
2007	9.14E+06	5.79E+06		1.49E+07	1.95E+07	-30.4%
2008	1.55E+07	6.08E+06		2.16E+07	2.46E+07	-14.0%
2009	1.20E+07	6.11E+06		1.81E+07	2.41E+07	-33.0%
2010	1.99E+07	6.53E+06		2.64E+07	4.23E+07	-60.3%
2011	1.82E+07	6.44E+06		2.47E+07	3.49E+07	-41.6%
2012	6.92E+06	6.21E+06		1.31E+07	1.94E+07	-47.6%
2013	1.59E+07	6.43E+06		2.23E+07	2.50E+07	-12.3%
2014	2.84E+07	6.96E+06		3.54E+07	4.59E+07	-29.8%
2015	3.25E+07	6.67E+06		3.91E+07	3.89E+07	0.6%
2016	1.76E+07	6.57E+06		2.42E+07	3.00E+07	-24.0%
2017	1.17E+07	6.42E+06		1.82E+07	2.21E+07	-21.8%
2018	1.86E+07	7.28E+06		2.59E+07	3.82E+07	-47.5%
2019	2.57E+07	6.99E+06		3.27E+07	4.04E+07	-23.4%
Total	**74.0%**	**26.0%**	**0.0%**	**4.34E+08**	**5.47E+08**	**-25.9%**

Table 4-21. Mann-Kendall Load Trends, 1983–2019

Constituent	**Nonpoint Sources**				**POTWs**			
	Sen Slope	*Kendall Tau*	*p-value*	*Trend*	*Sen Slope*	*Kendall Tau*	*p-value*	*Trend*
Nitrogen	-467	-0.012	0.927	↘	16,686	0.333	**0.004**	↗
Phosphorus	167	0.021	0.865	↗	167	0.664	**8.03E-09**	↗
Sediment	-560,775	-0.078	0.505	↘	-53	-0.057	0.628	↘
Sodium	546,910	0.229	0.198	↗	84,228	0.686	**8.18E-05**	↗

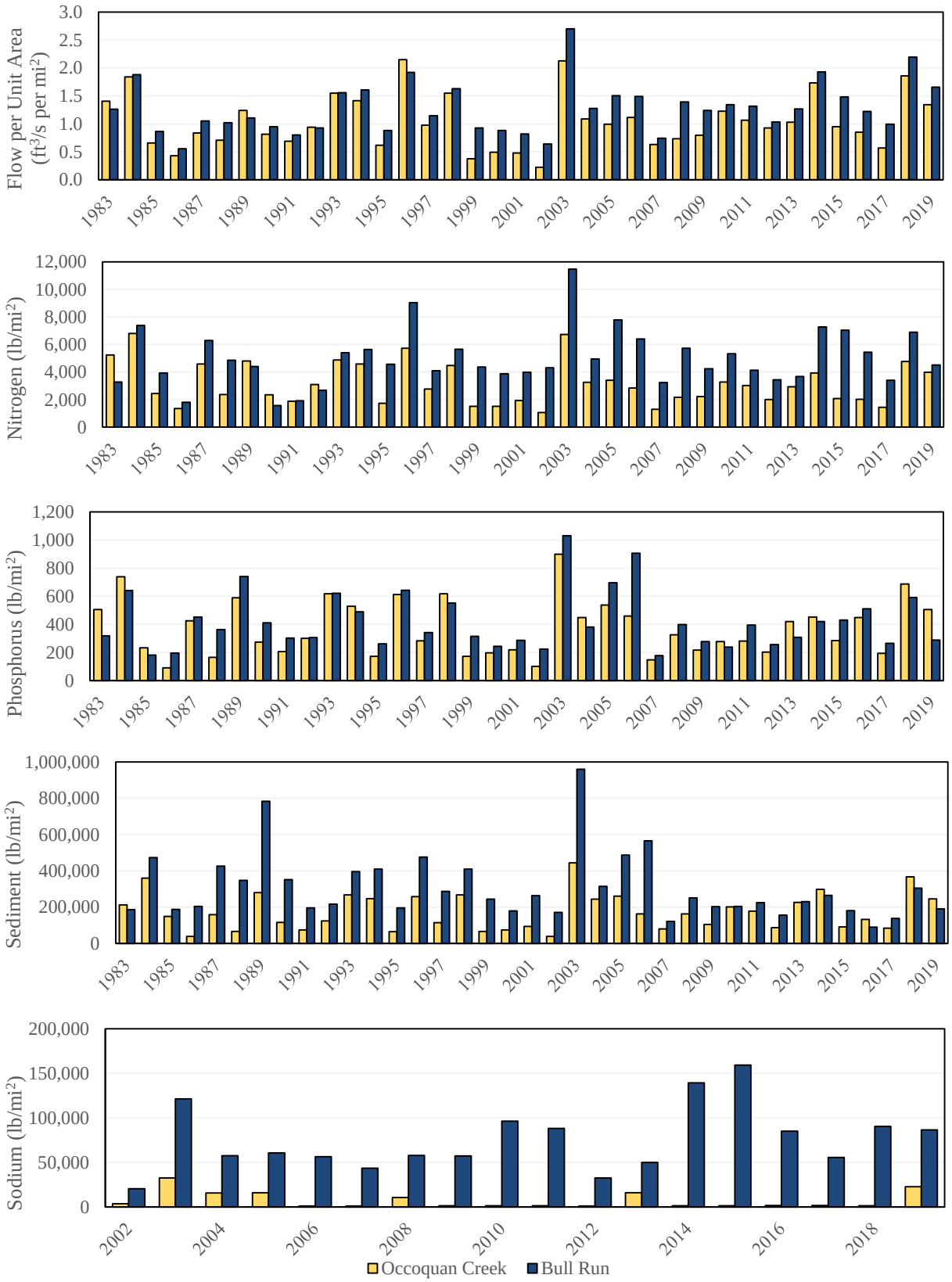

Figure 4-35. Annual Natural Flows and Nonpoint Source Loads Per Unit Area, 1983–2019

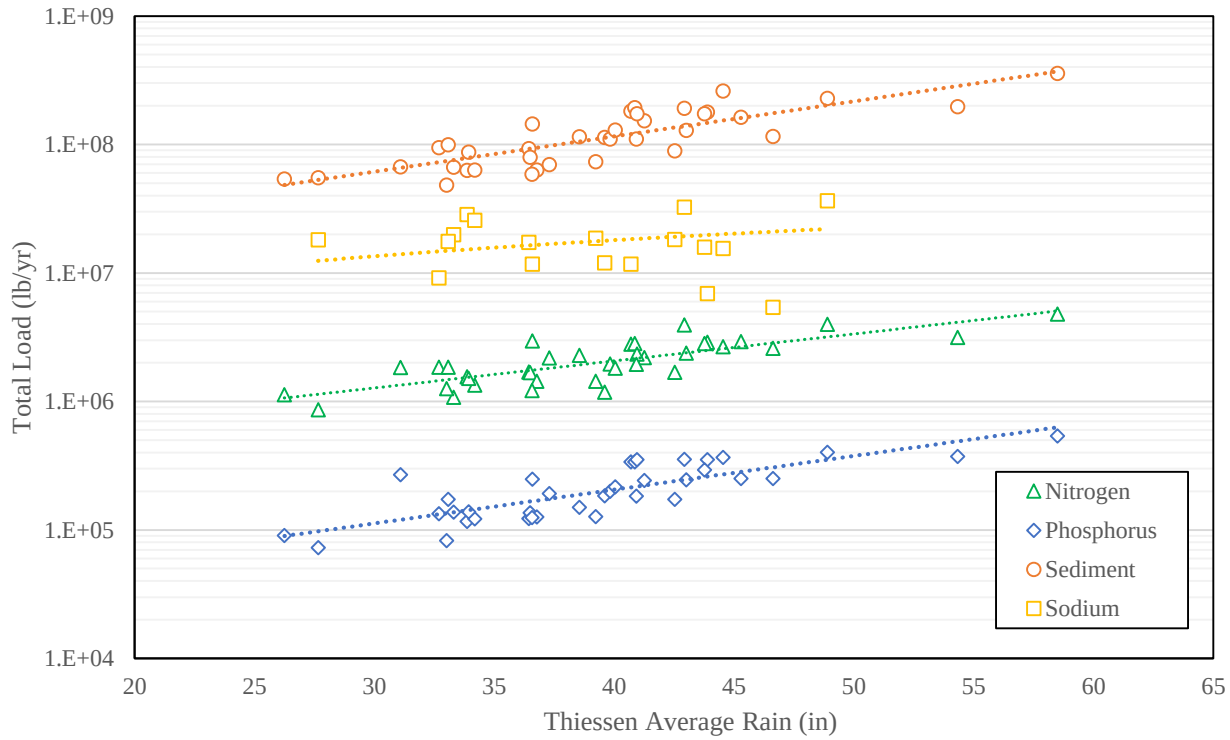

Figure 4-36. Relationship Between Nonpoint Source Loads and Rainfall

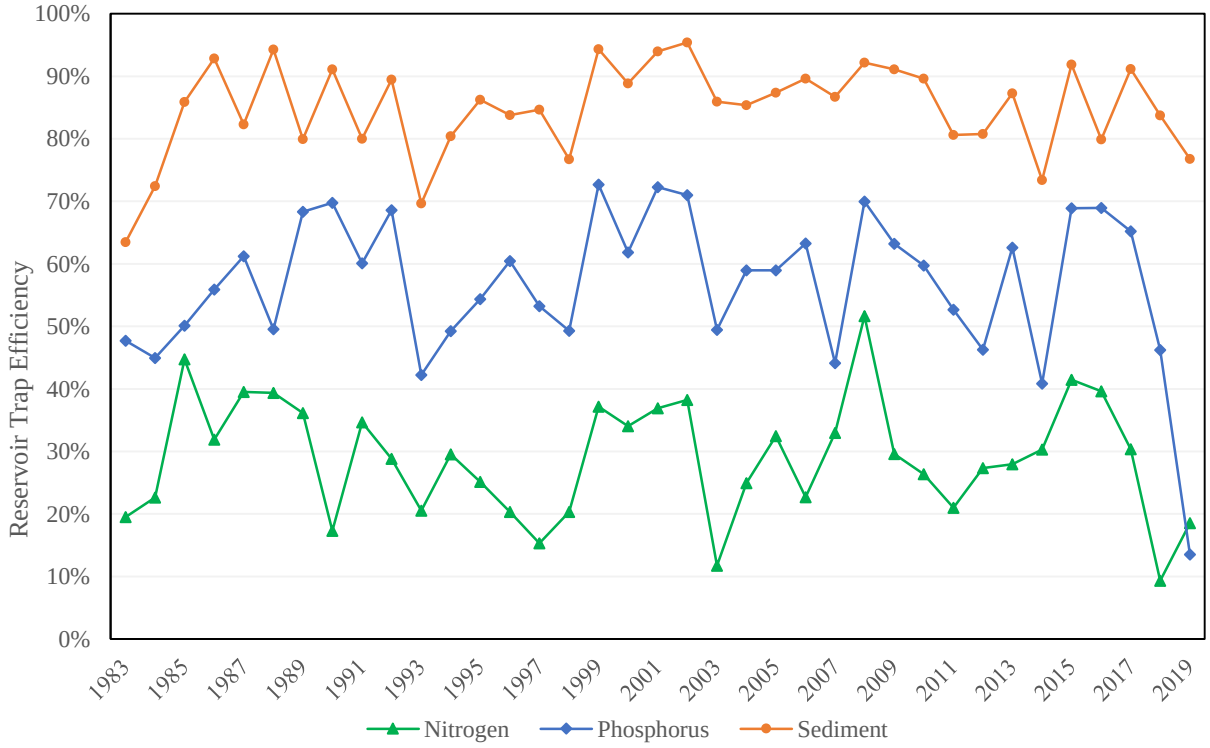

Figure 4-37. Trap Efficiency of the Occoquan Reservoir, 1983–2019

4.3 Reservoir Water Quality

4.3.1 Introduction

This section presents an analysis of different water quality parameters and constituents found in the Occoquan Reservoir based on data collected by the OWML. The analysis focuses on four (4) main stations: RE02, RE15, RE30, and RE35. RE02 is the station closest to the dam, the deepest part of the reservoir, and best represents the water quality at the Fairfax Water intake. RE15, which represents water quality at a mid-section of the reservoir, is located downstream of the Occoquan and Bull Run confluence and upstream of Ryons Dam, and about 6 miles upstream of the Occoquan Dam. RE30 is the station that represents the water quality in the Bull Run arm and RE35 describes water quality in the Occoquan Creek arm. These stations are located approximately 1.5 and 2 miles upstream of the confluence, respectively.

Analysis of reservoir water quality includes presentation of temperature and DO isopleths, seasonal average concentration graphs of different parameters, as well as time-series graphs. Reservoir data were divided into surface data, which corresponds to measurements taken at 1-foot depth, and bottom data, which includes measurements taken at the highest depth for a specific day and station. Mann-Kendall analysis was also performed for some constituents to determine if their behaviors showed any significant trends over time. Lastly, PCA was performed on nitrogen, phosphorus, sodium, and chloride to illustrate seasonal and spatial patterns, as well as their relationship with other water quality parameters. Available water quality data for the Occoquan Reservoir dates back to 1973.

4.3.2 Temperature

As mentioned in section 2.1, temperature has a great influence on biological and chemical processes that can affect the productivity of an aquatic system. Temperature measurements in lakes and reservoirs vary widely among seasons and show patterns of stratification. Thermal stratification occurs in lakes/reservoirs with moderate or high depths when surface water becomes warmer than bottom waters because of solar radiation and insufficient wind conditions that fail to overcome the density differences (because water density depends on temperature). During stratification, the water column divides into three zones: epilimnion (upper zone), metalimnion (middle zone), hypolimnion (bottom zone). During this period, oxygen may get depleted in the hypolimnion due to lack of circulation from the epilimnion, causing reducing conditions which can promote the release of constituents that affect water quality.

Lakes/reservoirs can have different circulation patterns depending on the location, climate, and morphometric characteristics of the waterbody. The Occoquan Reservoir has one single stratification period during the warmest season and mixes only once a year. Therefore, it can be classified as a warm monomictic reservoir. In temperate climates, such as Virginia, thermal stratification starts in late spring/early summer up until the surface water begins to cool during fall. This pattern can be observed in Figure 4-38, which shows the temperature isopleths at RE02 from December 2002 to November 2019. Isopleths, which are lines that connect points with equal temperatures, were constructed as contours in the figure by interpolating the observed water

temperature values at each depth. The dots on the figure represent the points at which actual data were recorded. The minor ticks on the horizontal axis indicate data recorded during March, May, August, and October. RE02 was chosen for this figure because it is the deepest part of the reservoir and less affected by wind mixing; therefore, thermal stratification is better seen. As expected, water temperature values from 2003 to 2019 are coolest during winter, ranging from 2 to 11°C and varying little with depth. Thermal stratification begins to show during late spring, when the water becomes warmer, reaching to temperatures up to 27°C. Stratification remains constant throughout the summer, with temperatures ranging between 18 and 32°C at the surface and between 9 and 25°C at bottom depths. Fall overturn typically occurs during October, and temperatures remain uniform at different depths until the early spring.

Figure 4-39 shows temperature profiles at RE02 during 2019. From January to March, the temperature is relatively constant throughout the entire depth. The lowest temperatures can be observed during these months, particularly in January, where the water was approximately 4°C. Thermal stratification appears to start in April and May, and is most noticeable from June to August. The most pronounced difference between surface and bottom temperatures for 2019 can be seen in July, where peak surface temperature was 30°C and the lowest bottom temperature was 16°C. Differences between surface and bottom temperatures start to diminish during September, for which there is only a 3°C difference observed. Fall overturn occurs during late September and early October. October and November have average temperatures of 22°C and 13°C respectively, with little variation throughout the water column.

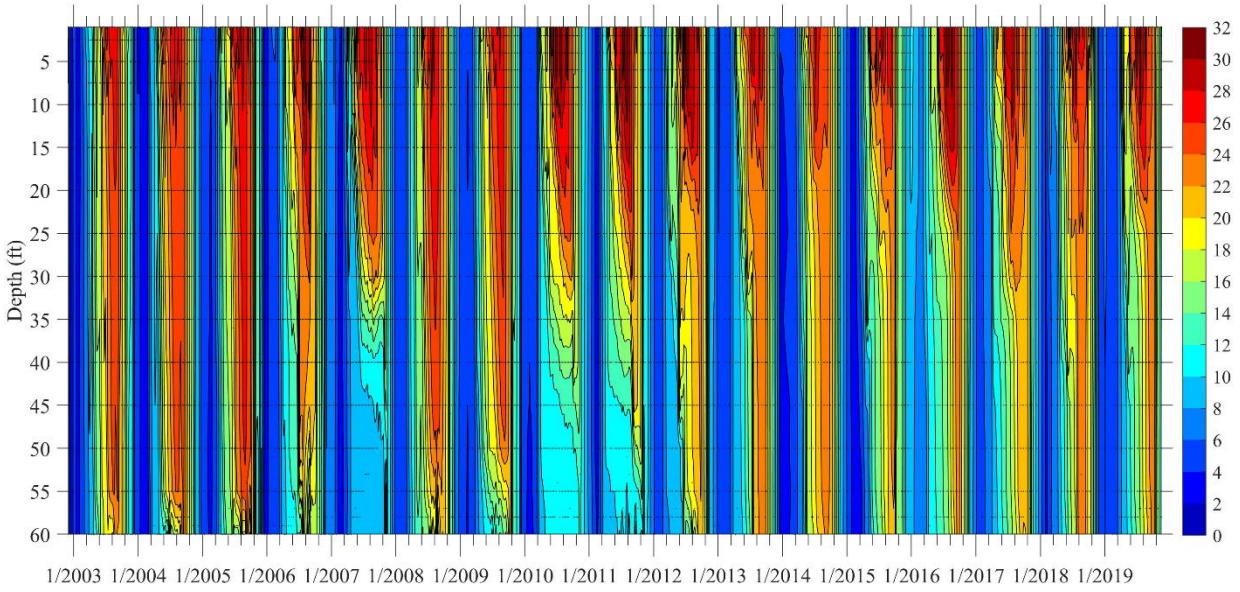

Figure 4-38. Temperature Isopleths at RE02, 2002–2019

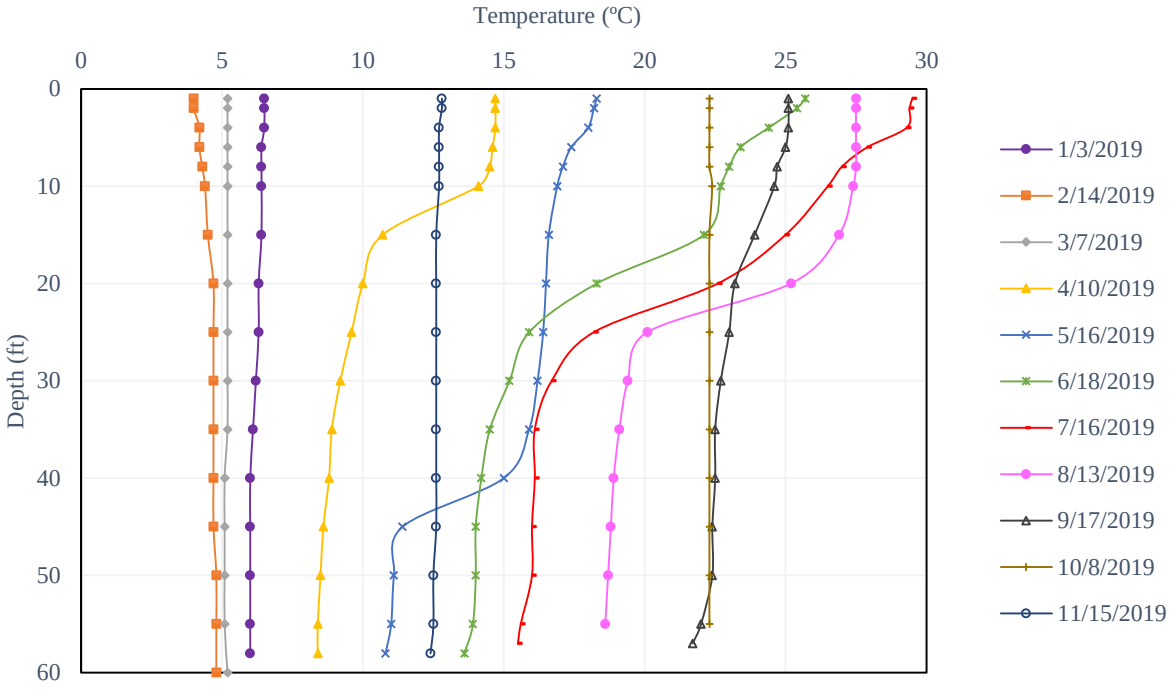

Figure 4-39. Temperature Profiles at Station RE02 for 2019

Relative Thermal Resistance to Mixing (RTRM) is a dimensionless parameter used to illustrate the stability of thermal stratification. This parameter is the result of the division of the density difference between adjacent waters (at different depths) and the density difference between waters with temperatures of 4°C and 5°C (since the density rate change is at its lowest value between these temperatures). The highest values of RTRM occur when density differences between adjacent layers are higher. Figure 4-40 presents the RTRM for the summer months of 2019, and shows that the most stable thermal stratification occurred on August 13, 2019. The maximum RTRM value of 119 was observed at a depth of 25 ft., indicating the position of the metalimnion/thermocline.

Figure 4-41 presents summer water temperatures at the surface and bottom depths of RE30 as a function of summer water temperatures at ST40/45, using data from 1973 to 2019. This graph illustrates how the water temperature at ST40/45 (black line in Figure 4-41) is cooler than the reservoir surface temperature and warmer than the reservoir bottom temperature. Since the density of water decreases with increasing temperature (after reaching its peak at 4°C), this graph also demonstrates that ST40/45 water is denser than reservoir epilimnetic waters and less dense than hypolimnetic waters, which are denser. Therefore, inflows from the Bull Run will tend to flow into the hypolimnion. This is an important observation because it suggests that the nitrate discharged in the MHR WRF effluent as a water quality strategy will flow to the hypolimnion where it is needed to maintain oxidized conditions.

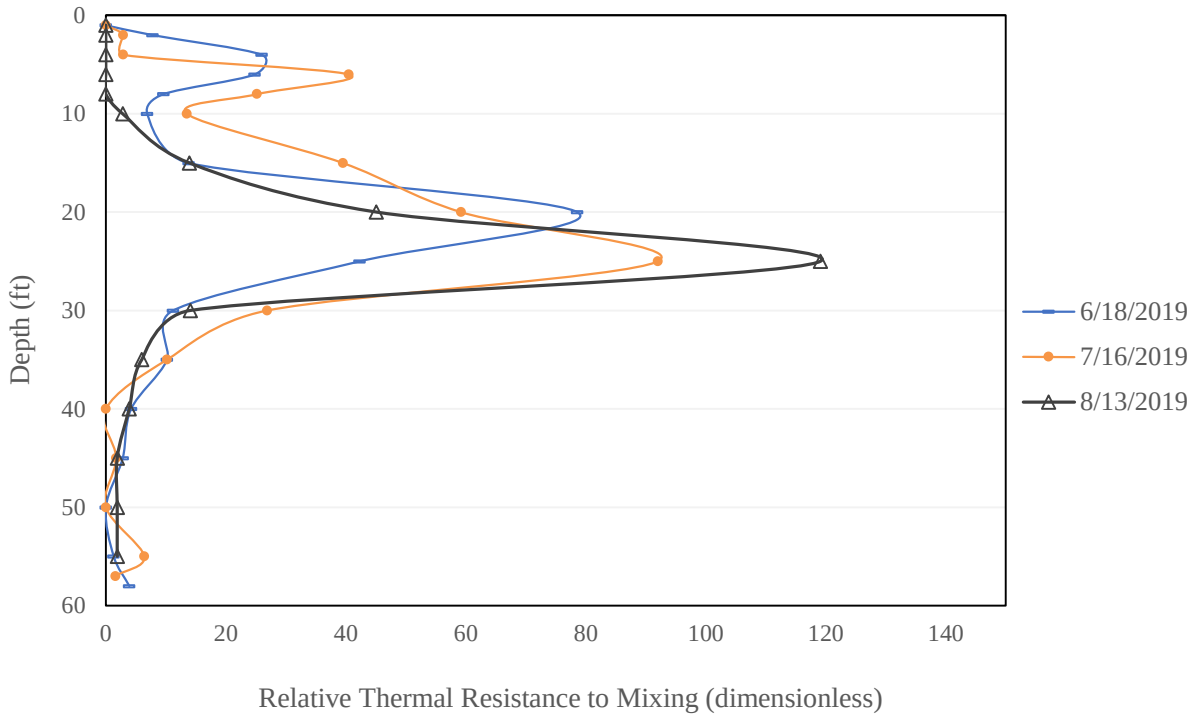

Figure 4-40. Relative Thermal Resistance to Mixing at Station RE02 for Summer Months

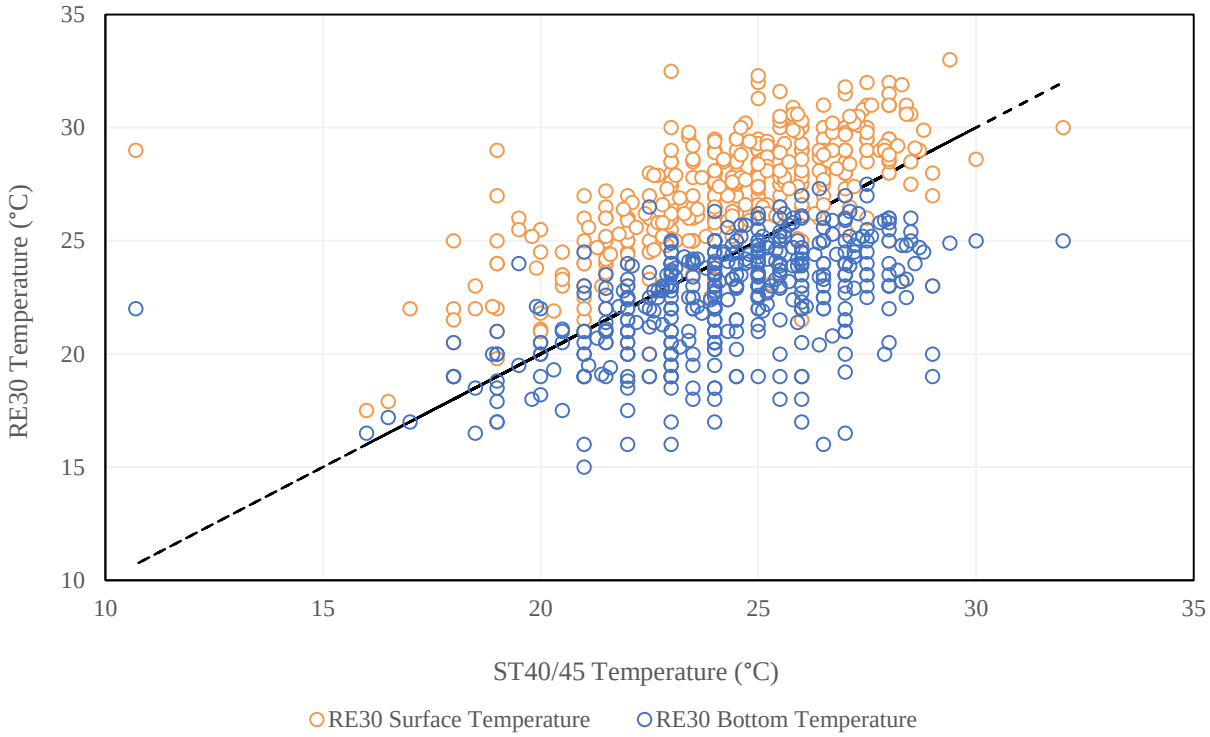

Figure 4-41. RE30 and ST40 Summer Water Temperature Comparison, 1973–2019

Table 4-22 summarizes water temperature data from 1973 to 2019 at each of the four main stations discussed in this assessment. Average, median, and standard deviation values are provided by season and depth. As mentioned previously, surface data correspond to measurements taken at 1-foot depths, while bottom data correspond to measurements taken at the greatest depth. All stations follow the same pattern: highest temperatures during summer, followed by fall, spring, and winter (same pattern shown in the stream monitoring station). The highest difference between surface and bottom average values can be observed in the summer (when thermal stratification is present), and this difference is more noticeable at stations RE02 and RE15, which are the deepest stations. Daily bottom water temperatures have not exceeded the VDEQ maximum temperature criteria of 32°C for Class III nontidal waters during the entire period of record and there have been very few instances where RE15, RE30, or RE35 have shown values slightly higher than 32°C at the surface (32.2°C–33.5 °C).

Table 4-22. Occoquan Reservoir Seasonal Average Temperature (°C), 1973–2019

Depth	Season	RE02			RE15			RE30			RE35		
		Mean	*Median*	*Standard Deviation*	*Mean*	*Median*	*Standard Deviation*	*Mean*	*Median*	*Standard Deviation*	*Mean*	*Median*	*Standard Deviation*
Surface	Winter	5.25	5.00	2.61	5.66	5.50	2.41	4.68	4.50	2.89	4.70	4.60	2.54
	Spring	14.91	15.25	5.59	15.63	16.00	5.54	15.39	15.80	5.55	15.29	15.90	5.57
	Summer	26.82	27.00	2.23	27.22	27.50	2.24	26.63	27.00	2.74	26.79	27.00	2.55
	Fall	18.75	19.00	5.34	18.44	18.50	5.75	16.90	16.90	6.06	17.41	17.50	5.99
Bottom	Winter	5.20	4.80	2.23	5.31	5.00	1.97	4.89	4.50	2.43	5.13	5.00	2.14
	Spring	9.77	9.80	2.86	10.82	11.00	3.18	12.99	13.50	4.06	12.07	12.35	3.72
	Summer	17.26	17.30	3.70	17.51	17.50	2.98	22.46	23.00	2.42	20.43	20.90	3.14
	Fall	16.81	17.25	4.68	15.82	16.50	4.54	15.61	15.50	5.40	16.20	16.70	5.27

The Mann-Kendall statistical test was performed for several water quality parameters for the surface and bottom water of the Occoquan Reservoir. Table 4-23 summarizes results for temperature, DO, and alkalinity trends. Temperature shows an increasing trend for almost all stations and seasons, for both surface and bottom waters, at $p<0.1$ (bold numbers). Similar increasing trends are observed at the stream stations. The only seasons that present decreasing trends at reservoir stations are spring and summer for bottom water at RE02.

Table 4-23. Mann-Kendall Trends for Reservoir Temperature, Dissolved Oxygen, and Alkalinity, 1973–2019

Station	Description	Season	Temperature				Dissolved Oxygen				Alkalinity			
			Sen Slope	*Kendall Tau*	*p-value*	*Trend*	*Sen Slope*	*Kendall Tau*	*p-value*	*Trend*	*Sen Slope*	*Kendall Tau*	*p-value*	*Trend*
RE02	Surface	Winter	0.053	0.285	**0.006**	↗	0.000	-0.001	1.000	↔	0.548	0.439	**1.8E-05**	↗
		Spring	0.046	0.248	**0.014**	↗	0.009	0.114	0.263	↗	0.524	0.658	**7.5E-11**	↗
		Summer	0.027	0.234	**0.021**	↗	0.030	0.328	**0.001**	↗	0.466	0.508	**4.8E-07**	↗
		Fall	0.036	0.260	**0.010**	↗	-0.010	-0.079	0.441	↘	0.545	0.467	**3.8E-06**	↗
	Bottom	Winter	0.018	0.122	0.236	↗	0.005	0.047	0.649	↗	0.611	0.470	**5.8E-06**	↗
		Spring	-0.027	-0.233	**0.021**	↘	-0.022	-0.123	0.226	↘	0.584	0.615	**1.1E-09**	↗
		Summer	-0.060	-0.265	**0.009**	↘	0.008	0.187	**0.065**	↗	0.601	0.310	**0.002**	↗
		Fall	0.006	0.028	0.790	↗	0.002	0.020	0.847	↗	0.758	0.458	**5.8E-06**	↗
RE15	Surface	Winter	0.036	0.194	**0.059**	↗	0.038	0.309	**0.003**	↗	0.464	0.372	**2.9E-04**	↗
		Spring	0.054	0.287	**0.005**	↗	0.008	0.123	0.226	↗	0.567	0.661	**5.8E-11**	↗
		Summer	0.031	0.272	**0.007**	↗	0.040	0.392	**1.0E-04**	↗	0.505	0.540	**1.2E-07**	↗
		Fall	0.037	0.230	**0.024**	↗	-4.93E-05	-0.002	0.993	↘	0.624	0.517	**3.6E-07**	↗
	Bottom	Winter	0.030	0.208	**0.044**	↗	0.016	0.107	0.302	↗	0.508	0.278	**0.007**	↗
		Spring	0.036	0.318	**0.002**	↗	-0.018	-0.151	0.137	↘	0.602	0.606	**2.0E-09**	↗
		Summer	0.068	0.300	**0.003**	↗	0.006	0.176	**0.083**	↗	0.622	0.359	**3.9E-04**	↗
		Fall	0.013	0.094	0.359	↗	0.024	0.193	**0.056**	↗	1.034	0.562	**2.7E-08**	↗
RE30	Surface	Winter	0.086	0.437	**2.0E-05**	↗	0.026	0.210	**0.041**	↗	0.957	0.578	**1.6E-08**	↗
		Spring	0.070	0.320	**0.002**	↗	0.006	0.077	0.452	↗	1.032	0.747	**1.5E-13**	↗
		Summer	0.052	0.418	**3.5E-05**	↗	0.045	0.306	**0.002**	↗	0.781	0.652	**1.1E-10**	↗
		Fall	0.049	0.271	**0.007**	↗	0.027	0.309	**0.002**	↗	0.897	0.630	**4.5E-10**	↗
	Bottom	Winter	0.055	0.325	**0.002**	↗	0.051	0.331	**0.001**	↗	0.875	0.523	**4.8E-07**	↗
		Spring	0.062	0.465	**4.3E-06**	↗	0.028	0.238	**0.019**	↗	0.994	0.713	**1.7E-12**	↗
		Summer	0.078	0.548	**1.2E-07**	↗	0.052	0.415	**4.0E-05**	↗	0.654	0.637	**2.8E-10**	↗
		Fall	0.044	0.245	**0.016**	↗	0.035	0.277	**0.006**	↗	0.905	0.652	**1.1E-10**	↗
RE35	Surface	Winter	0.052	0.292	**0.005**	↗	0.018	0.138	0.187	↗	0.408	0.409	**7.7E-05**	↗
		Spring	0.061	0.320	**0.002**	↗	0.009	0.154	0.128	↗	0.363	0.550	**5.1E-08**	↗
		Summer	0.052	0.384	**1.5E-04**	↗	0.017	0.201	**0.048**	↗	0.362	0.441	**1.3E-05**	↗
		Fall	0.037	0.230	**0.024**	↗	0.001	0.021	0.840	↗	0.531	0.480	**2.0E-06**	↗
	Bottom	Winter	0.023	0.148	0.156	↗	0.037	0.239	**0.021**	↗	0.378	0.316	**0.002**	↗
		Spring	0.048	0.440	**1.4E-05**	↗	0.018	0.097	0.340	↗	0.341	0.491	**1.2E-06**	↗
		Summer	0.073	0.282	**0.005**	↗	-0.001	-0.006	0.956	↘	0.221	0.132	0.193	↗
		Fall	0.017	0.093	0.364	↗	0.001	0.003	0.985	↗	0.574	0.460	**5.4E-06**	↗

4.3.3 Dissolved Oxygen

Recalling from previous sections, oxygen is added to the reservoir from the atmosphere through diffusion or by photosynthesis from aquatic plants. If photosynthesis rates are high, the water may even get supersaturated during sunny days. However, when thermal stratification is present, circulation of oxygen (as well as other gases and nutrients) is impeded due to the difference in water densities between adjacent layers. This results in reduced oxygen levels in the hypolimnion. If respiration rates and bacterial decomposition of organic matter are high, DO gets depleted. Oxygen may also get consumed through chemical oxidation of dissolved organic matter. Hypolimnetic anoxia can cause the release of undesirable constituents, including phosphorus, ammonia, iron, and manganese, and result in fish kills.

DO concentrations for RE02 are presented in Figure 4-42. As with temperature, isopleths were drawn to show DO behavior throughout the water column and during thermal stratification. Minor ticks indicate the months of March, May, August, and October. DO levels are higher during the winter, early spring, and late fall, reaching a maximum value of 21.6 mg/l in 2018. During these periods, DO levels seem to change less with depth, since the water column is well-mixed. Meanwhile, the difference between surface and bottom DO is noticeable in late spring and

becomes more pronounced during the summer, when thermal stratification is occurring. Figure 4-43 shows the DO concentrations at RE02, expressed as percent saturation, for the same period. Lower percent saturation is mostly observed during summer, with minimum values approaching 0% at depths greater than 15 ft. There have also been periods of supersaturation, the highest of which (206%) occurred in fall 2007. Since field measurements are taken during the day, the supersaturation values observed may be the result of photosynthesis, where aquatic plants reduce CO_2 and oxidize water. However, these values may decrease at night when there is no solar radiation for photosynthesis and oxygen is instead consumed during photorespiration (in addition to animal and bacterial respiration).

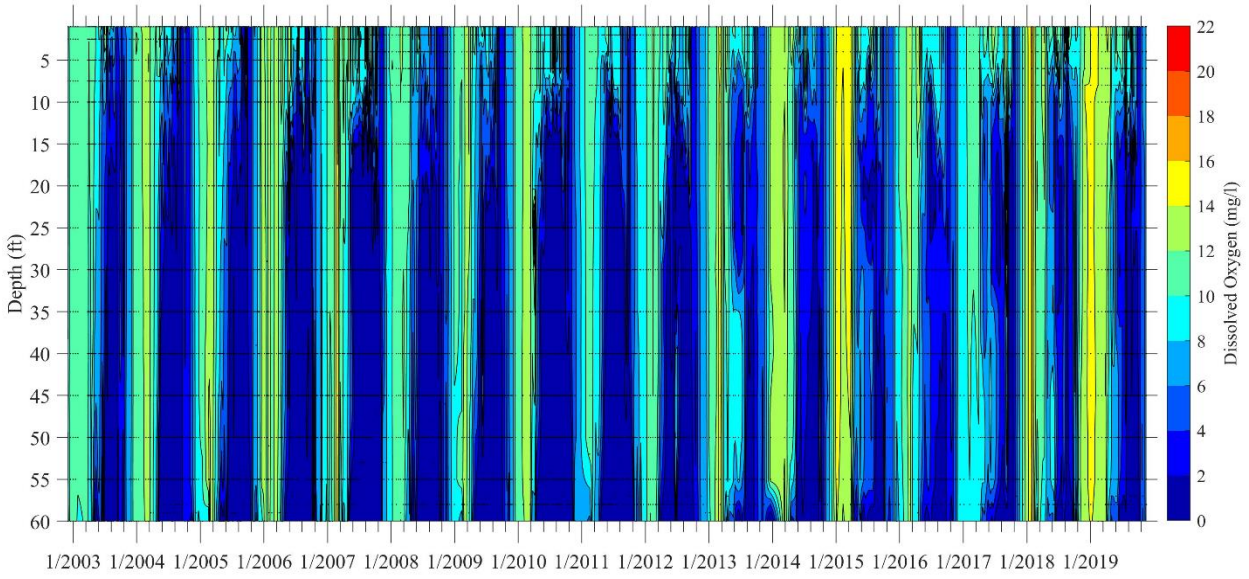

Figure 4-42. RE02 Dissolved Oxygen Isopleths, 2002–2019

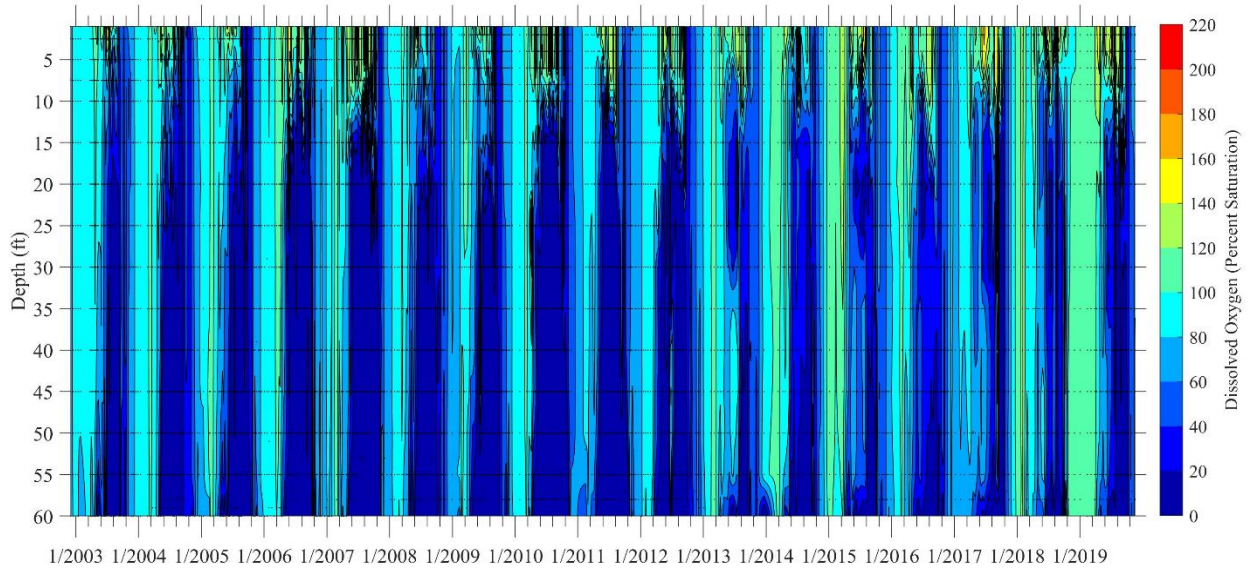

Figure 4-43. RE02 Percent Saturation Dissolved Oxygen Isopleths, 2002–2019

Figure 4-44 shows the DO profiles at RE02 for 2019, and provides a clear picture of monthly DO patterns. The highest DO concentrations are observed during January, with a maximum value of 14.6 mg/l, while lowest values (minimum of 0.4 mg/l) are seen in August at a depth of 20 ft. or deeper. From January to March and October to November, DO levels are relatively constant with depth. Differences throughout the water column start in April and are more pronounced during the summer months. The highest difference between surface and bottom DO are observed in August, when levels drop approximately 9 mg/l.

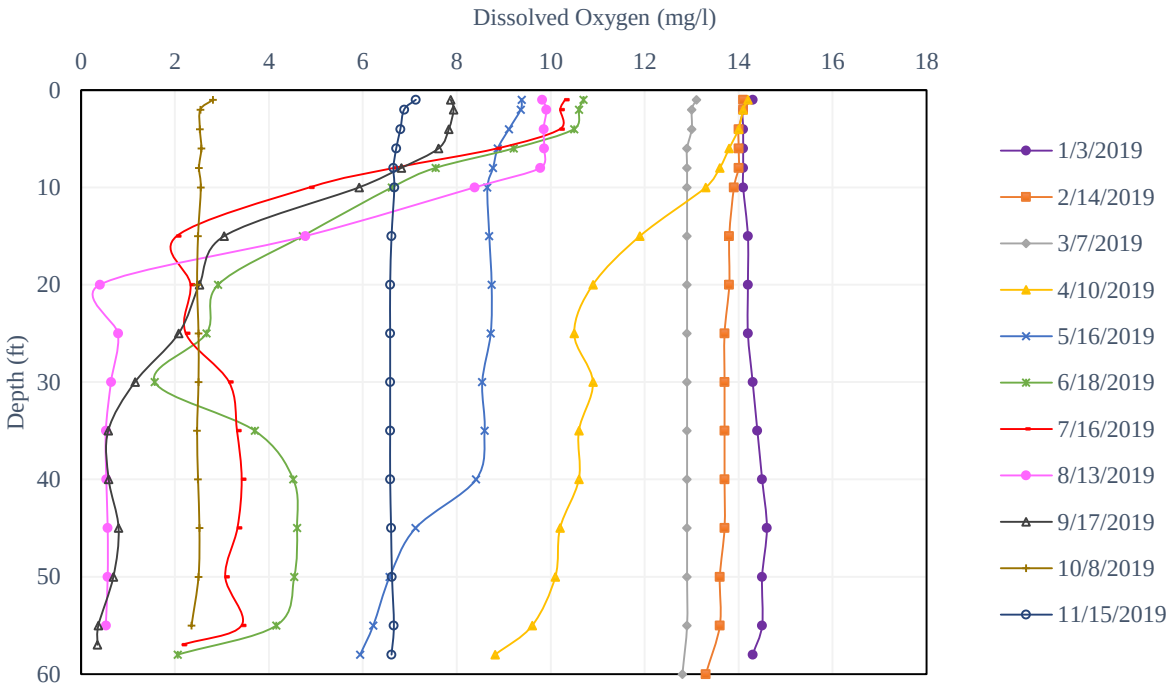

Figure 4-44. Dissolved Oxygen Profile at Station RE02, 2019

As shown for the stream stations, Table 4-24 presents the number of days from 2003 to 2019 that DO measurements at the reservoir were less than the 4 mg/l VDEQ standard, shown by station, year, and season. Van Den Bos (2003) reported 77 such occurrences in surface water and 1,782 for bottom waters from 1973 to 2002. Since 2003, there were 42 days that exhibited low DO in surface waters and 1,033 days in bottom waters. It should be noted that for the Occoquan Reservoir, the VDEQ standard refers only to epilimnetic waters when thermally stratified. When thermal stratification is not present, the DO criteria applies throughout the water column. The low DO occurrences in bottom waters presented in Table 4-24 are mainly a reflection of thermal stratification, as there are more occurrences in RE02, which is deeper than the other stations, and during summer, where temperature stratification is occurring. During winter, there were no DO levels less than 4 mg/l detected. The season with highest count of lower DO levels occurred during summer at the reservoir bottom and during fall at the surface. Since 2013, low DO level occurrences at the reservoir bottom have been somewhat lower than the preceding years. This may have been the result of the installation of the hypolimnetic oxygenation system completed in 2012.

Figure 4-45 shows the surface and bottom DO time series since 2003 to 2019 to illustrate the occurrences of DO levels less than 4 mg/l since 2013.

Table 4-24. Occoquan Reservoir Dissolved Oxygen Concentrations under 4 mg/l, 2003–2019

By Station		
Station	*Surface*	*Bottom*
RE02	42	335
RE15	0	305
RE30	0	144
RE35	0	249
Total	42	1033

By Season		
Season	*Surface*	*Bottom*
Winter	0	0
Spring	0	142
Summer	1	645
Fall	41	246
Total	42	1033

By Year		
Year	*Surface*	*Bottom*
2003	2	48
2004	5	74
2005	6	75
2006	1	71
2007	3	87
2008	5	70
2009	6	73
2010	2	92
2011	2	70
2012	2	80
2013	1	35
2014	1	27
2015	1	49
2016	2	49
2017	1	42
2018	0	31
2019	2	60
Total	42	1033

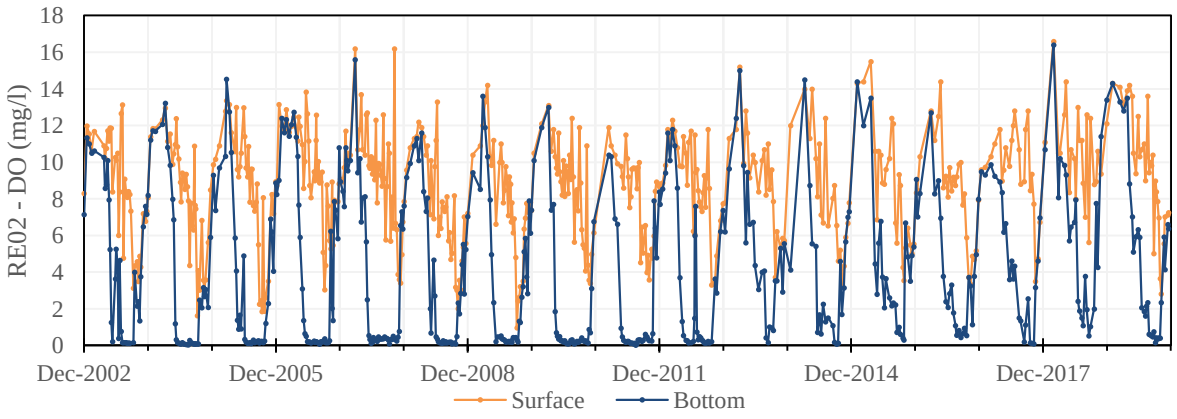

Figure 4-45. Dissolved Oxygen Time Series at RE02, 2003–2019

Table 4-25 shows seasonal average DO concentrations for each station and season from 1973 to 2019. In general, lower seasonal averages for surface DO were observed during fall and higher levels during winter. For bottom waters, the lowest values are observed during summer and highest during winter. These values match the annual circulation pattern of the reservoir explained previously, where biological activity consumes oxygen and thermal stratification prevents oxygen from being replenished during summer, resulting in low DO levels. Winter DO levels may be higher because biological activity tends to decrease during winter and gas solubility increases with decreasing temperatures. It should be noted that even though the Mann-Kendall results for temperature show increasing trends (and DO tends to follow an opposite pattern to temperature), results for DO, presented in Table 4-23, indicate all significant trends are increasing. These results contrast the behaviors at stream stations, where most temperature trends are positive and most DO trends are negative. Significant trends at the reservoir can be observed at the following stations: for surface water: at RE02 during summer, at RE15 during winter and summer, at RE30 during winter, summer, and fall, and at RE35 during summer; for bottom waters: at RE02 during summer, at RE15 during summer and fall, at RE30 during all seasons, and RE35 during winter.

Table 4-25. Occoquan Reservoir Seasonal Average Dissolved Oxygen, 1973–2019

Depth	Season	RE02			RE15			RE30			RE35		
		Mean	*Median*	*Standard Deviation*	*Mean*	*Median*	*Standard Deviation*	*Mean*	*Median*	*Standard Deviation*	*Mean*	*Median*	*Standard Deviation*
Surface	Winter	10.78	11.00	1.83	11.63	11.60	1.52	12.33	12.30	1.72	12.17	12.40	1.41
	Spring	10.70	10.70	1.64	10.82	10.85	1.67	10.06	10.00	1.95	10.51	10.48	1.61
	Summer	8.37	8.45	1.95	9.83	9.75	1.83	9.51	9.40	2.30	9.05	9.01	1.83
	Fall	5.97	5.90	2.27	9.06	9.00	1.82	9.51	9.36	1.91	9.02	9.10	1.79
Bottom	Winter	9.90	10.00	2.12	10.40	10.66	2.08	12.00	12.00	2.02	11.41	11.54	1.92
	Spring	5.82	6.00	3.94	6.06	6.40	3.88	7.88	8.20	3.21	7.15	8.00	3.83
	Summer	0.57	0.20	1.07	0.52	0.20	1.01	2.56	1.90	2.41	1.32	0.38	2.00
	Fall	3.04	2.85	2.69	4.07	4.15	3.33	7.42	7.81	2.67	6.03	6.60	3.30

4.3.4 pH and Alkalinity

Table 4-26 presents seasonal average and median pH values for the Occoquan Reservoir from 1973 to 2019 for stations RE02, RE15, RE30, and RE35. Both average and median values for surface waters are higher during summer and lower during winter for all stations. Reservoir pH values for the entire period of record average between 6.4 to 7.5 at the surface, and 6.3 to 7 at the bottom. Surface water values are higher than the bottom water values during spring, summer, and fall. RE15 surface pH values are higher than the other stations. There is no particular trend in bottom waters.

Figure 4-46 shows pH time series from 2003 to 2019 for the different reservoir stations. Dashed lines on this figure represent VDEQ pH range for class III nontidal waters as reference. These criteria apply to the entire column when reservoir is not thermally stratified and to epilimnetic waters when stratification is present. pH values range from 5.1 to 9.5 at RE02, 6.2 to 9.6 at RE15, 6.8 to 9.4 at RE30, and 6.3 to 9.1 at RE35. Since 2003, pH values greater than 9.0 have been observed only in surface water and mainly at RE15, with a peak value of 9.6 during summer 2007. pH values less than 6.0 have only been observed at RE02 bottom waters, with minimum value of

5.1 during summer 2012. pH peaks may be caused by CO_2 removal during photosynthesis, while pH dips may be related to rainfall events and/or CO_2 addition due to microbial decomposition.

Table 4-26. Occoquan Reservoir Seasonal Average and Median pH*, 1973–2019

Depth	Season	RE02		RE15		RE30		RE35	
		Mean	*Median*	*Mean*	*Median*	*Mean*	*Median*	*Mean*	*Median*
Surface	Winter	6.4	7.0	6.9	7.3	6.7	7.2	6.6	7.1
	Spring	6.8	7.3	6.9	7.3	6.8	7.3	6.7	7.2
	Summer	7.3	7.7	7.5	8.3	7.2	7.7	7.1	7.6
	Fall	6.9	7.0	7.1	7.4	7.1	7.3	7.0	7.2
Bottom	Winter	6.5	7.0	6.9	7.2	6.3	7.4	6.7	7.1
	Spring	6.5	6.9	6.7	6.9	6.7	7.2	6.6	7.0
	Summer	6.6	6.8	6.7	6.9	6.8	7.0	6.6	6.8
	Fall	6.8	6.9	6.9	7.0	7.0	7.2	6.8	7.0

* seasonal average corresponds to the average of the H+ concentration; median values correspond to standard pH units.

Figures 4-47 and 4-48 present seasonal average total alkalinity at the Occoquan Reservoir from 1973 to 2019. Surface seasonal average alkalinity ranges between 17–70 mg/l at RE02, 18–78 mg/l at RE15, 13–104 mg/l at RE30, and 19–74 mg/l at RE35, all as $CaCO_3$. Bottom seasonal average alkalinity is generally somewhat higher with values between 13–105 mg/l at RE02, 19–97 at RE15, 26–108 mg/l at RE30, and 19–81 mg/l at RE35, all as $CaCO_3$. Surface waters show higher average total alkalinity waters during fall. Higher values for bottom waters are seen during summer for all stations except RE30, which has higher values during fall for both surface and bottom waters. The lowest values for surface and bottom waters were observed during winter, followed by spring. RE30 has higher values than the rest of the stations during all seasons in surface waters. This is generally true for bottom waters also, except during summer, where all stations show similar ranges. The higher alkalinity values observed at RE30 match the higher values observed at ST40/45, all of which correspond to the Bull Run arm and are influenced by the MHR WRF high alkalinity.

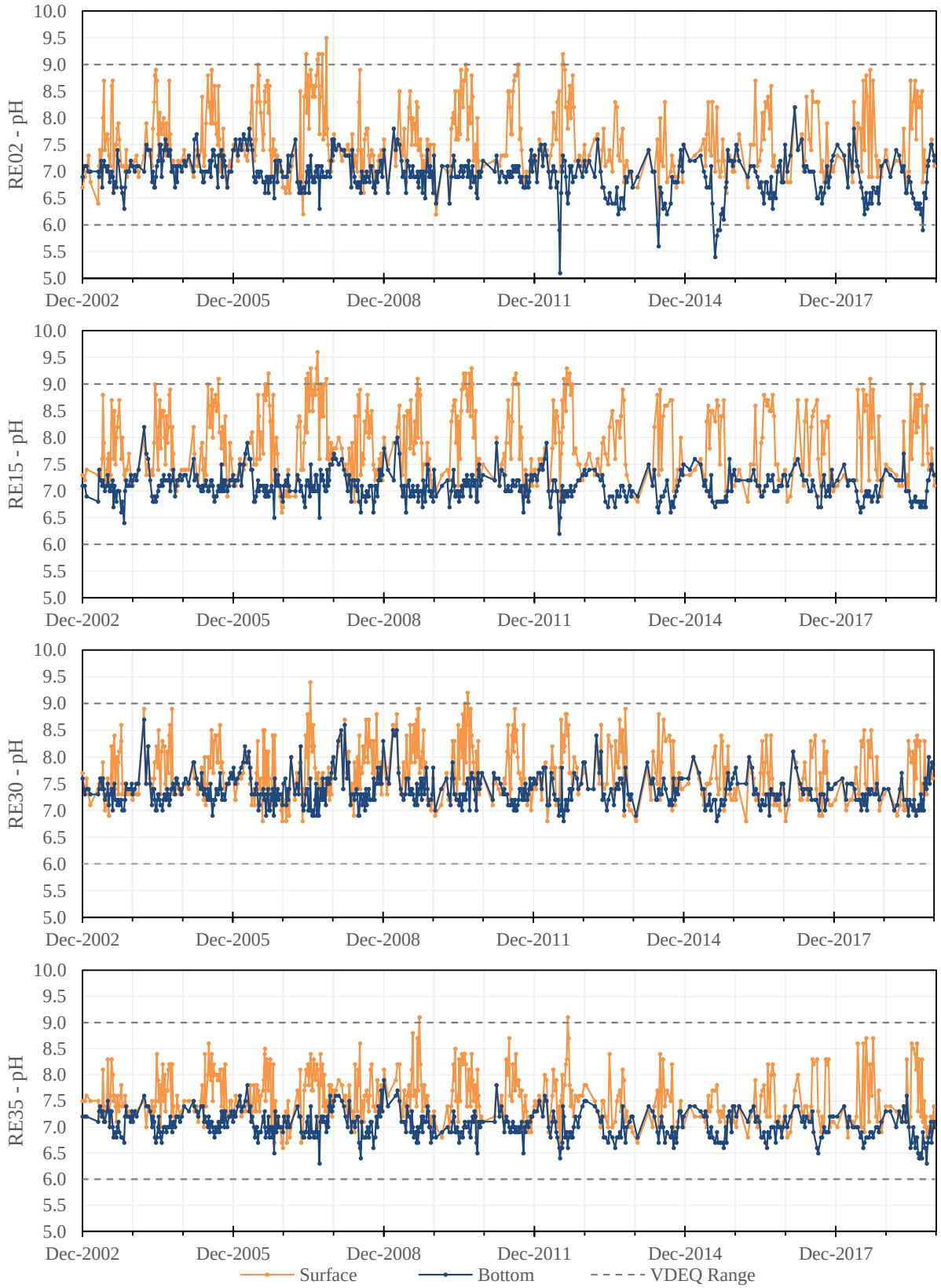

Figure 4-46. pH Time Series at Reservoir Stations, 2003–2019

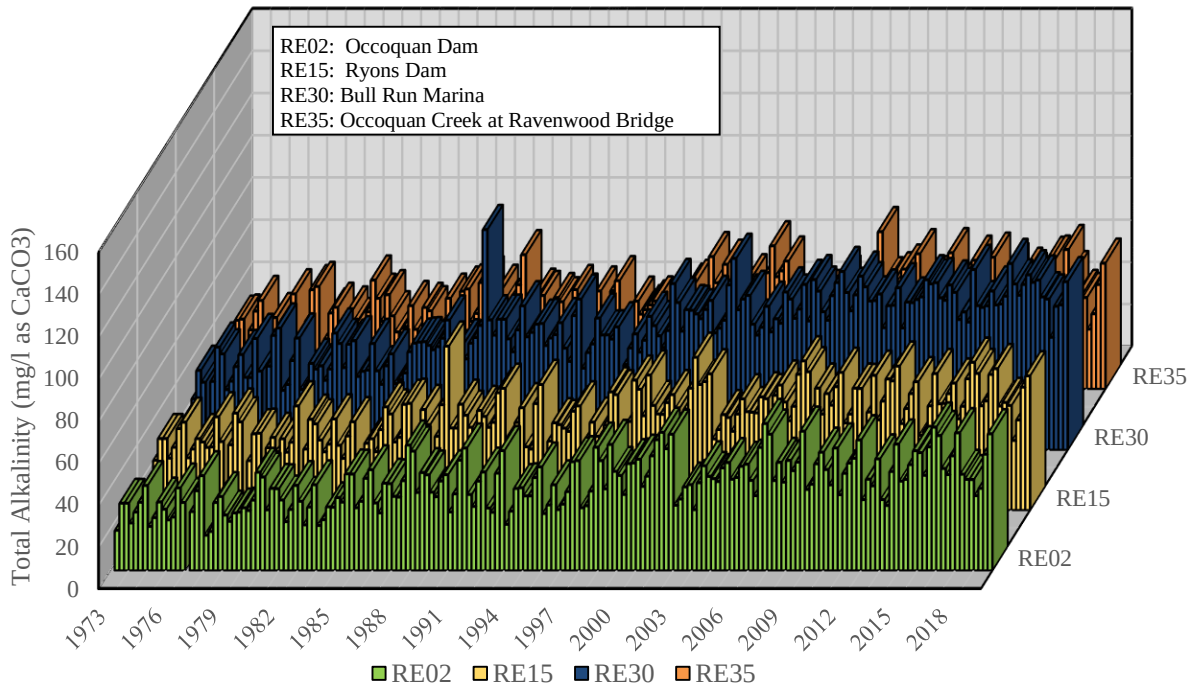

Figure 4-47. Seasonal Average Total Alkalinity in Reservoir Surface Waters, 1973–2019

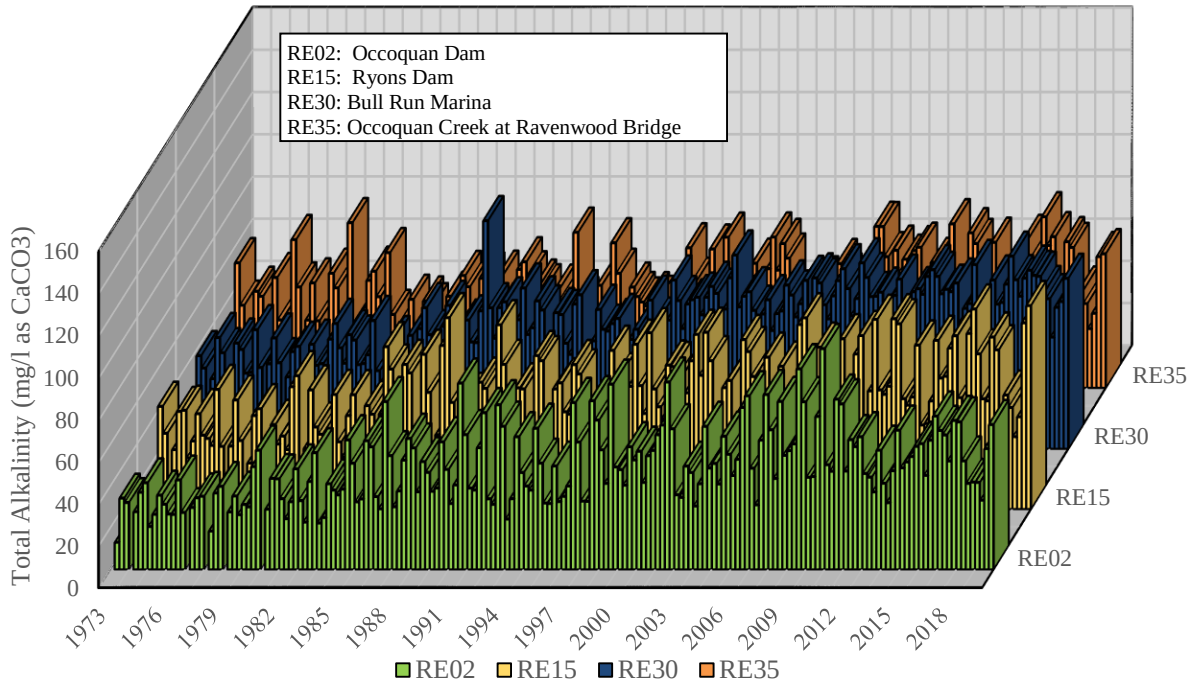

Figure 4-48. Seasonal Average Total Alkalinity in Reservoir Bottom Waters, 1973–2019

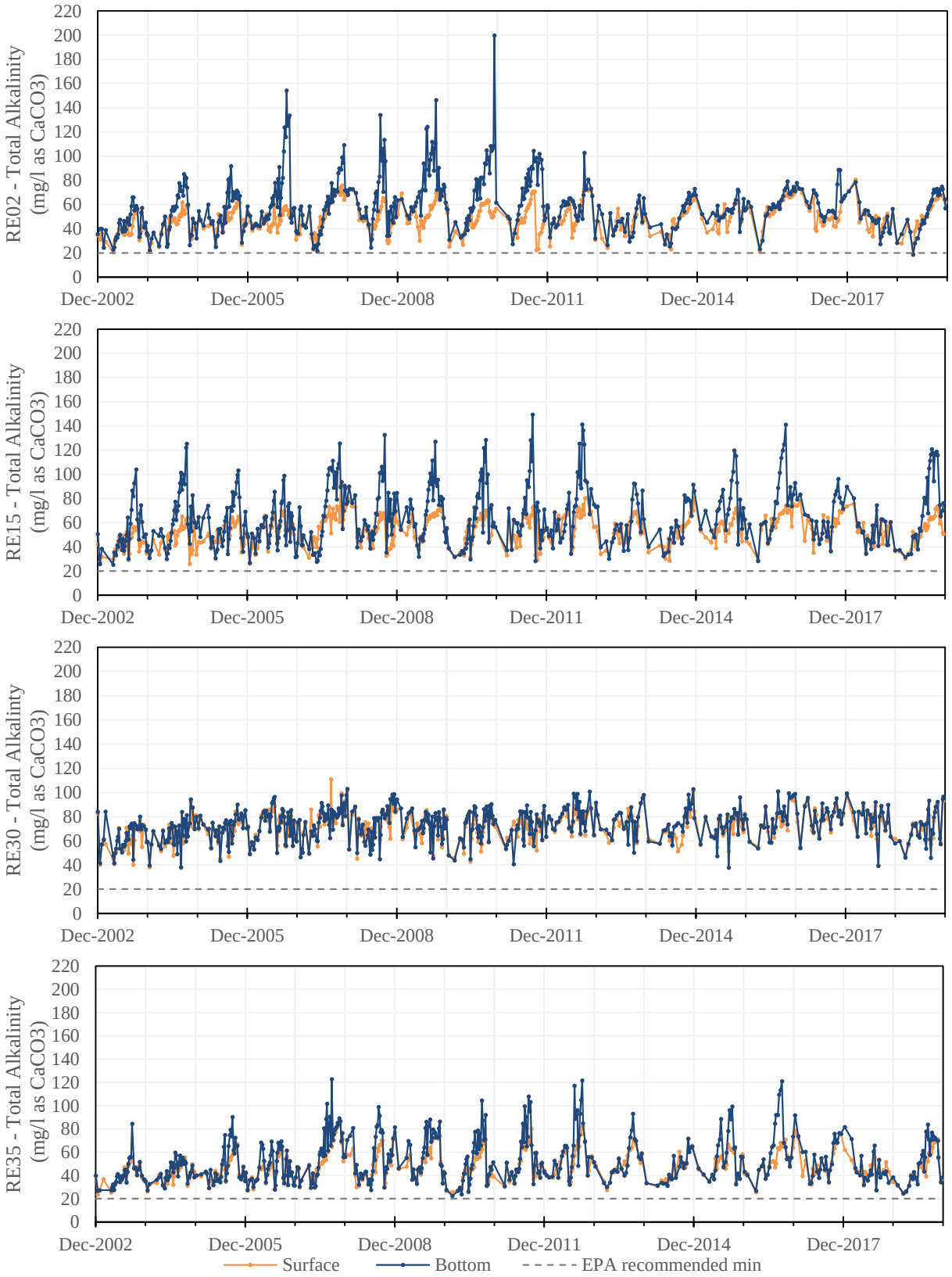

Figure 4-49. Total Alkalinity Time Series at Reservoir Stations, 2003–2019

Figure 4-49 shows alkalinity time series from 2003. Again, as mentioned, total alkalinity tends to be higher at the bottom than at the surface for all stations, although, the difference is less marked at the inflow reservoir stations (RE30 and RE35) than at the other stations. RE02 has a higher total alkalinity range, from 18 to 200 mg/l as $CaCO_3$, with three noticeable peaks in bottom waters (199.9, 154.5, and 146.6 mg/l as $CaCO_3$), all of which occurred during fall. Alkalinity values since 2003 for other stations ranged from 25 to 150 mg/l as $CaCO_3$ at RE15, 38 to 111 mg/l as $CaCO_3$ at RE30, and 22 to 123 mg/l as $CaCO_3$ at RE35. During this period, there was only one date (March 2019) where alkalinity was slightly lower (18 mg/l as $CaCO_3$) than the 20 mg/l as $CaCO_3$ recommended by the USEPA in the Aquatic Life Criteria, which may have been due to higher rainfall during that month.

Mann-Kendall test results in Table 4-23 and seasonal average figures (4-47, 4-48), show an increasing alkalinity trend for all stations and all seasons (with the exception of bottom water alkalinity at RE35 during summer). Upward reservoir trends coincide with alkalinity trends observed at stream monitoring stations. These may be due to higher alkalinity discharges since MHR WRF's inception in 1978, and to nitrate discharges into the reservoir promoting denitrification (which produces alkalinity) when thermal stratification occurs and DO levels are low, also causing bottom alkalinity values to be higher than surface waters. This likely also explains higher total alkalinity values observed during summer and fall in bottom waters.

4.3.5 Oxidation-Reduction Potential

Many important biochemical processes involve oxidation-reduction reactions (transfer of electrons). Oxidation-reduction conditions in lakes and reservoirs are determined by the balance between photosynthesis and respiration. During photosynthesis, solar energy is used by plants to reduce CO_2 (which is stored as organic matter) and oxidize water; during respiration of organisms, reduced products are oxidized. For the oxidation of organic matter, microbes utilize oxygen as an electron acceptor, since it is the oxidant that yields them the maximum energy. If DO is not available or has been used up, the next most efficient oxidant is used, until all oxidants or organic matter is consumed.

ORP is a parameter that serves as an indicator of the overall intensity of the oxidizing or reducing conditions in a system. It is a measurement that represents the voltage necessary to prevent the flow of electrons between the environment and a reference electrode. ORP is expressed as millivolts, with positive potentials indicating relatively oxidizing conditions and negative potentials indicating reducing conditions. ORP measurements are useful to qualitatively interpret concentrations and/or forms in which nutrients, organic carbon, DO, and metals are found in aquatic systems, thus helping predict positive or negative impacts. Aerobic environments typically have redox potentials higher than approximately 350 mV and DO depletion is associated with ORP values of approximately 200 mV (Kalff, 2002). Table 4-27 obtained from (Stumm and Morgan, 1996) presents the most efficient electron acceptors used after DO is depleted. As indicated, the next most efficient electron acceptor is nitrate. If DO and nitrate are depleted, anaerobic conditions are established and organisms shift to the next electron acceptors, namely iron and manganese, which get reduced and released from sediments, consequently releasing orthophosphate

phosphorus bound to iron, and thus degrading water quality. For this reason, during thermal stratification, the MHR WRF discharges effluent with high concentrations of oxidized nitrogen (nitrate) into the reservoir to keep reservoir bottom waters oxidized. As shown in Figure 4.41 from section 4.5.2, inflows from Bull Run tend to mix with reservoir bottom waters. With nitrate present in the hypolimnion, organisms are able to use NO_3^- ions as terminal electron acceptors, thus preventing the release of nutrients and metals. As the nitrate flows along the reservoir, it gets denitrified. By the time it reaches the reservoir outlet, nitrate concentrations are much lower than the 10 mg/l limit established in the USEPA National Primary Drinking Water Regulations and VDEQ water quality criteria, and have historically never reached the 5 mg/l denitrification trigger point under the *Occoquan Policy*.

Table 4-27. Sequential Electron Acceptors in the Absence of Oxygen

Redox Couple	E_7 (mV)	DO (mg/l)
Nitrate → Nitrite	450 − 400	4.0
Nitrate →Nitrogen gas	450 − 350	0.4
Manganese (IV) →Manganese(II)	300 − 200	0.1
Iron(III) →Iron(II)	300 − 200	0.1
Sulfate →Sulfide	100 − 60	0.0
Carbon dioxide →Methane	< 0	0.0

Source: Stumm and Morgan, 1996

Seasonal average ORP values from 2001 to 2019 for the Occoquan Reservoir are presented in Table 4-28 (averages and standard deviation values were rounded to the nearest integer). ORP average values range between 378 and 477 mV for reservoir surface waters, and between 187 and 466 mV for bottom waters. At RE02, average surface ORP was higher than average bottom ORP during all seasons. Average ORP values for all stations are lowest during the summer, particularly in bottom waters, which is due to the effect of higher rates of organic matter decomposition during warmer months. During this decomposition process, oxygen gets consumed. When DO values approach zero and anoxic conditions appear, ORP values also drop. The lowest average values at the reservoir bottom at RE02 (232 mV), RE15 (187 mV), and RE35 (207 mV) occur during summer, and coincide with low DO average values seen for bottom waters in Table 4-25 (0.57 mg/l, 0.52 mg/l, 1.32 mg/l, respectively). Average summer ORP for RE30 bottom waters, on the other hand, was 401 mV (2.56 mg/l DO), which may be the result of the MHR WRF highly nitrified effluent discharge into the reservoir.

The following two figures illustrate ORP behavior at RE02, which is the deepest station and, experiences a more stable thermal stratification. Figure 4-50 is a time series of ORP from 2003 to 2019 at RE02. It can be observed that since 2013, as with the DO time series for RE02 in section 4.5.3, ORP at bottom waters are somewhat higher than during previous years when ORP reached negative values and approached zero on several occasions during the summer months. After 2013, no negative ORP values have been recorded, which may be attributed to the presence of the hypolimnetic oxygenation system helping maintain oxidized conditions. Figure 4-51 shows the

ORP profile for RE02 during 2019. As may be observed, the lowest ORP values for 2019 (200 to 300 mV) occurred during the months of January, April, May, and September, and remained fairly constant throughout the water column. The ORP value during January coincides with lower ORP values observed since August 2018 (Figure 4-50). The lower values during late spring and early fall may have been influenced by the beginning and ending of the thermal stratification period. During July, ORP went from 314 mV at the top to 265 mV at the bottom. August values vary a little more with depth, ranging from 395 mV at the top to 229 mV at the bottom. ORP for the remaining months was higher than 320 mV.

Table 4-28. Seasonal Average Oxidation-Reduction Potential at Reservoir Stations, 2001–2019

Depth	Season	RE02			RE15			RE30			RE35		
		Mean	*Median*	*Standard Deviation*	*Mean*	*Median*	*Standard Deviation*	*Mean*	*Median*	*Standard Deviation*	*Mean*	*Median*	*Standard Deviation*
Surface	Winter	469	463	100	462	466	93	460	471	96	456	455	89
	Spring	455	465	100	446	464	100	447	456	100	451	477	102
	Summer	415	424	118	378	392	103	394	407	102	399	413	112
	Fall	477	482	117	457	468	107	459	471	101	464	471	106
Bottom	Winter	459	455	98	453	452	96	458	472	93	462	462	87
	Spring	447	465	123	446	448	119	449	464	107	442	451	125
	Summer	232	207	170	187	131	153	401	410	120	207	141	159
	Fall	380	408	177	393	423	177	466	483	108	414	449	161

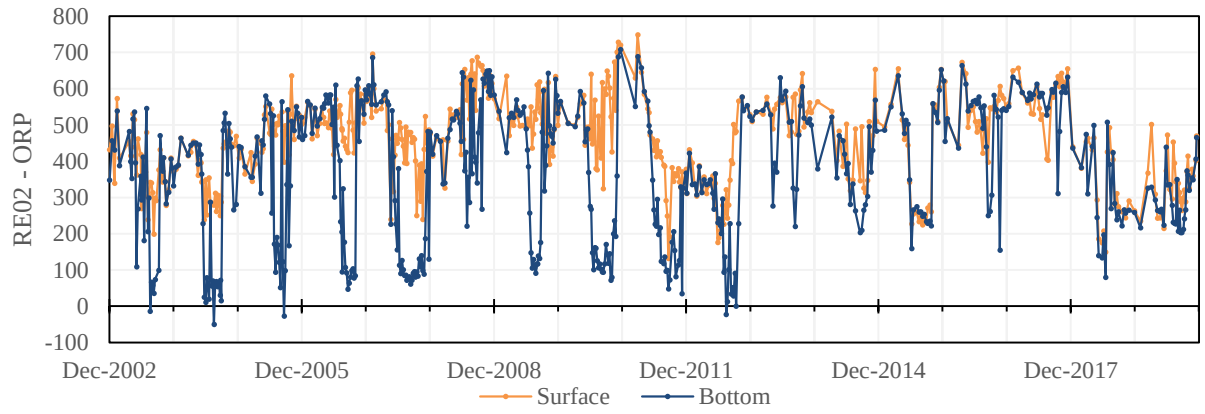

Figure 4-50. Oxidation-Reduction Potential Time Series at RE02, 2003–2019

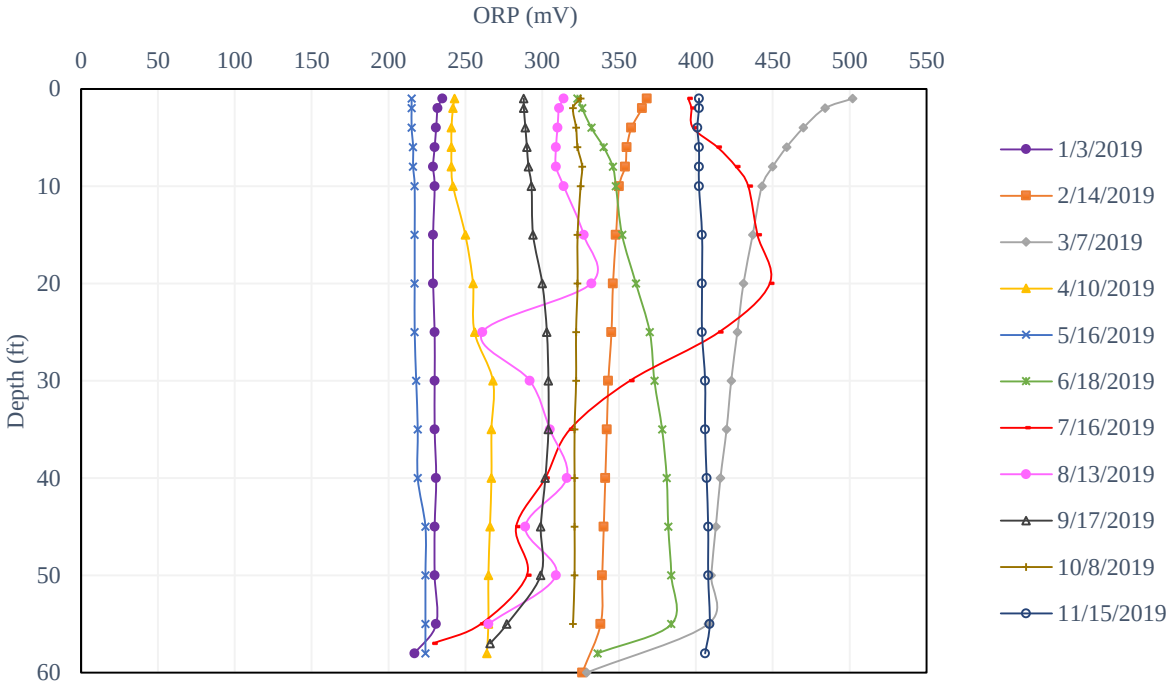

Figure 4-51. Oxidation-Reduction Potential Profile at RE02, 2019

4.3.6 Total Dissolved Solids, Conductivity, and Hardness

Conductivity is used to assess the effect of TDS such as minerals, salts, and ions at the reservoir stations. Because conductivity is more readily measured than TDS, TDS data are only available for RE02 (mainly surface values), whereas conductivity data are available for all stations. Using the TDS data collected at RE02, the ratio of TDS to conductivity was estimated to be 0.6:1 (Figure 4-52). A minimum average value of 79 µS/cm and maximum average value of 736 µS/cm was observed for both surface and bottom waters (Figures 4-53 and 4-54). However, despite similar average conductivity values throughout the water column, bottom conductivity was somewhat higher than surface conductivity during most of the period of record. Also observed from Figures 4-53 and 4-54, as with stream monitoring stations, RE30 (which represents water at the Bull Run arm) has higher average conductivity (144–736 µS/cm) than RE35 (which represents water at the Occoquan Creek arm), which has the lowest values (79–427 µS/cm). RE30 is influenced by the MHR WRF, as mentioned in the stream water quality section. Higher values were observed during the fall for all stations at both surface and bottom waters with the exception of RE35, in which higher values occurred during winter. Lowest values for all stations were generally seen during spring.

RE02 average conductivity ranged between 101 and 611 µS/cm at the surface, and between 109 and 609 µS/cm at the bottom for the period of record. Figure 4-55 shows the conductivity profile for RE02 during 2019. Values for conductivity during this year ranged between 107 and 373 µS/cm. Lowest values were seen during January and February, while the highest values were seen

during March and from September to November. All surface TDS values recorded for RE02, which represents the water quality at the Fairfax Water Griffith plant intake, were below the 500 mg/l recommended in the National Secondary Drinking Water Standards. Estimated values for bottom TDS at RE02, based on the ratio from Figure 4-52, show only two values to be slightly higher than 500 mg/l, which occurred during winter 1999 (502 mg/l and 508 mg/l). However, as Mann-Kendall results indicate in Table 4-29, conductivity trends are increasing for all analyzed stations and during all seasons, at 90% confidence intervals or greater; therefore, conductivity values should continue to be monitored to ensure that levels at the outflow are maintained under this secondary limit. Upward conductivity trends are likely due to agricultural and urban runoff, point source discharges, and the overall increasing salinization of the waters of the watershed. Since trends are increasing at all stations, this indicates runoff coming from both Occoquan Creek and Bull Run. Trend slopes at RE30 are higher than at other stations, which is likely because the Bull Run side of the reservoir is more urbanized, in addition to the influence from the MHR WRF.

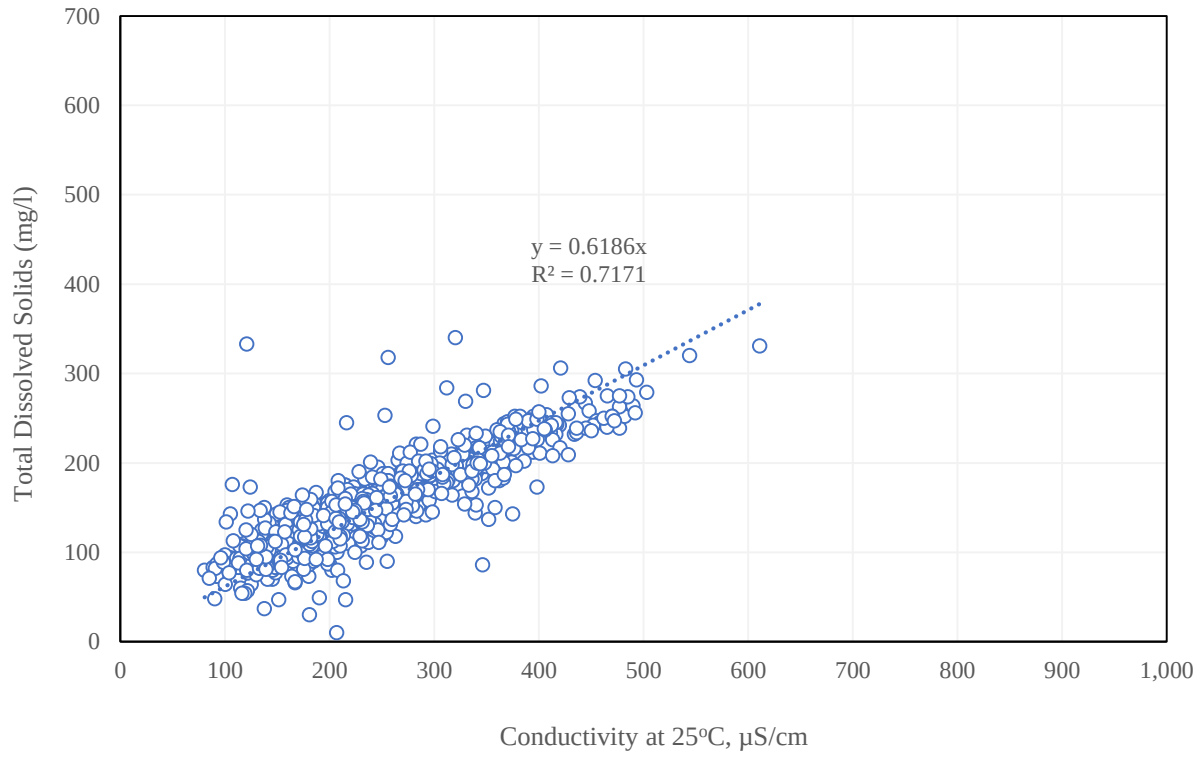

Figure 4-52. Total Dissolved Solids and Specific Conductance Correlation at RE02, 1979–2019

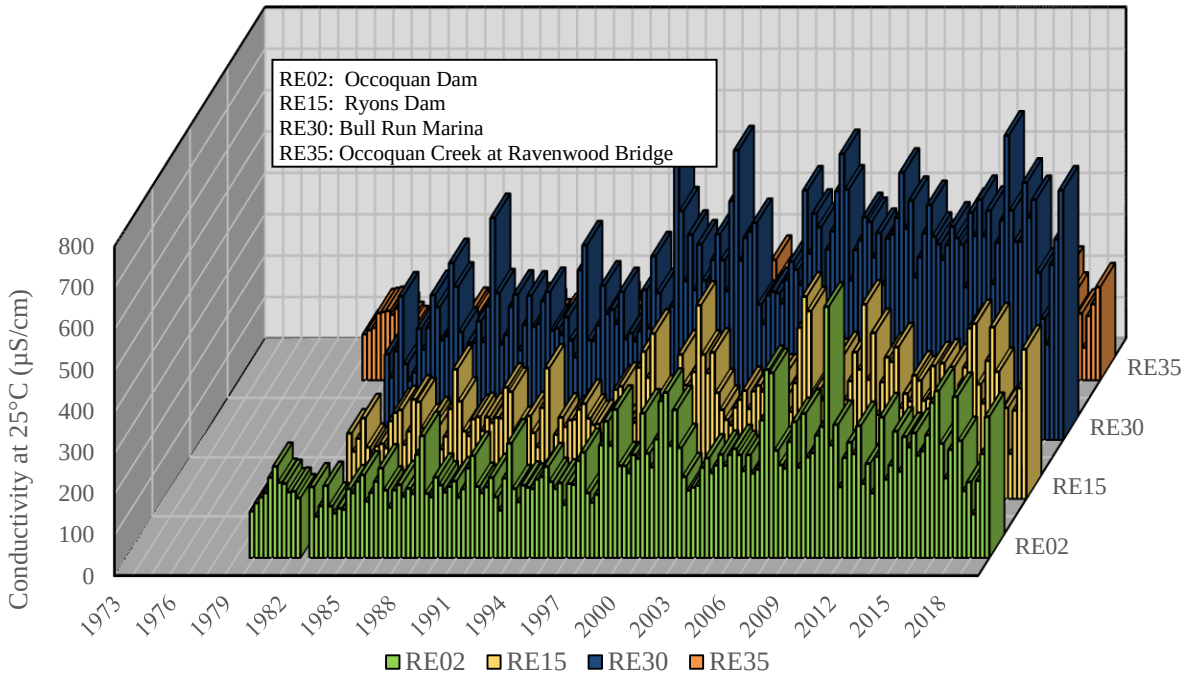

Figure 4-53. Specific Conductance Seasonal Average in Reservoir Surface Waters, 1973–2019

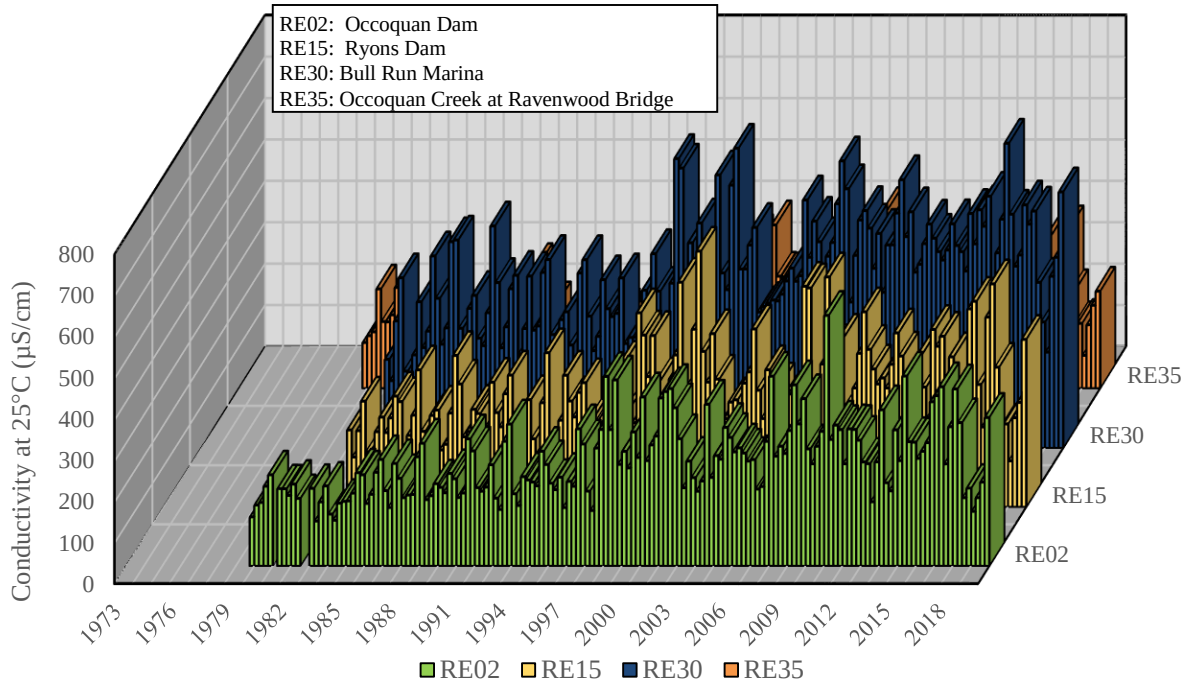

Figure 4-54. Specific Conductance Seasonal Average in Reservoir Bottom Waters, 1973–2019

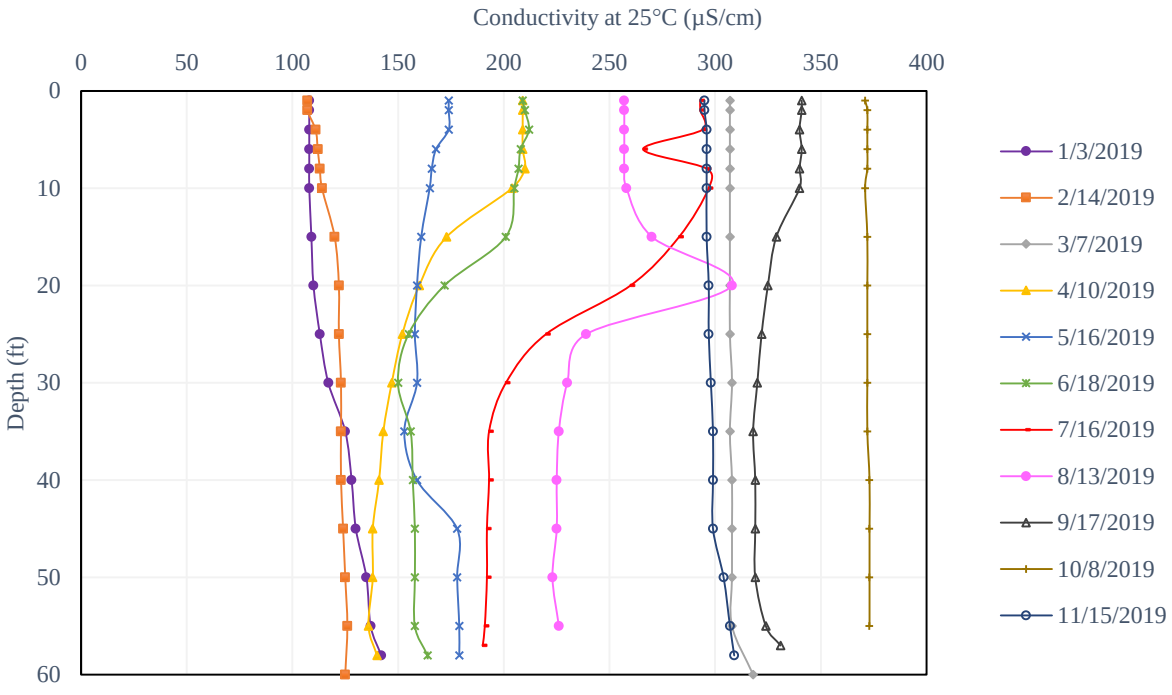

Figure 4-55. Specific Conductance Profiles at Station RE02, 2019

Table 4-29. Mann-Kendall Reservoir Conductivity and Hardness Trends, 1979–2019

Station	Description	Season	Conductivity				Hardness			
			Sen Slope	*Kendall Tau*	*p-value*	*Trend*	*Sen Slope*	*Kendall Tau*	*p-value*	*Trend*
RE02	Surface	Winter	3.693	0.446	**5.3E-05**	↗	1.600	0.373	**0.007**	↗
		Spring	4.190	0.574	**2.4E-07**	↗	1.337	0.509	**1.6E-04**	↗
		Summer	2.830	0.430	**1.0E-04**	↗	0.874	0.275	**0.042**	↗
		Fall	3.634	0.384	**4.2E-04**	↗	1.191	0.317	**0.019**	↗
	Bottom	Winter	4.289	0.384	**0.001**	↗	1.885	0.394	**0.004**	↗
		Spring	4.77E-07	0.554	**4.8E-07**	↗	1.678	0.418	**0.002**	↗
		Summer	2.443	0.217	**0.050**	↗	-0.240	-0.079	0.567	↘
		Fall	3.704	0.401	**2.3E-04**	↗	0.967	0.339	**0.012**	↗
RE15	Surface	Winter	4.700	0.414	**3.2E-04**	↗				
		Spring	5.087	0.562	**1.1E-06**	↗				
		Summer	3.457	0.414	**3.2E-04**	↗		-		
		Fall	4.302	0.423	**2.4E-04**	↗				
	Bottom	Winter	7.025	0.432	**1.7E-04**	↗				
		Spring	5.336	0.583	**3.6E-07**	↗				
		Summer	1.522	0.219	**0.058**	↗		-		
		Fall	4.376	0.363	**0.002**	↗				
RE30	Surface	Winter	9.137	0.511	**9.3E-06**	↗				
		Spring	10.427	0.651	**1.6E-08**	↗				
		Summer	7.765	0.511	**9.3E-06**	↗		-		
		Fall	7.914	0.459	**6.6E-05**	↗				
	Bottom	Winter	8.623	0.435	**1.6E-04**	↗				
		Spring	9.796	0.630	**4.6E-08**	↗				
		Summer	5.447	0.393	**0.001**	↗		-		
		Fall	5.795	0.345	**0.003**	↗				
RE35	Surface	Winter	2.194	0.410	**2.0E-04**	↗				
		Spring	2.338	0.533	**1.3E-06**	↗				
		Summer	1.564	0.376	**0.001**	↗		-		
		Fall	2.478	0.548	**4.8E-07**	↗				
	Bottom	Winter	2.539	0.349	**0.002**	↗				
		Spring	2.377	0.487	**1.0E-05**	↗				
		Summer	1.485	0.253	**0.022**	↗		-		
		Fall	2.523	0.509	**3.0E-06**	↗				

Hardness is the measure of divalent cations in water. In natural waters, the major contributors are calcium (Ca^{2+}) and magnesium (Mg^{2+}) and their sources are erosion from sedimentary rocks, seepage, and runoff from soils. Other divalent and trivalent ions can contribute to hardness, but they are almost always not significant contributions. There are no adverse health effects associated with hardness and no regulatory limits, but it is important to consider hardness for drinking water systems since it influences aesthetic acceptability for consumers, and because hard waters can cause scaling in distribution systems, as well as poor performance of soaps and detergents. According to hardness, waterbodies can be classified as soft (less than 17.1 mg/l); slightly hard (from 17.1 to 60 mg/l); moderately hard (from 60 to 120 mg/l); hard (from 120 to 180 mg/l); and very hard (higher than 180 mg/l) (McGowan, 2000). All hardness values refer to mg/l as $CaCO_3$.

Figure 4-56 presents a summary of hardness values for station RE02 from 1992 to 2019. RE02 was used for this graph due to data availability, since measurements for this station have been taken weekly since 1992 and measurements for the other stations have only been taken on a quarterly basis since 1993. Diamond markers in the graph represent average hardness values for surface (indicated with S-) and bottom waters (indicated with B-) by season. Blue lines represent hardness median values, outer limits of rectangles represent 25^{th} and 75^{th} percentiles, and whiskers indicate the most extreme points of the data without outliers. Red plus signs symbolize outliers. Average surface hardness at RE02 for the period of record was 76 mg/l during winter, 68 mg/l during spring, 71 mg/l during summer, and 82 mg/l during fall, all as $CaCO_3$. Average hardness

of bottom waters was 83 mg/l during winter, 70 mg/l during spring, 76 mg/l during summer, and 85 mg/l during fall, all as $CaCO_3$. In general terms, 75% percent of hardness values are below 105 mg/l as $CaCO_3$. Values for hardness present an upward trend for surface water during all seasons, and during winter, spring, and fall for bottom water, at $p<0.1$ (Table 4-29).

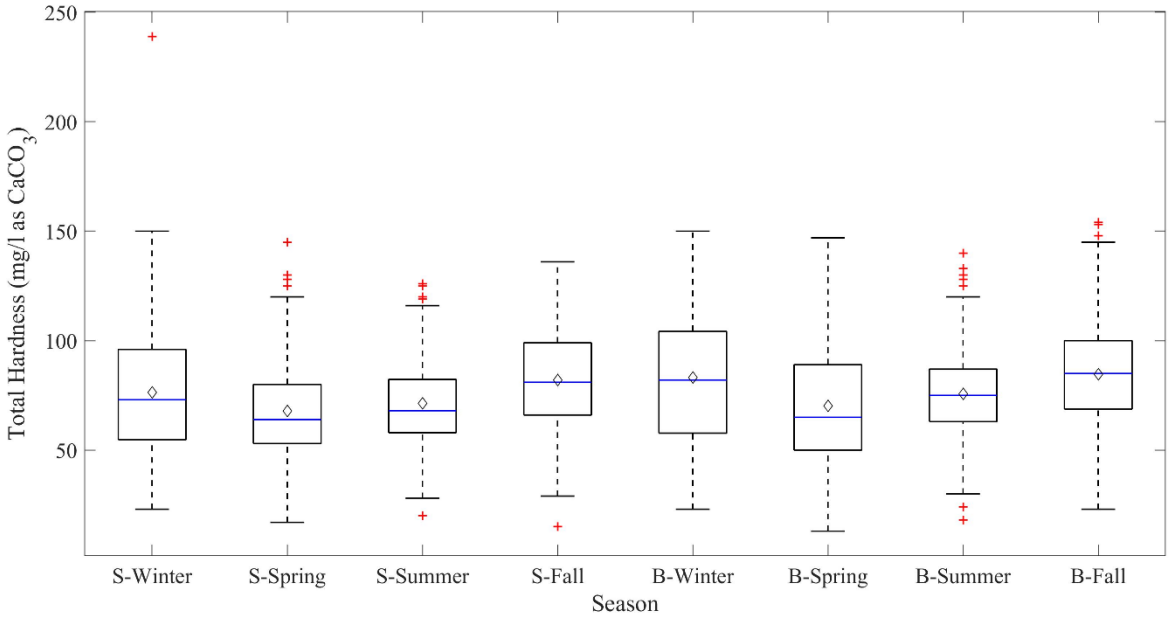

Figure 4-56. Hardness Statistical Summary at RE02, 1992–2019

4.3.7 Secchi Depth, Total Suspended Solids, Turbidity

As stated in section 4.3.5, TSS and turbidity are water quality parameters that indicate the presence of compounds that can affect water quality. TSS measures suspended particles in water, which include anything that is floating (larger than 2 microns) such as organic matter (algae, plankton, decomposing particles), inorganic matter, chemical precipitates, sediments, silt, sand, among others. Turbidity is the reduction of water clarity due to the presence of TSS, as well as colored and fluorescent dissolved organic matter or other dyes. Secchi depth is also an indicator parameter; however, as opposed to turbidity, it measures water clarity or transparency. Secchi depth is obtained by lowering a black and white 8 in. (20 cm) disk into the reservoir and observing the depth at which it disappears. The disk is then raised again and the depth at which it appears again is also observed. These two measurements are then averaged to obtain a transparency depth. Secchi depth measurements are taken from the water surface and are affected by turbidity and light attenuation through water depth. They are useful to assess productivity levels, presence of dissolved organic matter, and depth of plant growth, among other uses.

Secchi depth averages for the entire period of record at the Occoquan Reservoir were 46.3 inches at RE02, 37.6 inches at RE15, 29.2 inches at RE30, and 28.8 inches at RE35. Figure 4-57 shows seasonal average values of Secchi depth from 1973 to 2019. In general terms, higher clarity is observed at RE02 (higher Secchi depth), followed by RE15. Seasonally, a higher average at RE02 and RE15 is seen during summer, while RE30 and RE35 present higher averages during fall.

Figure 4-58 presents Secchi depth time series from 2003 to 2019. Several peaks are observed during winter and fall at RE30, the deepest Secchi depth being 171 inches on December 2017, followed by 152 inches on November 2019. At RE02, the highest peak was 111 inches, which was observed on July 2016. Secchi depths measurements since 2003 have ranged from 9 to 75 inches at RE15 and from 9 to 84 inches at RE35.

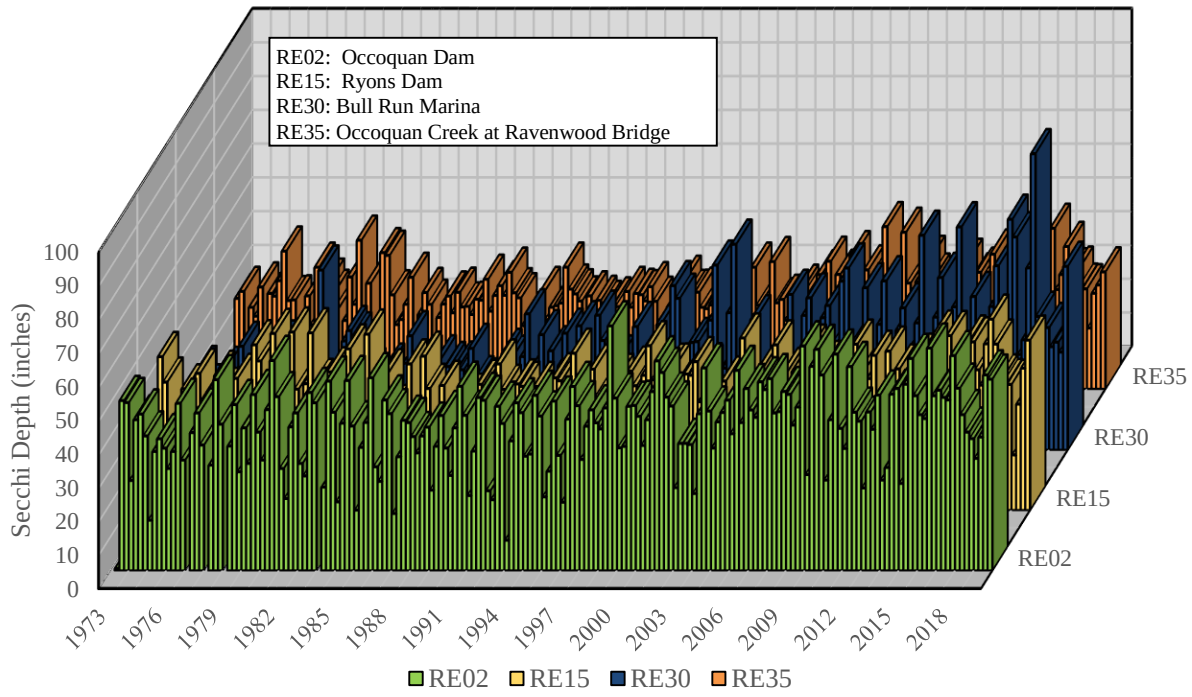

Figure 4-57. Occoquan Reservoir Seasonal Average Secchi Depth, 1973–2019

Figures 4-59 and 4-60 show seasonal average TSS concentrations for the reservoir stations for each of the years of the period of record. Average values for surface water range from 1.68 to 80.08 mg/l, and bottom water values range from 1.20 to 99.67 mg/l. It can be observed from the graphs that TSS values are higher at bottom waters than surface waters, especially from 1989 to 1996. From 1997 to 2019, average values were less than 26 mg/l at the surface, and less than 40 mg/l at the bottom. Total average surface TSS values for the entire period of record were 4.38 mg/l at RE02, 6.68 mg/l at RE15, 11.11 mg/l at RE30, and 9.50 mg/l at RE35. Total TSS averages for bottom waters were 10.89 mg/l at RE02, 17.50 mg/l at RE15, 21.55 mg/l at RE30, and 21.01 mg/l at RE35. As can be noticed from these averages and in the graphs, RE02 presented lower TSS values than the rest of the stations. TSS values showed no specific seasonal pattern. At the surface, TSS averages were higher during spring at all stations except RE15, which was higher during winter. At bottom waters, higher averages were seen during spring at RE02 and RE15, and during summer at RE30 and RE35 stations (Figure 4-61).

Since TSS and turbidity are both related and influenced by runoff, they show similar patterns (Figures 4-62 and 4-63). Seasonal average turbidity ranges from 2.23 to 62.67 NTU at the surface, and from 4.58 to 63.33 NTU at the bottom. Even though these turbidity maximum and minimum average values are similar, higher turbidity is seen at reservoir bottom waters on average. Turbidity values otherwise showed no particular pattern. Total seasonal average turbidity is shown in Figure 4-61. In surface waters, RE02, RE15, and RE35 presented higher turbidity during winter, and RE35 saw a higher average during spring. In bottom waters, RE02 showed higher average turbidity during spring, RE15 during winter (though average for all seasons are close), and RE30 and RE35 during summer. A recent peak observable from the TSS and turbidity graphs (Figures 4-59, 4-60, 4-62, 4-63) occurred during winter 2019 at station RE15, where surface waters presented 24 mg/l for TSS and 39.20 NTU, and bottom waters presented 26.90 mg/l TSS and 41.45 NTU. This peak could have been due to a higher rainfall-runoff from the Occoquan Creek arm, since this peak can also be noticed at RE35. Rainfall during winter 2019 was higher than winter rainfall values from the preceding 15 years.

Secchi depth, TSS, and turbidity are all related parameters. As it was observed, RE02 was the station with higher Secchi depth (more clarity), and lower TSS and turbidity values. This may be due to sedimentation of TSS; the sediment trap efficiency of the reservoir for TSS was 83% on average (Section 4.2.3.9). In addition, copper sulfate addition during previous years, and the installation of an aeration system (past) and a hypolimnetic oxygen system (present) may have led to reduced nutrient concentrations and therefore less algal growth. This may also be the reason summer Secchi depth values were higher at RE02 and RE15. In the stream monitoring section, it was stated that TSS and turbidity at Occoquan Creek presented higher values than Bull Run. This difference was not seen at the reservoir, where Bull Run (RE30) and Occoquan Creek (RE35) values were similar and, in some cases, Bull Run was slightly higher. In general, higher values were observed at the reservoir than at streams, which may be caused by additional runoff or erosion into the reservoir stations after inflow passed ST10 and ST40/45, or resuspension of sediments from water flow. Even so, Mann-Kendall test results for the reservoir stations indicate similar trends as the stream stations, with all statistically significant trends decreasing for TSS and turbidity (Table 4-30). Secchi depth, on the other hand, presents increasing trends for all stations, indicative of lower turbidity and TSS, though not all are statistically significant.

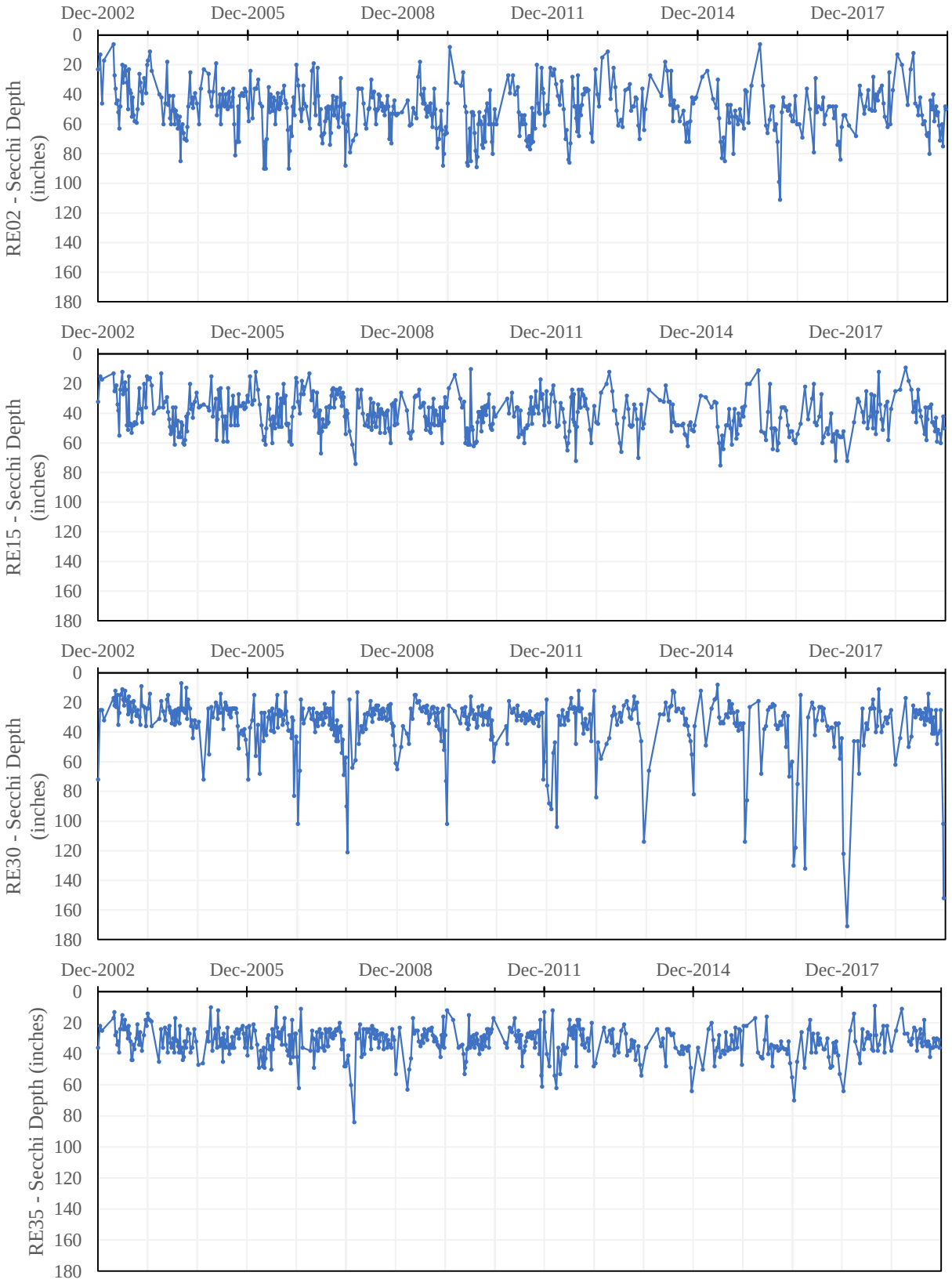

Figure 4-58. Secchi Depth Time Series at Reservoir Stations, 2003–2019

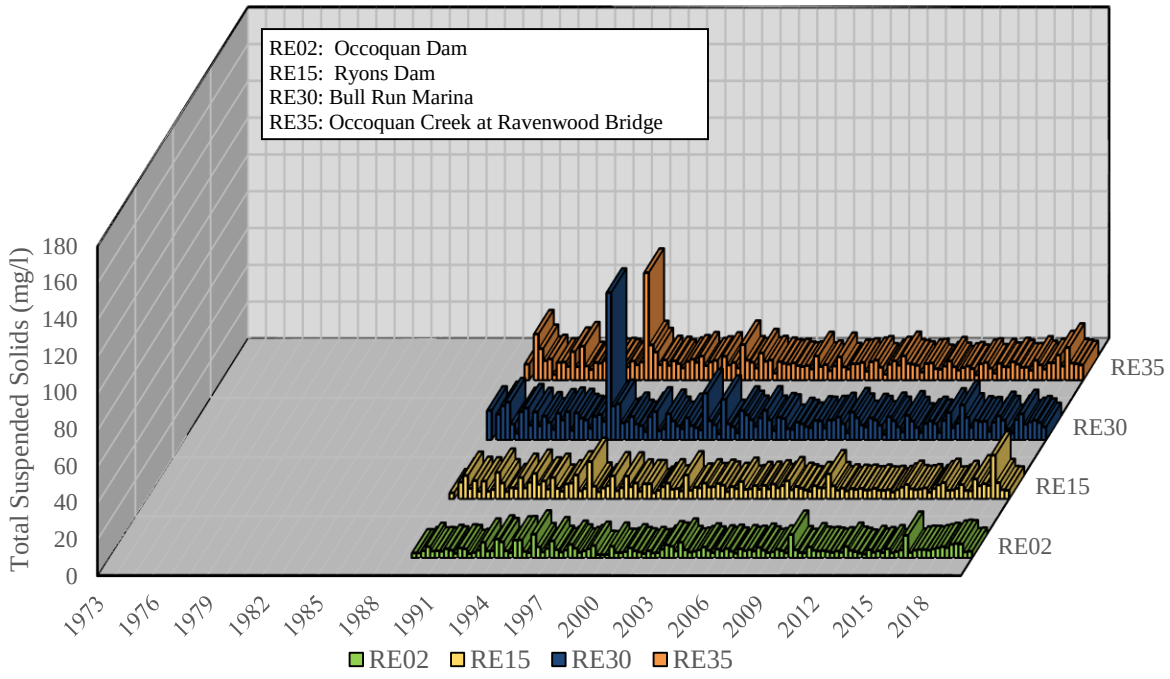

Figure 4-59. Seasonal Average Total Suspended Solids in Reservoir Surface Waters, 1973–2019

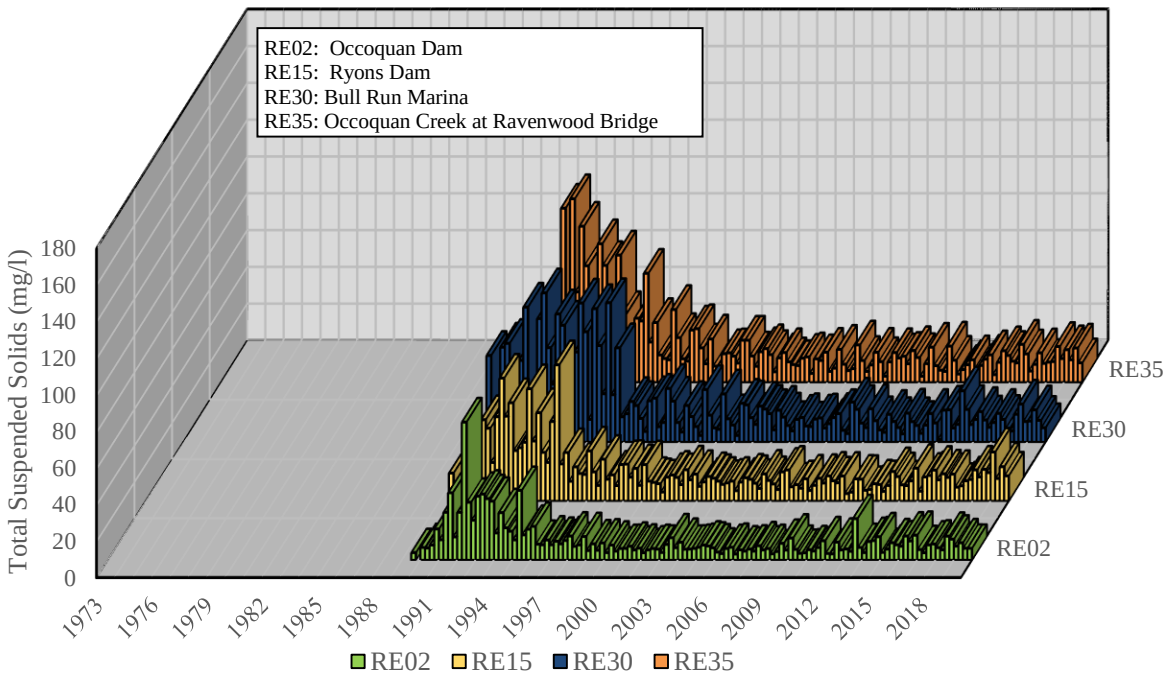

Figure 4-60. Seasonal Average Total Suspended Solids in Reservoir Bottom Waters, 1973–2019

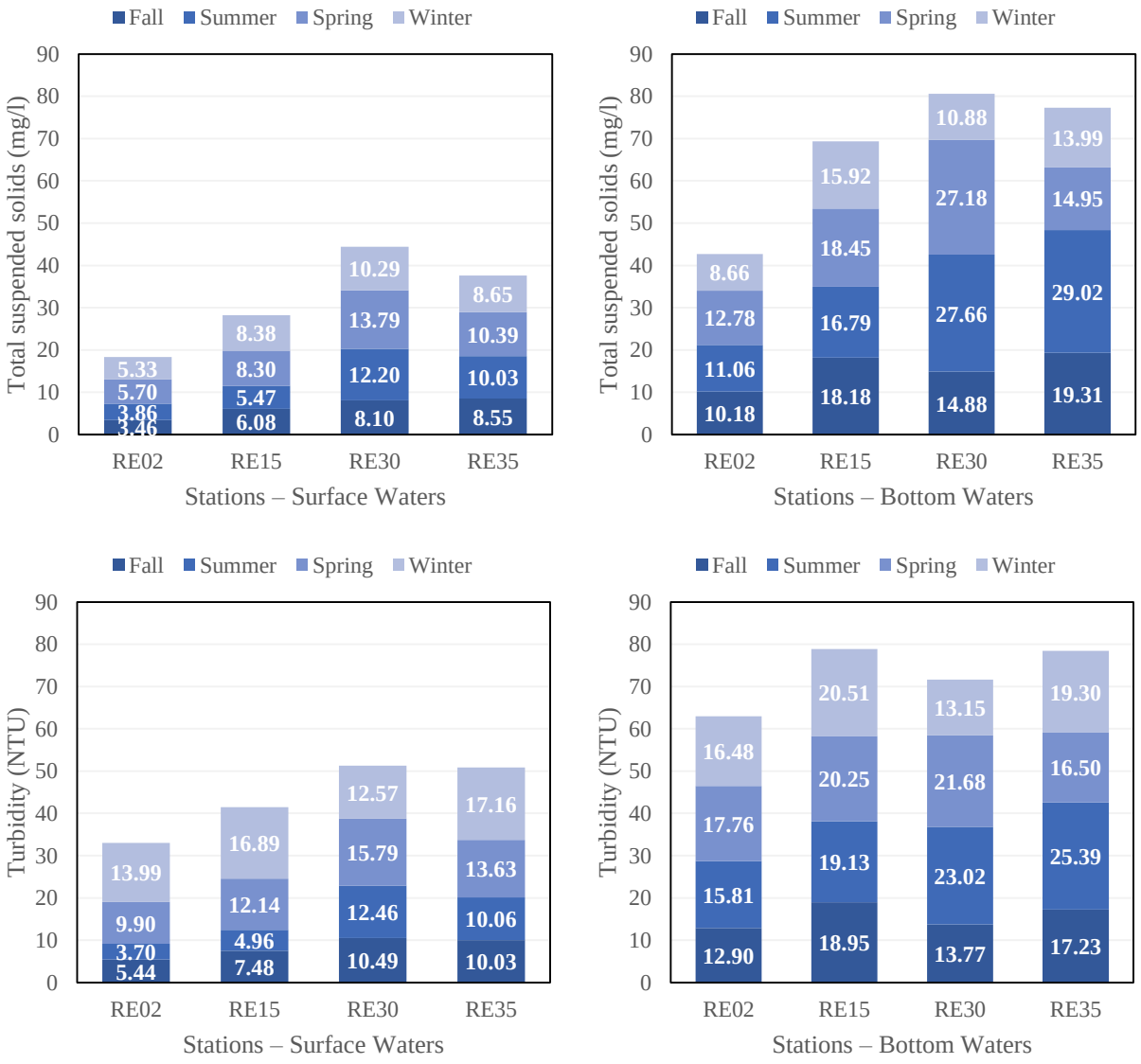

Figure 4-61. Overall Average Total Suspended Solids and Turbidity by Season at Occoquan Reservoir, 1989–2019

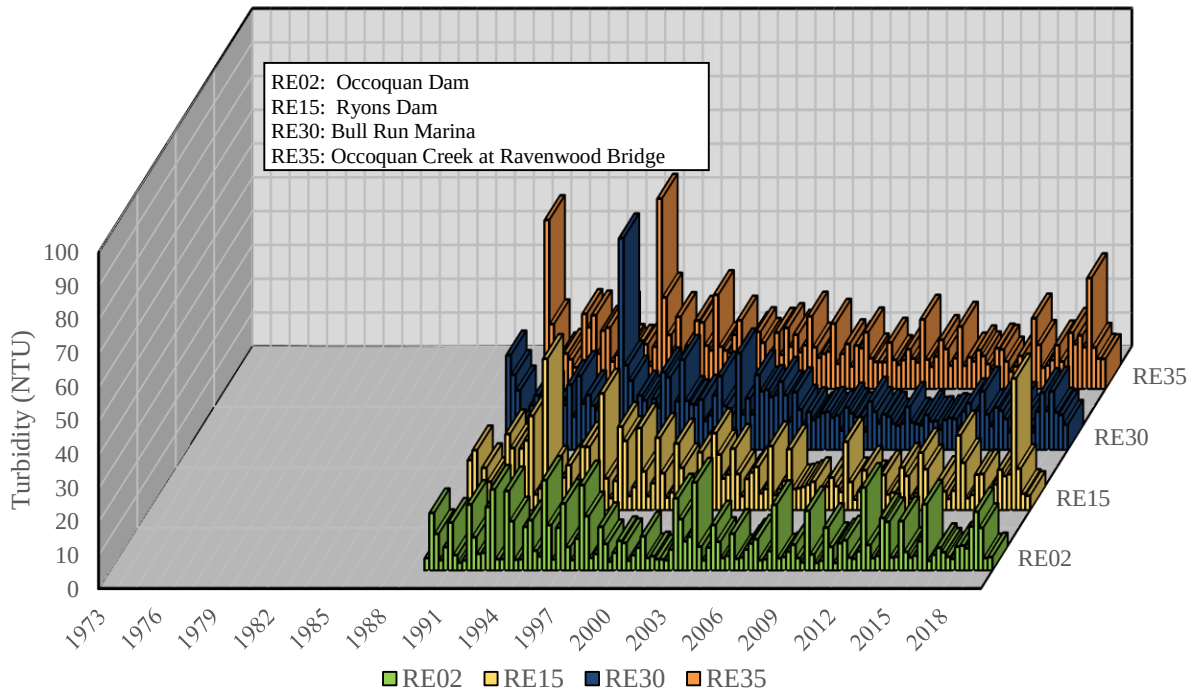

Figure 4-62. Seasonal Average Turbidity in Reservoir Surface Waters, 1973–2019

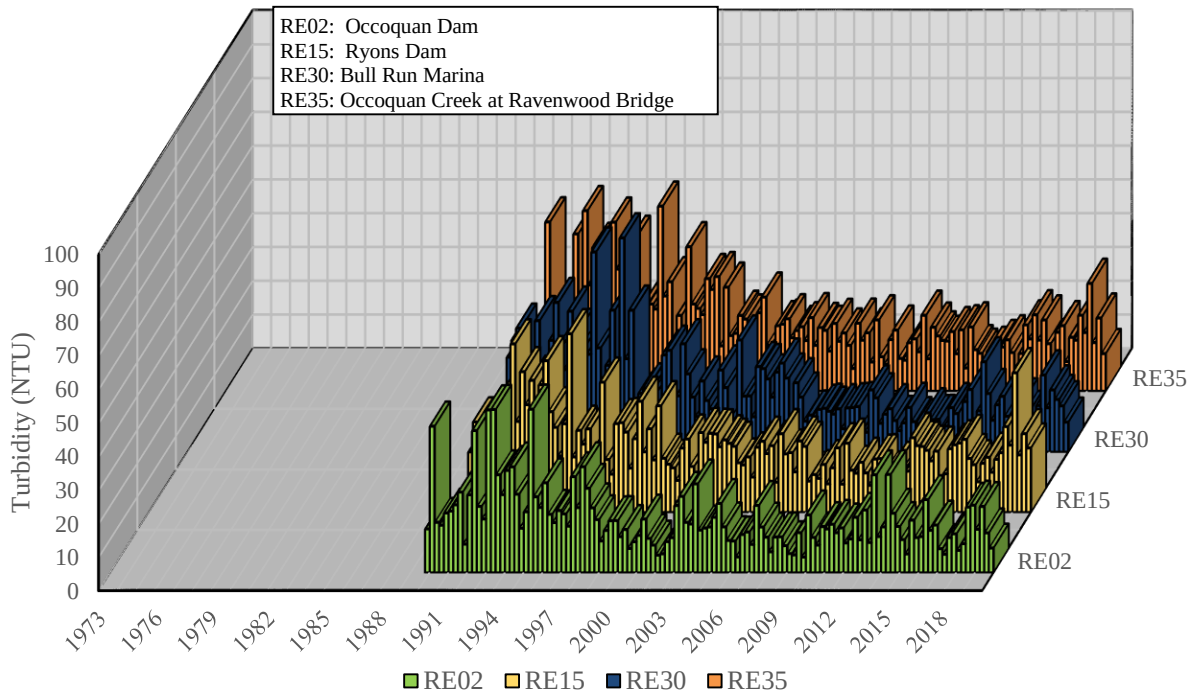

Figure 4-63. Seasonal Average Turbidity in Reservoir Bottom Waters, 1973–2019

Table 4-30. Mann-Kendall Reservoir Secchi Depth, Total Suspended Solids, and Turbidity Trends, 1973–2019

Station	Description	Season	Secchi				Total Suspended Solids				Turbidity			
			Sen Slope	*Kendall Tau*	*p-value*	*Trend*	*Sen Slope*	*Kendall Tau*	*p-value*	*Trend*	*Sen Slope*	*Kendall Tau*	*p-value*	*Trend*
RE02	Surface	Winter	0.341	0.279	**0.007**	↗	-0.038	-0.090	0.498	↘	-0.291	-0.246	**0.059**	↘
		Spring	0.414	0.424	**2.8E-05**	↗	-0.051	-0.210	0.108	↘	-0.126	-0.154	0.239	↘
		Summer	0.077	0.096	0.345	↗	0.011	0.080	0.541	↗	0.019	0.129	0.326	↗
		Fall	0.314	0.394	**9.7E-05**	↗	0.027	0.153	0.234	↗	-0.006	-0.024	0.865	↘
	Bottom	Winter					-0.212	-0.301	**0.020**	↘	-0.668	-0.434	**0.001**	↘
		Spring			-		-0.260	-0.398	**0.002**	↘	-0.512	-0.366	**0.005**	↘
		Summer					-0.066	-0.052	0.696	↘	-0.223	-0.241	**0.064**	↘
		Fall					-0.277	-0.315	**0.015**	↘	-0.192	-0.226	**0.077**	↘
RE15	Surface	Winter	0.152	0.135	0.191	↗	-0.103	-0.163	0.212	↘	-0.283	-0.209	0.108	↘
		Spring	0.269	0.346	**0.001**	↗	-0.112	-0.285	**0.028**	↘	-0.248	-0.269	**0.038**	↘
		Summer	0.040	0.076	0.458	↗	0.024	0.093	0.475	↗	0.004	0.021	0.887	↗
		Fall	0.278	0.389	**1.2E-04**	↗	-0.051	-0.269	**0.038**	↘	-0.154	-0.329	**0.011**	↘
	Bottom	Winter					-0.496	-0.361	**0.005**	↘	-0.593	-0.343	**0.008**	↘
		Spring			-		-0.652	-0.508	**8.7E-05**	↘	-0.716	-0.480	**2.1E-04**	↘
		Summer					-0.243	-0.252	**0.049**	↘	-0.147	-0.163	0.212	↘
		Fall					-0.348	-0.292	**0.025**	↘	-0.227	-0.237	**0.069**	↘
RE30	Surface	Winter	0.872	0.391	**1.6E-04**	↗	-0.037	-0.078	0.556	↘	-0.234	-0.276	**0.034**	↘
		Spring	0.230	0.421	**3.8E-05**	↗	-0.140	-0.295	**0.023**	↘	-0.290	-0.297	**0.022**	↘
		Summer	0.190	0.456	**6.4E-06**	↗	-0.116	-0.260	**0.041**	↘	-0.148	-0.310	**0.017**	↘
		Fall	0.582	0.572	**1.5E-08**	↗	-0.092	-0.338	**0.009**	↘	-0.247	-0.407	**0.002**	↘
	Bottom	Winter					-0.218	-0.237	**0.069**	↘	-0.265	-0.255	**0.050**	↘
		Spring			-		-1.000	-0.559	**1.6E-05**	↘	-0.692	-0.494	**1.3E-04**	↘
		Summer					-1.131	-0.561	**9.9E-06**	↘	-0.967	-0.545	**2.5E-05**	↘
		Fall					-0.402	-0.467	**3.1E-04**	↘	-0.425	-0.485	**1.8E-04**	↘
RE35	Surface	Winter	0.123	0.094	0.373	↗	-0.109	-0.214	0.101	↘	-0.286	-0.221	**0.090**	↘
		Spring	0.186	0.358	**4.8E-04**	↗	-0.041	-0.177	0.175	↘	-0.212	-0.274	**0.035**	↘
		Summer	0.145	0.297	**0.003**	↗	-0.060	-0.224	**0.080**	↘	-0.128	-0.216	**0.097**	↘
		Fall	0.215	0.369	**2.6E-04**	↗	-0.122	-0.467	**3.1E-04**	↘	-0.136	-0.320	**0.014**	↘
	Bottom	Winter					-0.425	-0.377	**0.004**	↘	-0.454	-0.283	**0.030**	↘
		Spring			-		-0.420	-0.462	**3.6E-04**	↘	-0.438	-0.366	**0.005**	↘
		Summer					-0.738	-0.406	**0.001**	↘	-0.735	-0.407	**0.002**	↘
		Fall					-0.434	-0.425	**0.001**	↘	-0.387	-0.425	**0.001**	↘

4.3.8 Nitrogen

Nitrogen forms analyzed for the reservoir stations included NH3-N, TKN, Ox-N, and TN. Data for NH3-N and Ox-N date back from 1973 and 1975, respectively, to present date. Data for TKN were collected from 1973 to 2004, from which point TN data were collected instead. TKN for the years where data were not available was calculated by subtracting Ox-N from TN. Prior to 2004, TN were calculated by summing TKN plus TN to present a complete timeline for all forms of nitrogen.

Figures 4-64 and 4-65 present seasonal average NH3-N for surface and bottom waters. Comparing both graphs, higher NH3-N seasonal average values can be seen at bottom waters, (ranging from 0.01 to 3.44 mg/l) than at surface waters (ranging from 0.01 to 0.62 mg/l). Comparing each station, higher NH3-N values are more frequently seen at RE02 at both depths than the rest of the stations throughout the years. However, in surface waters, due to peaks mainly observed in the early years of the period of record at RE30, total average NH3-N was similar for both stations (0.07 mg/l). Total averages for RE15 and RE35 were slightly lower, 0.05 mg/l and 0.06 mg/l, respectively. In bottom waters, high averages at RE02 were observed from 1987 to 2011, reaching a peak value of 3.44 mg/l in fall 2010. Averages before 1987 were below 0.93 mg/l, and averages after 2012 were

below 0.62 mg/l. This decrease in NH3-N at bottom waters since 2012 is probably a consequence of the installation of the hypolimnetic oxygenation system that was completed that year to help maintain oxidized conditions at RE02 during thermal stratification. For this reason, the total bottom average at RE15 (0.63 mg/l) was probably higher than RE02 (0.56 mg/l). Higher DO levels promote conversion of ammonia to nitrite and nitrate, since nitrification is an aerobic process. Total bottom NH3-N average for the entire period at RE30 was 0.17 mg/l, and 0.31 mg/l at RE5. Ammonia can be found in aquatic environments from natural sources such as decomposition of organic matter, animal and human waste, gas exchange with the atmosphere, and nitrogen fixation processes, or can enter via municipal and industrial discharges or agricultural runoff. The higher NH3-N concentrations seen at RE15 and RE02 bottom waters is probably an indication of the high organic matter content at these stations. The lower average at RE30 shows how NH3-N concentrations at the reservoir were not greatly affected by wastewater discharge from the Bull Run arm, since MHR WFR effluent NH3-N concentrations remained low, with a median value of 0.02 mg/l (1982–2019).

Seasonally, surface waters did not present one specific pattern. Higher NH3-N averages were seen during different seasons at each station (Figure 4-66). In bottom waters, higher values were seen during summer, which is probably an effect of the low DO concentrations observed during this season due to thermal stratification. RE02 and RE15 were the stations that presented lower DO values during summer (recall DO Table 4-25) and were also the ones that presented higher NH3-N averages. To understand the effect of the hypolimnetic oxygenation system on NH3-N, bottom water seasonal averages from 2003 to 2011 were compared to bottom water seasonal averages from 2012 to 2019 (Figure 4-67). This graph shows how NH3-N averages during summer decreased from 1.37 mg/l (before hypolimnetic oxygenation system) to 0.34 mg/l (after installation) at RE02. Values during the other seasons or stations did not exhibit any noticeable differences. During the period from 2012 to 2019, RE15 still remained with the highest average NH3-N, and the average at Occoquan Creek was higher than Bull Run. The effect of the oxygenation system can also be visualized in Figure 4-68, which presents NH3-N time series from 2003 to 2019. Additionally, this figure highlights the difference between surface and bottom water, and between RE02 and RE15 and the inflow reservoir stations. Seasonal variation can also be seen in these graphs, where peaks at bottom waters were generally seen during summer, followed by fall. The most recent noticeable peaks in bottom waters occurred in summer 2019. The only noticeable peak in surface waters occurred during spring 2008, with a value of 0.73 mg/l at RE30.

Mann-Kendall test results in Table 4-31 show statistically significant decreasing trends for surface waters at all stations and seasons. The only value that was not significant was the winter trend for RE30. Trends at bottom waters vary by station. RE02 and RE15 show an increasing trend but were only significant during spring at RE02 and fall at RE15. RE30, on the other hand, shows decreasing significant trends during all seasons. Trends at RE35 are mainly decreasing, except during fall, but none are significant. It should be noted that nitrogen trends decrease/increase slowly over time, as indicated by the minimal Sen slopes.

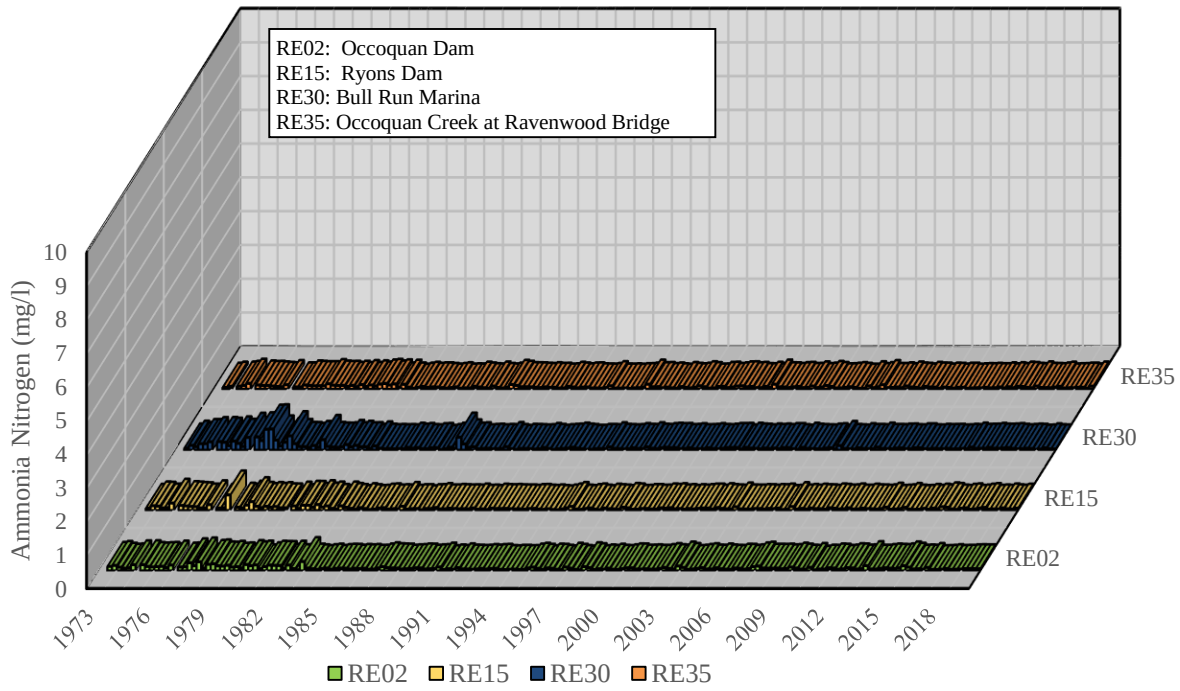

Figure 4-64. Seasonal Average Ammonia Nitrogen in Reservoir Surface Waters, 1973–2019

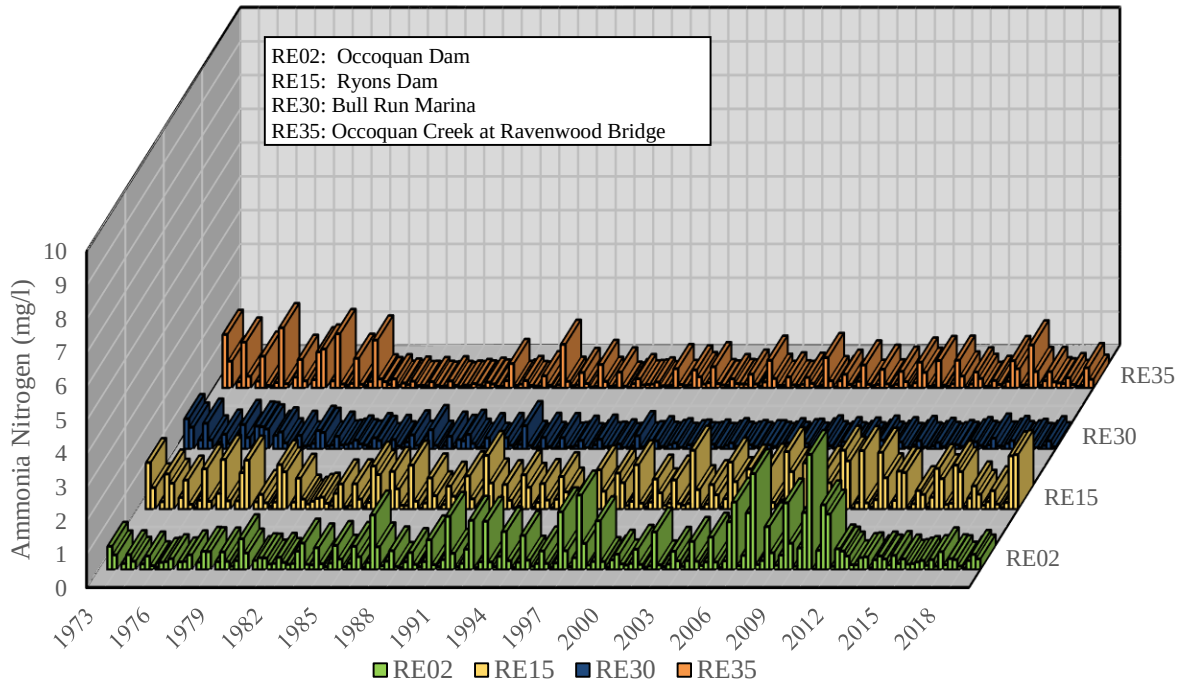

Figure 4-65. Seasonal Average Ammonia Nitrogen in Reservoir Bottom Waters, 1973–2019

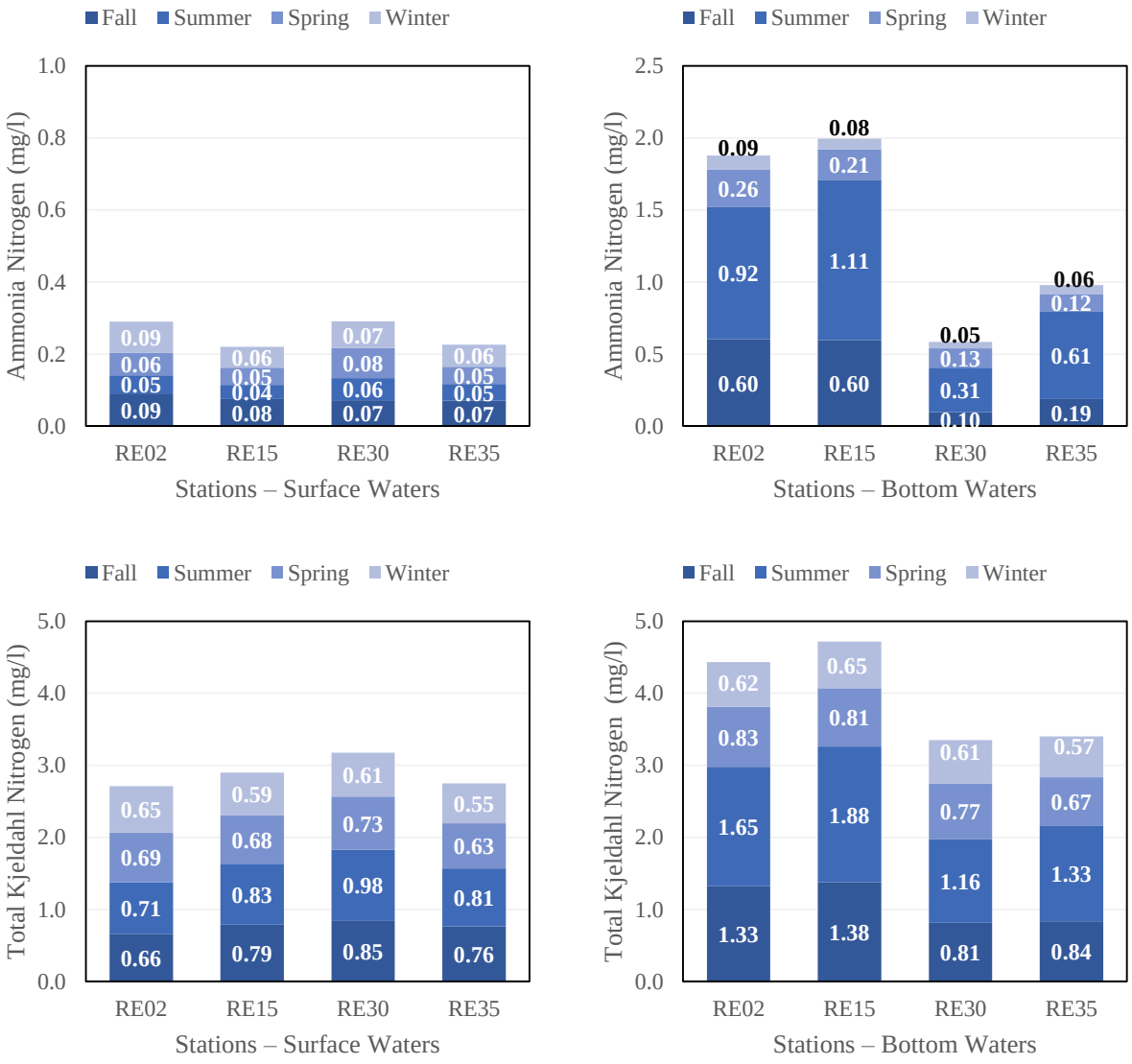

Figure 4-66. Overall Ammonia and Total Kjeldahl Nitrogen Average by Season at Occoquan Reservoir, 1973–2019

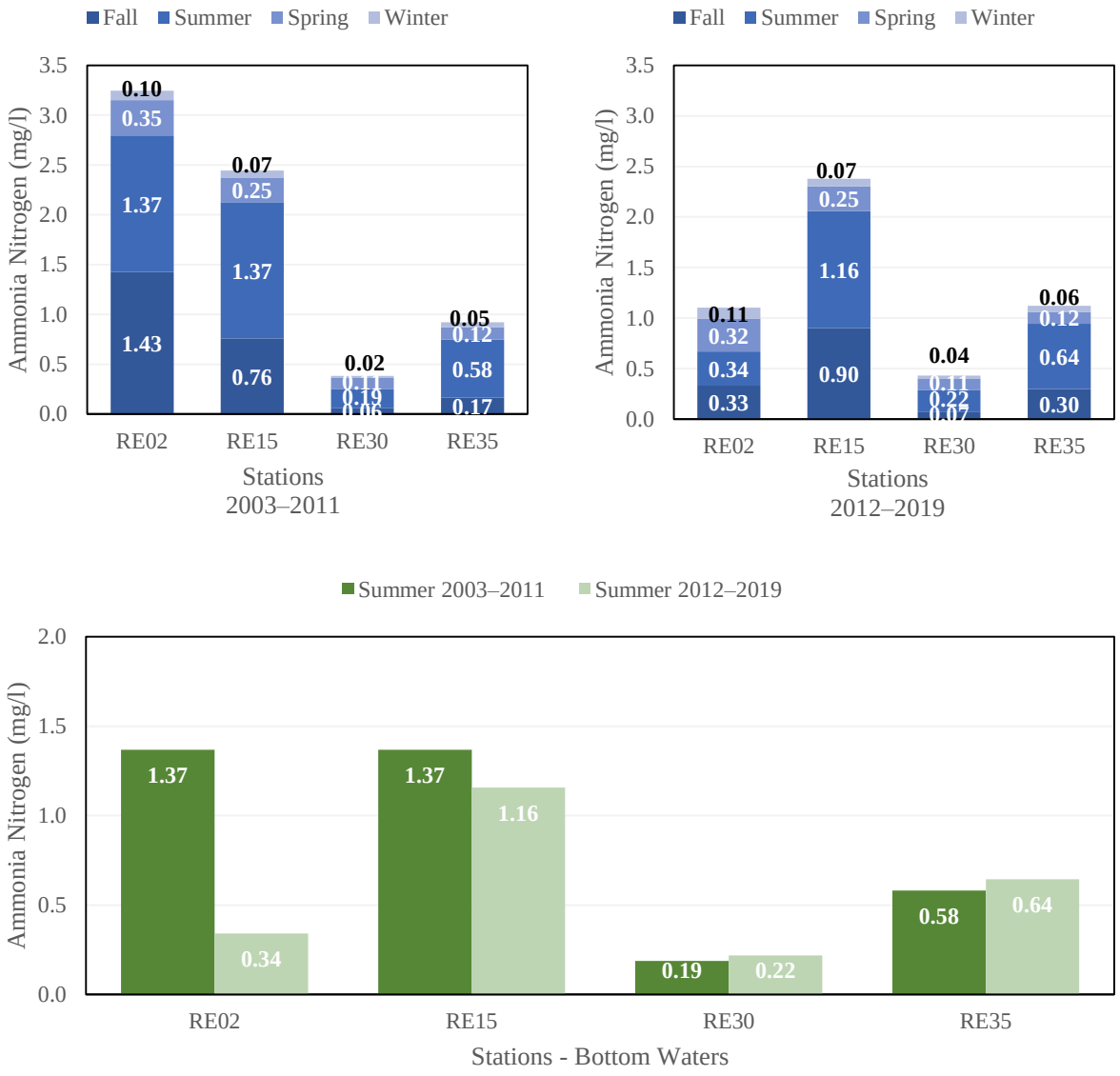

Figure 4-67. Seasonal Average Ammonia Before and After Installation of Hypolimnetic Oxygenation System

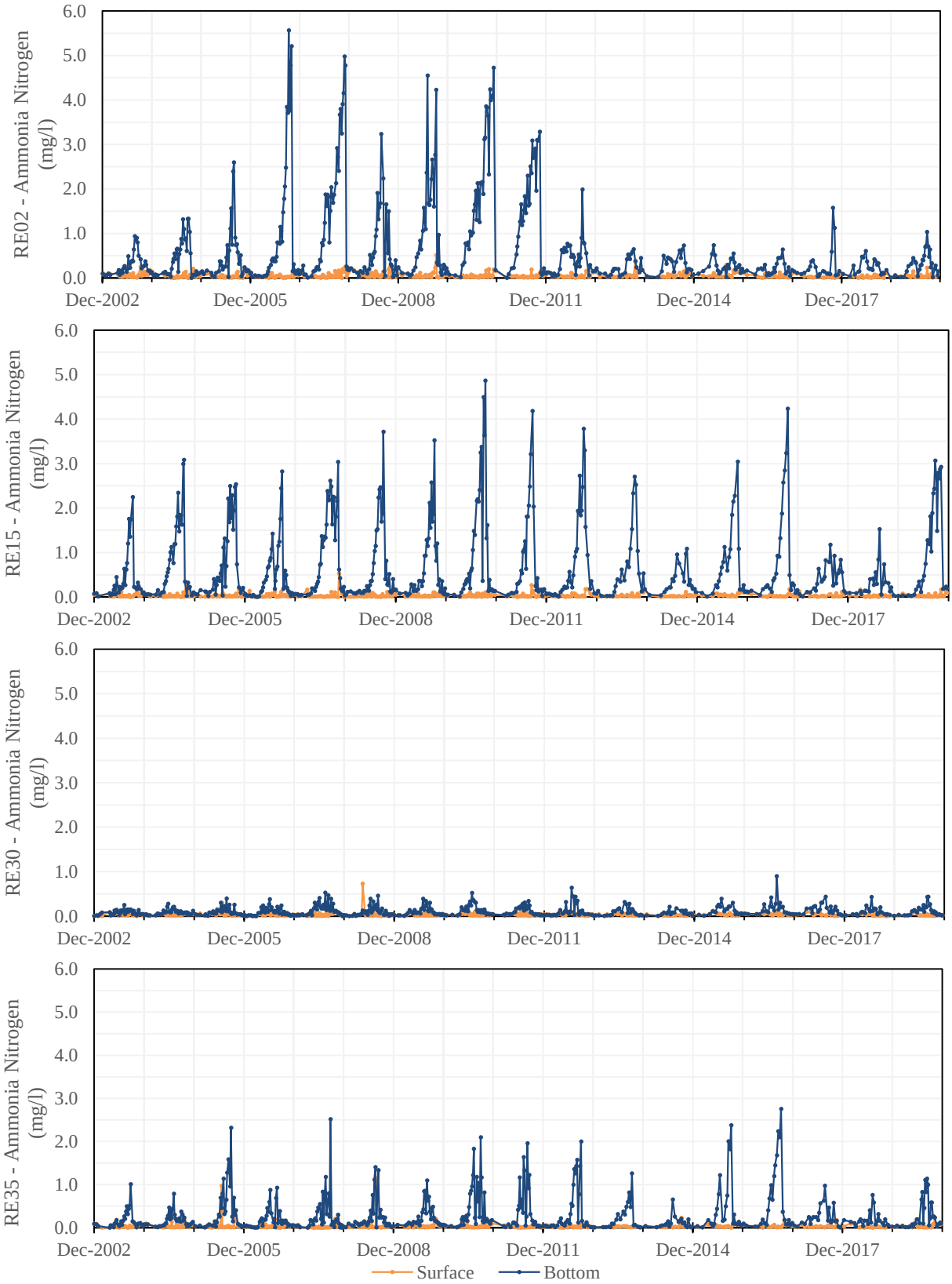

Figure 4-68. Ammonia Nitrogen Time Series at Reservoir Stations, 2003–2019

Table 4-31. Mann-Kendall Reservoir Nitrogen Species Trends, 1973–2019

Station	Description	Season	Ammonia Nitrogen				Total Kjedahl Nitrogen				Oxidized Nitrogen				Total Nitrogen			
			Sen Slope	*Kendall Tau*	*p-value*	*Trend*	*Sen Slope*	*Kendall Tau*	*p-value*	*Trend*	*Sen Slope*	*Kendall Tau*	*p-value*	*Trend*	*Sen Slope*	*Kendall Tau*	*p-value*	*Trend*
RE02	Surface	Winter	-0.001	-0.272	**0.008**	↘	-0.004	-0.231	**0.025**	↘	0.005	0.095	0.363	↗	-0.006	-0.113	0.278	↘
		Spring	-0.001	-0.320	**0.002**	↘	-0.003	-0.172	**0.094**	↘	0.004	0.131	0.207	↗	0.001	0.014	0.899	↗
		Summer	-0.001	-0.263	**0.009**	↘	0.002	0.197	**0.052**	↗	0.011	0.224	**0.031**	↗	0.009	0.202	**0.052**	↗
		Fall	-0.001	-0.221	**0.029**	↘	-0.001	-0.055	0.595	↘	0.021	0.376	**2.8E-04**	↗	0.015	0.337	**0.001**	↗
	Bottom	Winter	0.001	0.172	0.103	↗	-0.006	-0.294	**0.005**	↘	0.008	0.162	0.120	↗	-0.001	-0.016	0.883	↘
		Spring	0.003	0.312	**0.002**	↗	-0.004	-0.125	0.226	↘	0.006	0.121	0.244	↗	0.002	0.052	0.625	↗
		Summer	0.005	0.090	0.379	↗	-0.002	-0.029	0.783	↘	0.004	0.121	0.244	↗	-0.003	-0.030	0.777	↘
		Fall	0.002	0.082	0.420	↗	-0.003	-0.060	0.557	↘	0.022	0.307	**0.003**	↗	0.019	0.220	**0.034**	↗
RE15	Surface	Winter	-0.001	-0.279	**0.007**	↘	-0.001	-0.028	0.791	↘	0.009	0.165	0.113	↗	-0.002	-0.032	0.762	↘
		Spring	-0.001	-0.392	**1.3E-04**	↘	-0.003	-0.186	**0.071**	↘	0.009	0.216	**0.037**	↗	0.006	0.147	0.156	↗
		Summer	-0.001	-0.272	**0.007**	↘	0.003	0.200	**0.049**	↗	0.023	0.354	**0.001**	↗	0.025	0.372	**3.3E-04**	↗
		Fall	-0.001	-0.288	**0.004**	↘	-0.001	-0.083	0.414	↘	0.026	0.386	**1.9E-04**	↗	0.021	0.295	**0.004**	↗
	Bottom	Winter	0.000	-0.005	0.968	↔	-0.004	-0.162	0.120	↘	0.014	0.138	0.187	↗	0.002	0.049	0.646	↗
		Spring	0.001	0.069	0.507	↗	-0.005	-0.248	**0.015**	↘	0.006	0.186	**0.073**	↗	0.001	0.018	0.868	↗
		Summer	0.007	0.143	0.158	↗	0.005	0.086	0.399	↗	-0.002	-0.029	0.784	↘	0.004	0.065	0.538	↗
		Fall	0.007	0.182	**0.072**	↗	0.005	0.071	0.486	↗	0.036	0.265	**0.011**	↗	0.039	0.238	**0.022**	↗
RE30	Surface	Winter	-0.001	-0.162	0.116	↘	-0.003	-0.149	0.147	↘	0.027	0.179	**0.085**	↗	0.015	0.127	0.221	↗
		Spring	-0.001	-0.173	**0.092**	↘	-0.003	-0.140	0.173	↘	0.038	0.311	**0.003**	↗	0.026	0.269	**0.010**	↗
		Summer	-0.001	-0.427	**2.6E-05**	↘	4.0E-04	0.016	0.883	↗	0.075	0.410	**7.4E-05**	↗	0.073	0.414	**6.3E-05**	↗
		Fall	-0.002	-0.457	**6.1E-06**	↘	-0.004	-0.109	0.283	↘	0.046	0.188	**0.070**	↗	0.045	0.162	0.120	↗
	Bottom	Winter	-0.001	-0.261	**0.014**	↘	-0.006	-0.269	**0.010**	↘	0.020	0.117	0.261	↗	0.009	0.069	0.512	↗
		Spring	-0.001	-0.179	**0.081**	↘	-0.006	-0.248	**0.015**	↘	0.037	0.291	**0.005**	↗	0.024	0.287	**0.006**	↗
		Summer	-0.008	-0.542	**8.1E-08**	↘	-0.016	-0.425	**2.7E-05**	↘	0.080	0.384	**2.1E-04**	↗	0.058	0.327	**0.002**	↗
		Fall	-0.002	-0.405	**6.1E-05**	↘	-0.005	-0.191	**0.059**	↘	0.059	0.172	**0.098**	↗	0.055	0.192	**0.064**	↗
RE35	Surface	Winter	-0.001	-0.209	**0.047**	↘	-0.005	-0.231	**0.026**	↘	-0.008	-0.248	**0.017**	↘	-0.013	-0.295	**0.004**	↘
		Spring	-0.001	-0.242	**0.018**	↘	-0.005	-0.246	**0.016**	↘	-0.005	-0.198	**0.056**	↘	-0.009	-0.309	**0.003**	↘
		Summer	-0.001	-0.303	**0.003**	↘	-0.001	-0.068	0.509	↘	-0.004	-0.220	**0.034**	↘	-0.007	-0.220	**0.034**	↘
		Fall	-0.001	-0.252	**0.013**	↘	-0.002	-0.112	0.271	↘	-0.003	-0.099	0.343	↘	-0.006	-0.195	**0.060**	↘
	Bottom	Winter	-0.001	-0.155	0.145	↘	-0.005	-0.254	**0.014**	↘	-0.001	-0.022	0.837	↘	-0.008	-0.145	0.165	↘
		Spring	-3.6E-04	-0.063	0.545	↘	-0.005	-0.249	**0.015**	↘	-0.002	-0.071	0.500	↘	-0.008	-0.210	**0.043**	↘
		Summer	-0.002	-0.044	0.673	↘	-0.006	-0.090	0.379	↘	-0.002	-0.085	0.417	↘	-0.010	-0.168	0.107	↘
		Fall	0.001	0.104	0.309	↗	-0.005	-0.190	**0.061**	↘	-0.003	-0.088	0.400	↘	-0.008	-0.180	**0.083**	↘

Seasonal averages for TKN are higher than NH3-N but they show similar patterns, because TKN equals NH3-N plus organic nitrogen (Figures 4-69 and 4-70). Values at bottom waters show higher average TKN than surface waters. RE02 averages throughout the years range from 0.24 to 2.53 mg/l at surface waters and from 0.33 to 4.16 mg/l at bottom waters. Maximum averages for surface at RE02 can be seen from 1973 to 1989. Since then, values have been less than 1.0 mg/l. At bottom waters, several peaks can be seen since 1973, but after fall 2011, when average TKN was 2.63 mg/l, concentrations decreased to less than 1.18 mg/l, probably as a result of lower NH3-N concentrations, as explained previously. At RE15, surface water averages ranged from 0.25 to 2.09 mg/l and bottom water averages from 0.38 to 3.78 mg/l. The most recent peak values occurred during summer 2019 (2.09 mg/l) at surface waters, and during summer (2.43 mg/l) and fall 2019 (2.39 mg/l) at bottom waters. Surface Averages at RE30 ranged from 0.13 to 2.04 mg/l, and from 0.31 to 2.78 mg/l at bottom waters. Surface and bottom averages at RE35 ranged from 0.25 to 1.75 mg/l and 0.29 to 3.62 mg/l, respectively. Higher average concentrations in surface waters were observed at RE30, and higher average concentrations in bottom waters were observed at RE15. TKN seasonal averages were higher in summer at both depths (Figure 4-66). It can also be observed in this figure how a large part of TKN is composed of NH3-N.

Figure 4-71 shows surface and bottom time series for TKN since 2003. It can be observed that the difference between surface and bottom waters is more noticeable at RE02 and RE15 than at the reservoir inflow stations. The difference in TKN concentrations at RE02 from before and after the installation of the oxygenation system can also be seen in this graph. Additionally, it can be noticed that RE15 presents higher TKN concentrations than the rest of the stations during this period. The

highest surface water TKN concentration that was recorded from 2003 to 2019 corresponds to summer 2018, reaching a value of 14.21 mg/l at RE15. Several peaks can also be seen at RE30 at both surface and bottom waters, the highest being 10.60 mg/l in summer 2011 in bottom waters. Despite these peaks, TKN generally presented declining trends at surface and bottom waters, though only certain trends were significant (Table 4-31). At surface waters, upward trends were only seen during summer at RE05, RE15, and RE30. At bottom waters, upward trends occurred at RE15 during summer and fall but were not statistically significant.

In comparison to NH3-N and TKN, Ox-N concentrations were higher, especially at RE30 due to MHR WRF's highly nitrified effluent during summer months. Seasonal averages per year at the reservoir surface ranged between 0.04 and 3.38 mg/l at RE02, 0.02 and 5.83 mg/l at RE15, 0.26 and 13.36 mg/l at RE30, and 0.01 and 1.71 mg/l at RE35 (Figure 4-72). The three highest peaks at RE02 surface water occurred during winter 1999, 2001, and 2002, corresponding to values of 2.87 mg/l, 2.81 mg/l, 3.38 mg/l, respectively. The highest peaks at RE15 were also seen in 1999 and 2002, reaching values of 5.05 mg/l and 5.83 mg/l, respectively. Highest Ox-N surface averages were seen at RE30, while lowest averages were seen at RE35. Seasonal averages since 2003 surface waters have been below 1.95 mg/l at RE02, below 2.61 mg/l at RE15, and below 1.43 mg/l at RE35. At RE30, averages have generally been below 7.53 mg/l, with the exception of one noticeable peak of 11.93 mg/l in fall 2005. Seasonal averages at bottom waters ranged from 0.01 to 3.78 mg/l at RE02, 0.01 to 9.15 mg/l at RE15, 0.53 to 12.96 mg/l at RE30, and 0.01 to 3.42 at RE35 (Figure 4-73). Since 2003, averages for bottom waters have been below 2.18 mg/l at RE02, below 4.0 mg/l at RE15, and 1.62 mg/l at RE35. Like in surface waters, Ox-N averages at RE30 were mostly below 7.19, except during fall 2005, where a similar peak of 11.75 mg/l was observed in bottom waters.

Seasonally, higher values were mainly observed in winter or fall depending on the station and depth, and lower averages were seen during summer or spring (Figure 4-74). Lower Ox-N at the surface during summer and spring may be caused by nitrate uptake by algae to produce amino acids and other proteins. At bottom waters, Ox-N average concentrations were lower during summer at RE02, RE15, and RE35, while averages at RE30 were lower during spring. Ox-N average concentration at RE30 might have been lower during spring because this station receives the highly nitrified effluent from the MHR WRF during summer thereby increasing the concentrations. Lower Ox-N during summer at the other stations, despite high concentrations of nitrate coming from the MHR WRF, might be due to a decrease in DO levels during thermal stratification thus permitting denitrification. Later, when the water column starts to mix during fall, denitrification rates might start to lower before all the nitrate has been consumed resulting in higher Ox-N concentrations during fall and winter. Additionally, as it was stated in the Hydrometeorological Conditions section, the seasons with less average rainfall during the period of record were winter and fall, probably resulting in lower flow conditions and less dilution of Ox-N concentrations. Lastly, at RE02 and RE15, the NH3-N being nitrified during summer may contribute to the observed Ox-N concentrations (Figure 4-74).

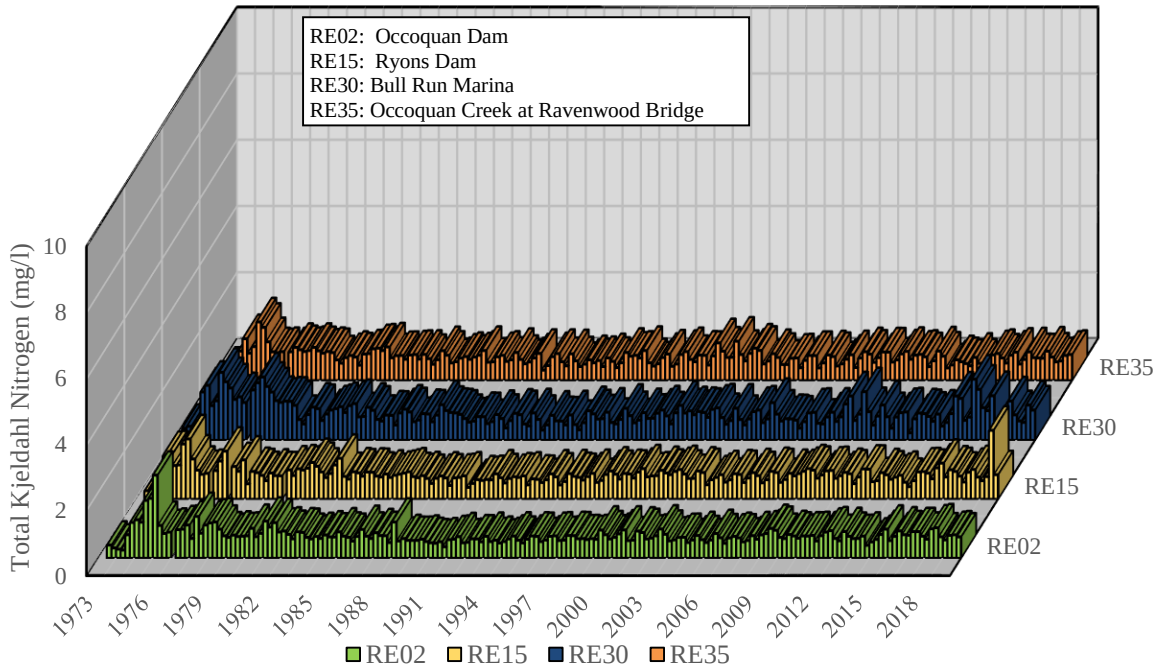

Figure 4-69. Seasonal Average Total Kjeldahl Nitrogen in Reservoir Surface Waters, 1973–2019

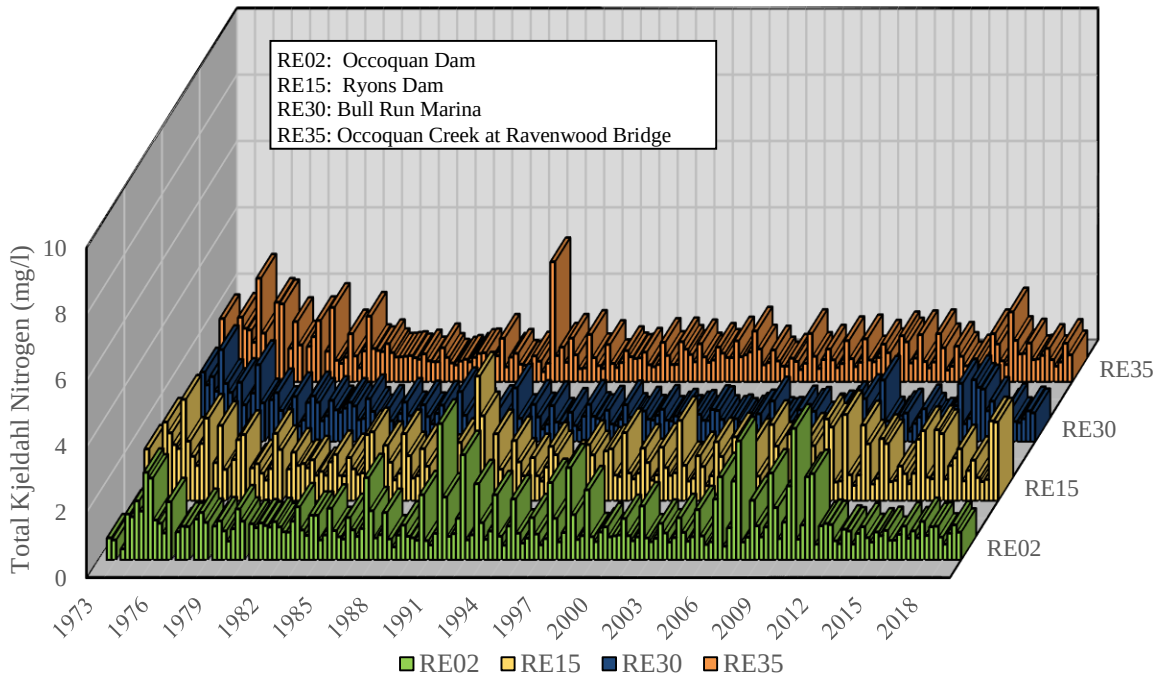

Figure 4-70. Seasonal Average Total Kjeldahl Nitrogen in Reservoir Bottom Waters, 1973–2019

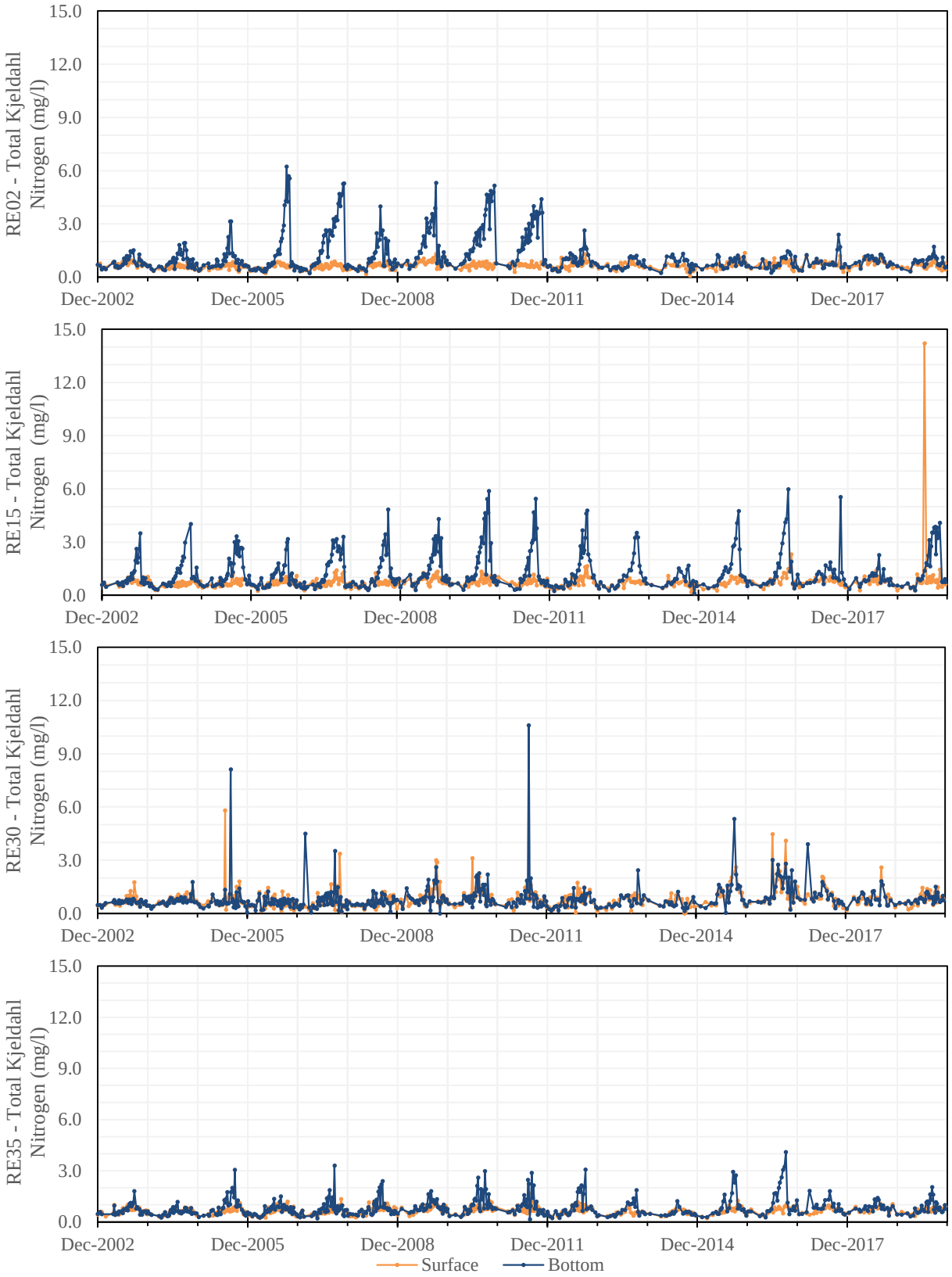

Figure 4-71. Total Kjeldahl Nitrogen Time Series at Reservoir Stations, 2003–2019

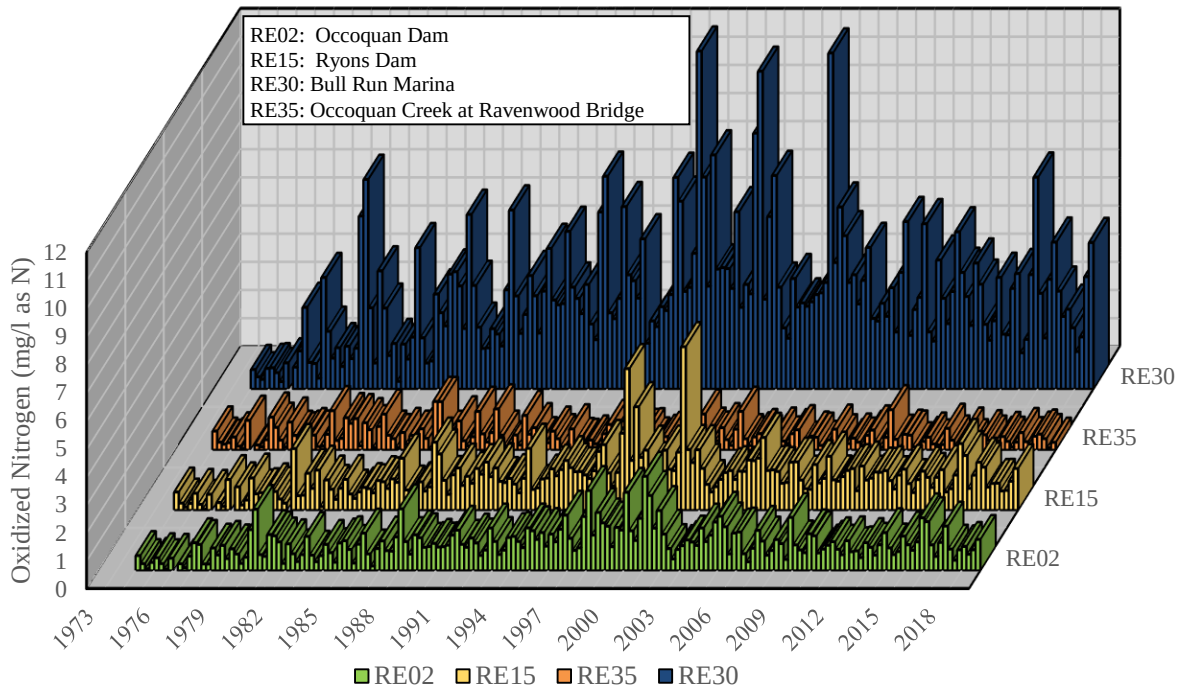

Figure 4-72. Seasonal Average Oxidized Nitrogen in Reservoir Surface Waters, 1973–2019

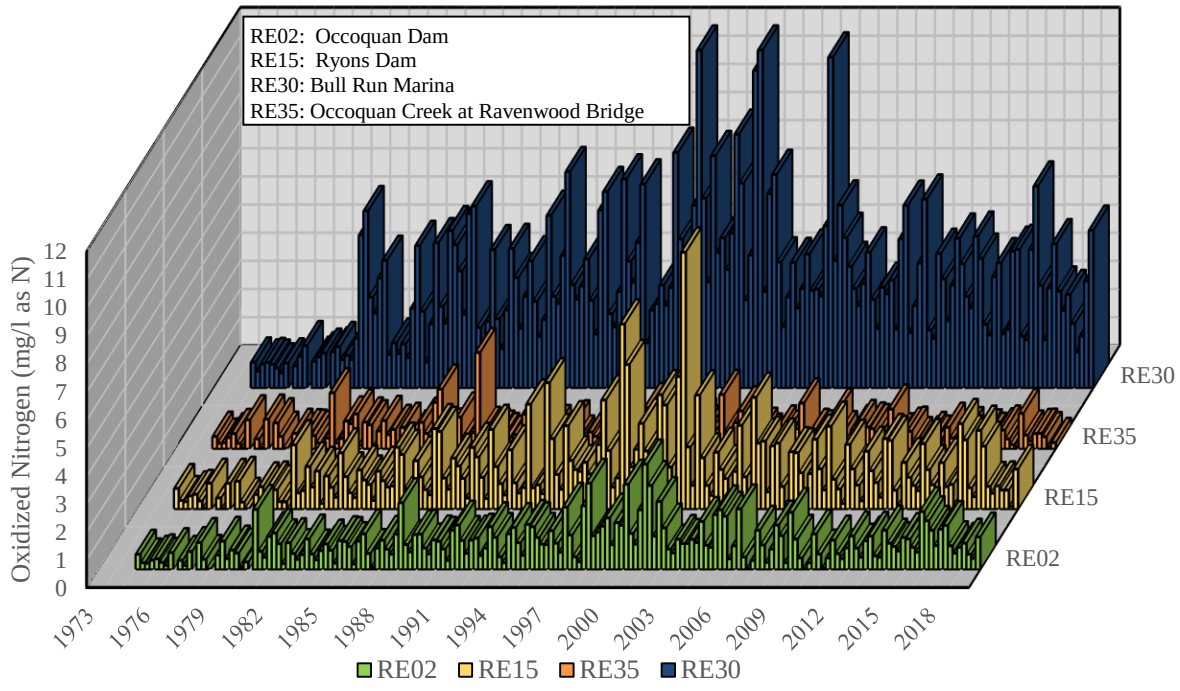

Figure 4-73. Seasonal Average Oxidized Nitrogen in Reservoir Bottom Waters, 1973–2019

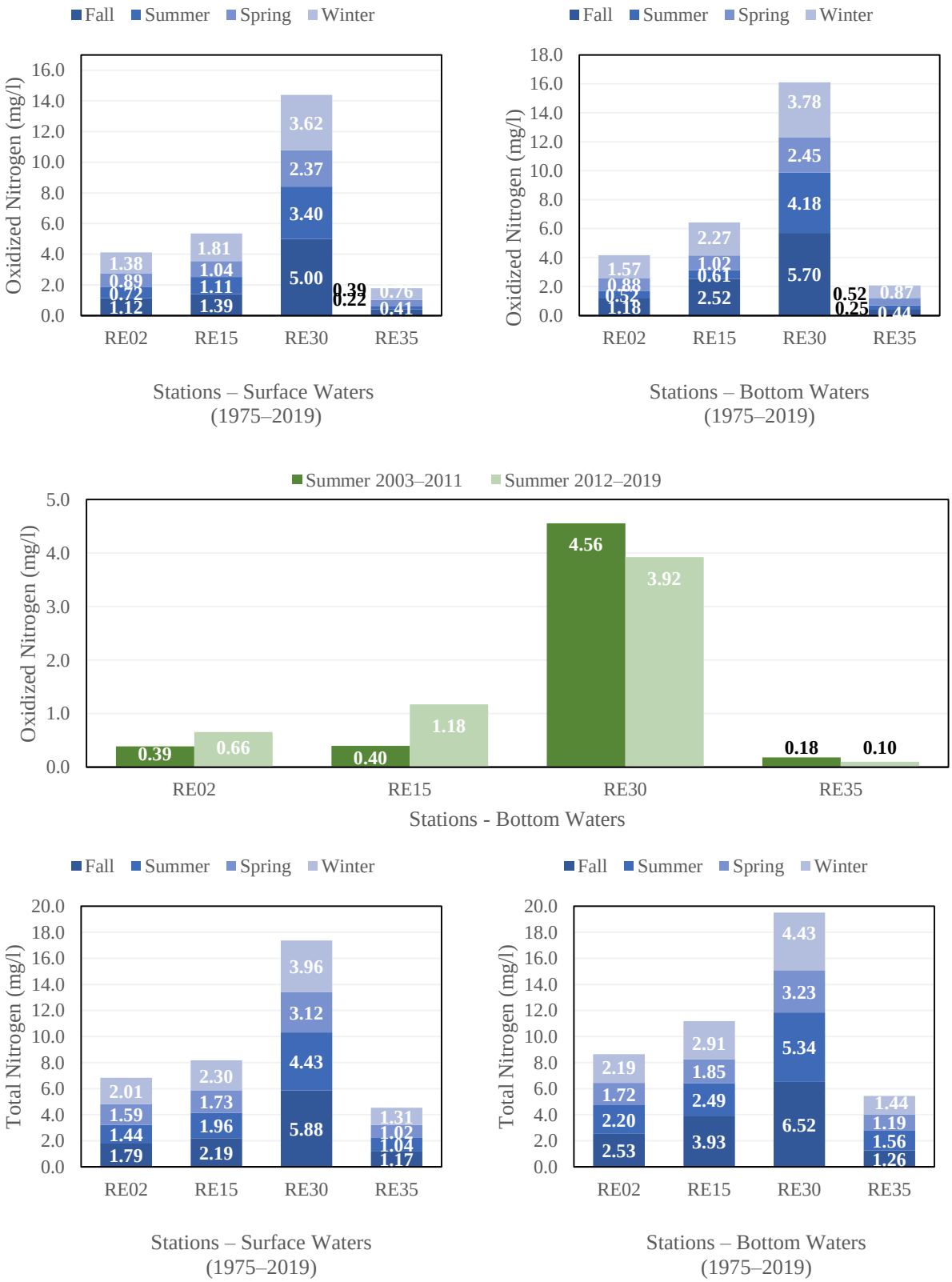

Figure 4-74. Overall Oxidized and Total Nitrogen Average by Season at Occoquan Reservoir, 1975–2019

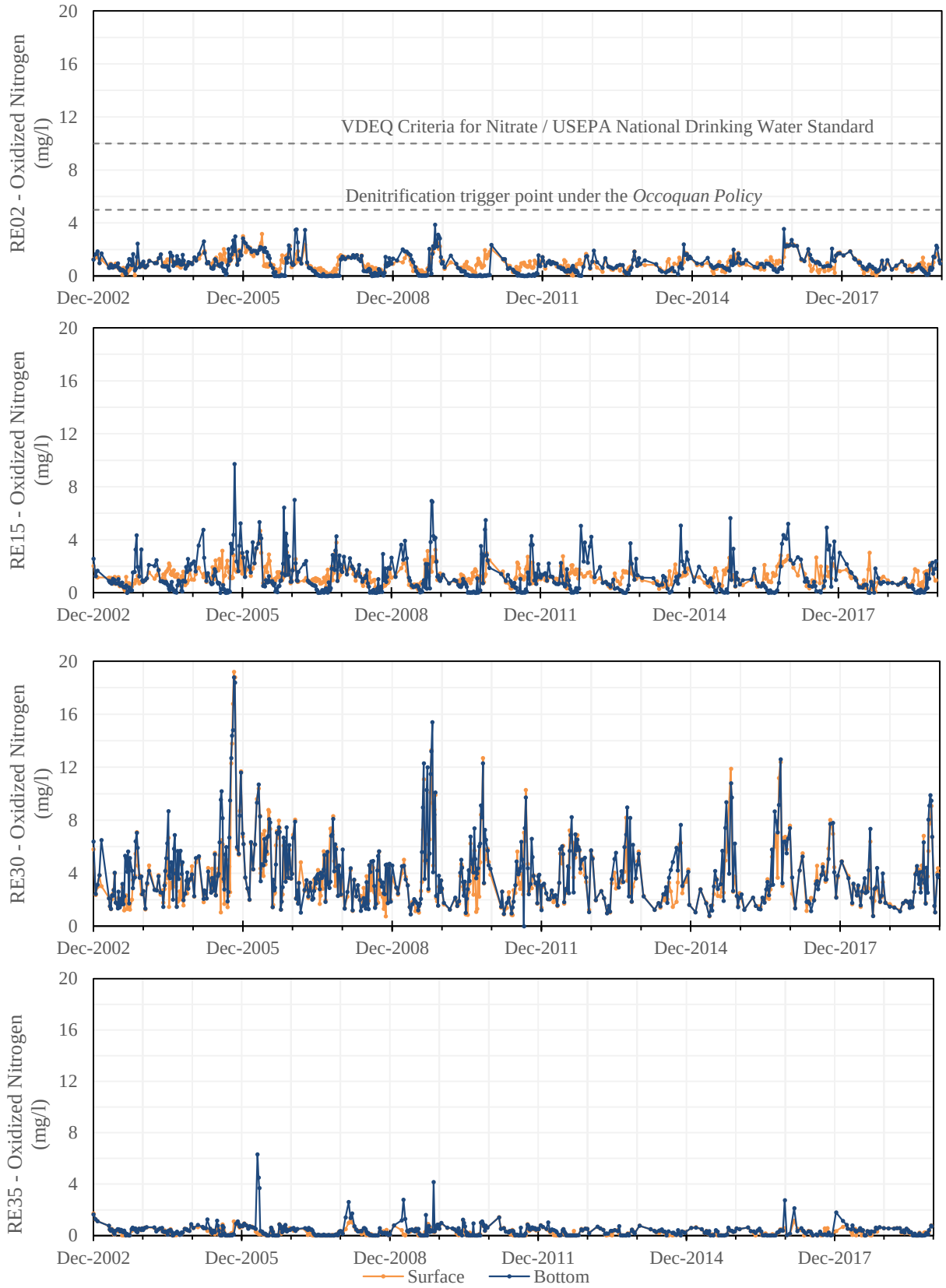

Figure 4-75. Oxidized Nitrogen Time Series at Reservoir Stations, 2003–2019

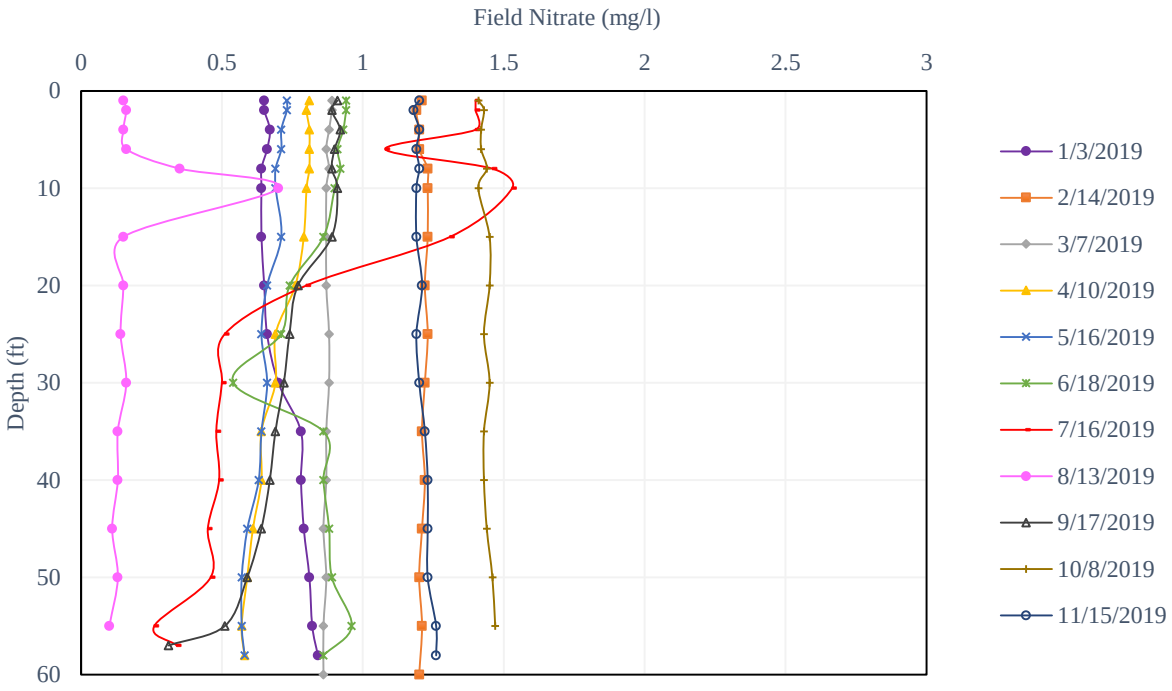

Figure 4-76. Field Nitrate Profiles at Station RE02, 2018

Ox-N time series from 2003 to 2019 are presented in Figure 4-75. In this graph, it can be observed how lowest values at both depths were seen at the Occoquan Creek and higher values were observed at Bull Run. Peak values at Bull Run in Figure 4-75 were seen during summer and fall. Despite high Ox-N concentrations at Bull Run, it can be observed that Ox-N decreased as it moved through the reservoir, maintaining values at the reservoir outlet well below the VDEQ and USEPA nitrate limit of 10 mg/l for drinking water and below the 5 mg/l trigger point of the *Occoquan Policy*. As mentioned, this decrease in nitrate through the reservoir may be a consequence of biological uptake and. Lower Ox-N values during summer at bottom waters correspond with lower DO during that season, and it may even be observed there were some dates when Ox-N was higher at surface waters than at bottom waters. Figure 4-76 illustrates field-measured nitrate concentrations throughout the water column during 2019 at RE02, where values were maintained below 2.60 mg/l. Overall, the months with higher Ox-N concentrations throughout the water column (1.18 to 1.47 mg/l) were October, November, and February. Additionally, a peak of 1.53 mg/l was observed during July at the surface but bottom waters remained below 0.52 mg/l.

Mann-Kendall test results for Ox-N in Table 4-31 show upward trends for RE02, RE15, and RE30 during all seasons and both depths, except for fall in RE30 at bottom waters. However, not all values are significant. Trends at RE35, on the other hand, show a downward tendency at surface and bottom waters, though significant values are only observed at the surface. This decreasing trend at RE35 matches decreasing tendency observed for Ox-N concentrations at ST40.

Figures 4-77 to 4-79, present seasonal averages of TN from 1973 to 2019, as well TN time series from 2003 to 2019. Since TN is the sum of the TKN and Ox-N, similar patterns can be observed

with them, mainly when compared to Ox-N due to higher concentrations observed at the reservoir. Higher average concentrations are observed at bottom waters than surface (though not as marked), at Bull Run than the rest of the stations, and during fall and winter. Lower values are seen at the Occoquan Creek, and mainly during spring. Mann-Kendall test results (Table 4-31), show upward trends at RE30 and downward trend at RE35, several being statistically significant. RE02 and RE15 vary by season and depth, however, significant trends at these stations are also increasing.

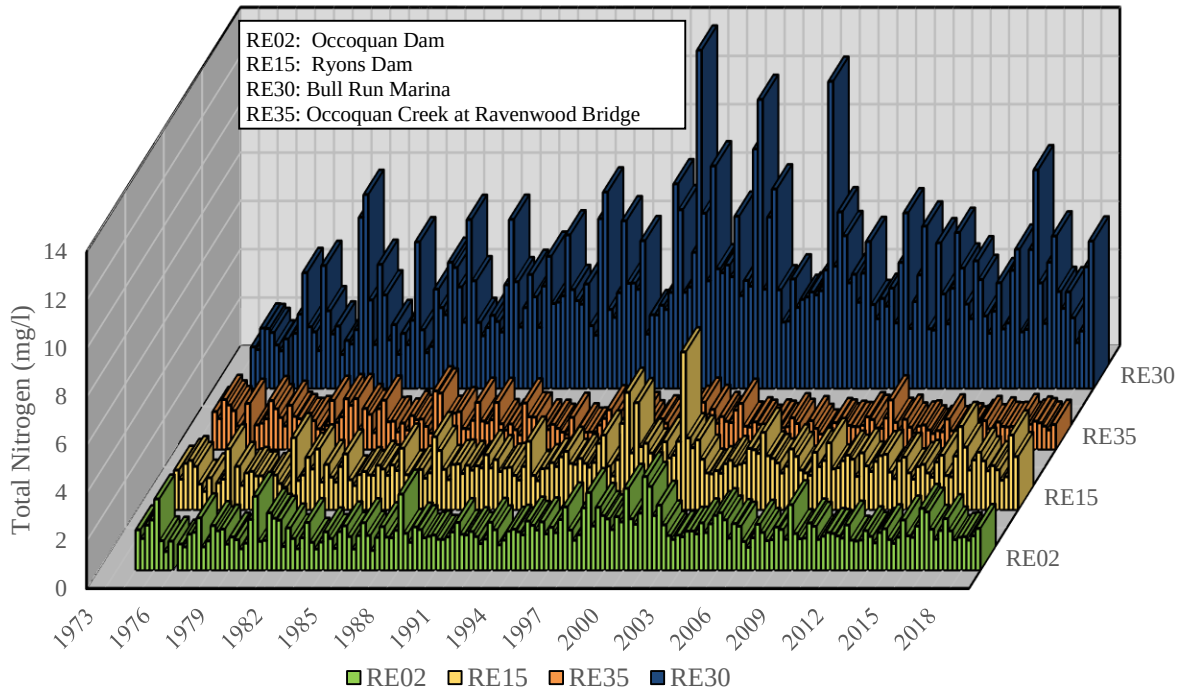

Figure 4-77. Seasonal Average Total Nitrogen in Reservoir Surface Waters, 1973–2019

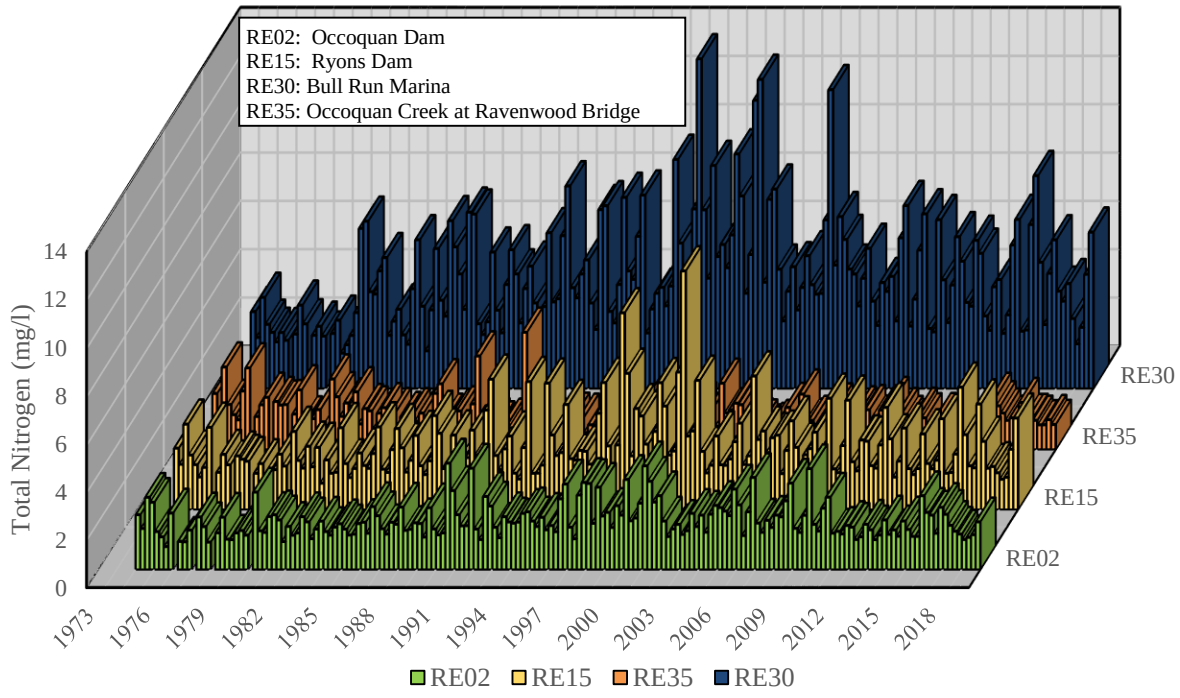

Figure 4-78. Seasonal Average Total Nitrogen in Reservoir Bottom Waters, 1973–2019

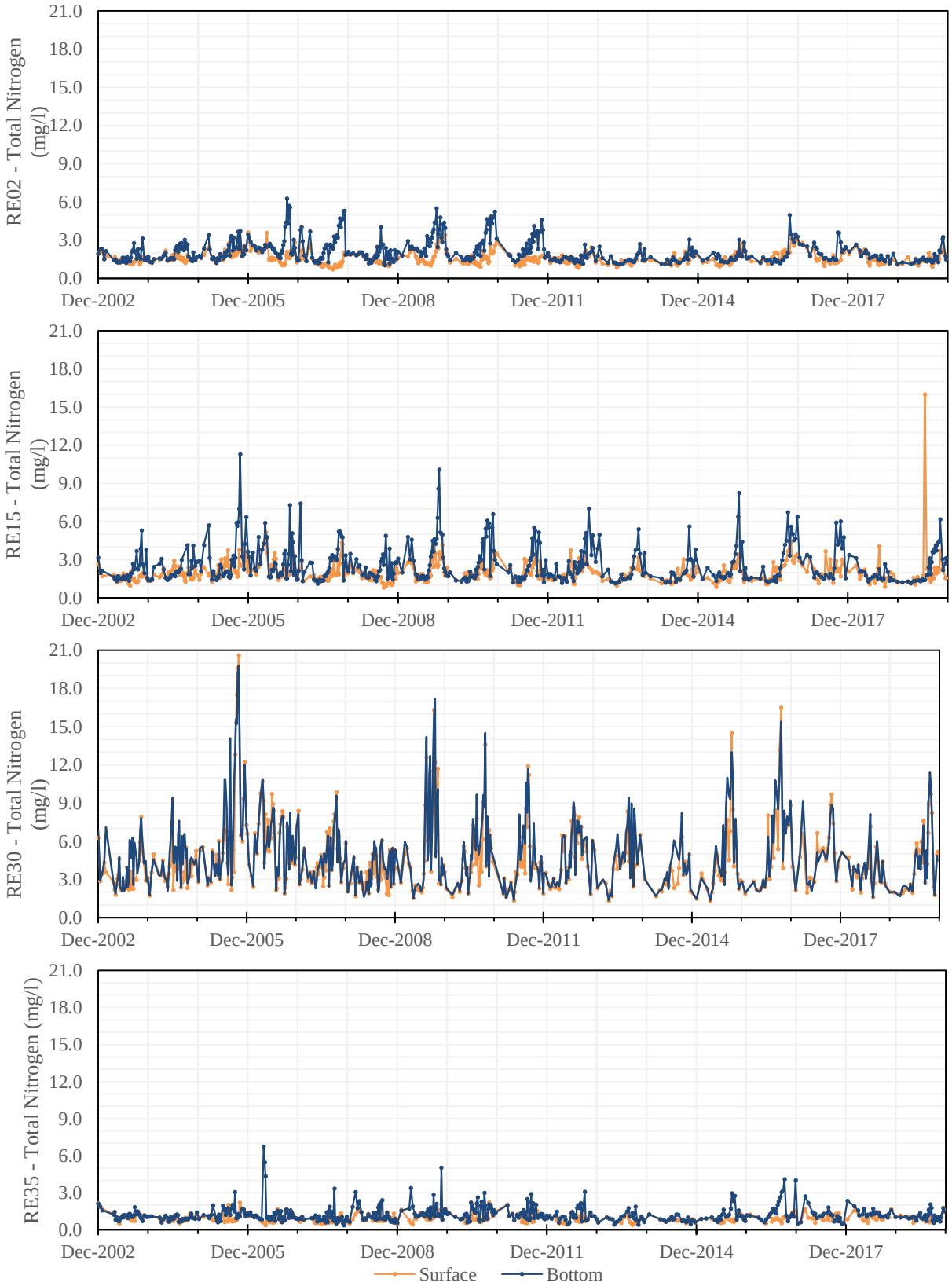

Figure 4-79. Total Nitrogen Time Series at Reservoir Stations, 2003–2019

4.3.9 Phosphorus

OP seasonal averages from 1973 to 2019 are presented for surface waters in Figure 4-80 and for bottom waters in Figure 4-81. Surface water averages all range from 0.01 mg/l to 0.06 mg/l as P at RE02, 0.07 mg/l as P at RE15, 0.26 mg/l as P at RE30, and 0.05 mg/l as P at RE35. The higher values observed at Bull Run correspond to the 1970s before the MHR WRF came into operation (averages from 0.05 to 0.26 mg/l as P). Since summer 1978, all average values at RE30 have been below 0.05 mg/l as P at the surface. Seasonal OP averages at bottom waters also range from 0.01 to 0.25 mg/l as P at RE02 and RE15, 0.22 mg/l as P at RE30, and 0.13 mg/l as P at RE35. Higher bottom averages (greater or equal to 0.10 mg/l as P) at stations RE15 and RE30 were also seen before the establishment of the MHR WRF and were probably caused by sewage discharges into the reservoir. RE02, on the other hand, does show high averages during summer and fall in 2006 and 2007, with peak average between 0.18 and 0.25 mg/l as P. It can be observed that averages at bottom waters tend to be higher than surface waters. This difference is also illustrated in Figure 4-82 which presents OP seasonal averages for the entire period of record. Values between stations present little difference, with slightly higher average observed at RE30 for surface water, which are probably due to the higher values before the MHR WRF's startup. Higher averages were seen at RE02 for bottom waters. Seasonally, a slightly higher value was seen during winter for surface waters at RE02 and RE15, and during summer at bottom waters for these stations. RE30 and RE35 did not exhibit significant variation among seasons.

Figure 4-83 presents OP time series from 2003 to 2019, where the most noticeable peaks were the ones responsible for previously mentioned higher seasonal averages at RE02 bottom waters. During this period, the highest concentration at RE02 during this period was 0.93 mg/l as P in fall 2007. A few peaks were also observed at RE15, the highest value being 0.39 mg/l as P during summer 2005. No significantly high peaks were observed at Bull Run or the Occoquan Creek stations, though RE35 showed slightly higher values during summer and fall 2006, reaching a value of 0.13 mg/l as P. Therefore, since the higher OP concentrations at RE02 and RE15 happened during the summer and fall, and values at the inflow reservoir stations were lower, they were most likely caused by phosphorus release from sediments when anaerobic conditions were present during thermal stratification. Also, comparing this figure with the Ox-N time series (Figure 4-75), peaks in OP generally coincide with lower nitrate values, (e.g. the highest peak of 0.93 mg/l at RE02 coincides with an Ox-N value of 0.03 mg/l; DO value of 0.52 mg/l; and 131mV for ORP). It should be noted that since 2012, lower values than previous years have been observed at RE02 probably due to the hypolimnetic oxygenation system (also illustrated in Figure 4-82). Fewer spikes have also been noticed at RE15 in the recent years. Comparing bottom waters from RE30 and RE35 during 2003 to 2019, it was observed that RE35 presented slightly higher values, reaching a peak of 0.17 mg/l as P, while concentration at RE30 remained less or equal to 0.05 mg/l as P. This was the case for surface waters where a few higher values were seen, the highest being 0.16 mg/l in 2018, when the rest of the stations remained less or equal to 0.07 mg/l as P.

Figures 4-84 and 4-85 show TP seasonal average concentrations by year for the period of record. Surface averages, ranging from 0.01 to 0.38 mg/l, tend to be lower than bottom averages, ranging between 0.01 to 0.87 mg/l. High values at RE30 were seen before the startup of the MHR WRF.

One of the highest averages during the period of record occurred in fall 1976 at bottom waters and was seen at RE02 (0.59 mg/l), RE15 (0.87 mg/l), and RE35 (0.55 mg/l), though it was most marked at RE15. Since then, values at RE15 and RE35 have remained lower. At RE02, other peaks were observed, the highest being 0.66 mg/l in 2007. Peaks concentrations since 2003 can be better observed in the TP time series (Figure 4-86), which even though higher, present similar pattern as OP, since OP is comprises a part of TP, roughly speaking around 24–30% (Figure 4-82). Other forms included in TP are organic phosphorus and particulate phosphorus. Since 2003, higher values at surface waters have been observed at the inflow reservoir stations than at RE02 and RE15, probably indicating external sources (e.g., runoff from watershed, point sources). At bottom waters, higher values were present at RE02 and RE15, indicating internal loading. TP values from 2003 to 2019 at Bull Run tend to be slightly lower than at the Occoquan Creek.

Mann-Kendall test results for OP show declining trends at all stations and seasons (Table 4-32). It should be noted not all trends were statistically significant and slopes values were low. Trends for TP were also mostly decreasing.

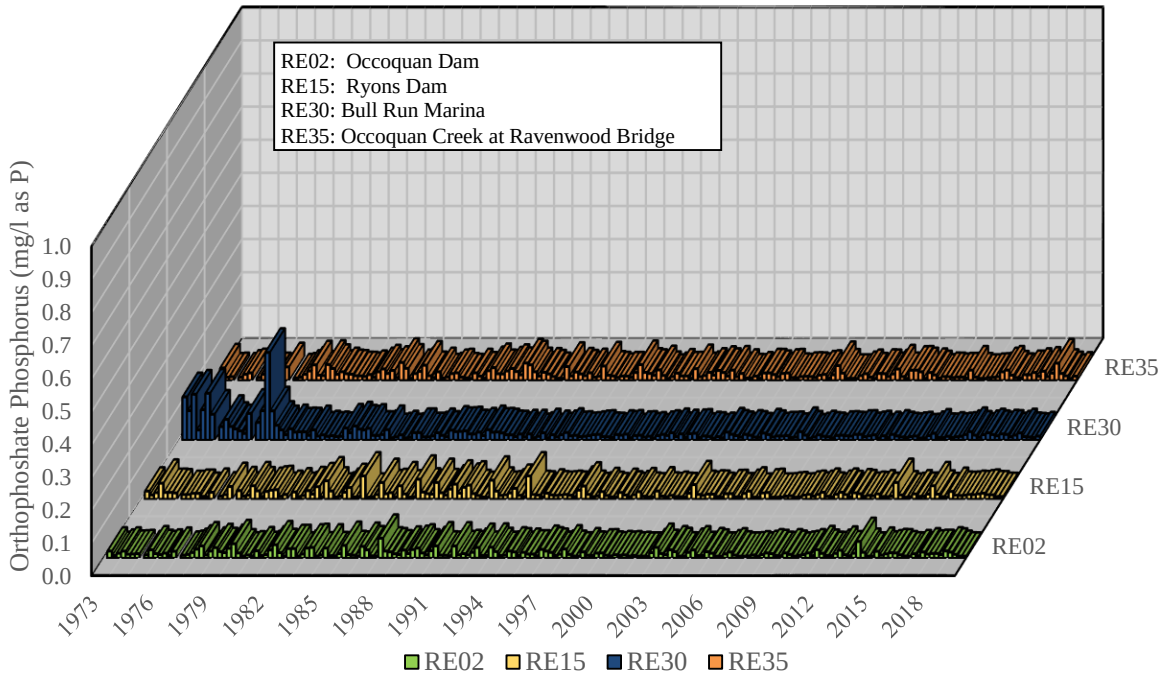

Figure 4-80. Seasonal Average Orthophosphate Phosphorus in Reservoir Surface Waters, 1973–2019

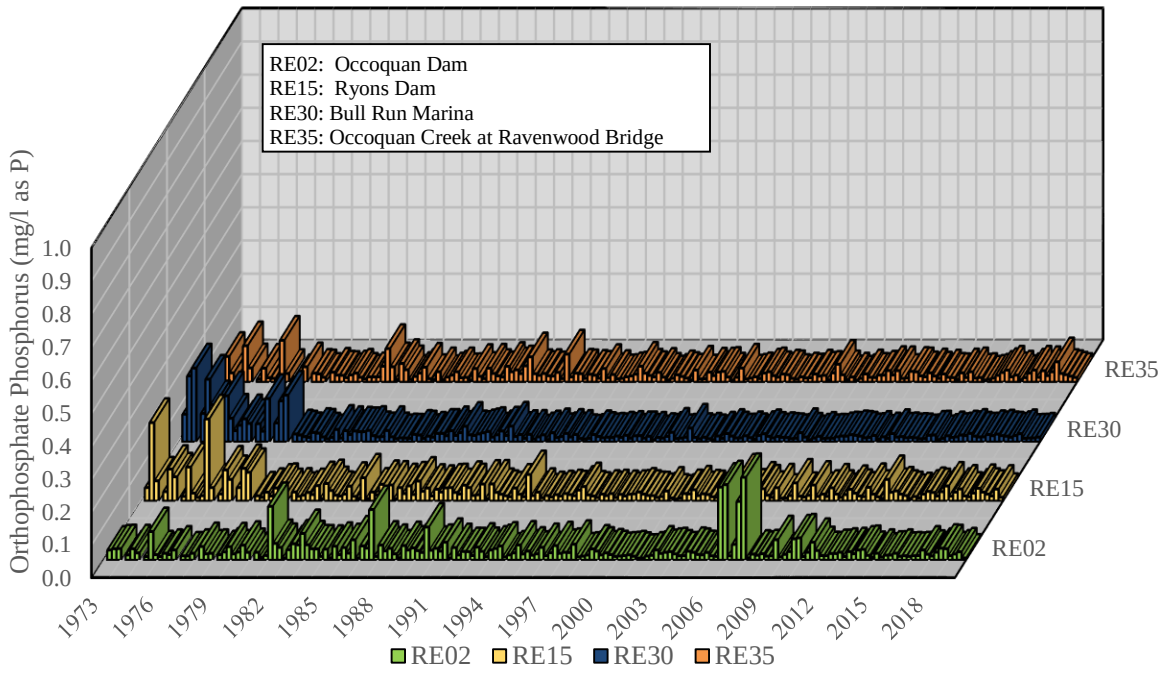

Figure 4-81. Seasonal Average Orthophosphate Phosphorus in Reservoir Bottom Waters, 1973–2019

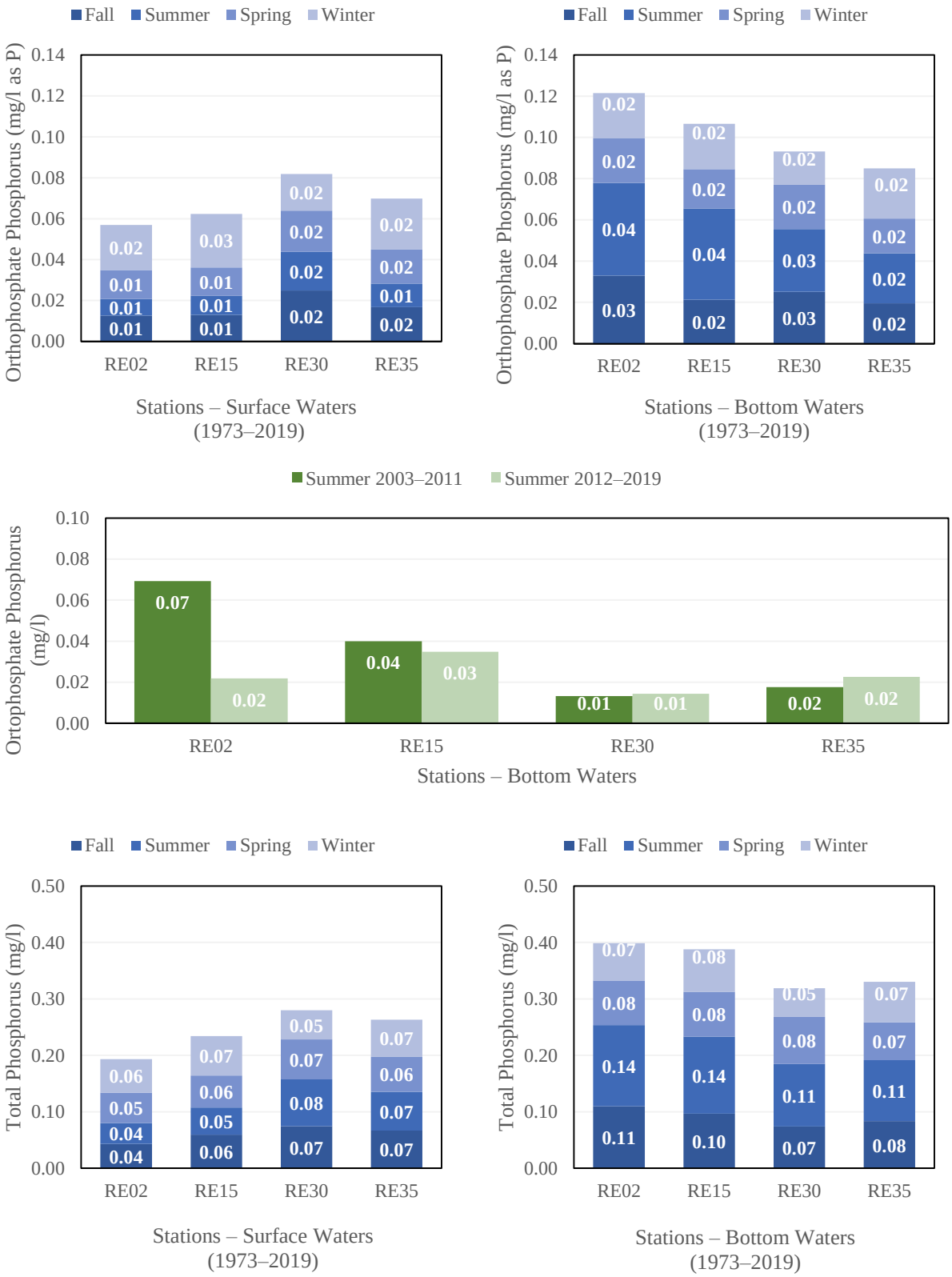

Figure 4-82. Overall Orthophosphate Phosphorus and Total Phosphorus Average by Season at Occoquan Reservoir, 1973–2019

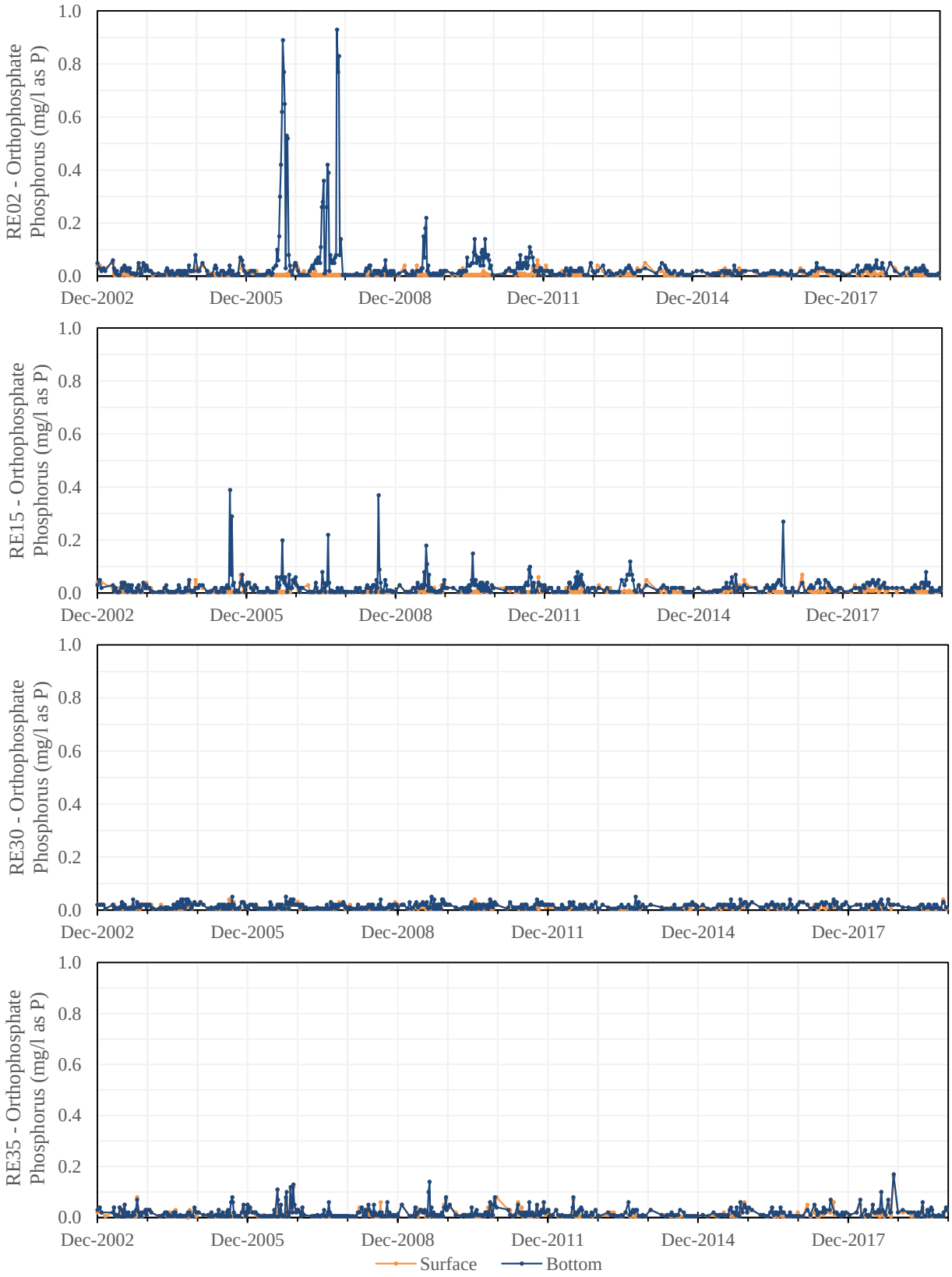

Figure 4-83. Orthophosphate Phosphorus Time Series at Reservoir Stations, 2003–2019

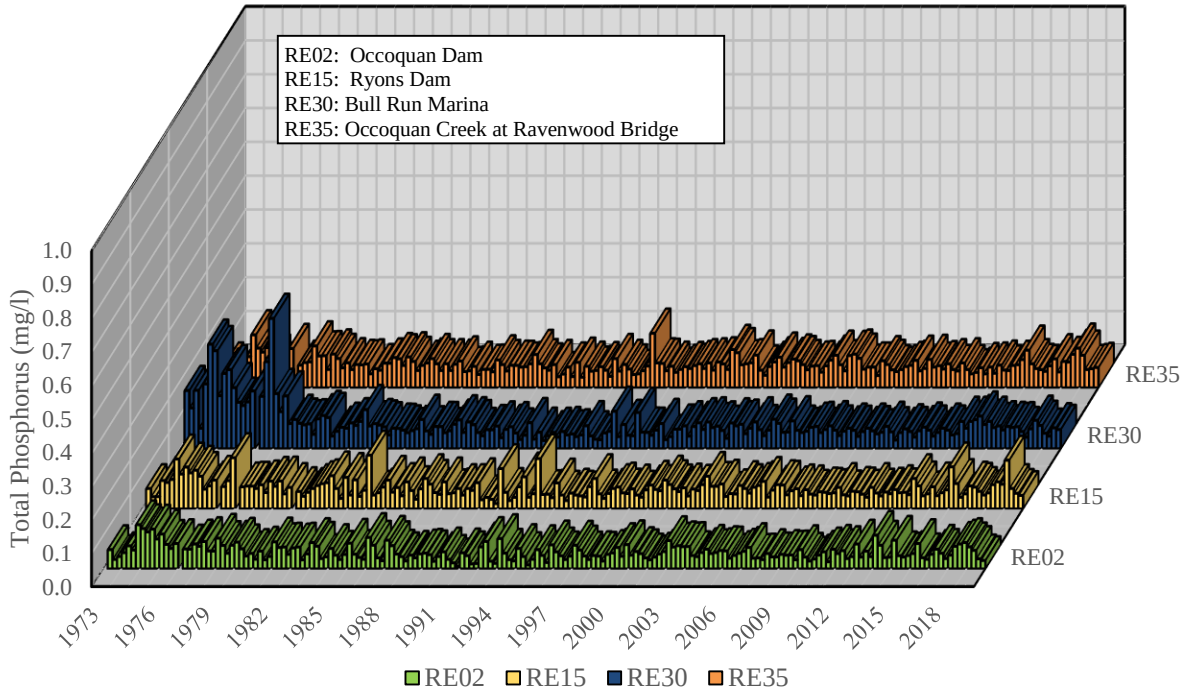

Figure 4-84. Seasonal Average Total Phosphorus in Reservoir Surface Waters, 1973–2019

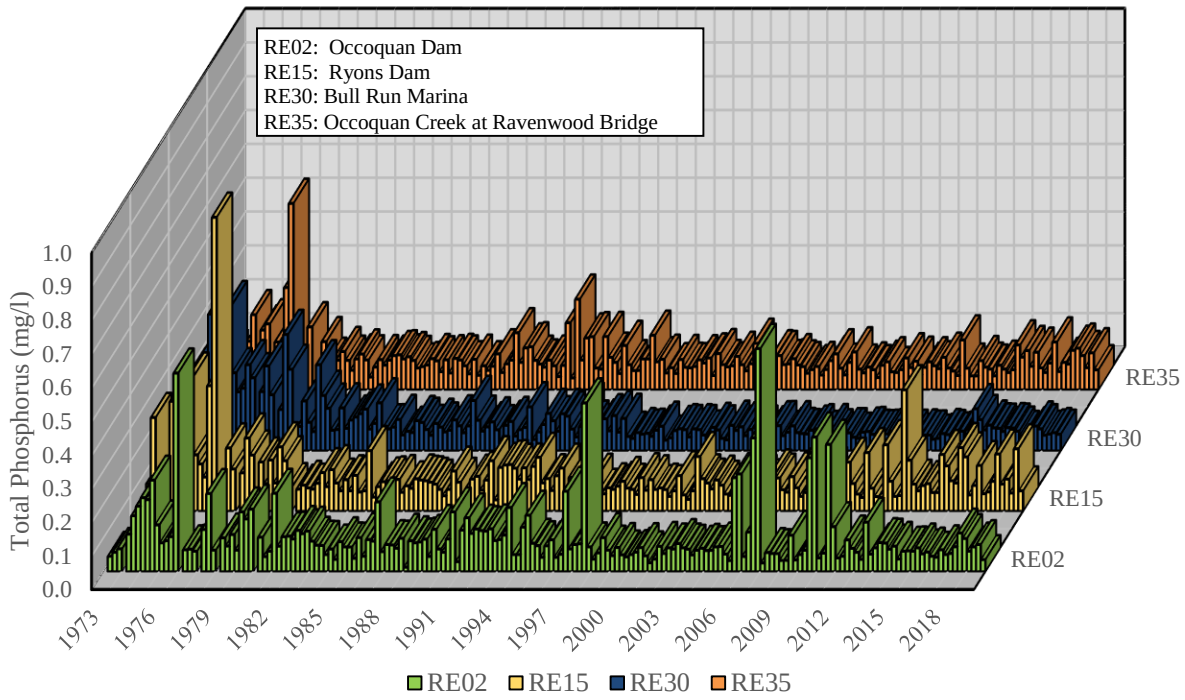

Figure 4-85. Seasonal Average Total Phosphorus in Reservoir Bottom Waters, 1973–2019

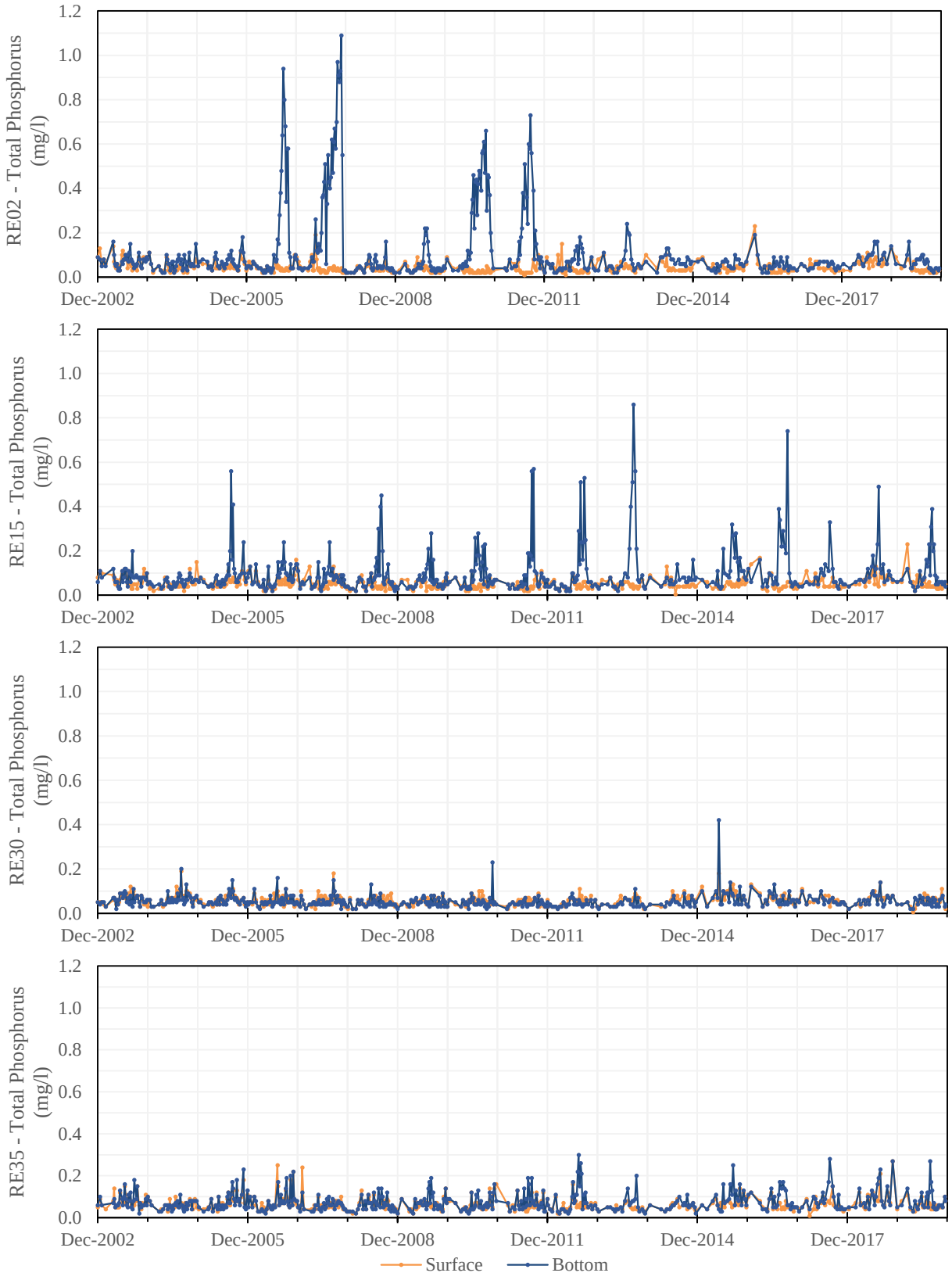

Figure 4-86. Total Phosphorus Time Series at Reservoir Stations, 2003–2019

Table 4-32. Mann-Kendall Reservoir Phosphorus Trends, 1973–2019

Station	Description	Season	Ortophosphate Phosphorus				Total Phosphorus			
			Sen Slope	*Kendall Tau*	*p-value*	*Trend*	*Sen Slope*	*Kendall Tau*	*p-value*	*Trend*
RE02	Surface	Winter	-2.5E-04	-0.170	**0.099**	↘	-0.001	-0.210	**0.042**	↘
		Spring	-2.2E-04	-0.303	**0.003**	↘	-3.5E-04	-0.212	**0.037**	↘
		Summer	-6.1E-05	-0.281	**0.006**	↘	-1.2E-04	-0.051	0.620	↘
		Fall	-6.0E-05	-0.091	0.373	↘	-3.5E-04	-0.205	**0.044**	↘
	Bottom	Winter	-0.001	-0.399	**1.7E-04**	↘	-0.002	-0.440	**2.4E-05**	↘
		Spring	-2.3E-04	-0.213	**0.036**	↘	-0.001	-0.301	**0.003**	↘
		Summer	-1.8E-04	-0.096	0.345	↘	-2.6E-04	-0.048	0.640	↘
		Fall	-5.0E-05	-0.054	0.601	↘	-0.001	-0.196	**0.054**	↘
RE15	Surface	Winter	-0.001	-0.356	**0.001**	↘	-0.001	-0.221	**0.032**	↘
		Spring	-2.8E-04	-0.361	**3.7E-04**	↘	-3.8E-04	-0.212	**0.037**	↘
		Summer	-7.3E-05	-0.254	**0.014**	↘	-1.2E-04	-0.080	0.436	↘
		Fall	-9.8E-05	-0.135	0.186	↘	-0.001	-0.247	**0.015**	↘
	Bottom	Winter	-4.5E-04	-0.270	**0.011**	↘	-0.001	-0.333	**0.001**	↘
		Spring	-3.2E-04	-0.330	**0.001**	↘	-0.001	-0.405	**6.6E-05**	↘
		Summer	-3.7E-04	-0.133	0.190	↘	0.001	0.082	0.420	↗
		Fall	-1.6E-04	-0.108	0.291	↘	-0.001	-0.187	**0.065**	↘
RE30	Surface	Winter	-3.1E-04	-0.358	**0.001**	↘	-3.3E-04	-0.201	**0.051**	↘
		Spring	-0.001	-0.495	**1.1E-06**	↘	-0.001	-0.339	**0.001**	↘
		Summer	-3.0E-04	-0.425	**2.7E-05**	↘	-3.9E-04	-0.202	**0.047**	↘
		Fall	-2.5E-04	-0.252	**0.013**	↘	-0.001	-0.276	**0.006**	↘
	Bottom	Winter	-1.4E-04	-0.183	**0.085**	↘	-0.001	-0.345	**0.001**	↘
		Spring	-0.001	-0.445	**1.1E-05**	↘	-0.001	-0.514	**3.8E-07**	↘
		Summer	-0.001	-0.488	**1.4E-06**	↘	-0.003	-0.660	**6.6E-11**	↘
		Fall	-2.6E-04	-0.195	**0.054**	↘	-0.001	-0.480	**2.0E-06**	↘
RE35	Surface	Winter	-2.2E-04	-0.171	0.105	↘	-3.9E-04	-0.148	0.158	↘
		Spring	-1.7E-04	-0.184	**0.071**	↘	-2.5E-04	-0.147	0.150	↘
		Summer	-7.2E-05	-0.144	0.162	↘	-9.9E-19	-0.001	1.000	↘
		Fall	-8.1E-05	-0.083	0.419	↘	-1.8E-04	-0.083	0.414	↘
	Bottom	Winter	-1.7E-04	-0.108	0.315	↘	-0.001	-0.210	**0.045**	↘
		Spring	-9.0E-05	-0.092	0.369	↘	-0.001	-0.265	**0.009**	↘
		Summer	-9.2E-05	-0.083	0.420	↘	-4.5E-04	-0.141	0.166	↘
		Fall	-6.7E-05	-0.061	0.557	↘	-0.001	-0.241	**0.018**	↘

4.3.10 Nitrogen: Phosphorus Ratios

Nitrogen and phosphorus are important nutrients required for aquatic plant growth. However, when they are present in excessive amounts in waterbodies they can cause eutrophication of waterbodies. The nitrogen to phosphorus (N:P) ratio provides an indication of what the limiting nutrient in a waterbody is. Phosphorus is usually the limiting nutrient in freshwaters. N:P ratios greater than 10.4:1 by mass (>23 by atoms) generally indicate phosphorus limitation in lakes (Wetzel, 2001). The limiting nutrient controls the pace at which algae and aquatics plants are produced and the species that may be present. Low N:P ratios tend to favor the growth of cyanobacteria (blue-green algae) which is not desirable because it can be toxic to consumer organisms, they can increase water turbidity, and they can increase water treatment requirements

by reducing filter operation efficiency, increasing taste and odor issues, and increasing possibility of formation of disinfection by-products.

The N:P ratio for the four reservoir stations analyzed was graphed for surface (Figure 4-87) and bottom waters (Figure 4-88). Analyzing N:P ratios it can be seen that the Occoquan Reservoir is generally phosphorus limited, with median ratios of 32 at surface waters and 25 at bottom waters for the entire period of record. N:P ratios tend to be higher at RE30 due to the nitrified effluent coming from the MHR WRF and lower at RE35. RE02 tends to experience lower N:P ratios at bottom waters mainly during the summer, probably the result of thermal stratification and a release of phosphorus when DO and oxidized nitrogen levels are low. Since 2003, N:P ratios at RE02 have ranged from 14 to 105 at the surface, and 6 to 107 at bottom waters. N:P ratios at RE15 range from 9 to 95 at the surface, and 6 to 86 at the bottom. At RE30 ratios range between 29 to 235, and 25 to 233 at the bottom. And at RE35, N:P ratios since 2003 range from 9 to 34 at the surface, and 9 to 53 at the bottom.

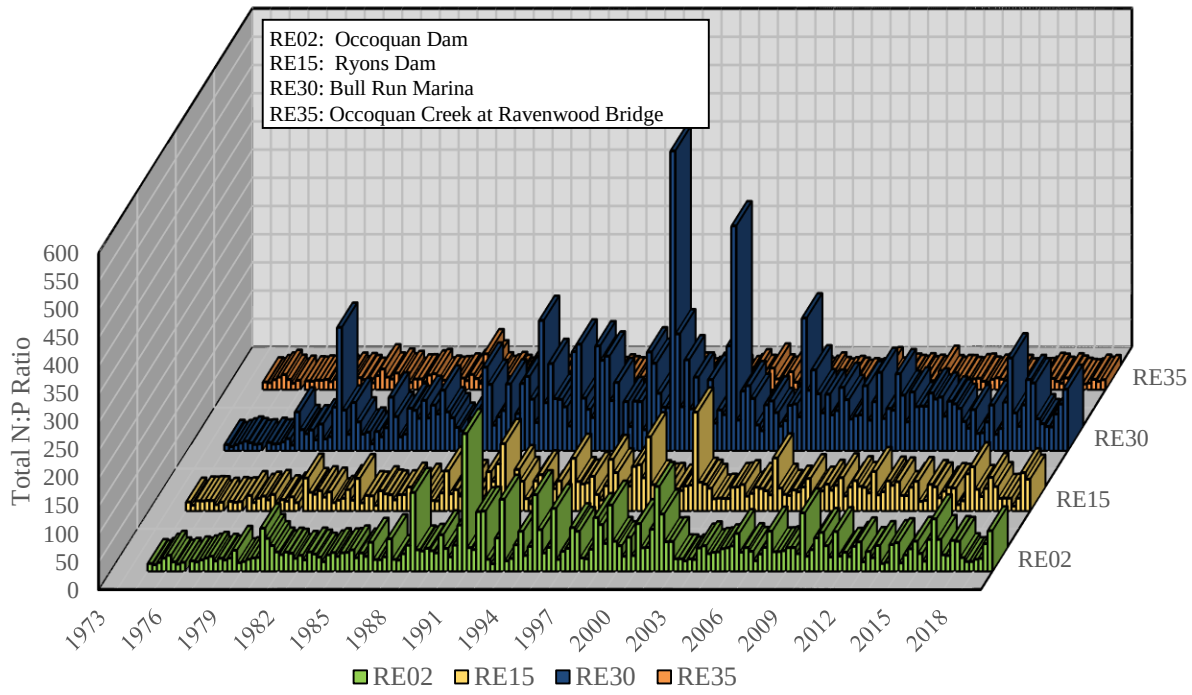

Figure 4-87. Seasonal Average Nitrogen to Phosphorus Ratio in Reservoir Surface Waters, 1973–2019

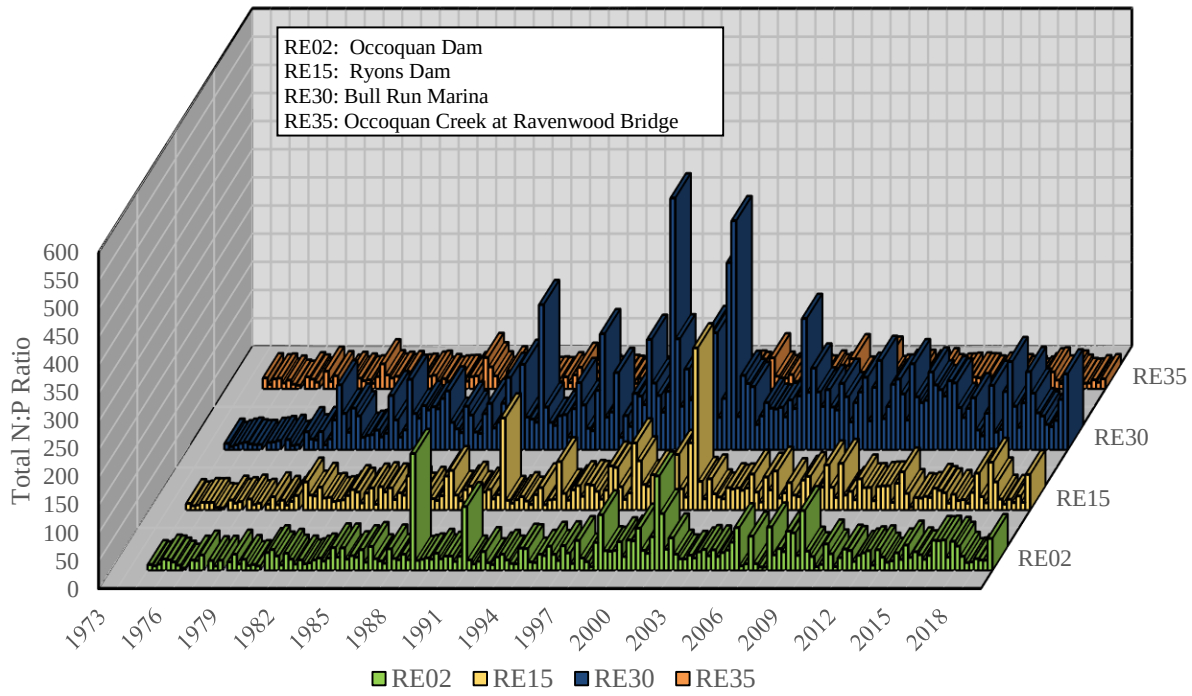

Figure 4-88. Seasonal Average Nitrogen to Phosphorus Ratio in Reservoir Bottom Waters, 1973–2019

4.3.11 Organic Carbon

Organic matter in lakes is an important source of nutrients and energy for organisms. However, high organic matter content in aquatic environments increases oxygen consumption, possibly leading to oxygen depletion, and nutrient release, which can lead to eutrophication. Furthermore, organic matter can react with chemicals added during water treatment and potentially form disinfection by-products (e.g., trihalomethanes, haloacetic acids) which have been associated with health problems. Lastly, high organic matter content can cause aesthetics problems by affecting the taste, odor, and color of water.

The amount of organic matter in the Occoquan Reservoir is measured in terms of the amount of organic carbon present, particularly DOC and TOC. DOC and TOC measurements have been collected since 1994 at RE02, and since 2006 for RE15, RE30, and RE35. Figure 4-89 shows seasonal average concentrations of DOC and TOC in surface and bottom water for the entire period. Overall, it can be observed there is little difference between surface and bottom water averages. At the surface, DOC seasonal averages range from 4.20 mg/l to 5.39 mg/l, while TOC surface seasonal averages range from 5.05 mg/l to 6.01 mg/l. At the bottom, DOC seasonal averages range from 3.83 mg/l to 6.78 mg/l, and TOC ranges from 4.54 mg/l to 7.70 mg/l. DOC and TOC averages tend to be slightly lower at RE30 at both depths, and averages are slightly higher during summer. Figures 4-90 and 4-91 show the time series for these parameters since 1994. It can be observed that RE02 is the station that experienced higher DOC peaks, reaching a

maximum value of 13.9 mg/l in spring 2000 and 13.2 mg/l in fall in bottom waters, and 13.1 mg/l during winter in surface waters. Values at RE15 were maintained below 10.8 mg/l, at RE30 below 12.3 mg/l, and below 9.9 mg/l at RE35. The highest TOC peak was also observed at RE02 in 1995 at both surface and bottom waters. Lower peaks at this station can be observed since 2012. RE30 presents three peak values, of 14.5, 14.1 and 12.8 mg/l during 2009 and 2012, however, it can also be noticed in this graph that values generally tend to be lower than the other stations.

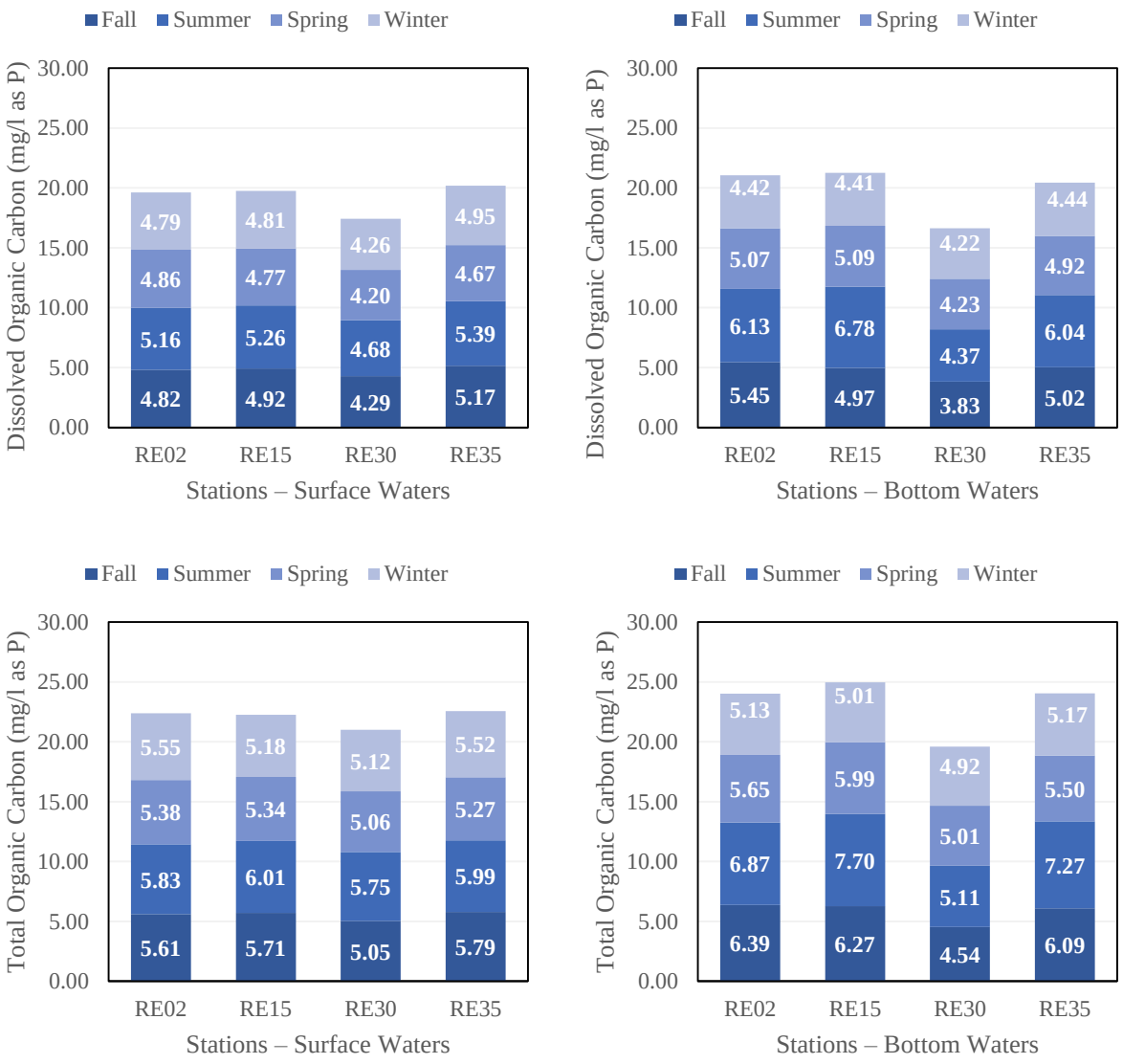

Figure 4-89. Overall Organic Carbon Average by Season at the Occoquan Reservoir, 1994–2019

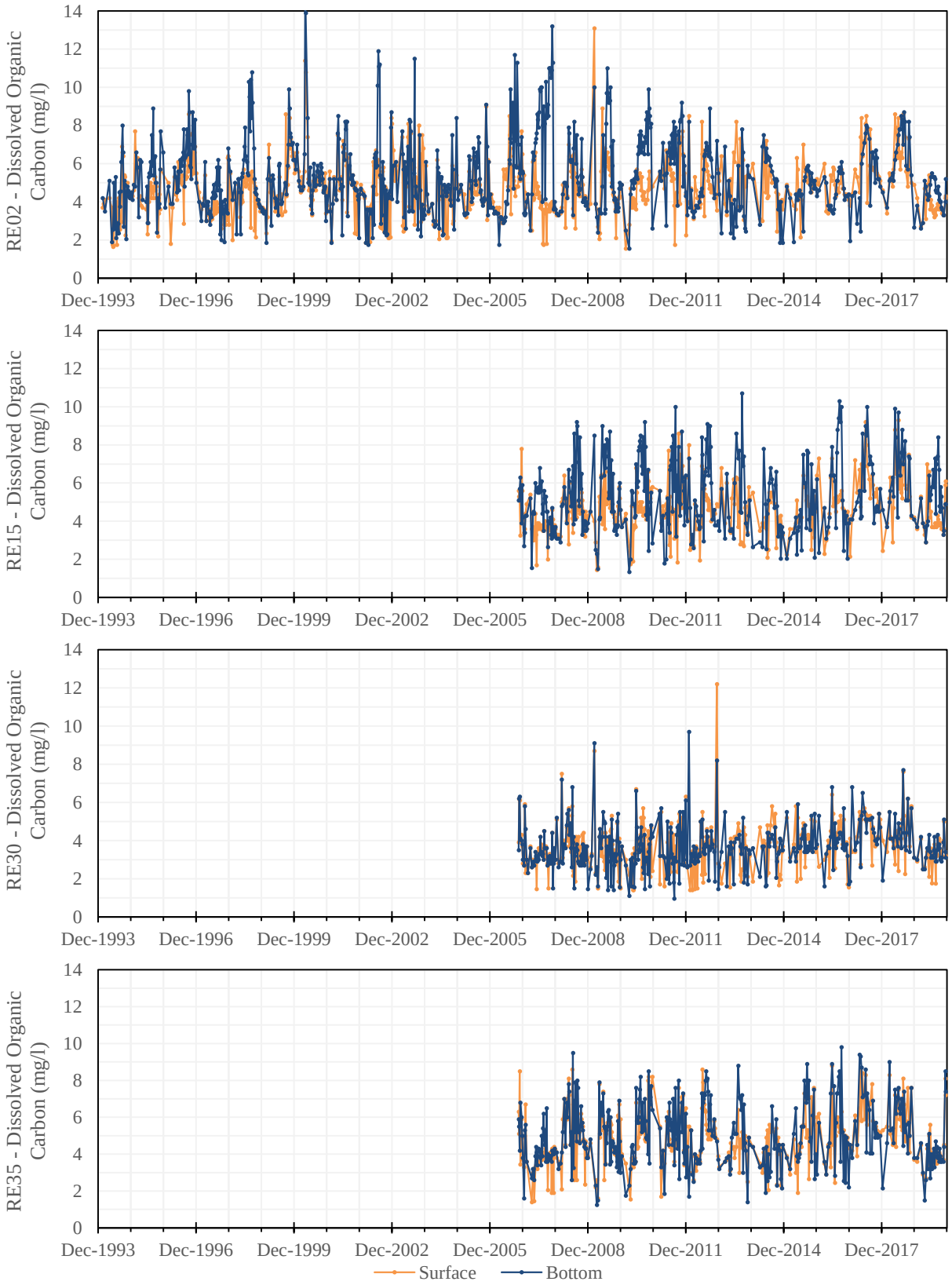

Figure 4-90. Dissolved Organic Carbon Time Series at Reservoir Stations, 1994–2019

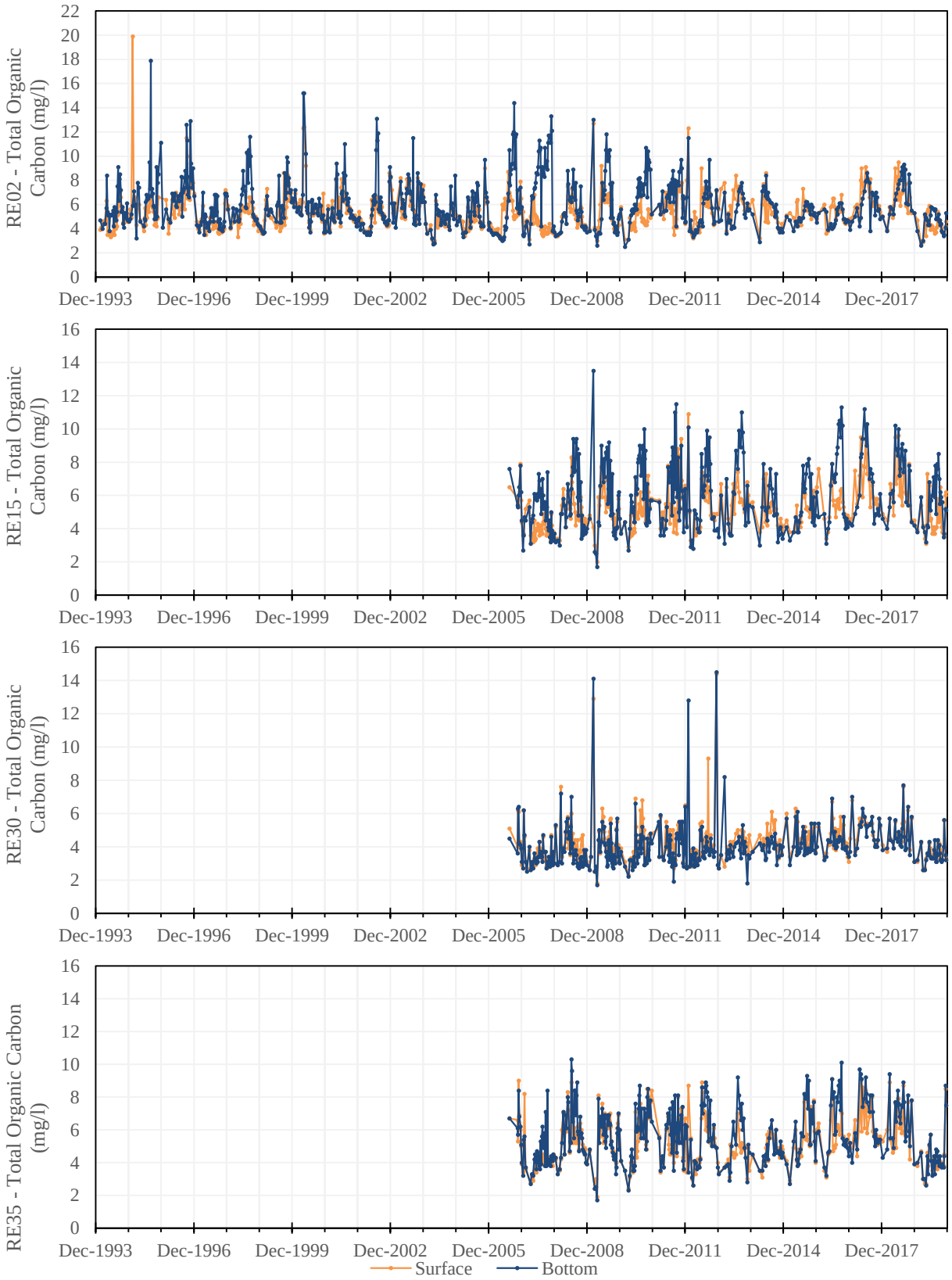

Figure 4-91. Total Organic Carbon Time Series at Reservoir Stations, 1994–2019

Mann-Kendall organic carbon trends are presented in Table 4-33. Trends for DOC seem to be mostly increasing but the only trends that were statistically significant were at RE02 surface water during spring and summer, at RE15 surface water during spring, and at RE30 bottom waters during summer. The only significant trend for TOC occurred during spring at RE30 surface water where an upward tendency was observed.

Table 4-33. Mann-Kendall Reservoir Organic Carbon Trends, 1994–2019

Station	Description	Season	Dissolved Organic Carbon				Total Organic Carbon			
			Sen Slope	*Kendall Tau*	*p-value*	*Trend*	*Sen Slope*	*Kendall Tau*	*p-value*	*Trend*
RE02	Surface	Winter	0.030	0.151	0.290	↗	0.002	0.012	0.947	↗
		Spring	0.049	0.339	**0.016**	↗	0.027	0.173	0.225	↗
		Summer	0.048	0.292	**0.038**	↗	0.048	0.210	0.140	↗
		Fall	0.011	0.095	0.508	↗	0.001	0.009	0.965	↗
	Bottom	Winter	-0.008	-0.034	0.826	↘	-0.015	-0.077	0.597	↘
		Spring	0.014	0.065	0.659	↗	-0.022	-0.117	0.415	↘
		Summer	0.021	0.138	0.332	↗	-0.013	-0.077	0.597	↘
		Fall	0.010	0.083	0.567	↗	-0.021	-0.071	0.628	↘
RE15	Surface	Winter	0.043	0.128	0.583	↗	0.084	0.282	0.200	↗
		Spring	0.112	0.359	**0.100**	↗	0.114	0.231	0.300	↗
		Summer	0.108	0.282	0.200	↗	0.043	0.099	0.661	↗
		Fall	0.008	0.011	1.000	↗	0.025	0.121	0.584	↗
	Bottom	Winter	0.020	0.092	0.712	↗	0.022	0.026	0.951	↗
		Spring	-0.010	-0.039	0.903	↘	-0.019	-0.077	0.760	↘
		Summer	0.094	0.256	0.246	↗	0.060	0.165	0.443	↗
		Fall	0.009	0.055	0.827	↗	0.012	0.011	1.000	↗
RE30	Surface	Winter	0.017	0.051	0.855	↗	0.035	0.103	0.669	↗
		Spring	0.082	0.282	0.200	↗	0.100	0.359	**0.100**	↗
		Summer	0.065	0.205	0.360	↗	0.046	0.209	0.324	↗
		Fall	0.041	0.209	0.324	↗	0.034	0.143	0.511	↗
	Bottom	Winter	0.009	0.116	0.625	↗	0.001	0.000	1.000	↔
		Spring	0.048	0.179	0.428	↗	0.082	0.282	0.200	↗
		Summer	0.066	0.462	**0.033**	↗	0.058	0.319	0.125	↗
		Fall	0.067	0.275	0.189	↗	0.073	0.275	0.189	↗
RE35	Surface	Winter	0.040	0.179	0.428	↗	0.077	0.128	0.583	↗
		Spring	0.029	0.077	0.760	↗	0.062	0.154	0.502	↗
		Summer	0.098	0.256	0.246	↗	0.003	0.011	1.000	↗
		Fall	0.004	0.033	0.913	↗	-0.016	-0.033	0.913	↘
	Bottom	Winter	0.064	0.256	0.246	↗	0.060	0.205	0.360	↗
		Spring	0.069	0.103	0.669	↗	0.101	0.154	0.502	↗
		Summer	0.020	0.026	0.951	↗	0.054	0.121	0.584	↗
		Fall	-0.020	-0.099	0.661	↘	-0.006	-0.055	0.827	↘

4.3.12 Chlorophyll-*a*

Chlorophyll-*a*, the primary photosynthetic pigment in plants, and provides an overall estimate of the amount of algae present in the reservoir. Chlorophyll-*a* is a response variable that can be used to assess and prevent eutrophic conditions. Nutrients nitrogen and phosphorus are the main cause of eutrophication, and algal blooms appear in response to nutrient enrichment. VDEQ criteria for chlorophyll-*a* states that the 90th percentile of the data collected between April 1 and October 31 at surface waters (at a depth less or equal to 1 meter) in the lacustrine zone of the Occoquan Reservoir should not exceed 35 µg/l for each of the two most recent monitoring years.

Figure 4-92 presents the seasonal average chlorophyll-*a* concentrations from 1973 to 2019. Seasonal averages at RE02 range from 0.05 to 58.52 µg/l, the highest values observed in winter 1986. Other high values were 33.73 µg/l in summer 1975, 33.04 µg/l in fall 1976, and more recently 30.89 µg/l in summer 2003. Since then, chlorophyll-*a* seasonal averages at RE02 have been lower than 30 µg/l. At RE15, seasonal averages range from 0.05 µg/l up to 32.75 µg/, the highest average observed during fall 1977, followed by 31.75 µg/l in fall 2016, and 31.75 µg/l in fall 1978. At inflow station RE30, highest values were observed before the MHR WRF's start up, reaching up to 64 µg/l in summer 1975. In the last twenty years, the highest seasonal average observed was 30.87 µg/l during winter 2001. Other than that, values have remained less than 30 µg/l. Seasonal averages at RE35 have ranged from 6.36 µg/l to 36.33 µg/l. Overall, chlorophyll-*a* tends to be lowest in winter at all stations. Higher concentrations tend to be observed at RE15 and RE35, even though these stations did not present peaks as high as RE02 and RE30 during the period of record. The higher chlorophyll-*a* averages at RE35 may be the result of agricultural runoff from this less urbanized watershed arm. Figure 4-93 shows the seasonal average of chlorophyll-*a* for the entire period of record. It can be observed that seasonally, RE02 presents higher values during spring and summer, RE15 during summer and fall, and the inflow reservoir stations during summer. It should be noted that from 1973 to 2011 copper sulfate was added during summer by Fairfax Water to manage algal production.

Figure 4-94 presents chlorophyll-*a* time series from 2003 to 2019. It can be observed in this figure that the high seasonal average that occurred during summer 2003 at RE02 (Figure 4-92) was the result of the chlorophyll-*a* peak concentration of 79 µg/l recorded during the month of June. After 2003, concentrations have generally been lower. Since then, 2018 was the only year where several values were higher than 35 µg/l, reaching 49.20 µg/l, 50.60 µg/l, and 37.80 µg/l during April, June, and August, respectively. This higher chlorophyll-*a* concentrations during 2018 were also seen at RE15. Concentrations at the Occoquan Creek are generally higher than at Bull Run. It should be noted that in spite of peaks observed at the other stations, RE02 values have remained lower than the rest of the stations. With the exception of 2003 and 2018, the 90th percentile of the data from April to October at RE02 have been lower than the VDEQ limit. This may be the result of the reservoir trapping efficiency of nutrients coming from the inflow. Additionally, hypolimnetic oxygenation might help maintain chlorophyll-*a* levels by keeping oxidized conditions and helping prevent the release of nutrients which can increase algae growth.

Mann-Kendall test results for chlorophyll-*a* show different trends depending on the season and station (Table 4-34). However, the only significant trends occurred at RE15, with a positive trend in winter and a negative in fall, and at RE30 with a negative trend during summer.

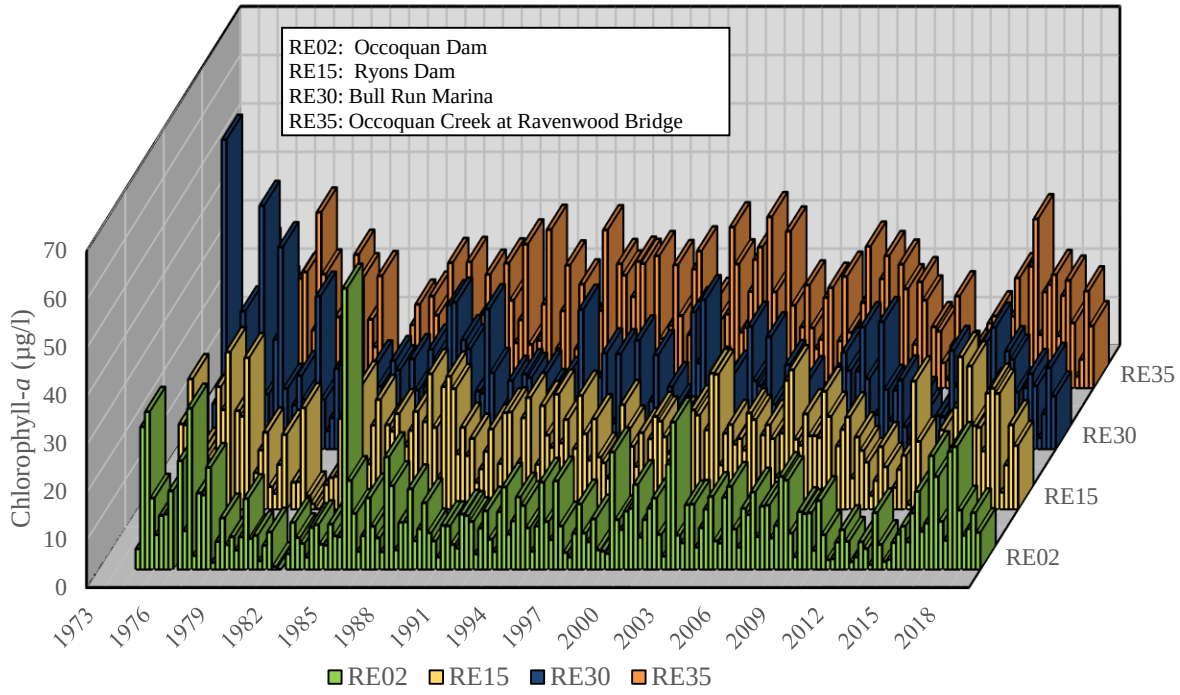

Figure 4-92. Seasonal Average Chlorophyll-*a* in Reservoir Surface Waters, 1973–2019

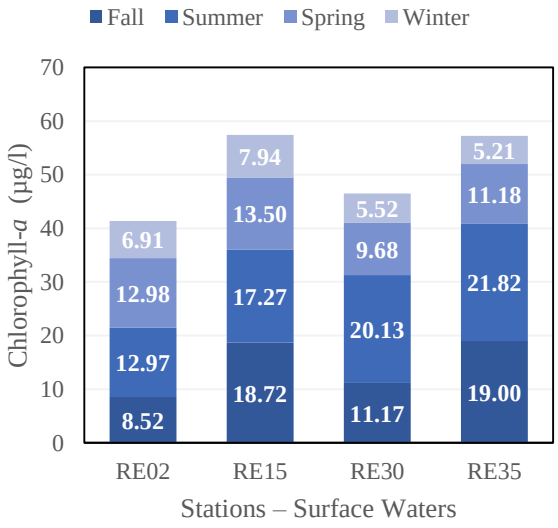

Figure 4-93. Overall Chlorophyll-*a* Average by Season at Occoquan Reservoir, 1975–2019

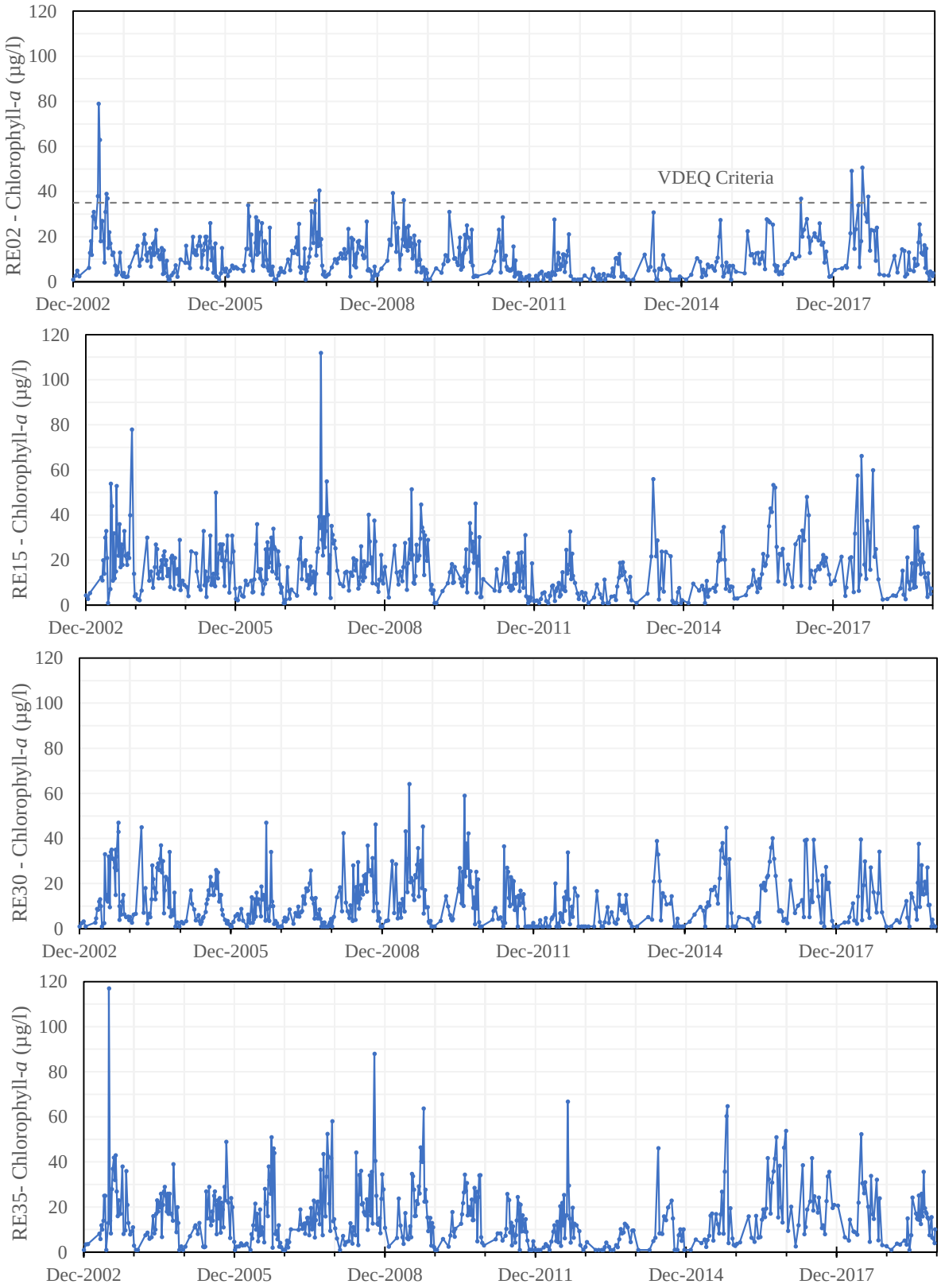

Figure 4-94. Chlorophyll-*a* Time Series at Reservoir Stations, 2003–2019

Table 4-34. Mann-Kendall Reservoir Chlorophyll-*a*, Sodium and Chloride Trends*, 1975–2019

Station	Description	Season	Chlorophyll-*a*				Sodium				Chloride			
			Sen Slope	*Kendall Tau*	*p-value*	*Trend*	*Sen Slope*	*Kendall Tau*	*p-value*	*Trend*	*Sen Slope*	*Kendall Tau*	*p-value*	*Trend*
RE02	Surface	Winter	-0.005	-0.013	0.907	↘	0.274	0.150	0.405	↗	0.635	0.176	0.343	↗
		Spring	0.048	0.057	0.591	↗	0.400	0.294	**0.096**	↗	0.672	0.275	0.120	↗
		Summer	0.100	0.154	0.140	↗	0.046	0.046	0.820	↗	0.099	0.033	0.880	↗
		Fall	-0.024	-0.046	0.667	↘	0.376	0.150	0.405	↗	0.401	0.111	0.544	↗
	Bottom	Winter					0.367	0.176	0.325	↗	1.000	0.221	0.232	↗
		Spring					0.729	0.281	0.112	↗	1.396	0.294	**0.096**	↗
		Summer					-0.006	-0.007	1.000	↘	0.137	0.085	0.649	↗
		Fall					0.554	0.333	**0.058**	↗	0.774	0.255	0.150	↗
RE15	Surface	Winter	0.104	0.241	**0.020**	↗	0.316	0.150	0.405	↗	0.629	0.162	0.387	↗
		Spring	0.085	0.081	0.440	↗	0.540	0.412	**0.019**	↗	0.786	0.307	**0.081**	↗
		Summer	0.091	0.145	0.162	↗	-0.108	-0.046	0.820	↘	0.011	0.007	1.000	↗
		Fall	-0.180	-0.246	**0.018**	↘	0.614	0.255	0.150	↗	0.766	0.203	0.256	↗
	Bottom	Winter					-0.067	-0.033	0.880	↘	0.036	0.015	0.967	↗
		Spring					0.815	0.359	**0.041**	↗	1.231	0.333	**0.058**	↗
		Summer					0.080	0.072	0.705	↗	0.058	0.046	0.820	↗
		Fall					0.494	0.242	0.173	↗	0.748	0.255	0.150	↗
RE30	Surface	Winter	0.010	0.023	0.830	↗	0.540	0.206	0.266	↗	0.500	0.132	0.484	↗
		Spring	-0.002	0.000	1.000	↔	0.951	0.464	**0.008**	↗	1.656	0.425	**0.015**	↗
		Summer	-0.186	-0.222	**0.032**	↘	0.086	0.059	0.762	↗	0.328	0.059	0.762	↗
		Fall	-0.107	-0.142	0.171	↘	0.582	0.216	0.225	↗	0.707	0.242	0.173	↗
	Bottom	Winter					0.364	0.147	0.434	↗	0.236	0.044	0.837	↗
		Spring					0.946	0.412	**0.019**	↗	1.452	0.373	**0.034**	↗
		Summer					-0.031	-0.033	0.880	↘	0.222	0.072	0.705	↗
		Fall					0.568	0.176	0.325	↗	0.600	0.255	0.150	↗
RE35	Surface	Winter	0.042	0.155	0.137	↗	0.265	0.176	0.343	↗	0.271	0.059	0.773	↗
		Spring	0.002	0.002	0.992	↗	0.325	0.477	**0.006**	↗	0.483	0.425	**0.015**	↗
		Summer	-0.073	-0.109	0.295	↘	0.099	0.111	0.544	↗	0.099	0.059	0.762	↗
		Fall	-0.041	-0.041	0.696	↘	0.425	0.373	**0.034**	↗	0.501	0.373	**0.034**	↗
	Bottom	Winter					0.257	0.147	0.434	↗	0.371	0.103	0.592	↗
		Spring					0.358	0.373	**0.034**	↗	0.452	0.255	0.150	↗
		Summer					0.046	0.046	0.820	↗	0.038	0.033	0.880	↗
		Fall					0.278	0.307	**0.081**	↗	0.514	0.281	0.112	↗

*Sodium and chloride Trends correspond to the period from 2002 to 2019

4.3.13 Sodium and chloride

Excessive salt can corrode pipes, cause poor tasting water, and affect aquatic life. Natural salt levels can increase by the influence of road salt, sewage effluents, fertilizers, water softeners, and water treatment chemicals. Salt is generally present as sodium chloride. USEPA drinking water advisory guideline indicates a sodium threshold of 20 mg/l for people that required to be on a low sodium diet, and between 30 mg/l to 60 mg/l as the taste threshold (USEPA, 2018). The VDEQ human health criterion to maintain adequate taste and aesthetic qualities for chloride is 250 mg/l applies at the drinking water intake. This limit is the same as the secondary maximum contaminant level (SMCL) indicated by the USEPA in the Secondary Drinking Water standards. VDEQ indicates a threshold of 230 mg/l of chloride for freshwater aquatic life (for chronic toxicity – four-day average concentration).

Sodium and chloride have been measured at the Occoquan Reservoir since 2002. Figures 4-95 and 4-96 show the time series for these two ions. There is little difference between surface and bottom waters. Sodium surface/bottom averages from 2002 to 2019 are 20.46/20.73 mg/l at RE02, 22.46/23.13 mg/l at RE15, 37.68/38.72 mg/l at RE30, and 13.30/13.53 mg/l at RE35. Chloride surface/bottom averages are 30.73/32.76 mg/l at RE02, 33.45/34.55 mg/l at RE15, 54.33/55.83

mg/l at RE30, and 20.86/21.05 mg/l at RE35. Higher averages were observed at RE30. Peak concentrations at all stations were observed during the months of January to April (most during March) and are likely influenced by road salt application during winter months. At RE02, the highest sodium peaks observed were 68.3 mg/l and 66.9 mg/l in February 2011 and April 2015, while the highest chloride values were 150 mg/l in April 2009 and 155mg/l on March 2015.

Mann-Kendall trends where calculated for sodium and chloride from 2002 to 2019 (Table 4-34). Trends for sodium are generally increasing, with few exceptions, though not all values are statistically significant. Chloride trends are all increasing but not all significant. Significant values occurred generally in spring and one during fall.

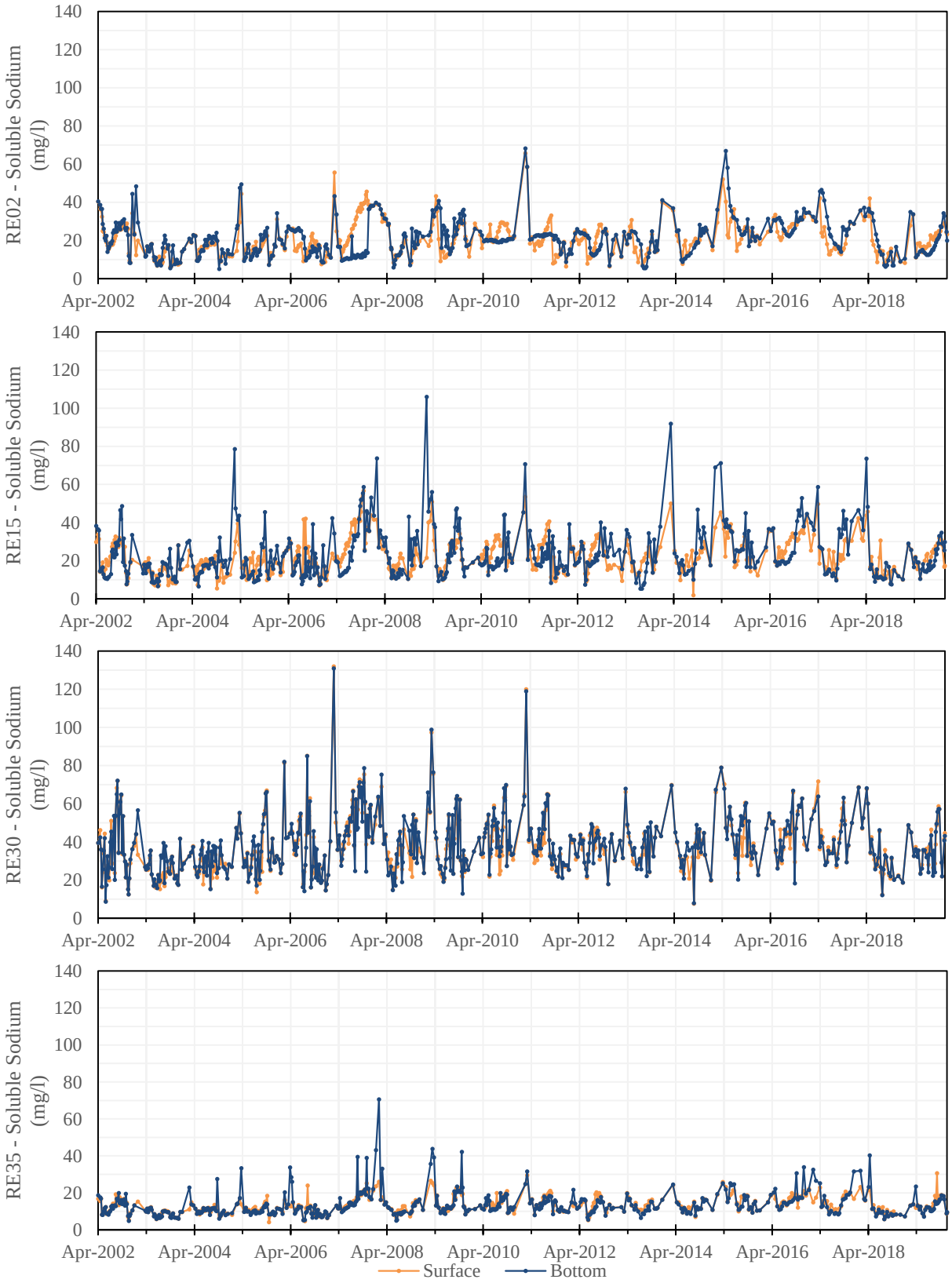

Figure 4-95. Sodium Time Series at Reservoir Stations, 2002–2019

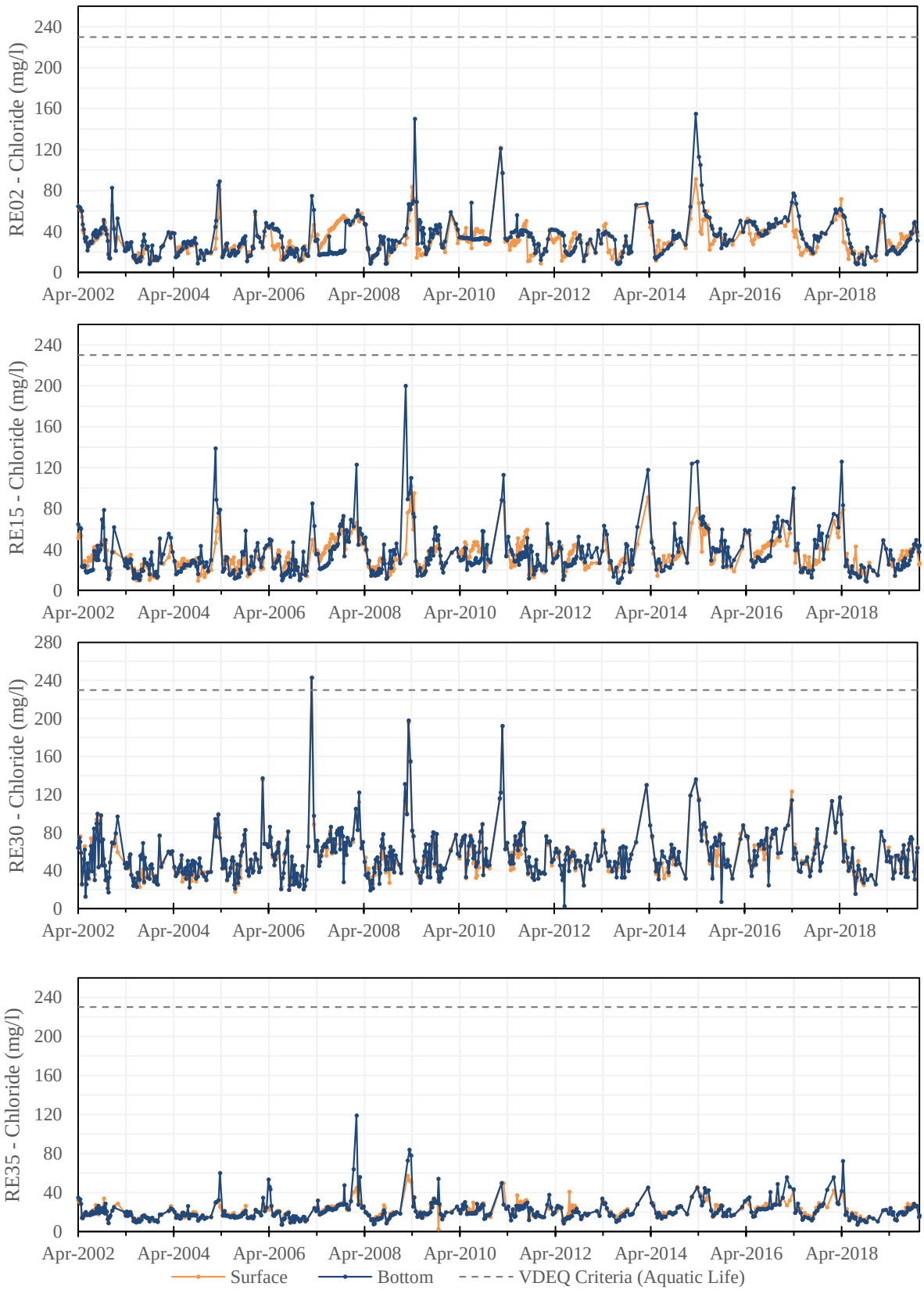

Figure 4-96. Chloride Time Series at Reservoir Stations, 2002–2019

4.3.14 Iron and Manganese

High levels of iron and manganese are undesirable in drinking water treatment because they can cause aesthetic effects, such as unpleasant tastes and odors, as well as technical effects, such as corrosion and staining. USEPA Secondary Drinking Water Standards recommend a SMCL of iron of 0.3 mg/l (300 µg/l) to prevent rusty color, reddish/orange staining, and metallic taste. This value is also indicated by the VDEQ criteria for surface water used as a public water supply and refers to the value at the drinking water intake. USEPA indicates a manganese SMCL of 0.05 mg/l (50 µg/l) to prevent black/brown color, black staining, and bitter metallic taste. In lakes and reservoirs, release of iron and manganese from sediments indicate anaerobic conditions, and it is undesirable because phosphorus that is bound to iron can get released to the water column as well. High amounts of phosphorus concentrations can lead to nutrient enrichment and eutrophication problems.

Iron and manganese have been measured in the Occoquan Reservoir since 2006 on a quarterly basis. Figure 4-97 presents the time series of soluble iron and Figure 4-98 shows the time series for soluble manganese for the period of record. Overall, values tend to be higher at the bottom (5 to 7110 µg/l iron; 5 to 8390 µg/l manganese) than at the surface (5 to 645 µg/l iron and 5 to 313 µg/l manganese). Higher concentrations are seen at RE02 and RE15, mainly during summer (particularly August) probably as a result from sediment release due to oxygen depletion during thermal stratification. When higher soluble iron values were observed at RE02 (1220 to 6240 µg/l), OP concentrations ranged between 0.02 and 0.3 mg/l. Since 2012, both soluble iron and manganese concentrations at RE02 have been lower than previous years probably due to the effect of the hypolimnetic oxygenation system. There are no noticeable iron and manganese peaks at RE30 possibly because of the nitrate addition from the MHR WRF's discharge at this arm. In general peaks, at RE35 are somewhat lower than at RE15 and tend to occur during summer.

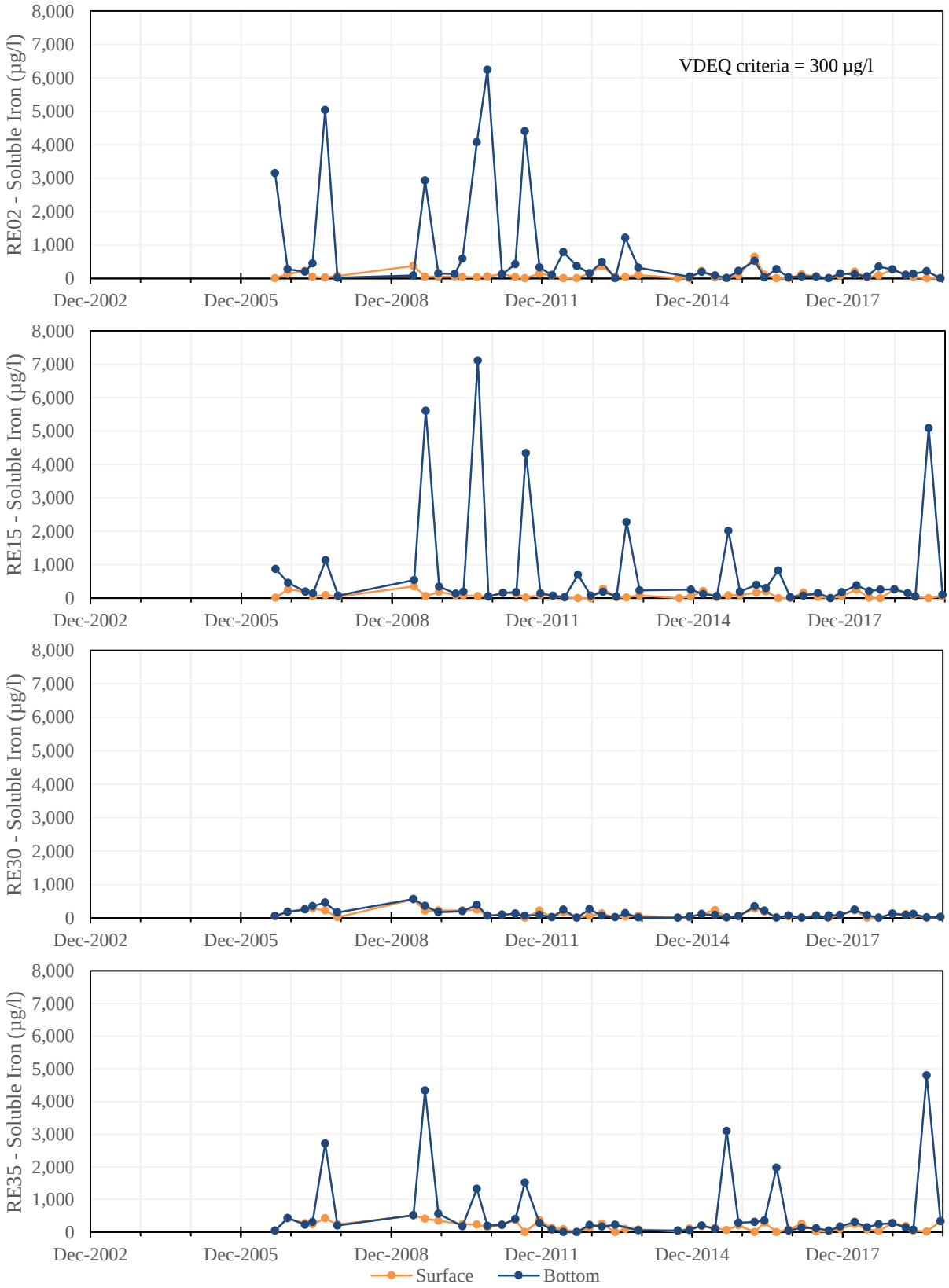

Figure 4-97. Soluble Iron Time Series at Reservoir Stations, 2003–2019

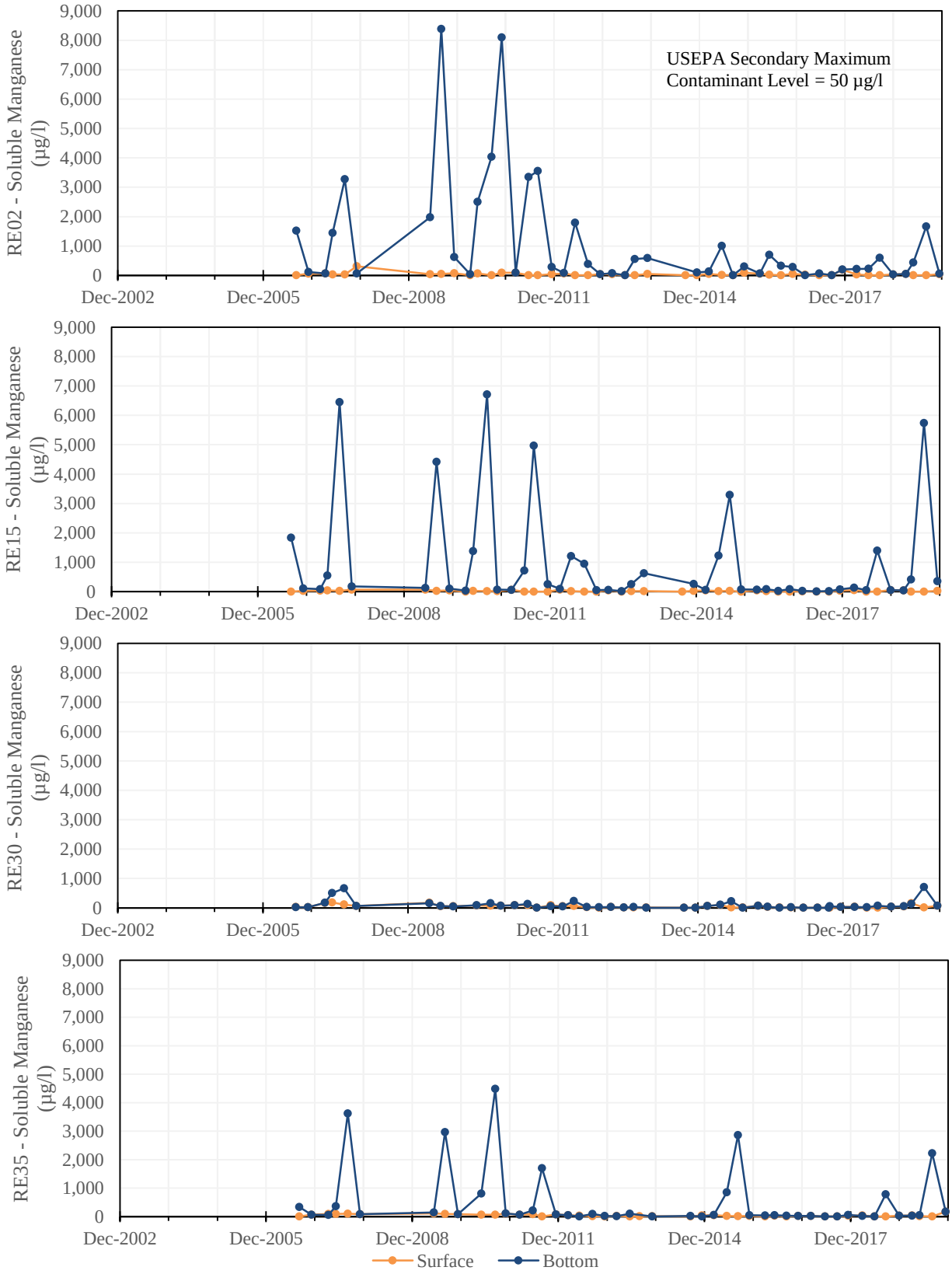

Figure 4-98. Soluble Manganese Time Series at Reservoir Stations, 2003–2019

4.3.15 Principal Component Analysis

PCA was performed on NH3-N, TKN, Ox-N, TN, OP, TP, sodium, and chloride (dependent variables) to identify dominant patterns in time and space. Then, the independent variables (i.e. temperature, DO, pH, total alkalinity, TSS, ORP, DOC, TOC, and rain) were projected into PC space to illustrate the relationships between these parameters and the dominant patterns plotted. Data used for this analysis corresponds to the period from 2002 to 2019. PCA was performed for surface water as well as for bottom water.

A resampling-based stopping rule was applied to both surface and bottom data to determine which PC modes should be evaluated (i.e., which data patterns are statistically significant). Results from this stopping rule are shown in Figures 4-99 and 4-100. Values on the x-axis indicate the PC mode number and the y-axis refers to the respective latent scores (eigenvalues) of the original data. The total variance within the data is explained by the sum of all these PC modes. PC modes with higher eigenvalue contribute more to the variance in the data. The blue, black, and red lines represent the 50%, 90%, and 95% confidence bounds thresholds calculated, respectively. It can be observed from the figures that for both depths, two patterns (PC1 and PC2) were significant at a 95% confidence bound (that is, eigenvalue of modes 1 and 2 are above the 95% confidence line).

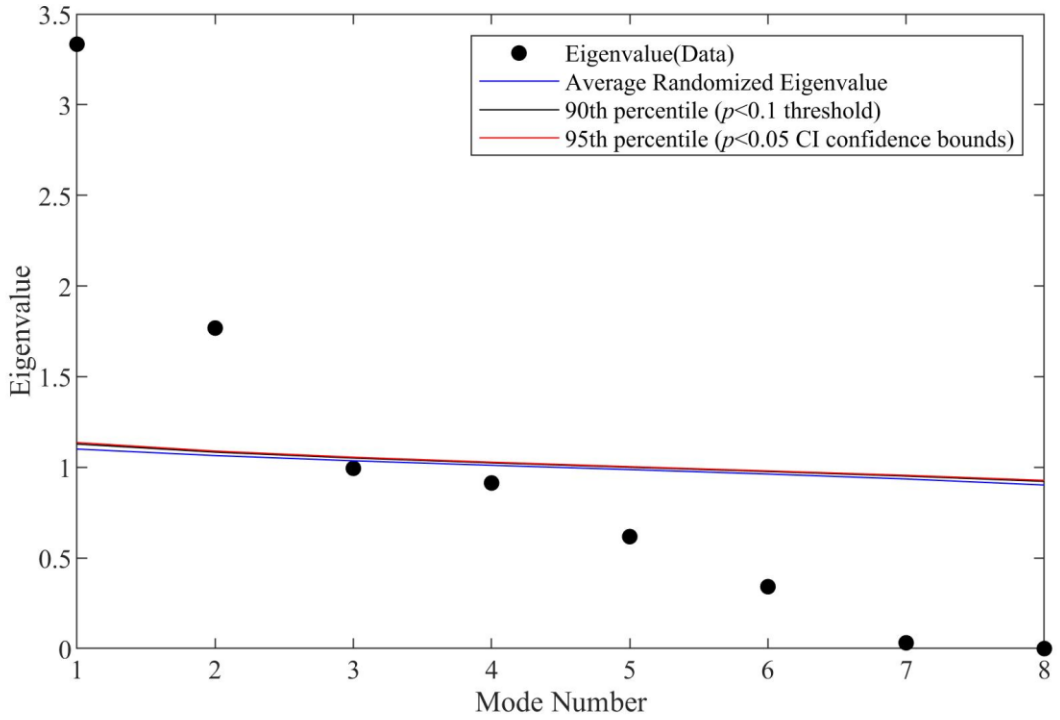

Figure 4-99. Advanced Stopping Rule for Surface Water PCA Data

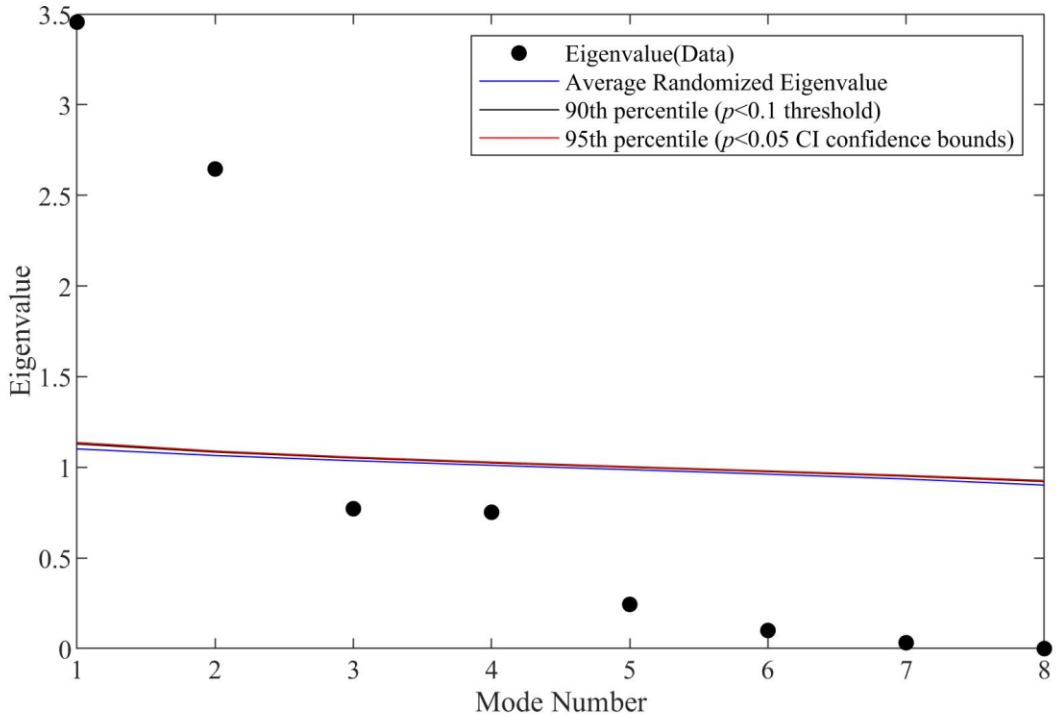

Figure 4-100. Advanced Stopping Rule for Bottom Water PCA Data

Figures 4-101 and 4-102 show the PCA biplots for surface data by station and by season. These biplots will be discussed in three (3) parts: significant PC modes observed for dependent variables, possible drivers for the patterns observed, and relation between observations and variables. The two significant modes previously identified are illustrated in the biplots, with PC1 (x-axis) explaining 41% of the data variability, and PC2 (y-axis) explaining 22%. Total variance explained by these two significant modes for surface water was 63%. Vectors that are labeled in black correspond to the dependent variables on which the PCA was performed, while the blue vectors refer to the independent variables that were projected. In addition, a non-parametric bootstrap method was employed to calculate confidence bounds and confirm which variables contributed significantly to the patterns represented by each PC mode. The primary pattern for surface water data (PC1) shows that samples with high Ox-N, TN, TKN, sodium, and chloride concentrations (all these plot on the positive side of the PC1 scale) had lower concentrations of OP and TP (these plot on the negative side of the PC1 scale). NH3-N (just barely on the negative side of the PC1 scale) did not contribute significantly to PC1, Ox-N and TN contribute to PC1 at $p<0.10$, and the rest of the variables contributed at $p<0.05$. PC2 grouped all the nutrient forms and chloride was separated. Sodium did not contribute significantly to PC2. Ox-N, TKN, and TN contributed at $p<0.10$, and the rest of the variables contributed at $p<0.05$. Since TN is mostly comprised of Ox-N, they tend to load on the same direction and with similar magnitudes. This is also observed for OP and TP, as well as DOC and TOC. Vectors leaning along the x-axis mainly contribute to PC1, while vectors leaning along the y-axis mainly contribute to PC2.

To determine which independent variables are possible drivers of the dominant patterns seen in the dependent variables the biplot is analyzed by quadrant. Independent variables (blue labeled vectors) and dependent variables (black labeled vectors) are positively related to one another if they are loading in the same direction (quadrant). Independent and dependent variables are negatively (inversely) related to one another if the vectors are loading in the opposite quadrants. It can be observed in Figures 4-101 and 4-102 that higher total alkalinity, DO, pH, and temperature were related with higher sodium and chloride. Conversely, lower sodium and chloride concentrations were observed at high organic carbon content and high rainfall. OP, TP, and NH3-N were positively related to organic carbon and to a lesser degree to rain (rain vector is shorter than organic carbon vectors), which may indicate that some phosphorus and NH3-N presence in surface water is due to runoff from the watershed. Additionally, TKN, TN, and Ox-N were positively related to TSS, while phosphorus was inversely related with temperature, DO, pH, and total alkalinity. Confidence intervals were also determined for the independent variables to which of the variables should be considered significant predictors of the independent variables. All variables, with the exception of ORP (which was not significant), were considered significant predictors of the patterns observed patterns in surface waters at $p<0.05$.

Lastly, PC scores (observations) for surface waters are analyzed by station (Figure 4-101) and by season (Figure 4-102). As with the independent variables, data are analyzed by quadrant. Scores, whether by station or season, and vectors plotted in the same quadrant are positively related. Figure 4-101, which presents the information by station, shows that more phosphorus and organic matter were seen at RE35 (more agricultural) than RE30, whereas more TKN, Ox-N, and TN was observed at RE30 than RE35. This is probably due to the nitrified discharges of the MHR WRF into Bull Run. Even though most of the effluent flows into the hypolimnion, about 15–20% mixes with the epilimnion (Cubas et al., 2019), which may explain why some nitrate is present at the surface, though at considerably lower concentrations than bottom waters as seen in Ox-N graphs in previous sections. More sodium and chloride is seen at RE30 than RE35, probably due to wastewater discharge and runoff from a more urbanized watershed. Lower concentrations tend to be seen at RE02. Seasonally, more TKN, Ox-N, and TN is observed during summer and/or fall (Figure 4-102).

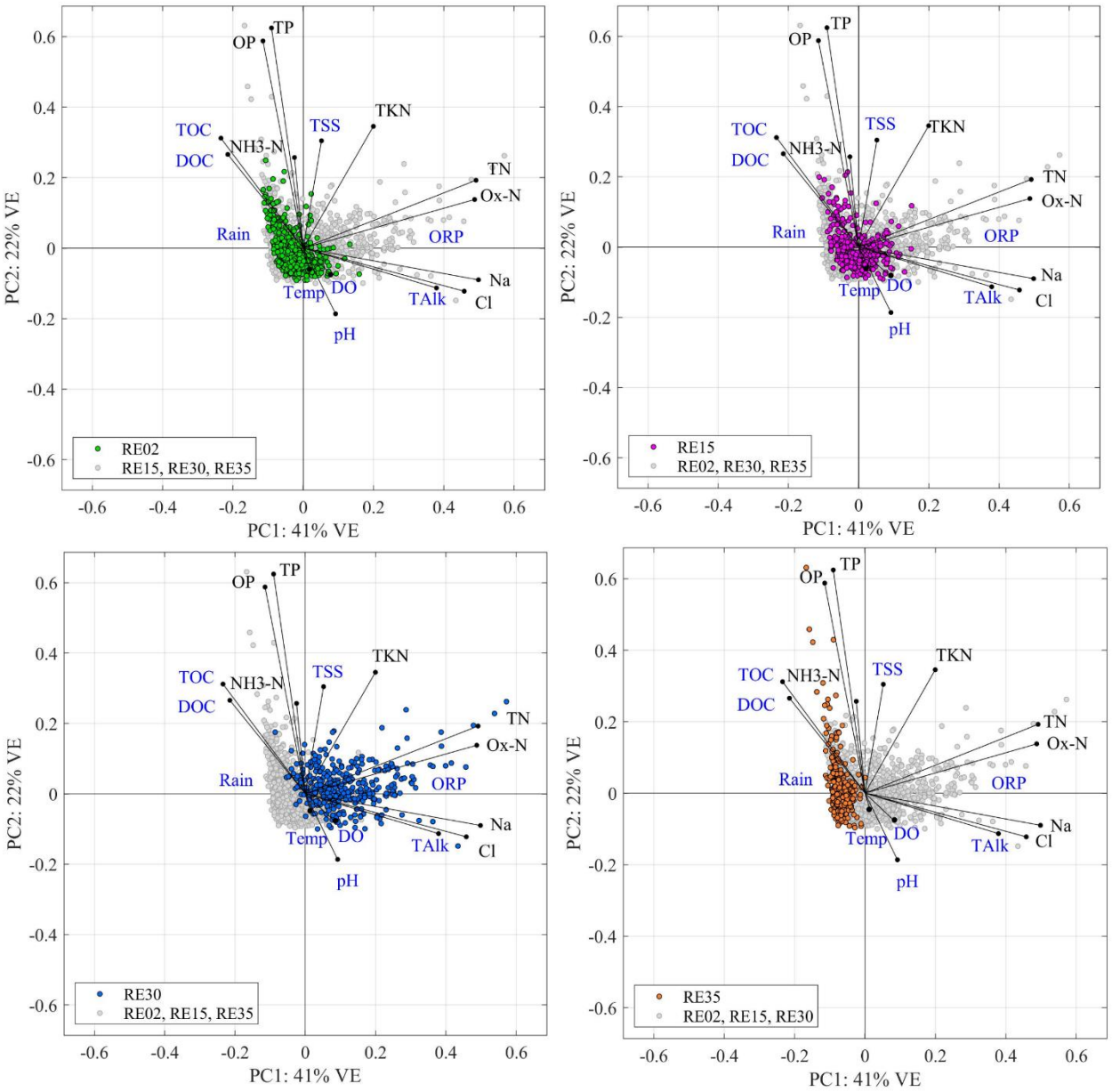

*NH3-N = ammonia nitrogen; TKN = total Kjeldahl nitrogen; Ox-N = oxidized nitrogen; TN = total nitrogen; OP = orthophosphate phosphorus; TP = total phosphorus; Na = sodium; Cl = chloride; DO = dissolved oxygen; ORP = oxidation-reduction potential; Temp = temperature; Talk = total alkalinity; TSS = total suspended solids; DOC = dissolved organic carbon; TOC = total organic carbon;

Figure 4-101. PCA for Surface Water by Station, 2002–2019

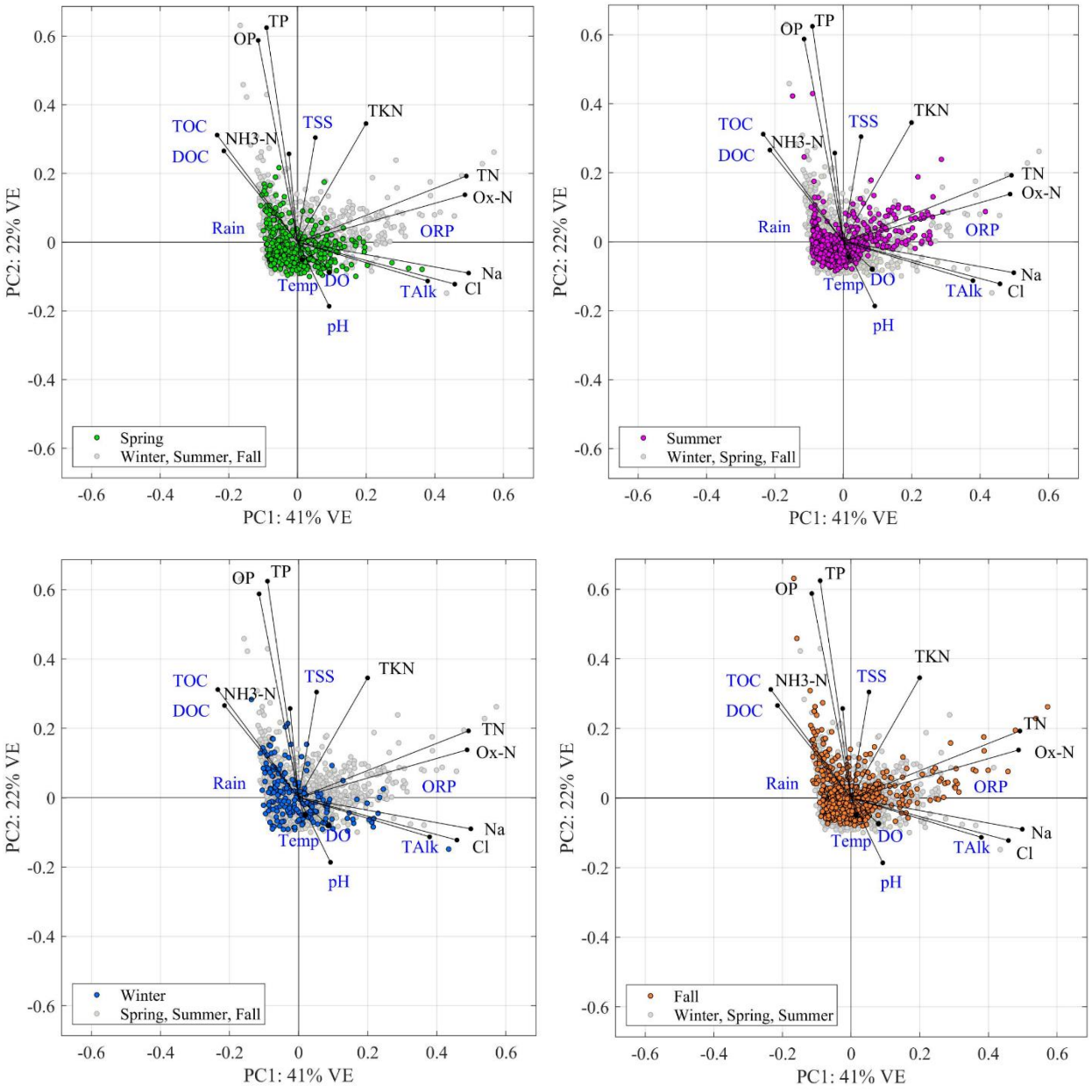

*NH3-N = ammonia nitrogen; TKN = total Kjeldahl nitrogen; Ox-N = oxidized nitrogen; TN = total nitrogen; OP = orthophosphate phosphorus; TP = total phosphorus; Na = sodium; Cl = chloride; DO = dissolved oxygen; ORP = oxidation-reduction potential; Temp = temperature; Talk = total alkalinity; TSS = total suspended solids; DOC = dissolved organic carbon; TOC = total organic carbon;

Figure 4-102. PCA for Surface Water by Season, 2002–2019

Like it was done for surface water data, PCA biplots for bottom water data are presented in Figures 4-103 and 4-104. The two modes that present statistically significant patterns (i.e., 95% confidence interval) are PC1 (x-axis) and PC2 (y-axis), explaining 43% and 33% of the variability, respectively. Total variance explained by PC1 and PC2 at bottom waters was 76%. All dependent variables were statistically significant for PC1 at $p<0.05$. PC1 grouped Ox-N, TN, sodium, and chloride together (positive) and NH3-N, TKN, OP and TP together (negative). This indicates that when high concentrations of one group were present, lower concentrations of the other group were observed. As mentioned for the surface data, Ox-N and TN load in the same direction and at similar magnitudes because Ox-N makes up a significant part of TN. This is especially true in bottom waters when the MHR WRF discharges nitrified effluent into the reservoir (RE30) during summer. The lower concentrations of OP when higher concentrations of Ox-N are present probably occurs because when DO levels are low, microorganisms use nitrate as a terminal electron acceptor, preventing the reduction of other elements, such as iron, which can release OP into the water column. The lower concentrations of NH3-N when higher Ox-N concentrations are seen are probably due to nitrate maintaining oxidized conditions that prevent ammonia release from sediments. Since sodium chloride (NaCl) is a common deicer and commonly used for industrial purposes, these ions are positively related with one another.

PC2 grouped all the dependent variables together and the independent variables DO and ORP are located in the opposite quadrant. Ox-N, sodium and chloride are not significant for PC2, TN is significant at $p<0.10$, and all other dependent variables are significant at $p<0.05$.

Analyzing the relation between dependent and independent variables by quadrants, it can be observed that DO and ORP are inversely related with OP and TP. This might be because low DO conditions can lead to low ORP and release of OP from sediments. DO and ORP are also inversely related with NH3-N and TKN, likely because low DO conditions inhibit nitrification (an aerobic process) and promote release of ammonia from sediments increasing NH3-N buildup. Higher DOC and TOC are positively associated with higher NH3-N, TKN, OP, and TP. Because organic carbon is an indicator of organic matter, higher values may indicate higher organic content from which OP and NH3-N (via ammonification) can be derived. Otherwise, higher positive association of organic carbon and phosphorus might mean both constituents are being released from sediments. NH3-N, TKN, OP, and TP vectors are also loading in the same direction as temperature and TSS, though in smaller magnitudes. In other words, higher temperature results in lower DO solubility, as well as low DO levels due to the occurrence of thermal stratification in summer. Na, Cl, Ox-N, and TN were positively associated with pH and alkalinity. It should be noted that independent variables were all significant at $p<0.05$.

Analyzing the PC scores by station (Figure 4-103) it can be observed that, as with surface data, samples at RE30 have higher concentrations of Ox-N, TN, sodium, and chloride than samples at RE35. However, Figure 4-103 shows these concentrations have reduced when flow reaches RE02. Ox-N reduction is likely due to denitrification occurring during anaerobic conditions. More DOC, TOC, OP, TP and NH3-N are observed at RE02 and RE15 than at the inflow stations.

Seasonally, higher concentrations of nutrients, ions, organic carbon, TSS and rainfall are all seen during summer and fall possibly due to all the processes occurring during thermal stratification

during these periods. Conversely, less phosphorus, NH3-N, and organic carbon is observed during spring and winter (Figure 4-104).

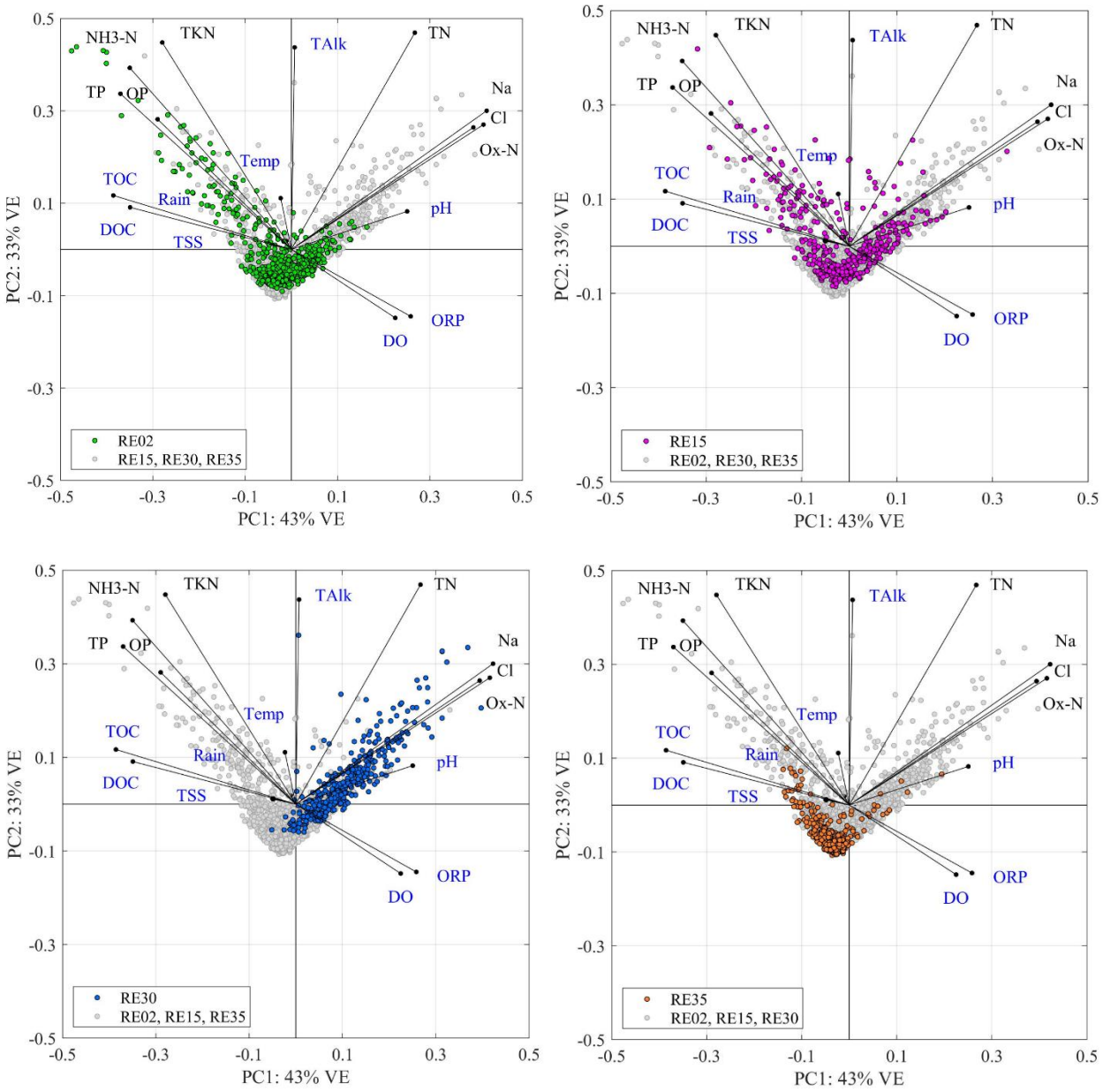

*NH3-N = ammonia nitrogen; TKN = total Kjeldahl nitrogen; Ox-N = oxidized nitrogen; TN = total nitrogen; OP = orthophosphate phosphorus; TP = total phosphorus; Na = sodium; Cl = chloride; DO = dissolved oxygen; ORP = oxidation-reduction potential; Temp = temperature; Talk = total alkalinity; TSS = total suspended solids; DOC = dissolved organic carbon; TOC = total organic carbon;

Figure 4-103. PCA for Bottom Water by Station, 2002–2019

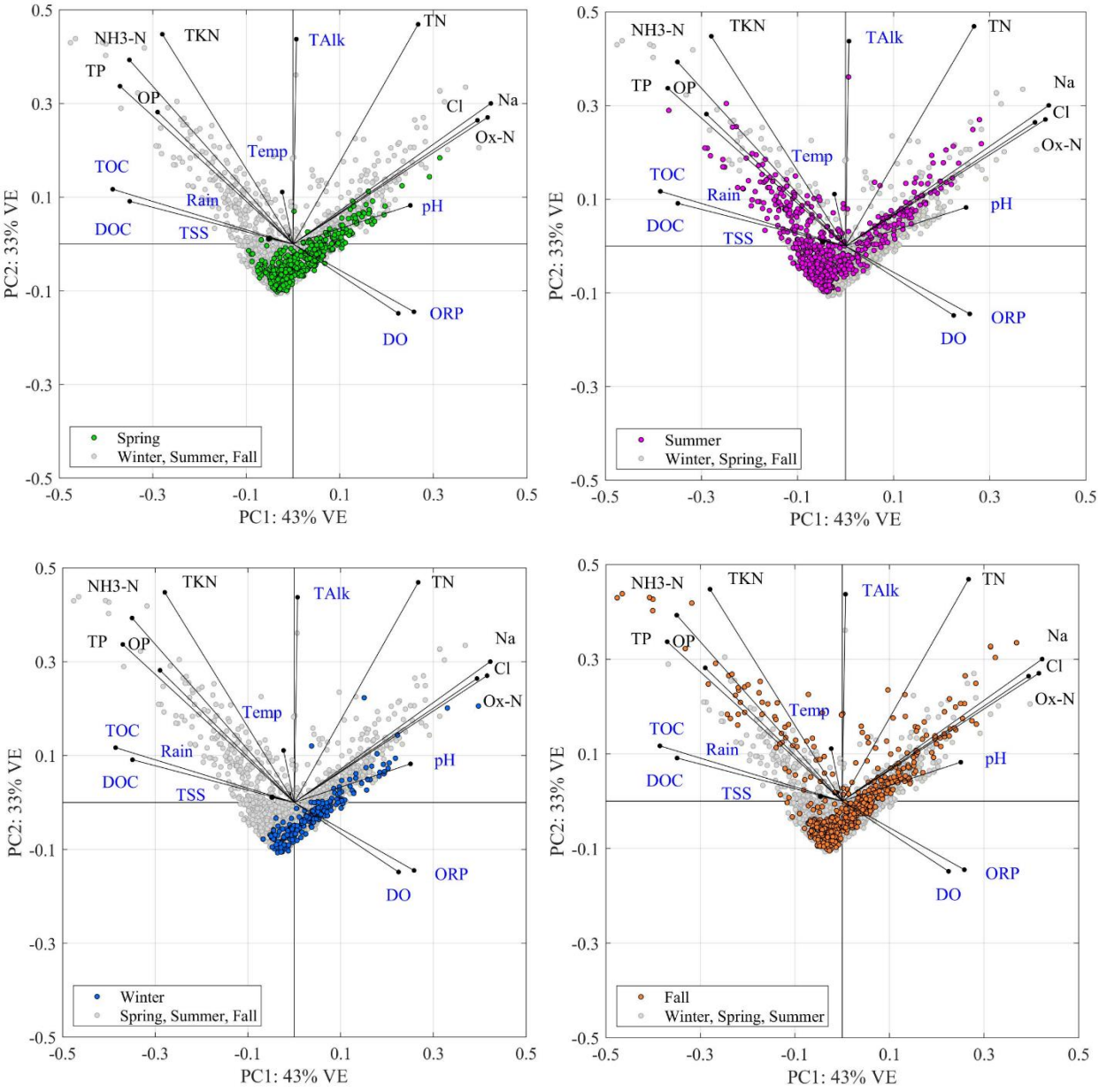

*NH3-N = ammonia nitrogen; TKN = total Kjeldahl nitrogen; Ox-N = oxidized nitrogen; TN = total nitrogen; OP = orthophosphate phosphorus; TP = total phosphorus; Na = sodium; Cl = chloride; DO = dissolved oxygen; ORP = oxidation-reduction potential; Temp = temperature; Talk = total alkalinity; TSS = total suspended solids; DOC = dissolved organic carbon; TOC = total organic carbon;

Figure 4-104. PCA for Bottom Water by Season, 2002–2019

4.4 Trophic State Assessment

4.4.1 Introduction

As stated in Chapter 3, the trophic state of the Occoquan Reservoir was assessed using Carlson's Index, the Vollenweider Model, and the Rast, Jones, and Lee Model. Trophic state assessments provide an indication of the biological productivity and nutrient levels of a particular waterbody. These empirical models do not provide a detailed description of all the processes that can influence eutrophication in waterbodies. However, they can be useful for determining or evaluating management practices.

4.4.2 Carlson's Trophic State Index

Figure 4-105 presents the seasonal average time series from 1973 to 2019 of Carlson's TSI for the Occoquan Reservoir. This graph was constructed by calculating the TSI of seasonal average values of Secchi depth, chlorophyll-*a*, and TP for each year at RE02, RE15, RE30, and RE35. Overall, it can be observed from the figure that values mostly range within the 50 and 70 eutrophic boundary. TSI values calculated with chlorophyll-*a* tend to be lower than TSI values calculated using the other two parameters. This difference is more pronounced during winter, but can also be seen in spring and fall. During summer, however, chlorophyll-*a* TSI tends to be closer to TSI values calculated with Secchi depth and TP, perhaps because it is the algae growing season during which growth is mainly limited by nutrient availability. Carlson (1977) suggested that when TSI calculated with different variables differed, priority should be given to chlorophyll-*a* and Secchi depth during summer, and TP during the other seasons. However, TSI values calculated with chlorophyll-*a* and Secchi depth should be interpreted with caution during the years when copper sulfate was applied to the Occoquan Reservoir between the months of May and September to control algae growth. For this reason, TSI values calculated with TP might best represent trophic state for the reservoir. In general, the phosphorus index has the advantage of being relatively stable year-round.

Table 4-35 presents seasonal average and median values for Carlson's TSI for the entire period of record. It can be observed from the table that Secchi depth and TP TSI values tend to be lower at RE02 and RE15 than the rest of the stations during all seasons except winter. Chlorophyll-*a* TSI values at RE02 tends to be lower than the inflow stations during summer and fall, and higher than the inflow stations during winter and spring. Within each station, chlorophyll-*a* TSI values tend to be lower during winter. Secchi depth and TP TSI, on the other hand, do not show a specific pattern. At RE02 and RE15, averages are generally higher during winter and lower during summer. At RE30, lower TSI values were seen during winter. At RE35, higher values were seen during summer.

Table 4-36 shows the Mann-Kendall test results for Carlson's TSI calculated for the reservoir. Since these indices are based on seasonal average concentrations of Secchi depth, chlorophyll-*a*, and TP, trends generally follow the same pattern as the variables themselves (section 4.3). Secchi depth TSI presents downward trends at all stations and seasons, generally at $p<0.1$. TP also presents downward trends at RE02, RE15, and RE30, several with high confidence values. TP TSI

trends at RE35 were not statistically significant. Chlorophyll-*a* TSI trends differ among stations and seasons. The only significant results were at RE15, which presented an upward trend during winter and a downward trend during fall, and at RE35, which presented an upward trend during winter and downward trends during summer and fall.

TSI has been used by VDEQ to assess nutrient impact on Virginia lakes and reservoirs. However, it should be noted that since 2010, VDEQ has replaced the use of TSI for the evaluation of nutrient impact in 187 lakes/reservoirs, including the Occoquan Reservoir, with the use of nutrient criteria (i.e., 35 µg/l limit for chlorophyll-*a* and 40 µg/l limit for TP if algaecide treatment is applied, measured at surface of the lacustrine zone) to protect aquatic life and recreational designated uses (VDEQ, 2019).

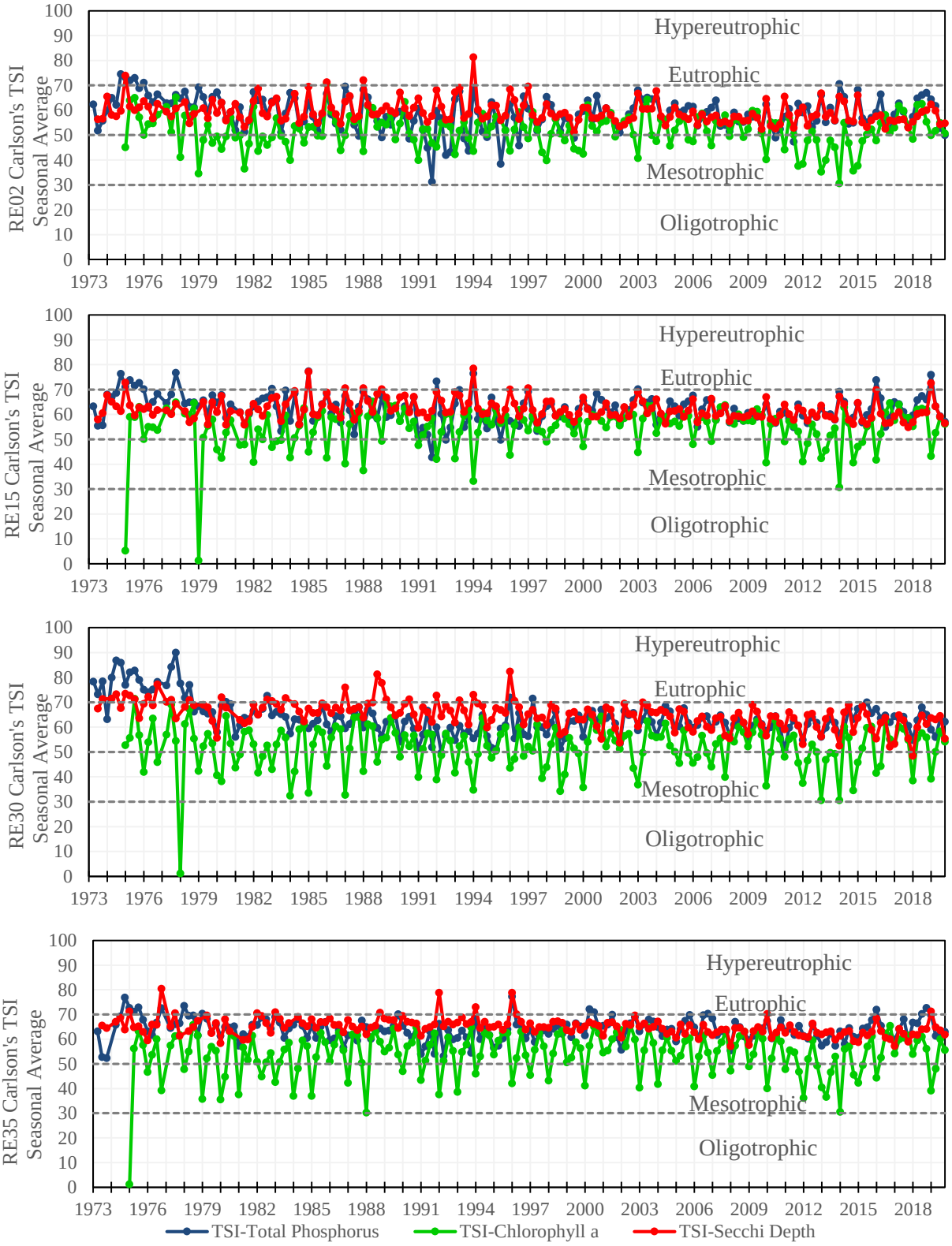

Figure 4-105. Seasonal Average Carlson's Trophic State Index for Occoquan Reservoir Surface Waters, 1973–2019

Table 4-35. Seasonal Average* and Median Carlson's Trophic State Index, 1973–2019

Station	Season	TSI SD		TSI CHL		TSI TP	
		Average	*Median*	*Average*	*Median*	*Average*	*Median*
RE02	Winter	61.55	62.11	49.57	46.39	62.96	60.56
	Spring	59.32	59.07	55.74	54.64	61.66	60.56
	Summer	56.12	56.56	55.74	54.12	56.17	53.20
	Fall	57.02	57.14	51.62	46.58	58.46	53.20
RE15	Winter	64.18	64.41	50.92	47.67	65.39	63.19
	Spring	62.26	62.54	56.13	54.56	62.45	60.56
	Summer	58.72	58.40	58.55	57.26	59.96	57.34
	Fall	60.75	61.29	59.34	58.39	63.06	60.56
RE30	Winter	59.45	61.29	47.36	40.70	61.10	57.34
	Spring	66.95	67.13	52.87	48.18	65.56	60.56
	Summer	66.54	66.54	60.05	58.39	67.84	65.41
	Fall	61.80	63.44	54.28	48.58	66.30	63.19
RE35	Winter	63.45	64.41	46.80	42.01	64.40	60.56
	Spring	64.77	64.41	54.28	52.37	63.81	60.56
	Summer	64.81	64.91	60.84	59.89	65.11	63.19
	Fall	64.20	64.41	59.48	57.30	64.74	63.19

*TSI of seasonal average of Secchi Depth (SD), chlorophyll-*a* (CHL), and total phosphorus (TP).

Table 4-36. Mann Kendall Carlson's Trophic State Index Trends, 1973–2019

Station	Season	TSI Secchi Depth				TSI Chlorophyll-a				TSI Total Phosphorus			
		Sen Slope	*Kendall Tau*	*p-value*	*Trend*	*Sen Slope*	*Kendall Tau*	*p-value*	*Trend*	*Sen Slope*	*Kendall Tau*	*p-value*	*Trend*
RE02	Winter	-0.173	-0.286	**0.005**	↘	-0.076	-0.108	0.300	↘	-0.155	-0.258	**0.012**	↘
	Spring	-0.130	-0.398	**1.0E-04**	↘	0.006	0.010	0.930	↗	-0.097	-0.212	**0.037**	↘
	Summer	-0.022	-0.096	0.345	↘	0.067	0.131	0.207	↗	-0.052	-0.051	0.620	↘
	Fall	-0.095	-0.394	**9.7E-05**	↘	-0.044	-0.062	0.557	↘	-0.135	-0.205	**0.044**	↘
RE15	Winter	-0.109	-0.204	**0.049**	↘	0.193	0.193	**0.063**	↗	-0.081	-0.124	0.232	↘
	Spring	-0.113	-0.346	**0.001**	↘	0.044	0.059	0.577	↗	-0.104	-0.212	**0.037**	↘
	Summer	-0.014	-0.076	0.458	↘	0.051	0.123	0.237	↗	-0.038	-0.080	0.436	↘
	Fall	-0.106	-0.389	**1.2E-04**	↘	-0.077	-0.224	**0.031**	↘	-0.146	-0.247	**0.015**	↘
RE30	Winter	-0.445	-0.508	**9.9E-07**	↘	0.070	0.066	**0.531**	↗	-0.156	-0.232	**0.024**	↘
	Spring	-0.146	-0.421	**3.8E-05**	↘	-0.011	-0.020	0.853	↘	-0.214	-0.339	**0.001**	↘
	Summer	-0.109	-0.456	**6.4E-06**	↘	-0.096	-0.222	**0.032**	↘	-0.081	-0.202	**0.047**	↘
	Fall	-0.263	-0.568	**1.9E-08**	↘	-0.087	-0.131	**0.207**	↘	-0.162	-0.276	**0.006**	↘
RE35	Winter	-0.182	-0.256	**1.4E-02**	↘	0.092	0.092	0.379	↗	-0.058	-0.095	0.368	↘
	Spring	-0.099	-0.358	**4.8E-04**	↘	-0.010	-0.026	0.807	↘	-0.062	-0.147	0.150	↘
	Summer	-0.072	-0.297	**0.003**	↘	-0.035	-0.109	0.295	↘	0.000	-0.001	1.000	↔
	Fall	-0.099	-0.369	**2.6E-04**	↘	-0.002	-0.004	0.977	↘	-0.043	-0.083	0.414	↘

4.4.3 Vollenweider Model

The Vollenweider Input-Output Phosphorus Loading Model was applied to the Occoquan Reservoir to determine its trophic state from 1974 to 2019. The assumptions the model follows were previously explained in Section 3.8. Two important limitations when applying this model to the Occoquan Reservoir is the assumption it behaves like a CSTR, since the reservoir more closely resembles a plug-flow reactor, and the assumption that there is no internal loading, since there is phosphorus release from sediments when reducing conditions are present. Figure 4-106 presents phosphorus loading per unit of surface area graphed against the areal hydraulic loading (calculated as mean depth divided by mean residence time) for each year of the period of record (blue circles). It can be observed from the graph that even though some years have lower phosphorus loading than others, all values are located within the hypereutrophic zone. Phosphorus loading values (per unit area) ranged from 5.2 to 39.4 $g/m^2/yr$, with the reservoir receiving approximately 18 $g/m^2/yr$ of phosphorus load in 2019. Hydraulic loading (flushing rate) values for the reservoir averaged 98 m/yr for the period of record.

Figure 4-107 further illustrates the reservoir hypereutrophic state by comparing the actual annual phosphorus load (tons per year) into the Occoquan Reservoir with the respective estimated upper eutrophic boundary load. Actual phosphorus load values are higher than the boundary loads during the entire period of record. Since both the actual and estimated boundary loads are affected by the same hydrometeorological conditions (i.e., rainfall-runoff),

Phosphorus loads were also normalized by dividing by the eutrophic and mesotrophic upper boundary values to provide a clearer picture of trends (Figure 4-108). It can be noticed from this figure that the resulting ratio of the actual phosphorus load to both trophic boundaries presents a negative trend line, which indicates a positive impact of nutrient management strategies on reservoir water quality. These trends were confirmed with the Mann-Kendall test result indicating a downward trend for both ratios at a 95% confidence interval (p-value = 0.031).

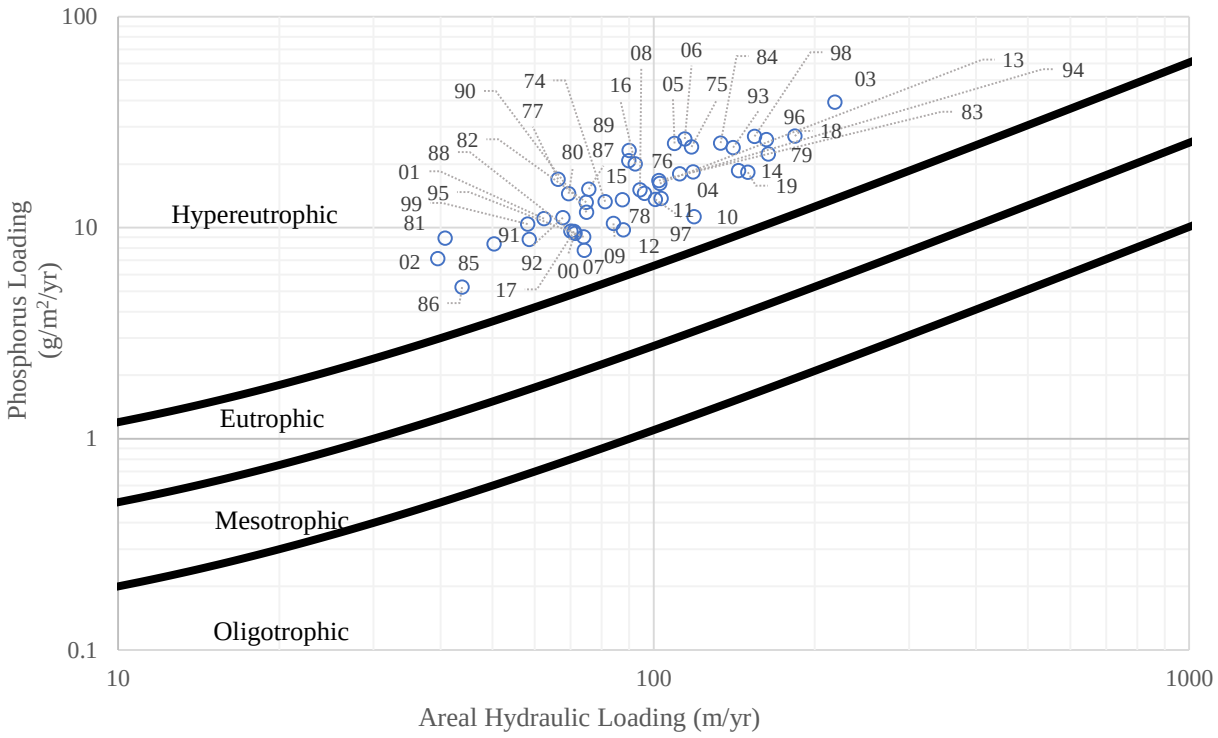

Figure 4-106. Vollenweider Model for the Occoquan Reservoir, 1974–2019

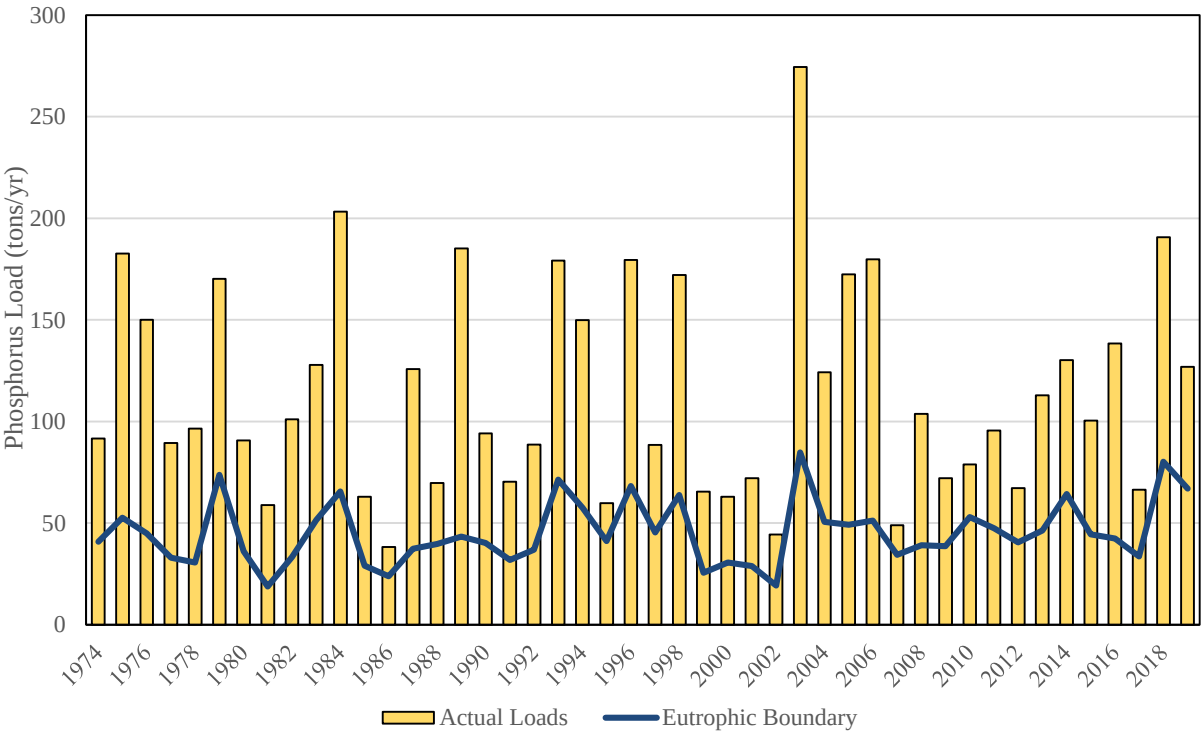

Figure 4-107. Annual Occoquan Reservoir Phosphorus Loads and Eutrophic Boundary

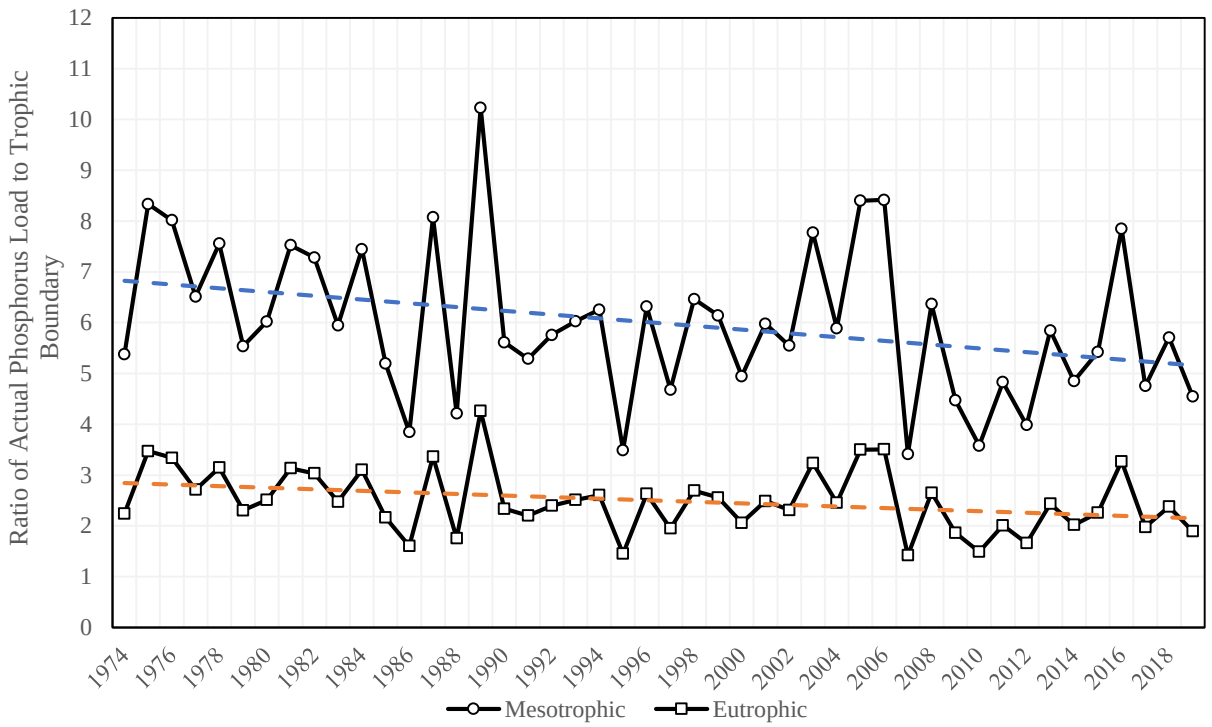

Figure 4-108. Actual Phosphorus Loads to Vollenweider Trophic State Boundaries Ratio

4.4.4 Rast, Jones, and Lee Model

Figure 4-109 presents a comparison of average summer chlorophyll-*a* concentrations predicted for the Occoquan Reservoir with Rast, Jones, and Lee's Model versus actual concentrations observed from 1974 to 2019. The dashed line on the graph represents the trendline of the predicted summer chlorophyll-*a* concentrations, which illustrates a negative slope over time, though the slope is lower than in the previous assessment (Van Den Bos, 2003). It can also be noticed from the graph that observed concentrations were generally lower than predicted concentrations. These lower observed values may have been influenced by the application of copper sulfate during the earlier years, though recent observed values also tend to be lower than predicted. Since 2003, observed values were greater than predicted only in 2003, 2007, 2009, 2010, and 2018. Rast et al. (1983) indicated that measured values may deviate from predicted when the assumptions of the model are not satisfied (e.g., steady-state conditions), or when phosphorus concentrations are present in forms that are unavailable for uptake and use by planktonic algae. Other reasons may be site-specific, such as internal phosphorus loading influencing algal growth.

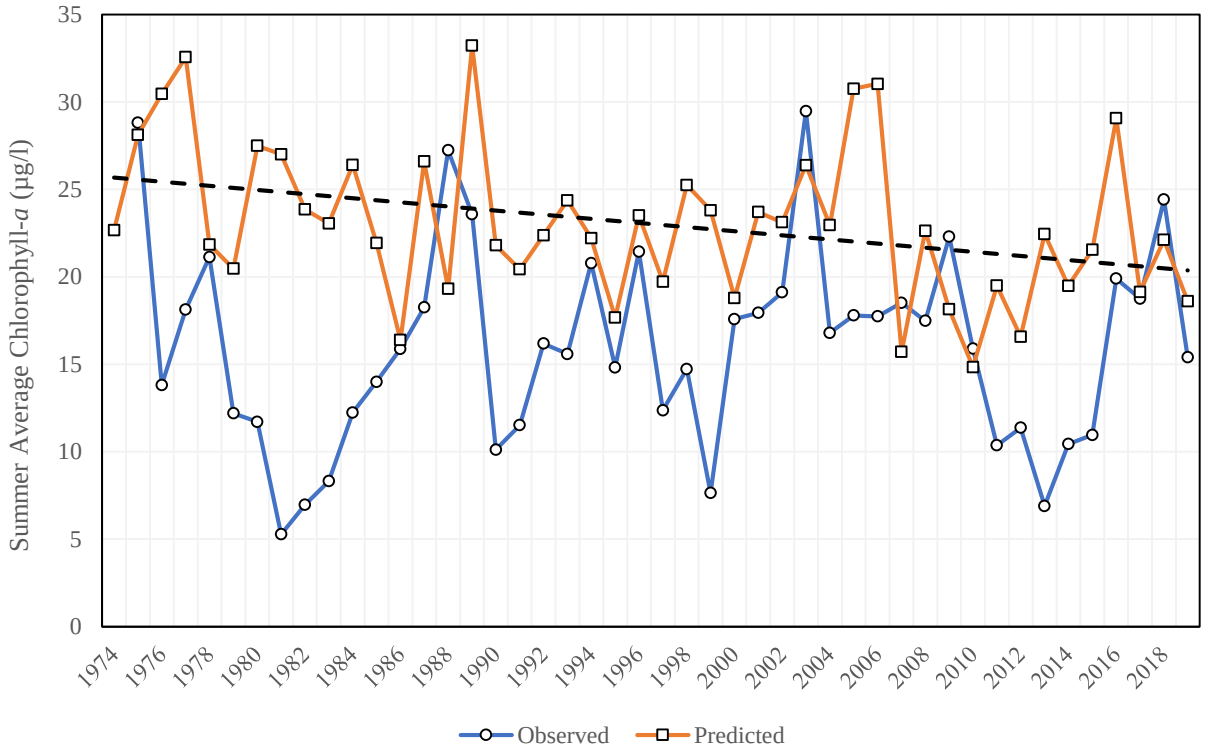

Figure 4-109. Rast, Jones, Lee Predicted Chlorophyll-*a* and Observed Values at the Occoquan Reservoir, 1974–2019

4.5 Synthetic Organic Compounds

4.5.1 Introduction

SOCs refer to anthropogenic chemicals which may be present in waterbodies. Examples include pharmaceuticals, pesticides, herbicides, solvents, and personal care products. The OWML maintains a database with 54 SOCs analyzed from water, fish, and sediment samples from the Occoquan stream and reservoir stations. Water and sediment samples are collected on a quarterly basis, and fish samples are collected semiannually. This section presents an analysis of the SOC data gathered from 2003 to 2019 at the Occoquan Reservoir and Watershed.

4.5.2 Water Samples

Table 4-37 indicates the number of water samples per station that were tested for SOC presence from 2003 to 2019 at the Occoquan Reservoir and Watershed. Stations included for this assessment were main reservoir stations (RE02, RE15, RE30, RE35), stream stations (ST10, ST25, ST30, ST40, ST45, ST70), and raw water samples taken at the Fairfax Water intake, as well as, finished water samples taken at the distribution point of Fairfax Water. The latter two stations only represent 12 of the water samples. During the period analyzed, 501 water samples were tested for the presence of 51 SOCs. The remaining compounds, heptachlor epoxide and benzene

hexachloride (delta isomer), were only tested in 381 of the water samples collected, and chlorpyrifos-methyl was only tested in 467 samples. Table 4-38 presents the number of water samples (and percentage of total) in which each SOC was detected (in order of prevalence), and the minimum, maximum, and average concentrations observed for each compound. As in the other sections of the document, negative values recorded were assumed as half of the detection limit. As a reference, Table 4-38 presents MCLs and maximum contaminant level goals (MCLGs) for SOCs indicated by the USEPA National Primary Drinking Water Regulations, as well as the VDEQ surface water numerical criteria for Human Health (public water supply use) and Aquatic Life Criteria (acute and chronic toxicity). Figure 4-110, shows the percentage of samples that presented quantifiable values (blue) and were below the quantification limit (yellow). Furthermore, Table 4-39 presents the number of detections of each SOC in the stations analyzed and Table 4-40 shows average concentrations of SOCs per stations.

It can be observed that the five (5) most detected SOCs (present in more than half the samples) were Bis(2-ethylhexyl) phthalate (95% of samples), Dibutyl Phthalate / Di-*n*-Butyl Phthalate (83% of samples), Diethyl Phthalate (81% of samples), Di-*n*-Octyl Phthalate (77% detection), and benzyl butyl phthalate (67% of samples). Phthalates (such as these SOCs) are chemicals that are commonly used as plasticizers (substance added to plastics to make them flexible). They can be found in products such as wall coverings, vinyl flooring, detergents, lubricating oils, personal care products (soaps, shampoos, perfumes, etc.), food packing, toys, pharmaceuticals and medical instruments (U.S. Food and Drug Administration [FDA], 2020). Figures 111-115 presents the time series for these compounds.

Of these five (5) compounds, one that exceeded the MCL and VDEQ human health numerical criteria was Bis(2-ethylhexyl) phthalate (DEHP, or Diethylhexyl phthalate). DEHP can be found in drinking water due to discharges from rubber and chemical factories. The potential long term-effects from exposure to levels above the MCL (6 µg/l) include reproductive and liver problems, and higher risk of cancer (USEPA, 2009b). At the Occoquan Reservoir and Watershed, concentrations ranged from <0.4 to 201 µg/l, the highest values (above 100 µg/l) observed in 2003 and 2004. The average concentration was 7.99 µg/l, increased due to these higher values seen. The median value during the period analyzed was 1.27 µg/l and, in the last three years all values have been less than the 6 µg/l stated as an MCL for drinking water (see Figure 4-111 for time series illustration). At the stream stations, this chemical was found at ST40 and ST45 in 89% and 100% of the samples, respectively, and in 95% of the samples at ST10. Average concentrations at the stations were, 12.21 µg/l at ST40, 2.29 µg/l at ST45, and 7.03 µg/l at ST10 (Table 4-40). At the reservoir stations, DEHP was detected in 93% of the samples at RE30 and concentrations averaged 8.18 µg/l, while at RE35 it was detected in 89% of the samples with an average concentration of 1.84 µg/l. These values indicate more presence of this SOC in the Bull Run arm (more developed drainage) than in the Occoquan Creek arm (mainly rural drainage). The detection percentage at RE02 and RE15 was 97%, with average concentrations of 7.08 µg/l and 5.55 µg/l, respectively.

Another one of the most detected phthalates for which the maximum value observed (12 µg/l) was higher than the VDEQ criteria (1 µg/l) was benzyl butyl phthalate. However, values for this SOC have generally been lower than the VDEQ criteria (Figure 4-115), averaging 0.37 µg/l from 2003

to 2019. This compound is commonly found in floor tiles. It can also be found in traffic cones and artificial leather. There is no MCL established for this SOC at present. The remaining three (3) phthalates did not exceed established criteria (where available).

Other prevalent SOCs and their detection percentages were: naphthalene (37%), pyrene (32%), dimethyl phthalate (32%), and phenanthrene (21%). Napthalene, pyrene, and phenanthrene are classified as polycyclic aromatic hydrocarbons (PAHs). PAHs can be produced in the burning of coal, oil, gas, wood, garbage, and tobacco (Centers for Disease Control and Prevention [CDC], 2009). PAHs are also present in products made from fossil fuels, such as asphalt. Most PAHs are manufactured for research purposes. A few of them (such as naphthalene, pyrene, and phenanthrene) are used to make plastics, dyes, and pesticides (Agency for Toxic Substances and Disease Registry [ASTDR], 1995). Napthalene's pesticide use is particularly as an insecticide. Pyrene is also used to make another PAH (benzo(a)pyrene). Phenanthrene is also used to make explosives and pharmaceuticals. Dimethyl phthalate is used as a plasticizer and for insect repellants. Average concentrations observed at the Occoquan Reservoir were 0.31 µg/l for naphthalene and pyrene, 0.23 µg/l for dimethyl phthalate, and 0.28 µg/l for phenanthrene. These compound do not have an MCL established and have not exceeded the VDEQ numerical criteria for human health. Other SOCs, such as atrazine and dual (metolachlor), that have been mentioned among the most prevalent with the phthalates in previous reports (OWML, 1998; Van Den Bos, 2003) were detected in 17% and 18% of the samples, respectively, since 2003.

SOCs that have exceeded the MCL established by the USEPA for drinking water (aside from DEHP, previously mentioned) are lindane, heptachlor, heptachlor epoxide, and benzo(a)pyrene. For lindane, since the detection limit (0.3 µg/l) is higher than the MCL (0.2 µg/l), it is not possible to determine exactly how many times it has exceed the MCL. However, there were 12 instances in which concentrations above 0.3 µg/l were recorded, for which four (4) occurred in 2004, one in 2013 and one in 2018, and the rest in 2014. It should be noted that lindane was only detected in 10% of the samples and only 2% of the samples were quantifiable. Lindane is an insecticide belonging to the family of cyclic chlorinated hydrocarbons (organochlorine insecticide) and is synthesized by the addition of chlorine to benzene in the presence of ultraviolet-light (USEPA, 1980). Lindane has been used to control pests on cattle, lumber, and gardens, and, in the pharmaceutical industry, as a treatment for lice and mites on humans (Nolan et al., 2012). In 2007, the USEPA banned lindane's use as an agricultural pesticide (USEPA, 2006). Long-term exposure to levels greater than the MCL can cause liver and kidney problems (USEPA, 2009b).

Heptachlor is also an organochlorine insecticide. Heptachlor epoxide is not commercially available but is a product of the oxidation of heptachlor (World Health Organization [WHO], 2004). Long-term exposure can cause liver damage and increase the risk of cancer (USEPA, 2009b). Heptachlor and heptachlor epoxide were detected in 4% and 3% of the samples, respectively, and only 1% and 0.4% of the samples were quantifiable. Quantifiable concentrations for heptachlor ranged from 0.4 to 0.7 µg/l (0.40 µg/l MCL) and were detected at RE02 (2004), RE15 (2016), ST25 (2003), and ST25 (2010). Quantifiable samples for heptachlor epoxide were detected at ST25 in 2010 (0.34 µg/l) and ST40 in 2011 (0.37 µg/l). The MCL for heptachlor epoxide 0.20 µg/l. VDEQ numerical criteria for these SOC are much lower than the MCL.

As mentioned, benzo(a)pyrene is also a PAH. In the Occoquan Reservoir and watershed, this SOC was found only in 2% of the samples and the only quantifiable concentration of 2.02 µg/l was observed at ST30 in 2015.

In addition to the compounds previously mentioned, other compounds have exceeded the VDEQ criteria for human health. These compounds and their percentage of detections in water samples are: acenaphthene (18%), benzo(a)anthracene (7%), chrysene (7%), benzene hexachloride (alpha isomer) (6%), benzo(b)fluoranthene (5%), benzo(k)fluoranthene (4%), benzene hexachloride (beta isomer) (3%), dieldrin (2%), Indeno(1,2,3-cd)pyrene (2%), and dibenz(a,h)anthracene (2%). Excluding dieldrin and benzene hexachlorides (which are organochlorine insecticides), these SOCs are all PAHs. The detection limit for most of these SOCs is higher than the VDEQ numerical criteria, except for acenapthene and chrysene. All quantifiable values of acenapthene occurred in 2014 in stream stations ST10, ST25, ST30, ST45, and ST70, and in reservoir stations RE02 and RE15. Concentrations ranged from 0.32 to 0.74 µg/l, and have only exceeded VDEQ criteria on one occurrence. Chrysene's quantifiable concentrations range from 0.18 to 2.28 µg/l, and have only exceeded the 1.2 µg/l VDEQ criteria for human health once in 2015 at ST30. Since the detection limit for the other mentioned SOCs is greater than the VDEQ criteria, the number of quantified samples, though few, represent exceedances of this criteria (Figure 4-110).

Table 4-37. Water Samples Analyzed Per Station, 2003–2019

Station	Start Date	End Date	Number of Samples per Station		
			Heptachlor Epoxide and Benzene Hexachloride (delta isomer)	*Chlorpyrifos-methyl*	*All other SOCs*
OCC_FIN	1/14/2003	5/6/2004	6	-	6
OCC_RAW	1/14/2003	5/6/2004	6	-	6
RE02	1/14/2003	9/17/2019	58	47	62
RE15	5/13/2003	9/17/2019	56	46	60
RE30	1/14/2003	9/17/2019	57	46	61
RE35	7/22/2008	6/20/2013	15	19	19
ST10	1/13/2003	9/16/2019	59	48	63
ST25	1/13/2003	9/16/2019	57	46	61
ST30	1/13/2003	9/16/2019	62	48	66
ST40	1/13/2003	6/18/2012	33	27	37
ST45	9/17/2012	9/16/2019	26	21	26
ST70	10/17/2005	4/5/2016	32	33	34
Total			**467**	**381**	**501**

Table 4-38. Synthetic Organic Compounds from Reservoir and Stream Water Samples, 2003–2019

SOC	Total Samples	Detections		Min	Max	Mean	EPA		VDEQ		
							MCL	*MCLG*	*Human Health*	*Aquatic Life*	
		Count	*Percent*	*(µg/l)*	*(µg/l)*	*(µg/l)*	*(µg/l)*	*(µg/l)*	*(µg/l)*	*(µg/l)**	*(µg/l)***
Bis(2-ethylhexyl)phthalate	501	478	95.41%	<0.4	201	7.99	6.00	0.00	3.2		
Dibutyl Phthalate; Di-n-Butyl Phthalate	501	418	83.43%	<0.3	6.16	0.52			20		
Diethyl Phthalate	501	408	81.44%	<0.5	7.19	0.55			600		
Di-n-Octyl Phthalate	501	386	77.05%	<0.5	18.4	1.33					
Benzyl butyl Phthalate	501	337	67.27%	<0.5	12.05	0.37			1		
Naphthalene	501	184	36.73%	<0.4	3.34	0.31					
Benzo(d,e,f)phenanthrene; Pyrene	501	161	32.14%	<0.3	1.34	0.31			20		
Dimethyl Phthalate	501	158	31.54%	<0.4	1.8	0.23			2000		
Phenanthrene	501	107	21.36%	<0.5	0.88	0.28					
Fluorene	501	100	19.96%	<0.4	0.61	0.22			50		
Metolachlor	501	92	18.36%	<0.2	1.63	0.27					
Acenaphthene; 1,2-Dihydroacenaphthylene	501	89	17.76%	<0.2	0.74	0.14			70		
Atrazine	501	83	16.57%	<0.4	2.69	0.44	3.00	3.00			
HCB; Hexachlorobenzene	501	83	16.57%	<0.5	<0.5	0.25	1.00	0.00	0.00079		
Fluoranthene	501	78	15.57%	<0.3	1.96	0.19			20		
Acenaphthylene	501	72	14.37%	<0.3	0.59	0.16					
Anthracene	501	52	10.38%	<0.2	9	0.33			300		
BHC (gamma isomer); Lindane	501	48	9.58%	<0.3	1.47	0.33	0.20	0.20	4.2	0.95	-
Triadimefon	501	42	8.38%	<0.6	1.38	0.33					
Benzo(a)anthracene	501	36	7.19%	<0.3	4.87	0.53			0.012		
Chrysene	501	36	7.19%	<0.3	2.28	0.31			1.2		
Benzene Hexachloride (alpha isomer)	501	30	5.99%	<0.3	1.15	0.35			0.0036		
Benzo(b)fluoranthene	501	27	5.39%	<0.4	2.51	0.44			0.012		
Benzo(k)fluoranthene	501	22	4.39%	<0.4	3.06	0.58			0.12		
DCPA; Chlorthal dimethyl	501	21	4.19%	<0.2	0.38	0.11					
Heptachlor	501	19	3.79%	<0.2	0.7	0.20	0.40	0.00	0.000059	0.52	0.0038
Terbufos	501	19	3.79%	<0.4	4.39	1.43					
Carbazole; 9-Azafluorene; Dibenzopyrrole; Diphenylenin	501	18	3.59%	<0.6	3.12	0.46					
Fenchlorphos; Ronnel	501	18	3.59%	<0.4	0.93	0.24					
Simazine	501	18	3.59%	<0.5	<0.5	0.25	4.00	4.00			
Benzene Hexachloride (beta isomer)	501	17	3.39%	<0.3	0.9	0.47			0.08		
Pendimethalin; Prowl	501	17	3.39%	<0.7	0.73	0.37					
Chlorpyrifos-methyl	381	12	3.15%	<0.4	3.16	0.47					
Heptachlor Epoxide	467	14	3.00%	<0.3	0.37	0.18	0.20	0.00	0.00032	0.52	0.0038
DDVP; Dichlorvos; UDVF	501	15	2.99%	<0.6	<0.6	0.30					
Fenoprop; Silvex; 2,4,5-TP	501	13	2.59%	<0.4	<0.4	0.20	50	50	100		
Ethylparathion; Parathion; Thiophos	501	12	2.40%	<0.4	2.2	0.37				0.065	0.013
Chlorothalonil	501	12	2.40%	<0.5	<0.5	0.25					
Dieldrin	501	11	2.20%	<0.5	1.17	0.33			0.000012	0.24	0.056
Indeno(1,2,3-cd)pyrene; o-Phenylenepyrene	501	10	2.00%	<0.2	1.37	0.38			0.012		
2,4,5-T	501	9	1.80%	<0.3	0.33	0.17					
Benzo(a)pyrene	501	9	1.80%	<0.2	2.02	0.38	0.20	0.00	0.0012		
Dibenz(a,h)anthracene	501	9	1.80%	<0.3	4.72	1.21			0.0012		
Carbaryl; Sevin	501	8	1.60%	<0.4	1.85	0.41				2.1	2.1
Propazine	501	8	1.60%	<0.4	1.14	0.42					
Diazinon; Dimpylate	501	7	1.40%	<0.2	<0.2	0.10				0.17	0.17
Fensulfothion	501	7	1.40%	<0.5	0.76	0.36					
Benzo(g,h,i)perylene	501	7	1.40%	<0.2	3.88	1.07					
Malathion; Mercaptothion; Carbofos; Maldison	501	4	0.80%	<0.4	1.57	0.54				-	0.10
Mevinphos; Phosdrin	501	2	0.40%	<0.5	<0.5	0.25					
Ethoprop; Ethoprophos	501	2	0.40%	<0.3	0.43	0.29					
Benzene Hexachloride (delta isomer)	467	1	0.21%	<0.5	<0.5	0.25					
Phorate; Timet	501	1	0.20%	3.81	3.81	3.81					
Etridiazole	501	1	0.20%	<0.3	<0.3	0.15					

**Acute Toxicity* ***Chronic Toxicity*

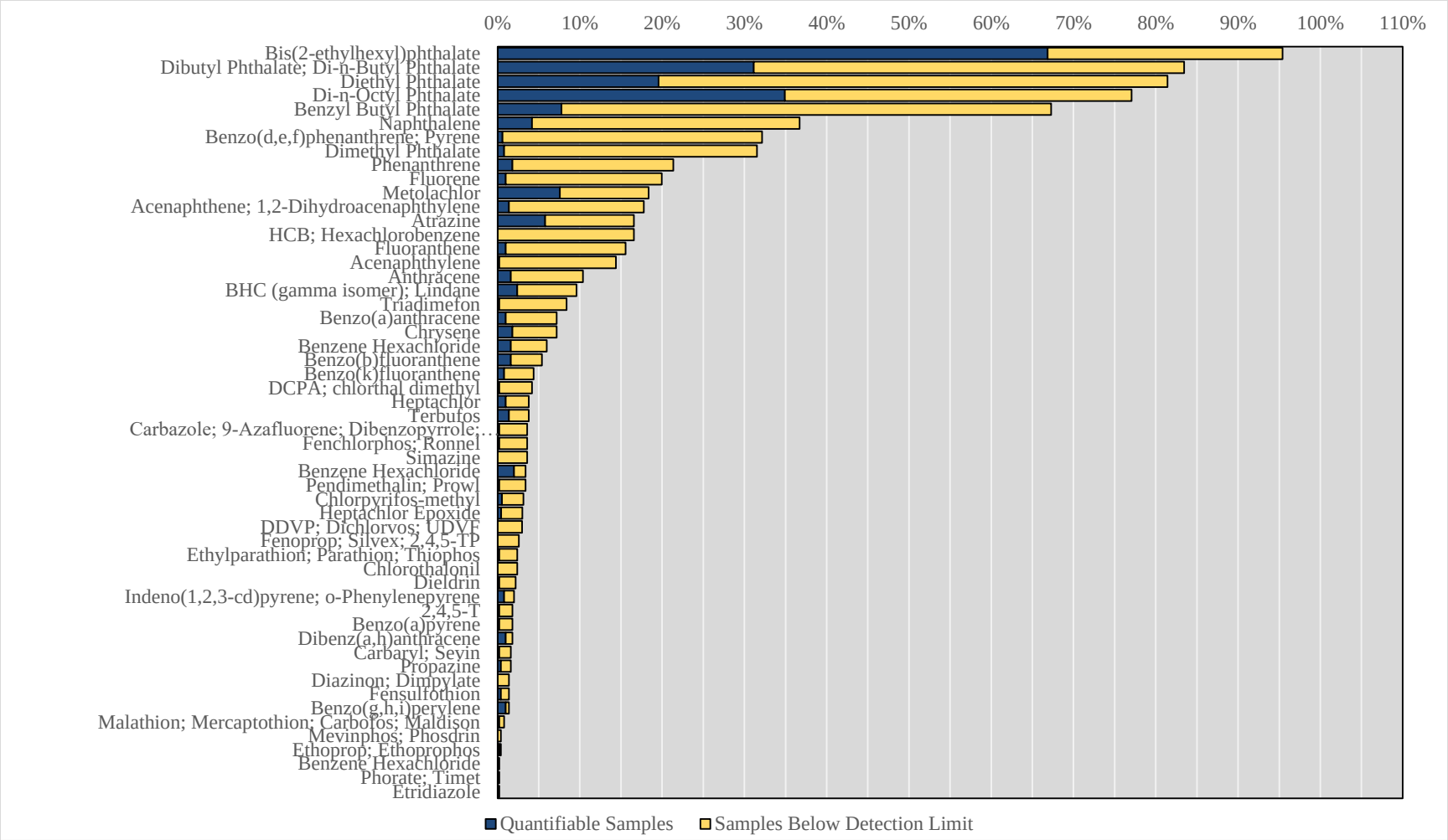

Figure 4-110. Synthetic Organic Compounds Detected in Reservoir and Stream Water Samples, 2003–2019

Table 4-39. Distribution of Synthetic Organic Compounds Detected in Water Samples, 2003–2019

SOC	Detections	Number of Detections Per Station											
		OCC_FIN	*OCC_RAW*	*RE02*	*RE15*	*RE30*	*RE35*	*ST10*	*ST25*	*ST30*	*ST40*	*ST45*	*ST70*
Bis(2-ethylhexyl)phthalate	478	5	6	60	58	57	17	60	61	63	33	26	32
Dibutyl Phthalate; Di-n-Butyl Phthalate	418	3	2	54	49	51	18	55	51	55	25	26	29
Diethyl Phthalate	408	2	2	49	50	50	17	52	50	53	26	26	31
Di-n-Octyl Phthalate	386	6	4	47	45	45	19	47	47	52	29	15	30
Benzyl Butyl Phthalate	337	4	4	44	40	43	15	40	41	44	27	16	19
Naphthalene	184	1	1	23	25	25	7	24	22	26	12	9	9
Benzo(d,e,f)phenanthrene; Pyrene	161	0	0	17	21	20	11	17	20	20	14	9	12
Dimethyl Phthalate	158	1	2	21	20	19	2	22	19	23	12	11	6
Phenanthrene	107	1	1	12	15	15	5	13	16	11	6	7	5
Fluorene	100	0	0	13	17	11	1	13	15	9	4	11	6
Metolachlor	92	1	1	13	14	5	5	14	18	12	2	3	4
Acenaphthene; 1,2-Dihydroacenaphthylene	89	0	0	10	13	11	2	12	11	11	5	8	6
Atrazine	83	1	1	12	14	3	6	14	15	11	0	3	3
HCB; Hexachlorobenzene	83	1	0	8	15	16	2	6	10	8	2	9	6
Fluoranthene	78	0	0	8	10	10	4	10	12	9	5	5	5
Acenaphthylene	72	0	0	11	11	7	1	7	10	11	3	8	3
Anthracene	52	0	0	8	9	6	1	5	8	7	2	4	2
BHC (gamma isomer); Lindane	48	1	0	7	4	4	0	8	9	6	0	7	2
Triadimefon	42	0	0	6	5	7	2	6	3	6	1	2	4
Benzo(a)anthracene	36	0	0	5	6	5	1	3	6	4	3	3	0
Chrysene	36	0	0	4	6	3	0	5	6	5	3	2	2
Benzene Hexachloride	30	0	0	2	3	3	0	4	4	3	2	4	5
Benzo(b)fluoranthene	27	0	0	5	4	3	1	4	2	1	3	1	3
Benzo(k)fluoranthene	22	0	0	5	3	3	1	3	2	1	2	1	1
DCPA; chlorthal dimethyl	21	0	0	2	3	2	1	2	5	4	1	0	1
Heptachlor	19	0	0	5	3	1	0	1	5	1	1	2	0
Terbufos	19	0	0	5	2	2	0	1	4	3	1	0	1
Carbazole; 9-Azafluorene; Dibenzopyrrole; Diphenylenimine	18	0	0	2	2	1	0	3	2	3	0	3	2
Fenchlorphos; Ronnel	18	0	0	3	1	2	0	1	4	4	1	2	0
Simazine	18	0	0	2	4	4	1	3	1	1	0	1	1
Benzene Hexachloride	17	0	0	2	4	2	1	2	2	2	0	1	1
Pendimethalin; Prowl	17	0	0	3	1	2	1	2	4	3	1	0	0
Chlorpyrifos-methyl	12	0	0	1	1	1	0	3	2	1	1	1	1
Heptachlor Epoxide	14	0	0	0	1	0	0	2	4	3	2	1	1
DDVP; Dichlorvos; UDVF	15	0	0	2	2	1	0	2	2	3	0	2	1
Fenoprop; Silvex; 2,4,5-TP	13	0	0	1	2	1	0	2	2	2	0	1	2
Ethylparathion; Parathion; Thiophos	12	0	0	2	0	2	0	1	4	2	0	0	1
Chlorothalonil	12	0	0	2	1	2	2	1	1	2	0	0	1
Dieldrin	11	0	0	1	1	0	2	1	3	2	1	0	0
Indeno(1,2,3-cd)pyrene; o-Phenylenepyrene	10	0	0	2	2	1	1	0	1	1	1	1	0
2,4,5-T	9	0	0	1	1	1	0	1	2	1	0	1	1
Benzo(a)pyrene	9	0	0	2	2	2	0	0	0	1	1	0	1
Dibenz(a,h)anthracene	9	0	0	1	1	0	1	1	2	1	1	1	0
Carbaryl; Sevin	8	0	0	2	1	1	0	1	1	0	0	1	1
Propazine	8	0	0	2	0	0	0	2	3	1	0	0	0
Diazinon; Dimpylate	7	0	0	1	0	1	0	0	1	2	0	1	1
Fensulfothion	7	0	0	1	0	1	0	1	1	1	0	2	0
Benzo(g,h,i)perylene	7	0	0	1	1	0	1	0	1	1	0	1	1
Malathion; Mercaptothion; Carbofos; Maldison	4	0	0	3	0	0	0	0	1	0	0	0	0
Mevinphos; Phosdrin	2	0	0	0	0	1	0	1	0	0	0	0	0
Ethoprop; Ethoprophos	2	0	0	0	0	0	0	0	0	0	1	0	1
Benzene Hexachloride	1	0	0	1	0	0	0	0	0	0	0	0	0
Phorate; Timet	1	0	0	1	0	0	0	0	0	0	0	0	0
Etridiazole	1	0	0	0	0	0	0	0	0	0	0	0	1

Table 4-40. Average Concentrations of Synthetic Organic Compounds Detected in Water Samples, 2003–2019

SOC	Detections	Average Concentration Per Station (µg/l)											
		OCC_FIN	*OCC_RAW*	*RE02*	*RE15*	*RE30*	*RE35*	*ST10*	*ST25*	*ST30*	*ST40*	*ST45*	*ST70*
Bis(2-ethylhexyl)phthalate	478	34.48	28.44	7.08	5.55	8.18	1.84	7.03	10.82	9.11	12.21	2.29	3.50
Dibutyl Phthalate; Di-n-Butyl Phthalate	418	1.06	0.48	0.39	0.58	0.47	0.62	0.52	0.51	0.55	0.65	0.56	0.43
Diethyl Phthalate	408	0.80	1.51	0.49	0.52	0.46	0.29	0.69	0.47	0.67	0.41	0.86	0.41
Di-n-Octyl Phthalate	386	0.75	1.96	1.22	1.44	1.09	1.51	1.32	1.60	1.41	1.20	1.01	1.35
Benzyl Butyl Phthalate	337	0.39	3.63	0.32	0.37	0.30	0.29	0.39	0.30	0.35	0.38	0.25	0.25
Naphthalene	184	0.48	0.81	0.22	0.26	0.21	0.20	0.49	0.37	0.37	0.20	0.26	0.27
Benzo(d,e,f)phenanthrene; Pyrene	161	-	-	0.34	0.33	0.29	0.30	0.30	0.31	0.29	0.30	0.27	0.30
Dimethyl Phthalate	158	0.20	0.20	0.20	0.20	0.28	1.00	0.21	0.20	0.20	0.28	0.20	0.20
Phenanthrene	107	0.25	0.25	0.33	0.28	0.27	0.25	0.28	0.28	0.28	0.25	0.35	0.25
Fluorene	100	-	-	0.22	0.20	0.20	0.20	0.20	0.24	0.27	0.20	0.20	0.20
Metolachlor	92	0.28	0.29	0.23	0.27	0.13	0.30	0.30	0.36	0.20	1.00	0.10	0.10
Acenaphthene; 1,2-Dihydroacenaphthylene	89	-	-	0.15	0.14	0.10	0.10	0.15	0.15	0.15	0.10	0.17	0.14
Atrazine	83	0.40	0.41	0.43	0.38	0.28	0.47	0.56	0.51	0.39	-	0.20	0.37
HCB; Hexachlorobenzene	83	0.25	-	0.25	0.25	0.25	0.25	0.25	0.25	0.25	0.25	0.25	0.25
Fluoranthene	78	-	-	0.18	0.33	0.18	0.15	0.15	0.15	0.17	0.21	0.15	0.15
Acenaphthylene	72	-	-	0.15	0.19	0.15	0.15	0.15	0.15	0.15	0.15	0.15	0.15
Anthracene	52	-	-	0.10	0.26	0.18	0.10	0.12	1.29	0.10	0.34	0.10	0.10
BHC (gamma isomer); Lindane	48	0.46	-	0.31	0.50	0.21	-	0.34	0.32	0.36	-	0.32	0.23
Triadimefon	42	-	-	0.48	0.30	0.30	0.30	0.30	0.30	0.30	0.30	0.30	0.30
Benzo(a)anthracene	36	-	-	0.53	1.01	0.27	0.30	0.33	0.32	1.10	0.20	0.30	-
Chrysene	36	-	-	0.31	0.22	0.28	-	0.24	0.26	0.68	0.28	0.25	0.15
Benzene Hexachloride	30	-	-	0.60	0.45	0.15	-	0.40	0.40	0.47	0.15	0.37	0.25
Benzo(b)fluoranthene	27	-	-	0.60	0.79	0.32	0.25	0.24	0.37	1.02	0.28	0.25	0.23
Benzo(k)fluoranthene	22	-	-	0.80	0.96	0.23	0.20	0.22	0.23	3.06	0.25	0.20	0.20
DCPA; chlorthal dimethyl	21	-	-	0.10	0.10	0.10	0.10	0.10	0.16	0.10	0.10	-	0.10
Heptachlor	19	-	-	0.22	0.24	0.10	-	0.10	0.27	0.10	0.10	0.10	-
Terbufos	19	-	-	0.99	0.68	0.20	-	4.39	1.97	1.39	3.92	-	0.20
Carbazole; 9-Azafluorene; Dibenzopyrrole; Diphenylenimine	18	-	-	0.30	0.30	0.30	-	1.24	0.30	0.30	-	0.30	0.30
Fenchlorphos; Ronnel	18	-	-	0.20	0.20	0.20	-	0.20	0.38	0.20	0.20	0.20	-
Simazine	18	-	-	0.25	0.25	0.25	0.25	0.25	0.25	0.25	-	0.25	0.25
Benzene Hexachloride	17	-	-	0.49	0.41	0.37	0.40	0.53	0.52	0.60	-	0.84	0.15
Pendimethalin; Prowl	17	-	-	0.35	0.35	0.35	0.35	0.35	0.45	0.35	0.35	-	-
Chlorpyrifos-methyl	12	-	-	0.20	0.20	0.20	-	1.19	0.20	0.20	0.43	0.20	0.20
Heptachlor Epoxide	14	-	-	-	0.15	-	-	0.15	0.21	0.15	0.25	0.15	0.15
DDVP; Dichlorvos; UDVF	15	-	-	0.30	0.30	0.30	-	0.30	0.30	0.30	-	0.30	0.30
Fenoprop; Silvex; 2,4,5-TP	13	-	-	0.20	0.20	0.20	-	0.20	0.20	0.20	-	0.20	0.20
Ethylparathion; Parathion; Thiophos	12	-	-	1.20	-	0.20	-	0.20	0.20	0.20	-	-	0.20
Chlorothalonil	12	-	-	0.25	0.25	0.25	0.25	0.25	0.25	0.25	-	-	0.25
Dieldrin	11	-	-	0.25	0.25	-	0.25	0.25	0.56	0.25	0.25	-	-
Indeno(1,2,3-cd)pyrene; o-Phenylenepyrene	10	-	-	0.53	0.74	0.10	0.10	-	0.45	0.10	0.10	0.39	-
2,4,5-T	9	-	-	0.33	0.15	0.15	-	0.15	0.15	0.15	-	0.15	0.15
Benzo(a)pyrene	9	-	-	0.18	0.18	0.18	-	-	-	2.02	0.10	-	0.25
Dibenz(a,h)anthracene	9	-	-	4.72	2.36	-	0.15	0.15	1.25	0.41	0.15	0.41	-
Carbaryl; Sevin	8	-	-	1.03	0.20	0.20	-	0.20	0.20	-	-	0.20	0.20
Propazine	8	-	-	0.20	-	-	-	0.67	0.48	0.20	-	-	-
Diazinon; Dimpylate	7	-	-	0.10	-	0.10	-	-	0.10	0.10	-	0.10	0.10
Fensulfothion	7	-	-	0.76	-	0.25	-	0.25	0.25	0.25	-	0.38	-
Benzo(g,h,i)perylene	7	-	-	3.88	1.55	-	0.10	-	1.23	0.28	-	0.34	0.10
Malathion; Mercaptothion; Carbofos; Maldison	4	-	-	0.66	-	-	-	-	0.20	-	-	-	-
Mevinphos; Phosdrin	2	-	-	-	-	0.25	-	0.25	-	-	-	-	-
Ethoprop; Ethoprophos	2	-	-	-	-	-	-	-	-	-	0.43	-	0.15
Benzene Hexachloride	1	-	-	0.25	-	-	-	-	-	-	-	-	-
Phorate; Timet	1	-	-	3.81	-	-	-	-	-	-	-	-	-
Etridiazole	1	-	-	-	-	-	-	-	-	-	-	-	0.15

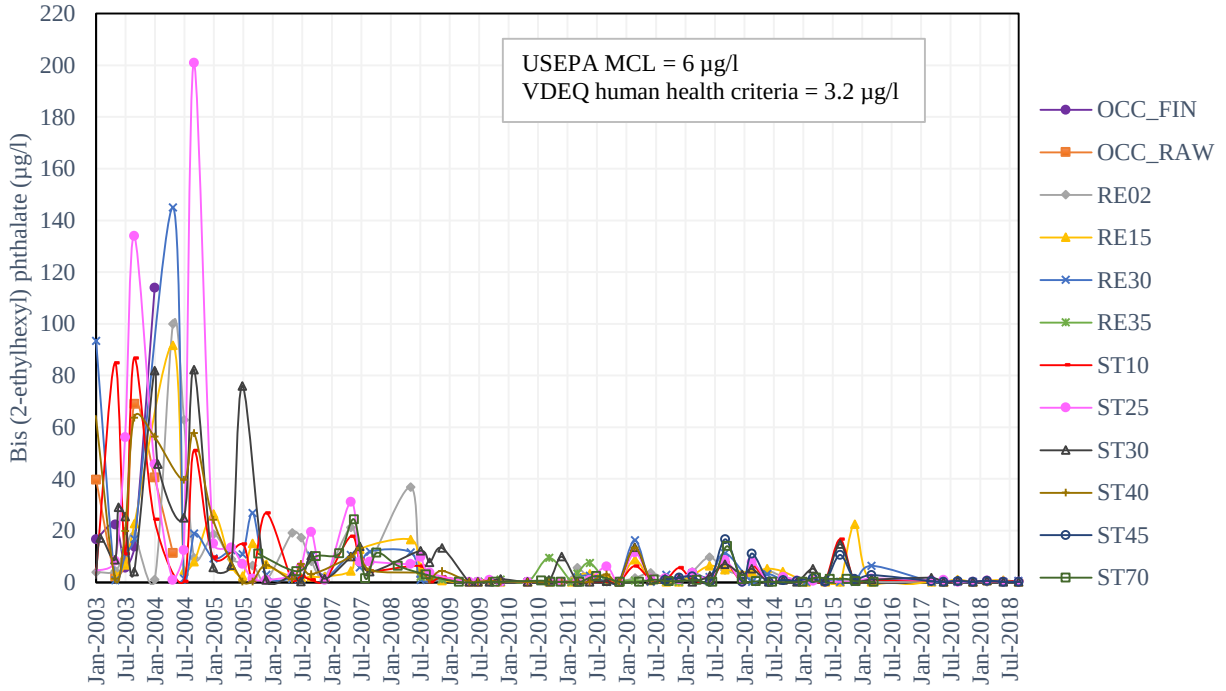

Figure 4-111. Time Series for Bis(2-ethylhexyl)phthalate by Station, 2003–2019

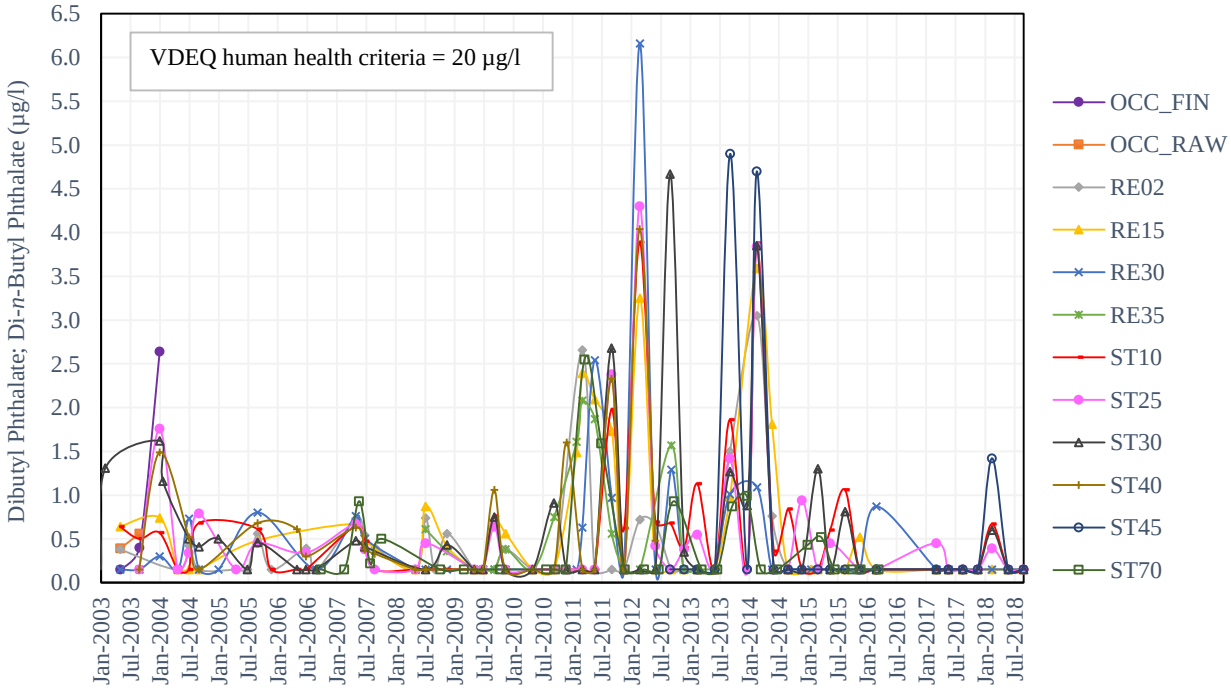

Figure 4-112. Time Series for Dibutyl Phthalate; Di-n-Butyl Phthalate by Station, 2003–2019

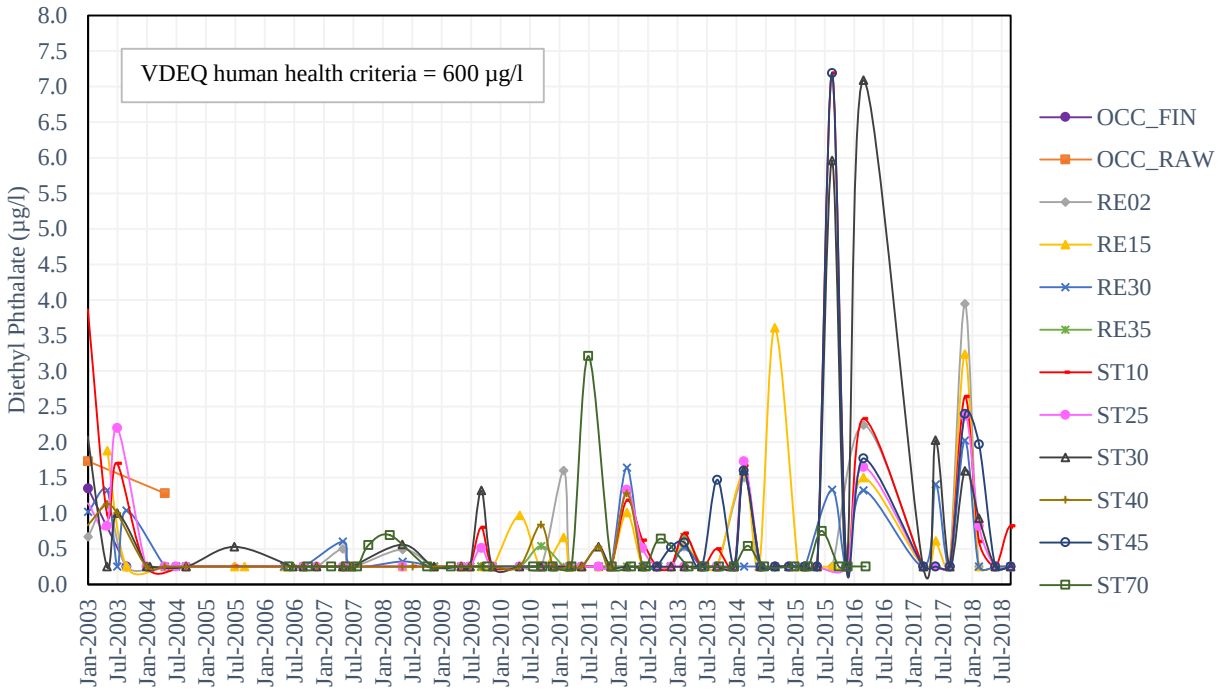

Figure 4-113. Time Series for Diethyl Phthalate by Station, 2003–2019

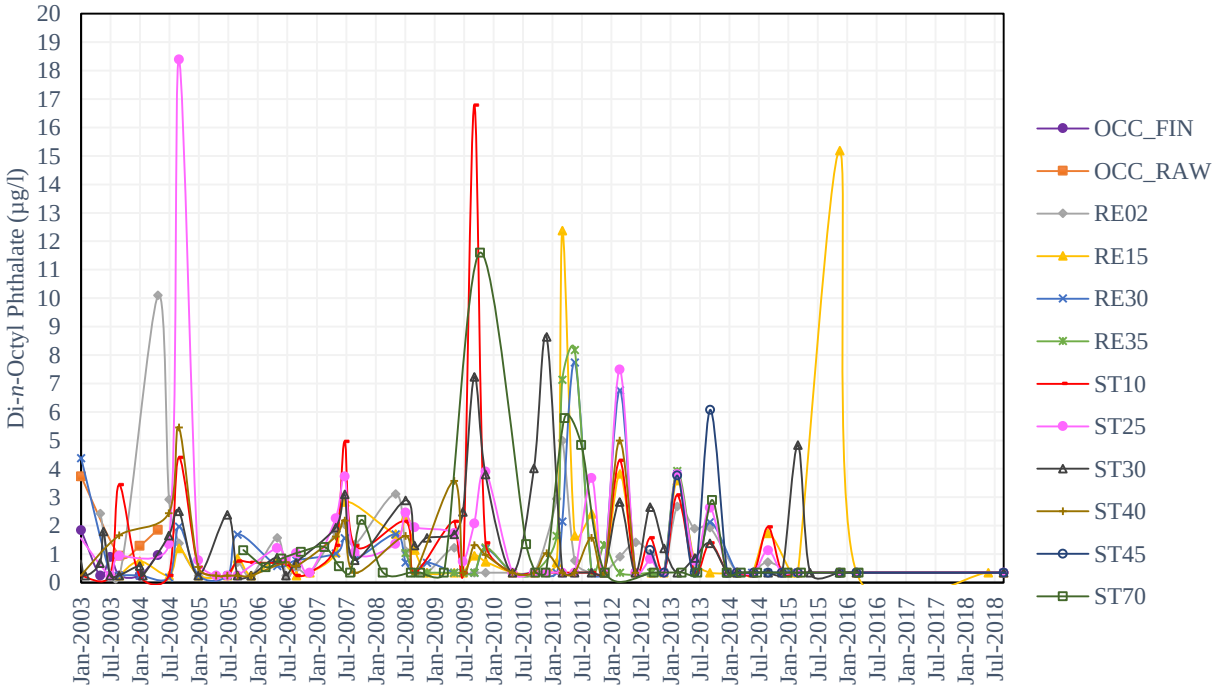

Figure 4-114. Time Series for Di-*n*-Octyl Phthalate by Station, 2003–2019

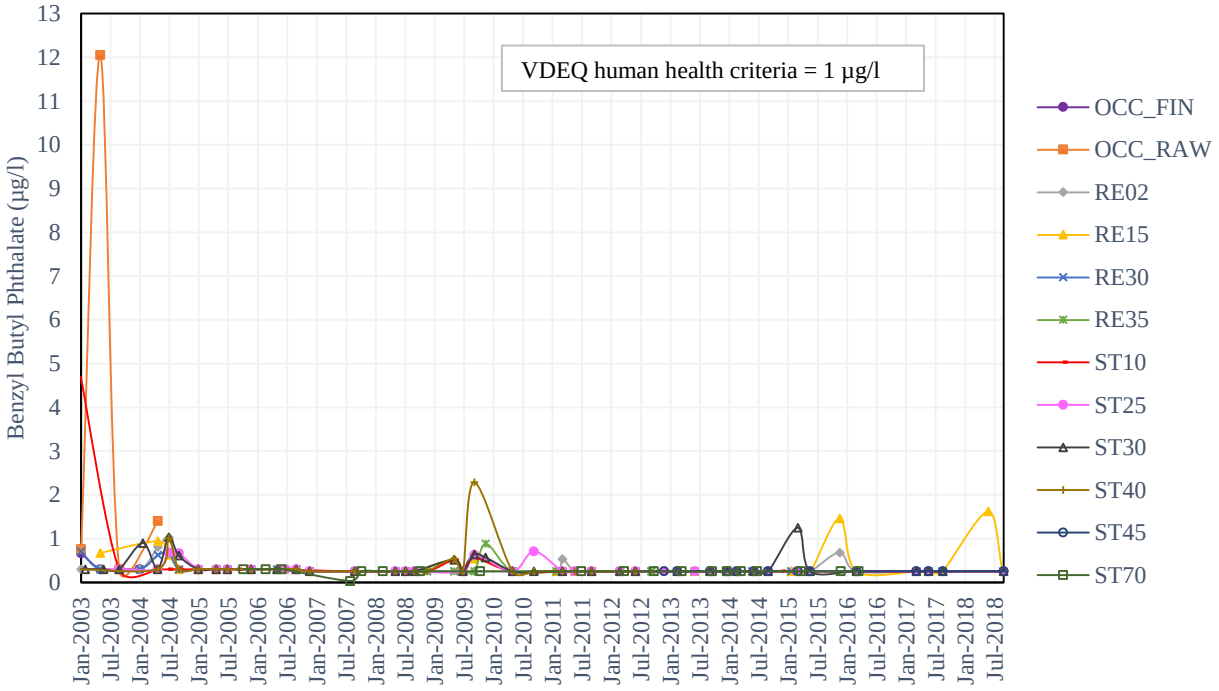

Figure 4-115. Time Series for Benzyl Butyl Phthalate by Station, 2003–2019

4.5.3 Fish Samples

The same compounds analyzed for in water samples were also analyzed for in fish samples from 2003 to 2019. Fish samples were taken at RE02, RE15, RE30, and RE35. A total of 87 fish samples (taken from bass, crappie, and catfish) were analyzed during this period. Table 4-41 details the number of SOCs analyzed for each station. Additionally, Table 4-42 presents the number of detections for each SOC (count and percentage of total samples), the minimum, maximum and average concentrations, and the number of detections observed at each station. Table 4-42 only shows the SOCs (31 compounds) that were detected at the reservoir stations analyzed (ordered by frequency). The remaining compounds (in comparison to the 54 compounds listed in Table 4-38) were not presented in the table because they were not detected in fish samples. Lastly, Figure 4-116 illustrates the percentage of samples that were quantifiable versus the percentage of samples that were below detection limit.

As it was observed in the water samples, the most prevalent compounds detected in fish samples were the phthalates, though some in different order. DEHP was the most detected SOC (detected in 97% of the samples), followed by diethyl phthalate which was detected in 94% of samples. For these two compounds, most of the samples were quantifiable (Figure 4-116), with values averaging 4.52 µg/g and 0.73 µg/g, respectively (Table 4-42). The next most frequently detected SOCs were dibutyl phthalate / Di-n-Butyl Phthalate (detected in 93% of samples), di-n-octyl phthalate (detected in 74% of the samples), and benzyl butyl phthalate (detected in 60% of the samples). Following these five (5) compounds, the next prevalent SOCs were naphthalene, phenanthrene,

and dimethyl phthalate, as with water samples. However, unlike water samples, pyrene was only detected in 2% of the fish samples, and anthracene followed dimethyl phthalate (23% detection). All other SOCs where detected in less than 10% of the samples.

Table 4-41. Fish Samples Analyzed Per Station

Station	Start Date	End Date	Number of Samples per Station
RE02	10/21/2003	6/12/2019	21
RE15	6/24/2003	9/11/2019	29
RE30	6/17/2003	9/11/2019	31
RE35	7/28/2009	6/2/2013	6
Total			**87**

Table 4-42. Synthetic Organic Compounds Detected in Fish Samples by Station, 2003–2019

SOC	Total Samples	Detections		Min	Max	Mean	Number of Detections by Stations			
		Count	*Percent*	*(µg/g)*	*(µg/g)*	*(µg/g)*	*RE02*	*RE15*	*RE30*	*RE35*
Bis(2-ethylhexyl)phthalate	87	84	96.55%	<0.04	82.56	4.52	21	28	29	6
Diethyl Phthalate	87	82	94.25%	<0.05	5.43	0.73	20	26	30	6
Dibutyl Phthalate; Di-n-Butyl Phthalate	87	81	93.10%	<0.03	0.35	0.04	21	26	28	6
Di-n-Octyl Phthalate	87	64	73.56%	<0.04	1.01	0.07	16	20	24	4
Benzyl Butyl Phthalate	87	52	59.77%	<0.05	0.42	0.05	12	18	17	5
Naphthalene	87	41	47.13%	<0.04	0.15	0.04	9	12	17	3
Phenanthrene	87	27	31.03%	<0.05	<0.05	0.02	7	7	11	2
Dimethyl Phthalate	87	23	26.44%	<0.04	0.25	0.05	6	8	9	0
Anthracene	87	20	22.99%	<0.02	0.07	0.02	7	8	5	0
Benzo(a)anthracene	87	9	10.34%	<0.06	<0.06	0.03	3	2	3	1
Benzene Hexachloride (alpha isomer)	87	6	6.90%	<0.03	0.04	0.02	1	2	2	1
Carbaryl; Sevin	87	6	6.90%	<0.04	<0.04	0.02	2	1	1	2
HCB; Hexachlorobenzene	87	5	5.75%	<0.05	<0.05	0.03	1	2	2	0
BHC (gamma isomer); Lindane	87	5	5.75%	<0.03	0.09	0.05	1	3	1	0
Atrazine	87	3	3.45%	<0.04	0.49	0.19	1	1	1	0
Simazine	87	3	3.45%	<0.05	0.41	0.15	1	1	1	0
Acenaphthene; 1,2-Dihydroacenaphthylene	87	3	3.45%	<0.02	<0.02	0.01	1	1	1	0
Acenaphthylene	87	3	3.45%	<0.03	0.31	0.15	2	1	0	0
Dibenz(a,h)anthracene	87	3	3.45%	<0.03	<0.03	0.02	0	1	2	0
Dieldrin	87	2	2.30%	0.06	0.07	0.07	1	1	0	0
Propazine	87	2	2.30%	<0.04	0.11	0.07	0	1	1	0
Fenoprop; Silvex; 2,4,5-TP	87	2	2.30%	<0.04	<0.04	0.02	0	1	1	0
DDVP; Dichlorvos; UDVF	87	2	2.30%	<0.06	<0.06	0.03	1	1	0	0
Fluoranthene	87	2	2.30%	<0.03	<0.03	0.02	0	1	1	0
Benzo(d,e,f)phenanthrene; Pyrene	87	2	2.30%	<0.06	0.07	0.05	0	1	1	0
Heptachlor Epoxide	87	1	1.15%	0.13	0.13	0.13	0	0	1	0
Ethoprop; Ethoprophos	87	1	1.15%	<0.03	<0.03	0.02	1	0	0	0
Benzo(b)fluoranthene	87	1	1.15%	<0.05	<0.05	0.03	0	1	0	0
Benzo(k)fluoranthene	87	1	1.15%	<0.04	<0.04	0.02	0	0	1	0
Chrysene	87	1	1.15%	0.06	0.06	0.06	0	0	1	0
Fluorene	87	1	1.15%	<0.04	<0.04	0.02	0	0	1	0

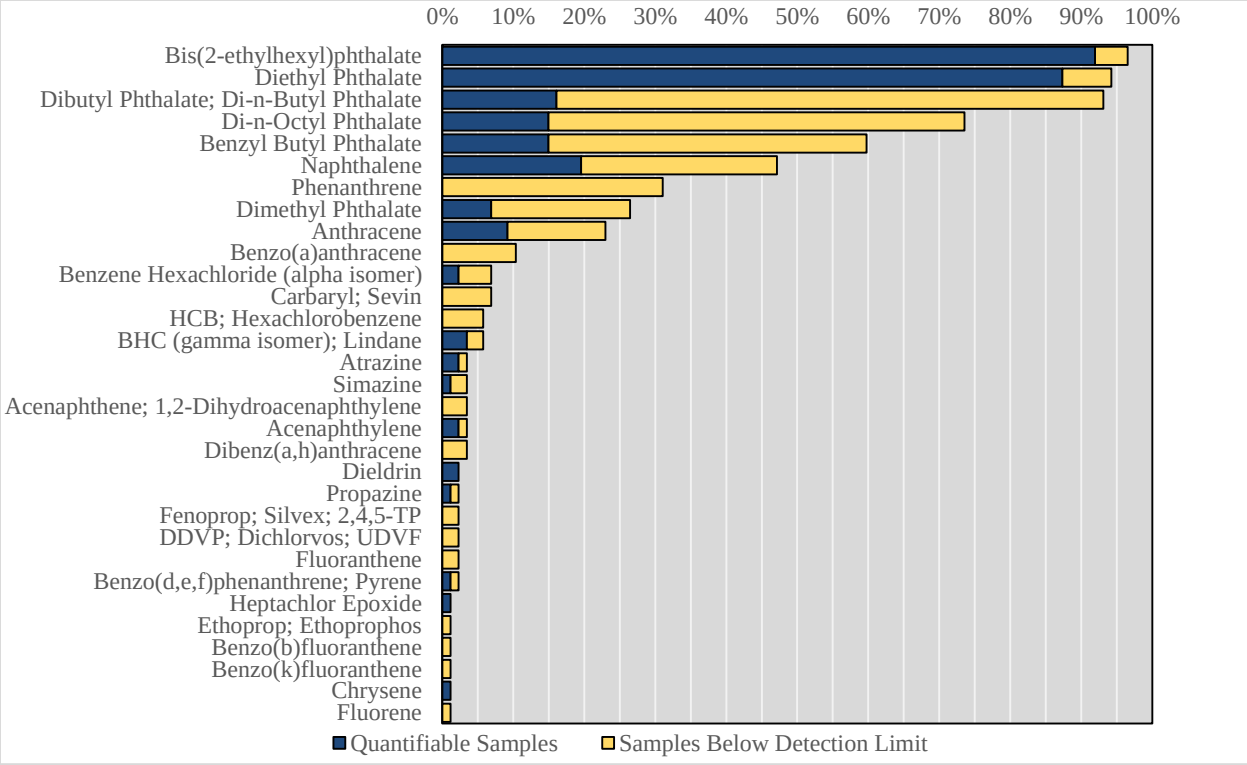

Figure 4-116. Synthetic Organic Compounds Detected in Fish Samples, 2003–2019

4.5.4 Sediment Samples

SOC results for sediment samples are shown in this section. Table 4-43 details the number of samples per station analyzed (RE02, RE15, RE30, RE35). SOC tested for sediment include the 54 compounds tested for water and fish samples with the exception of triadimefon, for which no data were available. Most SOCs were tested in the total 210 sediment samples collected from 2003 to 2019. However, heptachlor epoxide was only tested in 194 samples, dibutyl phthalate/di-*n*-butyl phthalate was tested in 209 samples, chlorothalonil and etridiazole were tested in 183 samples, chlorpyrifos-methyl was tested in 168 samples and indeno(1,2,3-cd)pyrene was tested in 162 samples.

Table 4-44 presents the number of detections for each SOC (count and percentage of total samples), the minimum, maximum and average concentrations, and the number of detections observed at each station. This table presents 43 chemical compounds that were detected at the reservoir stations. The remaining compounds (benzene hexachloride delta isomer, heptachlor, mevinphos, pendimethalin, phorate, propazine, silvex, simazine, parathion, and malathion) were not presented in the table since there were not detected in sediment samples. Figure 4-117 illustrates the percentage of samples that were quantifiable versus the percentage of samples that were below detection limit.

The most detected SOC in sediment samples was diethyl phthalate, detected in 90% of the samples, followed by dibutyl phthalate / Di-*n*-Butyl Phthalate with a detection percentage of 86%. DEHP

which was the most frequently detected SOC in water and fish samples, was the third most detected in sediment samples (close to 86% detections), followed by di-*n*-octyl phthalate which was detected in 79% of the samples. Pyrene, which was the seventh most detected SOC in water samples (32%) and only one of the least detected in fish samples (2%), was among the top five (5) detected SOC in sediment samples (65%). In contrast with water and sediment samples for which only nine (9) compounds were detected in more than 20% samples, 18 compounds were detected in more than 20% of sediment samples.

Table 4-43. Sediment Samples Analyzed Per Station

Station	Start Date	End Date	Number of Samples per Station					
			Heptachlor Epoxide	*Dibutyl Phthalate; Di-n-Butyl Phthalate*	*Chlorothalonil / Etridiazole*	*Chlorpyrifos-methyl*	*Indeno(1,2,3-cd)pyrene; o-Phenylenepyrene*	*All other SOCs*
RE02	1/14/2003	9/17/2019	60	64	55	50	48	64
RE15	1/14/2003	9/17/2019	60	64	55	50	48	64
RE30	1/14/2003	9/17/2019	60	63	55	50	48	64
RE35	9/16/2008	6/20/2013	14	18	18	18	18	18
Total			**194**	**209**	**183**	**168**	**162**	**210**

Table 4-44. Synthetic Organic Compounds Detected in Sediment Samples by Station, 2003–2019

SOC	Total Samples	Detections		Min	Max	Mean	Number of Detections by Stations			
		Count	*Percent*	*(µg/g as dry weight)*			*RE02*	*RE15*	*RE30*	*RE35*
Diethyl Phthalate	210	188	89.52%	<0.03	4.47	0.276	60	56	56	16
Dibutyl Phthalate; Di-n-Butyl Phthalate	209	180	86.12%	<0.02	1.53	0.138	55	58	51	16
Bis(2-ethylhexyl)phthalate	210	180	85.71%	<0.03	37.7	1.132	53	55	55	17
Di-n-Octyl Phthalate	210	165	78.57%	<0.05	3.71	0.250	49	47	51	18
Benzo(d,e,f)phenanthrene; Pyrene	210	137	65.24%	<0.04	0.3	0.139	37	36	49	15
Benzyl Butyl Phthalate	210	123	58.57%	<0.04	0.47	0.103	35	36	40	12
Fluoranthene	210	103	49.05%	<0.02	0.31	0.064	25	29	44	5
Naphthalene	210	101	48.10%	<0.03	0.97	0.098	32	30	32	7
Dimethyl Phthalate	210	87	41.43%	<0.03	1.64	0.083	24	29	30	4
Benzo(b)fluoranthene	210	82	39.05%	<0.04	0.47	0.103	22	23	35	2
Acenaphthene; 1,2-Dihydroacenaphthylene	210	76	36.19%	<0.01	0.12	0.031	25	25	24	2
Phenanthrene	210	71	33.81%	<0.04	0.19	0.078	21	19	28	3
Anthracene	210	64	30.48%	<0.01	0.15	0.037	20	17	27	0
Benzo(a)anthracene	210	62	29.52%	<0.04	0.11	0.141	14	15	26	7
Acenaphthylene	210	54	25.71%	<0.02	<0.30	0.029	16	19	18	1
Benzo(a)pyrene	210	51	24.29%	<0.03	0.46	0.099	10	14	24	3
Benzo(k)fluoranthene	210	51	24.29%	<0.03	0.57	0.146	13	13	23	2
Fluorene	210	50	23.81%	<0.03	0.04	0.024	14	15	19	2
Indeno(1,2,3-cd)pyrene; o-Phenylenepyrene	162	28	17.28%	<0.02	0.05	0.049	4	5	17	2
Chrysene	210	34	16.19%	<0.02	0.26	0.058	9	10	15	0
Benzene Hexachloride (alpha isomer)	210	27	12.86%	<0.02	0.31	0.063	9	7	10	1
Benzo(g,h,i)perylene	210	26	12.38%	<0.01	0.18	0.059	2	7	16	1
HCB; Hexachlorobenzene	210	18	8.57%	<0.04	<0.04	0.020	6	6	6	0
BHC (gamma isomer); Lindane	210	17	8.10%	<0.02	0.18	0.049	5	4	6	2
Dibenz(a,h)anthracene	210	11	5.24%	<0.02	0.06	0.045	1	2	7	1
DCPA; chlorthal dimethyl	210	9	4.29%	<0.02	<0.2	0.090	3	2	2	2
Diazinon; Dimpylate	210	9	4.29%	<0.01	<0.2	0.019	3	2	3	1
Metolachlor	210	8	3.81%	<0.2	<0.2	0.100	2	2	2	2
Ethoprop; Ethoprophos	210	8	3.81%	<0.02	0.13	0.029	2	2	4	0
DDVP; Dichlorvos; UDVF	210	7	3.33%	<0.04	<0.18	0.034	3	2	2	0
Benzene Hexachloride (beta isomer)	210	5	2.38%	<0.02	0.04	0.100	0	2	2	1
Heptachlor Epoxide	194	4	2.06%	<0.02	0.11	0.058	2	2	0	0
Chlorpyrifos-methyl	168	3	1.79%	<0.03	<0.03	0.015	0	1	1	1
Carbaryl; Sevin	210	3	1.43%	<0.03	<0.03	0.015	0	1	1	1
Terbufos	210	3	1.43%	<0.03	0.05	0.038	0	1	1	1
Fenchlorphos; Ronnel	210	2	0.95%	<0.13	0.44	0.253	1	1	0	0
2,4,5-T	210	2	0.95%	<0.02	<0.02	0.003	1	1	0	0
Carbazole; 9-Azafluorene; Dibenzopyrrole; Diphenylenimine	210	2	0.95%	<0.05	0.1	0.063	1	0	0	1
Etridiazole	183	1	0.55%	<0.02	<0.02	0.010	1	0	0	0
Chlorothalonil	183	1	0.55%	<0.06	<0.06	0.030	1	0	0	0
Atrazine	210	1	0.48%	<0.03	<0.03	0.015	0	1	0	0
Dieldrin	210	1	0.48%	<0.04	<0.04	0.020	1	0	0	0
Fensulfothion	210	1	0.48%	<0.04	<0.04	0.020	1	0	0	0

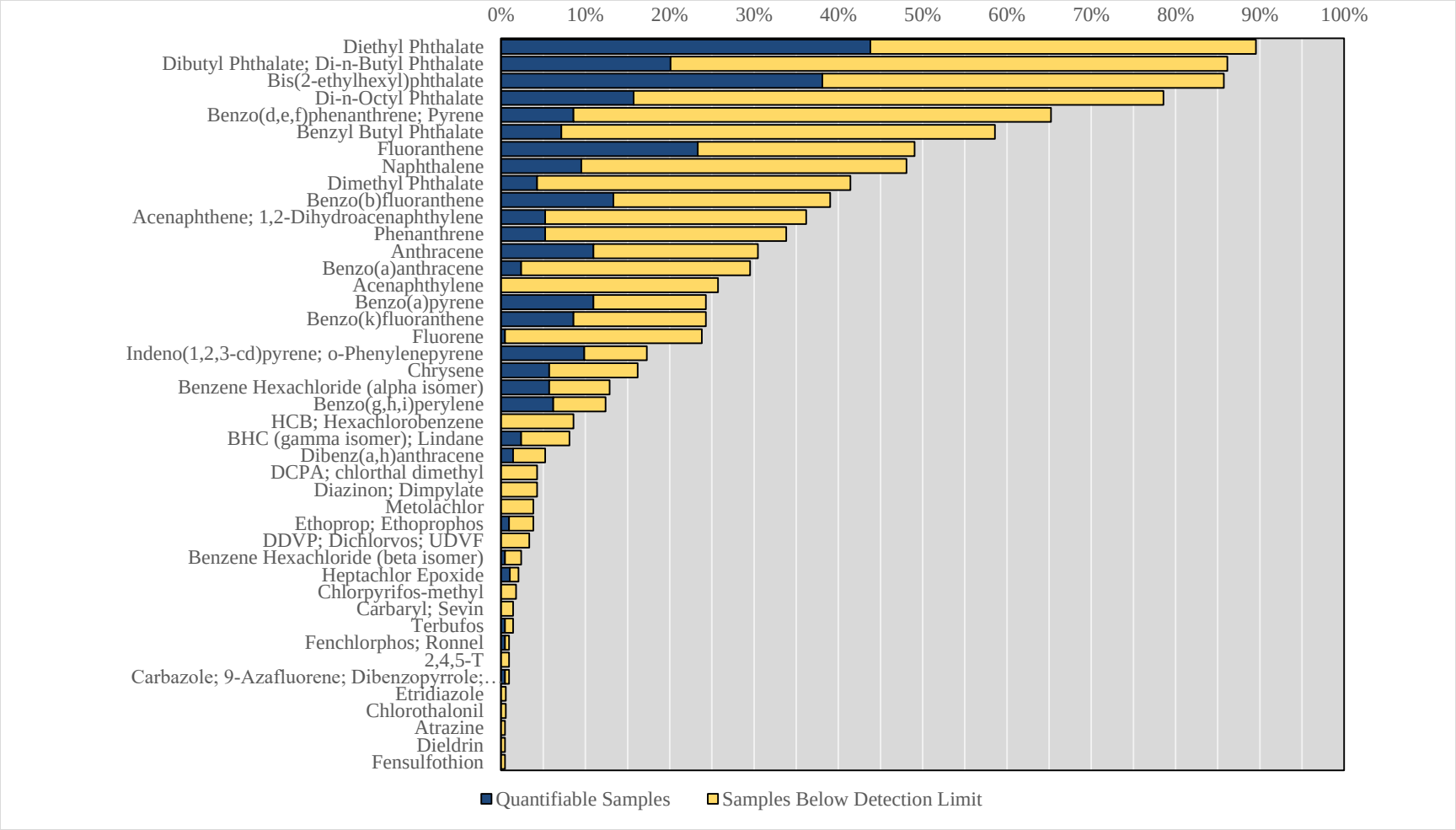

Figure 4-117. Synthetic Organic Compounds Detected in Sediment Samples, 2003–2019

CHAPTER 5. CONCLUSIONS AND RECOMMENDATIONS

While focusing on the 2003–2019 period, this assessment took into consideration all previous data from 1973 onwards, and used the earlier period as one against which the later period was compared. Changing trends in watershed and reservoirs take years to become apparent. Most plots and graphs, though, are only for the 2003–2019 period (the last major report was dated 2003) when the graphs would become impractical for the entire 47 period of record included in this assessment. Some broad conclusions can be drawn.

After analyzing long-term trends of different constituents, it can be concluded that the nitrate management strategy and the installation of the hypolimnetic oxygenation system have improved the water quality of the Reservoir. These strategies maintain oxidized conditions in hypolimnetic waters preventing the release of undesirable constituents such as OP, ammonia, iron, and manganese that negatively affect the water quality of the reservoir during periods of thermal stratification. Although high concentrations of nitrate (~14 mg-N/l) are discharged into Bull Run, Ox-N concentrations measured at the reservoir and stream outlet stations have not exceeded the established VDEQ and USEPA nitrate limit of 10 mg-N/l for drinking water and have always been below the 5 mg/l trigger point of the *Occoquan Policy*. Additionally, since 2012, concentrations for ammonia, OP, TP, iron, and manganese at RE02 bottom waters have decreased, as a result of the hypolimnetic oxygenation system operation.

Results from the Carlson's TSI and Vollenweider input-output model trophic state assessment indicate the reservoir remains a eutrophic/hypereutrophic waterbody. However, the ratio of phosphorus load to the trophic boundaries (mesotrophic and eutrophic) calculated with Vollenweider's model presented a downward trend, which indicates a positive impact of the management strategies implemented throughout the period of record. Furthermore, chlorophyll-*a* predictions using the Rast, Jones, Lee Model show a decreasing trend, but at a lower rate compared to previous water quality assessments. Actual concentrations observed for chlorophyll-*a* at the reservoir were generally lower than predicted values during the period of record. Trophic state assessments provide an indication of the biological productivity and nutrient levels in the reservoir. However, it is important to pair these assessments with long-term trend analyses of water quality parameters to obtain a more detailed description of the processes that can cause eutrophication and to determine water quality.

Five SOCs, belonging to the phthalates group, which are chemicals that are mainly used as plasticizers were often identified and measured in the reservoir. Of these five most-detected compounds, there were two that exceeded the MCL and/or VDEQ human health criteria sometimes which were Bis(2-ethylhexyl) phthalate (DEHP, or Diethylhexyl phthalate) and benzyl butyl phthalate. Other compounds that exceeded USEPA or VDEQ criteria were compounds that are classified as organochlorine insecticides and PAHs. As new information becomes available related to these emerging contaminants, continued monitoring, and SOC sediment release analysis is recommended. Additionally, an update of current SOCs monitored or new studies, such as the one performed on the "Impact of Indirect Potable Reuse on Endocrine Disrupting Compounds in the

Potomac River Basin" (Flanery, 2020), may be required to assess the effect of these chemical contaminants on water quality.

Finally, results also showed increasing sodium and chloride trends at reservoir stations, though not all trends were statistically significant. Sodium concentrations at RE02 have generally been maintained within the 30–60 mg/l USEPA guideline for the taste threshold, though some values have exceeded the lower threshold and the restricted diet level of 20 mg/l. Higher sodium load values were observed at the outflow station that at the inflow stations. The sodium and overall salt issue is one getting a lot of attention currently. A Salt Management Strategy SaMS was developed with input from a very wide variety of stakeholders in the Northern Virginia region. The OWML has also already started studies on this subject. Continued monitoring and evaluation are recommended.

There are two other areas of concern that likely will need attention in the near future: (i) endocrine-disrupting compounds, and, (ii) emerging contaminants per- and poly-fluorinated alkyl substances (PFAS), of which perfluorooctane sulfonate (PFOS) and perfluorooctanoic acid (PFOA) are two of the older ones that have been used. While endocrine-disrupting compounds have been focused upon quite a bit of late, attention is being placed on PFAS compounds, too. PFAS compounds are used in a very wide range of common products such as Teflon, are fairly ubiquitous, and are persistent in the environment. It is estimated that practically all human beings have measurable levels of PFAS in their bodies, and PFAS compounds have been linked to a variety of health conditions and diseases. Both the VDEQ and USEPA are working on establishing MCLs for PFAS compounds. OWML currently does not have much, if any, data on either (i) or (ii).

REFERENCES

Agency for Toxic Substances and Disease Registry. (1995). *Toxicological profile for polycyclic aromatic hydrocarbons*. P. H. S. U.S. Department of Health and Human Services. https://www.atsdr.cdc.gov/toxprofiles/tp69.pdf

Ambrosetti, W., Barbanti, L., and Sala, N. (2003). Residence time and physical processes in lakes. *Journal of limnology*, *62*, 1-15. https://doi.org/https://doi.org/10.4081/jlimnol.2003.s1.1

American Public Health Association. (1999). Standard methods for the examination of water and wastewate.

Augustyniak, R., Grochowska, J., Lopata, M., Parszuto, K., Tandyrak, R., and Tunowski, J. (2019). Sorption properties of the bottom sediment of a lake restored by phosphorus inactivation method 15 years after the termination of lake restoration procedures. *Water*, *11*. https://doi.org/https://doi.org/10.3390/w11102175

Babamoradi, H., van den Berg, F., and Rinnan, Å. (2013). Bootstrap based confidence limits in principal component analysis — A case study. *Chemometrics and Intelligent Laboratory Systems*, *120*, 97-105. https://doi.org/https://doi.org/10.1016/j.chemolab.2012.10.007

Beutel, M. (2016). The other internal loading — A look at nitrogen and mercury. *North American Lake Management Society (NALMS) Lakeline*, *36*, 13-16.

Beutel, M. W., and Horne, A. J. (1999). A review of the effects of hypolimnetic oxygenation on lake and reservoir water quality. *Lake and Reservoir Management*, *15*(4), 285-297. https://doi.org/https://doi.org/10.1080/07438149909354124

Bhagowati, B., and Ahamad, K. U. (2019). A review on lake eutrophication dynamics and recent developments in lake modeling. *Ecohydrology & Hydrobiology*, *19*(1), 155-166. https://doi.org/https://doi.org/10.1016/j.ecohyd.2018.03.002

Björk, S. (1988). Redevelopment of lake ecosystems: A case-study approach. *Ambio*, *17*(2), 90-98. http://www.jstor.org/stable/4313431

Boyer, E. W., Goodale, C. L., Jaworski, N. A., and Howarth, R. W. (2002). Anthropogenic nitrogen sources and relationships to riverine nitrogen export in the northeastern U.S.A. *Biogeochemistry*, *57-58*, 137-169. https://doi.org/10.1023/A:1015709302073

Brezonik, P. L. (1984). Trophic State Indices: Rationale for Multivariate Approaches. *Lake and Reservoir Management*, *1*(1), 441-445. https://doi.org/https://doi.org/10.1080/07438148409354553

Bruce, J. P., and Clark, R. H. (1966). *Introduction to hydrometeorology*. Pergamon Press Ltd. https://doi.org/https://doi.org/10.1016/C2013-0-01965-2

Bryhn, A. C., and Håkanson, L. (2007). A comparison of predictive phosphorus load-concentration models for lakes. *Ecosystems*, *10*(7), 1084-1099. https://doi.org/https://doi.org/10.1007/s10021-007-9078-z

Carleton, J. N., Grizzard, T. J., Godrej, A. N., Post, H. E., Lampe, L., and Kenel, P. P. (2000). Performance of a constructed wetlands in treating urban stormwater runoff. *Water Environment Research*, *72*(3), 295-304. https://doi.org/https://doi.org/10.2175/106143000X137518

Carlson, R. E. (1977). A trophic state index for lakes. *Limnology and Oceanography*, *22*(2), 361-369. https://doi.org/https://doi.org/10.4319/lo.1977.22.2.0361

Carmichael, W. W. (1994). The toxins of cyanobacteria. *Scientific American*, *270*(1), 78-86. https://doi.org/https://doi.org/10.1038/scientificamerican0194-78

Centers for Disease Control and Prevention. (2009). *Polycyclic aromatic hydrocarbons (PAHs)*. Retrieved December 28, 2020 from https://www.atsdr.cdc.gov/toxfaqs/TF.asp?id=377&tid=65

Charlton, M. N. (1980). Hypolimnion oxygen consumption in lakes: Discussion of productivity and morphometry Effects. *Canadian Journal of Fisheries and Aquatic Sciences, 37*, 1531-1539. https://doi.org/ https://doi.org/10.1139/f80-198

Cheng, V., Arhonditsis, G. B., and Brett, M. T. (2010). A revaluation of lake-phosphorus loading models using a Bayesian hierarchical framework. *Ecological Research, 25*(1), 59-76. https://doi.org/https://doi.org/10.1007/s11284-009-0630-5

Chesapeake Bay Program. (2008). *Chesapeake Bay 2007 health and restoration assessment* (EPA-903-R-08-002). U. S. E. P. Agency. https://www.chesapeakebay.net/what/publications/chesapeake_bay_2007_health_and_restoration_assessment

Congressional Research Service. (2016). *Clean Water Act: A summary of the law* (RL30030). https://crsreports.congress.gov/product/pdf/RL/RL30030

Cooke, G. D., Welch, E. B., Peterson, S., and Nichols, S. A. (2005). *Restoration and management of lakes and reservoirs, third edition*. CRC press.

Cubas, F. J., Holbrook, R. D., Novak, J. T., Godrej, A. N., and Grizzard, T. J. (2019). Effective depth controls the nitrate removal rates in a water supply reservoir with a high nitrate load. *Science of the Total Environment, 673*, 44-53. https://doi.org/https://doi.org/10.1016/j.scitotenv.2019.03.470

Donner, S. D., Kucharik, C. J., and Foley, J. A. (2004). Impact of changing land use practices on nitrate export by the Mississippi River. *Global Biogeochemical Cycles, 18*(I). https://doi.org/ https://doi.org/10.1029/2003GB002093

Dunalska, J. A., Wiśniewski, G., and Mientki, C. (2007). Assessment of multi-year (1956–2003) hypolimnetic withdrawal from Lake Kortowskie, Poland. *Lake and Reservoir Management, 23*(4), 377-387. https://doi.org/https://doi.org/10.1080/07438140709354025

Durães, N., Novo, L. A. B., Candeias, C., and da Silva, E. F. (2018). Chapter 2 - Distribution, transport and fate of pollutants. In A. C. Duarte, A. Cachada, & T. Rocha-Santos (Eds.), *Soil Pollution* (pp. 29-57). Academic Press. https://doi.org/https://doi.org/10.1016/B978-0-12-849873-6.00002-9

Fairfax Water. (2019). *Annual water quality report 2019*. https://www.fairfaxwater.org/sites/default/files/newsletters/ccr_2019.pdf

Fairfax Water. (2020). *Strategic plan 2025*. https://www.fairfaxwater.org/sites/default/files/about_us/Fairfax%20Water%20-%20Strategic%20Plan%202025.pdf

Flanery, A. (2020). *Impact of indirect potable reuse on endocrine disrupting compounds in the Potomac River Basin*.

Genkai-Kato, M., and Carpenter, S. R. (2005). Eutrophication Due to Phosphorus Recycling in Relation to Lake Morphometry, Temperature, and Macrophytes. *Ecology, 86*(1), 210-219. https://doi.org/https://doi.org/10.1890/03-0545

Grundy, R. D. (1971). Strategies for control of man-made eutrophication. *Environmental Science & Technology, 5*(12), 1184-1190. https://pubs.acs.org/doi/pdf/10.1021/es60059a011?casa_token=YqyIxnLAiHAAAAAA:u

l4wqo6a_Ng-fU8J1cZLc7h_qQzddVnZvaKLc-b6IjrprGCr9H4zV9Y8Ga7eYOznhZZaJS8QVg3QkvE
Harrison, J. A., Maranger, R. J., Alexander, R. B., Giblin, A. E., Jacinthe, P.-A., Mayorga, E., Seitzinger, S. P., Sobota, D. J., and Wollheim, W. M. (2009). The regional and global significance of nitrogen removal in lakes and reservoirs. *Biogeochemistry*, *93*(1/2), 143-157. https://doi.org/https://doi.org/10.1007/s10533-008-9272-x
Hawkins, P., Runnegar, M., Jackson, A. R. B., and Falconer, I. (1985). Severe hepatotoxicity caused by the tropical cyanobacterium (blue-green alga) Cylindrospermopsis raciborskii (Woloszynska) Seenaya and Subba Raju isolated from a domestic water supply reservoir. *Applied and Environmental Microbiology*, *50*(5), 1292-1295. https://doi.org/https://doi.org/10.1128/AEM.50.5.1292-1295.1985
Helsel, D. R., and Hirsch, R. M. (2002). *Statistical methods in water resources techniques of water resources investigations* (Book 4, chapter A3). U. S. G. Survey.
Hobbie, S. E., Finlay, J. C., Janke, B. D., Nidzgorski, D. A., Millet, D. B., and Baker, L. A. (2017). Contrasting nitrogen and phosphorus budgets in urban watersheds and implications for managing urban water pollution. *Proceedings of the National Academy of Sciences*, *114*(16), 4177-4182. https://doi.org/https://doi.org/10.1073/pnas.1618536114
Howarth, R. W., Marino, R., Lane, J., and Cole, J. J. (1988). Nitrogen fixation in freshwater, estuarine, and marine ecosystems. 1. Rates and importance. *Limnology and Oceanography*, *33*(4part2), 669-687. https://doi.org/https://doi.org/10.4319/lo.1988.33.4part2.0669
Johnston, C. A. (1999). *Development and evaluation of infilling methods for missing hydrologic and chemical watershed monitoring data* Virginia Polytechnic Institute and State University]. http://hdl.handle.net/10919/10028
Jones, R. A., and Lee, G. F. (1982). Recent advances in assessing impact of phosphorus loads on eutrophication-related water quality. *Water Research*, *16*(5), 503-515. https://doi.org/https://doi.org/10.1016/0043-1354(82)90069-0
Jones, R. A., and Lee, G. F. (1986). Eutrophication modeling for water quality management: An update of the Vollenweider-OECD model. *World Health Organization Water Quality Bulletin*, *11*, 67-74.
Kalff, J. (2002). *Limnology*. *Inland Water Ecosystems*. Prentice Hall, Inc.
Kohler, M. A., Nordenson, T. J., and Baker, D. R. (1959). *Evaporation maps for the United States* (Technical Paper No. 37). U.S. Department of Commerce, Weather Bureau.
Larsen, D. P., and Mercier, H. T. (1976). Phosphorus retention capacity of lakes. *Journal of the Fisheries Research Board of Canada*, *33*(8), 1742-1750. https://doi.org/https://doi.org/10.1139/f76-221
Lewtas, K., Paterson, M., Venema, H. D., and Roy, D. (2015). *Prairie lakes: Eutrophication and in-lake remediation treatments* (International Institute for Sustainable Development, Issue. https://www.iisd.org/system/files/publications/manitoba-prairie-lakes-remediation-literature-review.pdf
Lodhi, A. G., Godrej, A. N., Sen, D., and Baran, A. A. (2020). URUNME: A generic software for integrated environmental modeling. *Environmental Modelling & Software*, *134*. https://doi.org/https://doi.org/10.1016/j.envsoft.2020.104737
Lupon, A., Gerber, S., Sabater, F., and Bernal, S. (2015). Climate response of the soil nitrogen cycle in three forest types of a headwater Mediterranean catchment. *Journal of*

Geophysical Research: Biogeosciences, *120*(5), 859-875. https://doi.org/https://doi.org/10.1002/2014JG002791
Maavara, T., Parsons, C. T., Ridenour, C., Stojanovic, S., Dürr, H. H., Powley, H. R., and Van Cappellen, P. (2015). Global phosphorus retention by river damming. *Proceedings of the National Academy of Sciences of the United States of America*, *112*(51), 15603-15608. https://doi.org/https://doi.org/10.1073/pnas.1511797112
Malmaeus, J. M., and Håkanson, L. (2003). A dynamic model to predict suspended particulate matter in lakes. *Ecological Modelling*, *167*(3), 247-262. https://doi.org/https://doi.org/10.1016/S0304-3800(03)00166-2
Matsui, S., Ide, S., and Ando, M. (1995). Lakes and reservoirs: Reflecting waters of sustainable use. *Water Science and Technology*, *32*(7), 221-224. https://doi.org/https://doi.org/10.2166/wst.1995.0238
McGowan, W. (2000). *Water processing: residential, commercial, light-industrial, 3rd edition*. Water Quality Association.
Meals, D. W., Spooner, J., Dressing, S. A., and Harcum, J. B. (2011). *Statistical analysis for monotonic trends* (Tech notes 6). U. S. E. P. Agency. https://www.epa.gov/nps/nonpoint-source-monitoring-technotes
Metcalf and Eddy, Inc. (1970). 1969 Occoquan Reservoir Study. In.
Mulholland, P. J., and Elwood, J. W. (1982). The role of lake and reservoir sediments as sinks in the perturbed global carbon cycle. *Tellus*, *34*(5), 490-499. https://doi.org/https://doi.org/10.3402/tellusa.v34i5.10834
Nolan, K., Kamrath, J., and Levitt, J. (2012). Lindane toxicity: A comprehensive review of the medical literature. *Pediatric Dermatology*, *29*(2), 141-146. https://doi.org/https://doi.org/10.1111/j.1525-1470.2011.01519.x
Noor Halini, B., Razali, I., and Mohamad Hanif, O. (2011). Effects of thermal stratification on the concentration of iron and manganese in a tropical water supply reservoir. *Sains Malaysiana*, *40*(8), 821-825. http://inis.iaea.org/search/search.aspx?orig_q=RN:46135476
Northern Virginia Regional Comission. (2008). Occoquan Watershed - Where is it and what is in it. In.
NSTATE. (2016). *The geography of Virginia*. Retrieved December 27, 2020 from https://www.netstate.com/states/geography/va_geography.htm
Nürnberg, G. K. (1984). The prediction of internal phosphorus load in lakes with anoxic hypolimnia. *Limnology and Oceanography*, *29*(1), 111-124. https://doi.org/https://doi.org/10.4319/lo.1984.29.1.0111
Nürnberg, G. K. (2020). Hypolimnetic withdrawal as a lake restoration technique: determination of feasibility and continued benefits. *Hydrobiologia*, *847*(21), 4487-4501. https://doi.org/https://doi.org/10.1007/s10750-019-04094-z
Nygrén, N. A., Tapio, P., and Qi, Y. (2017). Lake management in 2030 — Five future images based on an international Delphi study. *Futures*, *93*, 1-13. https://doi.org/https://doi.org/10.1016/j.futures.2017.08.004
Occoquan Watershed Monitoring Laboratory. (1993). *A water quality assessment for the Occoquan Reservoir*.
Occoquan Watershed Monitoring Laboratory. (1998). *An updated water quality assessment for the Occoquan Reservoir and Tributary Watershed 1973–1997*.

Occoquan Watershed Monitoring Laboratory. (2011). *Bathymetric surveys of the Occoquan Reservoir and Fairfax Water solids storage quarry 2010*.
Olem, H., and Flock, G. (1990). *The lake and reservoir restoration guidance manual, Second edition* (EPA-440/4-90-006). U.S. Environmental Protection Agency. https://www.epa.gov/cwa-404/lake-and-reservoir-restoration-guidance-manual
Paerl, H. W., Fulton, R. S., Moisander, P. H., and Dyble, J. (2001). Harmful freshwater algal blooms, with an emphasis on cyanobacteria. *The Scientific World Journal*, *1*, 76-113. https://doi.org/https://doi.org/10.1100/tsw.2001.16
Pal, A., He, Y., Jekel, M., Reinhard, M., and Gin, K. Y.-H. (2014). Emerging contaminants of public health significance as water quality indicator compounds in the urban water cycle. *Environment International*, *71*, 46-62. https://doi.org/https://doi.org/10.1016/j.envint.2014.05.025
Peres-Neto, P. R., Jackson, D. A., and Somers, K. M. (2003). Giving meaningful interpretation to ordination axes: Assessing loadings significance in principal component analysis. *Ecology*, *84*(9), 2347-2363. https://doi.org/https://doi.org/10.1890/00-0634
Phyoe, W. W., and Wang, F. (2019). A review of carbon sink or source effect on artificial reservoirs. *International Journal of Environmental Science and Technology*, *16*(4), 2161-2174. https://doi.org/https://doi.org/10.1007/s13762-019-02237-2
Prince William County Service Authority. (2020). *Water treatment plants*. Retrieved December 27, 2020 from https://www.pwcsa.org/what-we-do/treatment-plants-0
Rast, W., Jones, R. A., and Lee, G. F. (1983). Predictive capability of US OECD phosphorus loading-Eutrophication response models. *Journal Water Pollution Control Federation*, *55*(7), 990-1003. https://www.researchgate.net/publication/297522110_Predictive_Capability_of_US_OECD_Phosphorus_Loading-Eutrophication_Response_Models
Rast, W., and Lee, G. (1978). *Summary analysis of the North American (US Portion) OECD Eutrophication Project: Nutrient loading - Lake response relationships and trophic state indices* (EPA/600/3-78/008). http://udspace.udel.edu/handle/19716/1386
Ripl, W. (1976). Biochemical oxidation of polluted lake sediment with nitrate: a new lake restoration method. *Ambio*, *5*(3), 132-135.
Rippy, M. A., Deletic, A., Black, J., Aryal, R., Lampard, J.-L., Tang, J. Y.-M., McCarthy, D., Kolotelo, P., Sidhu, J., and Gernjak, W. (2017). Pesticide occurrence and spatio-temporal variability in urban run-off across Australia. *Water Research*, *115*, 245-255. https://doi.org/https://doi.org/10.1016/j.watres.2017.03.010
Salas, E., and Subburayalu, S. (2019). Implications of climate change on nutrient pollution: a look into the nitrogen and phosphorus loadings in the Great Miami and Little Miami watersheds in Ohio. *AIMS Environmental Science*, *6*(3), 186-221. https://doi.org/https://doi.org/10.3934/environsci.2019.3.186
Schindler, D. W. (2006). Recent advances in the understanding and management of eutrophication. *Limnology and Oceanography*, *51*(1part2), 356-363. https://doi.org/https://doi.org/10.4319/lo.2006.51.1_part_2.0356
Seitzinger, S. P. (1988). Denitrification in freshwater and coastal marine ecosystems: Ecological and geochemical significance. *Limnology and Oceanography*, *33*(4part2), 702-724. https://doi.org/https://doi.org/10.4319/lo.1988.33.4part2.0702

Sen, P. K. (1968). Estimates of the regression coefficient based on Kendall's Tau. *Journal of the American Statistical Association*, *63*(324), 1379-1389. https://doi.org/https://doi.org/10.2307/2285891

Shuttleworth, W. J. (2007). Putting the 'vap' into evaporation. *Hydrology and Earth System Sciences*, *11*(1), 210-244. https://doi.org/https://doi.org/10.5194/hess-11-210-2007

Smith, R. A., Schwarz, G. E., and Alexander, R. B. (1997). Regional interpretation of water-quality monitoring data. *Water Resources Research*, *33*(12), 2781-2798. https://doi.org/https://doi.org/10.1029/97WR02171

Smith, V. H., and Schindler, D. W. (2009). Eutrophication science: Where do we go from here? *Trends in ecology & evolution*, *24*(4), 201-207. https://doi.org/https://doi.org/10.1016/j.tree.2008.11.009

Stets, E. G., Kelly, V. J., and Crawford, C. G. (2015). Regional and temporal differences in nitrate trends discerned from long-term water quality monitoring data. *Journal of the American Water Resources Association (JAWRA)*, *51*(5), 14. https://onlinelibrary.wiley.com/doi/epdf/10.1111/1752-1688.12321

Stumm, W., and Morgan, J. J. (1996). *Aquatic chemistry: Chemical equilibra and rates in natural waters*. John Wiley and Sons, Inc.

Tapp, J. S. (1978). Eutrophication analysis with simple and complex models. *Journal (Water Pollution Control Federation)*, *50*(3), 484-492. http://www.jstor.org/stable/25039576

Thomann, R. V., Winfield, R. P., Di Toro, D. M., and O'Connor, D. J. (1976). *Mathematical modeling of phytoplankton in Lake Ontario, Part 2, Simulations using Lake 1 Model* (EPA-600/3-76-065). http://udspace.udel.edu/handle/19716/1371

Thomas, A. G. (1986). Specific conductance as an indicator of total dissolved solids in cold, dilute waters. *Hydrological Sciences Journal*, *31*(1), 81-92. https://doi.org/https://doi.org/10.1080/02626668609491029

Trench, E. C. T., Moore, R. B., Ahearn, E. A., Mullaney, J. R., Hickman, R. E., and Schwarz, G. E. (2012). *Nutrient concentrations and loads in the Northeastern United States — Status and trends, 1975–2003: U.S. Geological Survey Scientific Investigations Report* (2011-5114). http://pubs.usgs.gov/sir/2011/5114

U.S. Environmental Protection Agency. (1979). *Lake and reservoir classification systems* (EPA-600/3-79-074). https://nepis.epa.gov/Exe/ZyPDF.cgi/9101QXT0.PDF?Dockey=9101QXT0.PDF

U.S. Environmental Protection Agency. (1980). *Aquatic water quality criteria for hexachlorocyclohexane* (EPA 440/5-80-054). https://www.epa.gov/sites/production/files/2019-03/documents/ambient-wqc-hexachlorocyclohexane-1980.pdf

U.S. Environmental Protection Agency. (1986). *Quality criteria for water* (EPA-400/5-86-001). https://www.epa.gov/sites/production/files/2018-10/documents/quality-criteria-water-1986.pdf

U.S. Environmental Protection Agency. (2000a). *Ambient Water Quality Criteria Recommendations. Lakes and Reservoirs in Nutrient Ecoregion IX*. (EPA 822-B-00-011). https://www.epa.gov/sites/production/files/documents/lakes9.pdf

U.S. Environmental Protection Agency. (2000b). *Nutrient criteria technical guidance manual — Lakes and reservoirs* (EPA-822-B00-001). https://www.epa.gov/sites/production/files/2018-10/documents/nutrient-criteria-manual-lakes-reservoirs.pdf

U.S. Environmental Protection Agency. (2006). *USEPA - Pesticides - Product cancellation order for Lindance* (EPA-HQ-OPP-2002-0202). https://www.govinfo.gov/content/pkg/FR-2006-12-13/pdf/FR-2006-12-13.pdf

U.S. Environmental Protection Agency. (2009a). *National lakes assessment: A collaborative survey of the nation's lakes* (EPA 841-R-09-001). https://www.epa.gov/sites/production/files/2013-11/documents/nla_newlowres_fullrpt.pdf

U.S. Environmental Protection Agency. (2009b). *National Primary Drinking Water Regulations* (EPA 816-F-09-004). https://www.epa.gov/sites/production/files/2016-06/documents/npwdr_complete_table.pdf

U.S. Environmental Protection Agency. (2016a). *National lakes assessment 2012: A collaborative survey of lakes in the United States* (EPA 841-R-16-113). https://www.epa.gov/sites/production/files/2016-12/documents/nla_report_dec_2016.pdf

U.S. Environmental Protection Agency. (2016b). *National Nonpoint Source Program — A catalyst for water quality improvements* (EPA 841-R-16-009). https://www.epa.gov/sites/production/files/2016-10/documents/nps_program_highlights_report-508.pdf

U.S. Environmental Protection Agency. (2018). *2018 Edition of the drinking water standards and health advisories tables* (EPA 822-F-18-001). https://www.epa.gov/sites/production/files/2018-03/documents/dwtable2018.pdf

U.S. Food and Drug Administration. (2020). *Phthlates*. Retrieved December 28, 2020 from https://www.fda.gov/cosmetics/cosmetic-ingredients/phthalates#top

U.S. Geological Survey. (2021). *Lakes and reservoirs*. Retrieved February 16, 2021 from https://www.usgs.gov/special-topic/water-science-school/science/lakes-and-reservoirs?qt-science_center_objects=0#qt-science_center_objects

Upper Occoquan Service Authority. (2020). *Upper Occoquan Service Authority, Leader in Water Reclamation and Reuse*. Retrieved December 27, 2020 from https://www.uosa.org/IndexUOSA.asp

Van Den Bos, A. C. (2003). *A water quality assessment of the Occoquan Reservoir and its tributary watershed: 1973–2002* Virginia Polytechnic Institute and State University]. http://hdl.handle.net/10919/34117

Van der Does, J., Verstraelen, P., Boers, P., Van Roestel, J., Roijackers, R., and Moser, G. (1992). Lake restoration with and without dredging of phosphorus-enriched upper sediment layers. *Hydrobiologia*, *233*(1), 197-210. https://doi.org/https://doi.org/10.1007/BF00016108

Virginia Cooperative Extension. (2000). *Agronomy handbook* (424-100). https://www.pubs.ext.vt.edu/424/424-100/424-100.html

Virginia Department of Environmental Quality. (2019). *Water quality assessment guidance manual for 2020* (305(b)/303(d) Integrated Water Quality Report). https://www.deq.virginia.gov/water/water-quality/assessments/wqa-guidance-manual

Virginia State Water Control Board. (2008). Virginia Administrative Code Chapter 740. Water reclamation and reuse regulation. *Virginia Register*, *24*(26). https://law.lis.virginia.gov/admincode/title9/agency25/chapter740/section10/

Virginia State Water Control Board. (2017a). *Water quality standards Part I. Surface water standards with general, statewide application. Numerical criteria for dissolved oxygen, pH, and maximum*

temperature (9VAC25-260-50.). https://law.lis.virginia.gov/pdf/admincode/9/25/260/50/
Virginia State Water Control Board. (2017b). *Water quality standards Part II. Standards with More Specific Application Criteria for man-made lakes and reservoirs to protect aquatic life and recreational designated uses from the impacts of nutrients.* (9VAC25-260-187). https://law.lis.virginia.gov/pdf/admincode/9/25/260/187/
Virginia State Water Control Board. (2019). *Water quality standards Part I. Surface water standards with general, statewide application. Criteria for Surface Water.* (9VAC25-260-140). https://law.lis.virginia.gov/admincode/title9/agency25/chapter260/section140/
Virginia State Water Control Board. (2020). *Water quality standards Part I. Surface Water Standards with General, Statewide Application Ammonia surface water quality criteria.* (9VAC25-260-155). https://law.lis.virginia.gov/pdf/admincode/9/25/260/155/
Vollenweider, R. A. (1968). *Scientific fundamentals of the eutrophication of lakes and flowing waters, with particular reference to nitrogen and phosphorus as factors in eutrophication* (DAS/CSI/62.27).
Vollenweider, R. A. (1975). Input-output models with special reference to the phosphorus loading concept in limnology. *Schweizerische Zeitschrift für Hydrologie, 37*(1), 53-84. https://doi.org/https://doi.org/10.1007/BF02505178
Vollenweider, R. A. (1976). Advances in defining critical loading levels for phosphorus in lake eutrophication. *Mem. 1st ital. Idrobiol., 33*, 53-58.
Wang, H., and Wang, H. (2009). Mitigation of lake eutrophication: Loosen nitrogen control and focus on phosphorus abatement. *Progress in Natural Science, 19*(10), 1445-1451. https://doi.org/https://doi.org/10.1016/j.pnsc.2009.03.009
Wetzel, R. G. (2001). *Limnology: Lake and river ecosystems*. San Diego: Academic Press.
World Health Organization. (2004). *Heptachlor and heptachlor epoxide in drinking-water* (WHO/SDE/WSH/03.04/99). https://www.who.int/water_sanitation_health/dwq/chemicals/heptachlor.pdf
Wu, Z., Liu, Y., Liang, Z., Wu, S., and Guo, H. (2017). Internal cycling, not external loading, decides the nutrient limitation in eutrophic lake: A dynamic model with temporal Bayesian hierarchical inference. *Water Research, 116*, 231-240. https://doi.org/https://doi.org/10.1016/j.watres.2017.03.039
Yang, K., Yu, Z., Luo, Y., Yang, Y., Zhao, L., and Zhou, X. (2017). Spatial and temporal variations in the relationship between lake water surface temperatures and water quality - A case study of Dianchi Lake. *Science of the Total Environment, 624*, 859-871. https://doi.org/https://doi.org/10.1016/j.scitotenv.2017.12.119
Yang, X. E., Wu, X., Hao, H.-l., and He, Z.-l. (2008). Mechanisms and assessment of water eutrophication. *Journal of Zhejiang University SCIENCE B, 9*(3), 197-209. https://doi.org/https://doi.org/10.1631/jzus.B0710626
Yuan, M., Carmichael, W. W., and Hilborn, E. D. (2006). Microcystin analysis in human sera and liver from human fatalities in Caruaru, Brazil 1996. *Toxicon, 48*(6), 627-640. https://doi.org/https://doi.org/10.1016/j.toxicon.2006.07.031